Understand the antiviral property of IFITM3 and identify viral counter measures

Yimeng Wang

Division of Experimental Medicine

McGill University, Montreal

December 2020

A thesis submitted to McGill University in partial fulfillment of the requirements of the degree of Ph.D. of Science.

Table of Contents

Abstract

Ever since crossed the species barrier to infect humans, HIV quickly became a global pandemic that claimed 37 million lives. Decades of intense research and tremendous support from global organizations have led to a deeper understanding of HIV and the rapid development of effective therapies for suppressing HIV viremia. Despite the immense efforts to research the cures and the vaccines, the answers are still not close to sight. Moreover, people with HIV and those at higher risk also face the lack of access to diagnosis, treatment and care. In 2019, there were 1.7 million reported new infections, which add up to 38 million people living with HIV globally. Therefore, continuous efforts are required to understand HIV virology and to find cures. My research focuses on understanding the interaction between the host restriction factors and HIV-1. At the early stage of HIV transmission, interferon-stimulated genes (ISGs) were critical in restricting the spread of HIV across species. To overcome the effects of the host restriction factors, HIV has evolved several accessory proteins to ablate the restriction factors. The HIV genome's plasticity also enables the virus to mutate its structural genes to escape the targeting by the host restriction factors. I aim to elucidate the molecular mechanism behind the arms race between the host restriction factors and HIV-1. This knowledge helps to pave the way to finding the effective vaccine epitopes. One of the ISGs, interferon-inducible transmembrane protein 3 (IFITM3), was reported to inhibit HIV-1 primary isolates, but not the transmitted founder strains. Studies have shown that IFITM3 prevents HIV-1 entry by hindering the formation of fusion pores. I have found that the HIV-1 envelope (Env) protein helps the resistant HIV-1 to overcome IFITM3 inhibition. By testing a group of transmitted founder strains and the primary isolates, I identified the HIV-1 that are resistant to IFITM3 inhibition. By performing mutagenesis studies on the HIV-1 Env, I discovered that HIV-1 mutates the V3 loop of Env to

counter fusion inhibition by IFITM3. I further tested these HIV-1 for their sensitivity to a group of neutralization antibodies. The IFITM3-resistant HIV-1 was shown resistant to neutralization antibodies that target the V3 loop. This observation suggests that Env with less exposed V3 loop is more resistant to IFITM3. The Env stability assay further attested that more stable Env proteins with V3 loop buried inside are more resistant to IFITM3 inhibition. However, incorporating IFITM3 in virions did not sensitize HIV-1 to entry inhibitors such as soluble CD4 or neutralization antibodies. Interestingly, I observed that 25-hydroxycholesterol, the product of another ISG cholesterol 25 hydroxylase (CH25H), potentiates the inhibitory activity of IFITM3 against HIV-1. Collectively, I have discovered the importance of the V3 loop of HIV-1 Env in modulating the viral response to IFITM3 inhibition, found that the extent of V3 loop exposure correlates with the Env sensitivity to IFITM3, and that the product of CH25H enhances the anti-HIV-1 effect of IFITM3.

Résumé

Depuis que le VIH a franchi la barrière des espèces pour infecter les humains, celui-ci est rapidement devenu responsable d'une pandémie mondiale causant 32,7 millions de victimes. Des années de recherche rigoureuse et un soutien important de la part d'organisations mondiales ont permis de mieux comprendre le VIH et de développer rapidement des thérapies efficaces pour supprimer la virémie du VIH. Malgré des immenses efforts de recherche sur les remèdes et les vaccins, les produits ne sont toujours pas à portée de main. En addition, les personnes séropositives et les personnes à haut risque sont également confrontées au manque d'accès à la prévention, au traitement et aux soins. En 2019, 1,7 million de nouvelles infections ont été confirmées, ce qui représente 38 millions de personnes vivant avec le VIH dans le monde. Des efforts continus sont donc nécessaires pour comprendre la virologie du VIH et pour trouver des remèdes. Mes recherches se concentrent sur la compréhension de l'interaction entre les facteurs de restriction de l'hôte et le VIH-1. Au stade aigu de la pathogenèse du VIH, les gènes stimulés par l'interféron (ISG) sont essentiels pour limiter la propagation du VIH entre les différentes espèces. Pour surmonter les effets des facteurs de restriction de l'hôte, le VIH a développé plusieurs protéines accessoires pour éliminer les facteurs de restriction. La flexibilité du génome du VIH permet également au virus de muter ses gènes de structure pour échapper au ciblage par les facteurs de restriction de l'hôte. Mon objectif est d'élucider le mécanisme moléculaire qui se cache derrière la course aux armements entre les facteurs de restriction de l'hôte et le VIH-1. Cette connaissance aide à ouvrir la voie à la découverte d'épitopes efficaces pour la confection d'un vaccin. L'un des GSI, la protéine transmembranaire 3 inductible par l'interféron (IFITM3), inhibe les isolats primaires du VIH-1, mais pas les souches fondatrices transmises. Des études ont montré que l'IFITM3 empêche l'entrée du VIH-1 en entravant la formation de pores de

fusion. J'ai découvert que la protéine de l'enveloppe du VIH-1 (Env) aide le VIH-1 résistant à surmonter l'inhibition de l'IFITM3. En testant un groupe de souches fondatrices transmises et les isolats primaires, j'ai identifié les souches qui sont sensibles ou résistants à l'inhibition d'IFITM3. En effectuant des études de mutagenèse sur la protéine Env du VIH-1, j'ai découvert que le VIH-1 muter dans la boucle V3 de l'Env contre l'inhibition de la fusion par IFITM3. J'ai ensuite testé ces VIH-1 pour leur sensibilité à un groupe d'anticorps de neutralisation. Le VIH-1 résistant à l'IFITM3 s'est également révélé résistant aux anticorps de neutralisation qui ciblent la boucle V3. Cette observation suggère que l'Env avec une boucle V3 moins exposée est plus résistant à l'IFITM3. Le test de stabilité Env a en outre attesté que les protéines Env plus stables avec une boucle V3 enfouie à l'intérieur de la protéine sont plus résistantes à l'inhibition d'IFITM3. Cependant, l'incorporation d'IFITM3 dans les virions n'a pas sensibilisé le VIH-1 aux inhibiteurs d'entrée tels que les CD4 solubles, ou les anticorps de neutralisation. Il est intéressant de noter que le 25-hydroxycholestérol, le produit d'une autre hydroxylase du cholestérol ISG 25 (CH25H), potentialise l'activité inhibitrice de l'IFITM3 contre le VIH-1. Collectivement, j'ai découvert l'importance de la boucle V3 de l'Env du VIH-1 dans la modulation de la réponse virale à l'inhibition de l'IFITM3, j'ai constaté que l'étendue de l'exposition de la boucle V3 est en corrélation avec la sensibilité de l'Env à l'IFITM3, et que le produit de la CH25H renforce l'effet anti-VIH-1 de l'IFITM3.

Contribution to original knowledge

This thesis has identified the viral mechanism that antagonizes IFITM3 inhibition for the first time. IFITM3 protein is an essential effector of the interferon-mediated viral immunity that inhibits the entry of a broad spectrum of viruses. Previous studies of other viruses have identified their envelope proteins to play a pivotal role in resisting IFITM3 inhibition. The results from Chapter 3.1 have revealed that Env is the viral protein that HIV-1 uses to overcome IFITM3 inhibition. The mutagenesis studies mapped the IFITM3 resistance property to the V3 loop of Env. Furthermore, the underlying mechanisms of the HIV-1 escape of IFITM3 have been elucidated. The IFITM3-resistant Env was shown to be associated with higher sensitivity to sCD4 and 17b antibody. The results highlighted the critical correlation between the conformation of Env and the viral resistance to IFITM3. The effects of SNP rs34481144 and rs12252 of IFITM3 on its expression and the anti-HIV-1 activity have been studied. The results have implicated the importance of overcoming IFITM3 for HIV-1 to establish successful infection in humans. This thesis also investigated the interplay between IFITM3 and 25HC in HIV-1 inhibition for the first time. The results have shed light on the enhancement of IFITM3 anti-HIV-1 activity by another interferon-inducible restriction factor.

Contribution of Authors

This thesis has been prepared following the guideline provided by McGill Graduate and Postdoctoral Studies and written in the traditional monograph style. The author of this thesis is the contributor to most of the experimental results. The contributions of other individuals to the data and materials are acknowledged in the overview of each chapter. These works will not be used in any other thesis. My supervisor Dr. Chen Liang provided editorial support in the preparation of this thesis.

In Chapter I, the topics related to the research objectives are introduced. The history and epidemiology of HIV are briefly summarized. The virology of HIV-1 and the IFN-triggered innate immune responses to HIV-1 are described in detail as they are closely related to the foundation of my research objectives. At the end of the chapter, I introduced the hypotheses and the research aims of my study.

In Chapter II, I described the protocols used for each experiment, as well as the sources of the biological and non-biological reagents used. A special acknowledgement to Dr. Eric O. Freed for providing the NL(AD8-1) DNA construct, Dr. Andrés Finzi for providing all the JRFL mutant constructs, Dr. Bluma Brenner for providing the human peripheral blood samples and HIV-1 patients PBMCs, and Dr. Yiming Shao for providing Han Chinese HIV-1 patient blood samples. Also, special thanks to the postdoctoral fellow Dr. Zhen Wang, who helped to construct the V3 loop NL4-3 mutants.

In Chapter III, all the results are described. A special acknowledgement to our research assistant Qinghua Pan for helping me with testing the TF viruses (Figure 16) and quantifying the RT activity of the viruses. The HIV-1 Env stability test by radioimmunoprecipitation (Figure 23)

was performed by the postdoctoral fellow Dr. Shilei Ding from Dr. Finzi's lab. The manuscript adopted for some of the data presented in Chapter 3.1 is listed below:

Wang, Y., Pan, Q., Ding, S., Wang, Z., Yu, J., Finzi, A., ... & Liang, C. (2017). The V3 loop of HIV-1 Env determines viral susceptibility to IFITM3 impairment of viral infectivity. *Journal of virology*, *91*(7).

In Chapter IV, I discussed my results in the context of the literature and highlighted the relevance of my study to the field of HIV-1 and the importance of my research to the development of possible novel HIV treatments.

The published works not included in this thesis to which I have contributed listed below:

Beitari, S., **Wang, Y.**, Liu, S. L., & Liang, C. (2019). HIV-1 envelope glycoprotein at the interface of host restriction and virus evasion. *Viruses*, *11*(4), 311.

Qian, J., Le Duff, Y., **Wang, Y.**, Pan, Q., Ding, S., Zheng, Y. M., ... & Liang, C. (2015). Primate lentiviruses are differentially inhibited by interferon-induced transmembrane proteins. *Virology*, *474*, 10-18.

List of Figures

List of Tables

List of Acronyms

25HC	25-hydroxy cholesterol
A	Adenosine
AIDS	Acquired Immunodeficiency Syndrome
ALIX	ALG-interacting protein X
AMP	Adenosine monophosphate
APOBEC3G	Apolipoprotein B mRNA editing enzyme catalytic polypeptide-like 3G
ARD	Arginine-rich domain
ATCC	American Type Culture Collection
BST-2/CD317	Bone marrow stromal antigen
C	Cytosine
CA	Capsid/p24
CARDs	Caspase activation and recruitment domains
cART	Combination antiretroviral therapy
CBFβ	Core Binding Factor β
CBMCs	Cord blood-derived mononuclear cells
CCR5	C-C chemokine receptor type 5
CDC	United States Centers of Disease Control and Prevention

CDK9	Cyclin-dependent kinase 9
cDNA	Complementary DNA
cGAMP	cyclic GMP-AMP
cGAS	cyclic GMP-AMP synthase
CH25H	Cholesterol 25 hydroxylase
CIL	Conserved intracellular loop
Co-IP	Co-immunoprecipitation
CTCF	CCCTC-binding factor
CTD	Carboxyl terminal domain
CXCL10	C-X-C motif chemokine 10
CXCR4	C-X-C chemokine receptor type 4
Cyc T1	Cyclin T1
CypA	Cyclophilin A
dGTP	Deoxyguanosine triphosphate
DMEM	Dulbecco's Modified Eagle Medium
DNA	Deoxyribonucleic acid
dNTP	Deoxynucleotide triphosphate
dNTPase	Deoxynucleotide triphosphate hydrolase

DRB	5,6-dichloro-1-beta-D-ribofuranosylbenzimidazole
DSIF	DRB sensitivity inducing factor
dsRNA	Double-stranded RNA
ECL	Enhanced chemiluminescence
ELISA	Enzyme-linked immunosorbent assay
Env	Envelope glycoprotein
EP	Eppendorf
EPR	Electron paramagnetic resonance
ER	Endoplasmic reticulum
ESCRT	Endosomal sorting complex required for transport
FBS	Fetal bovine serum
FDA	Food and Drug Administration
G	Guanosine
GAF	IFNγ activation factor
Gag	Group-specific antigens
Gag-Pol	Gag-protease-reverse transcriptase-integrase polyprotein
GAP	GTPase-activating proteins
GBP5	Guanylate binding protein 5

GMP	Guanosine monophosphate
Gp41	Glycoprotein 41 KDa
Gp120	Glycoprotein 120 KDa
Gp160	Glycoprotein 160 KDa
GPI	C-terminal glycosyl-phosphatidylinositol
GTP	Guanosine triphosphate
GTPase	Guanosine triphosphate hydrolase
HCV	Hepatitis C Virus
HIV	Human Immunodeficiency Virus
HPV-16	Human Papillomavirus-16
HRhV	Human Rhinovirus
HRoV	Human Rotavirus
HRP	Hourseradish peroxidase
IAV	Influenza A virus
IBV	Influenza B virus
IFI16	Interferon inducible protein 16
IFITMs	Interferon-induced transmembrane proteins
IFN	Interferon

IFNAR	Interferon α receptors
IFNGR	Interferon γ receptors
IFNLR	Interferon λ receptors
IL-6	Interleukin 6
IN	Integrase
IRF3	Interferon regulatory transcription factor 3
IRF7	Interferon regulatory transcription factor 7
ISGF3	IFN stimulated gene factor 3
ISGs	Interferon stimulated genes
ISRE	IFN-stimulated response element
IκB	Nuclear factor of kappa light polypeptide gene enhancer in B-cells inhibitor
JAK1	Janus kinase 1
JGH	Jewish General Hospital
KO	Knock out
LEDGF/p75	the Lens epithelium-derived growth factor
LTR	Long terminal repeats
MA	Matrix/p17
MARCH8	Membrane-associated really interesting new gene C4HC3 8

MAVS	Mitochondrial antiviral signaling protein
MCMV	Murine cytomegalovirus
MDM	Monocyte derived macrophages
MLV	Murine leukemia virus
mRNA	Messenger RNA
MTb	Mycobacterium tuberculosis
Mx2/MxB	Myxovirus resistant protein 2/B
MyD88	Myeloid differentiation primary response protein 88
NC	Nucleocapsid/p7
NEB	New England Biolabs
Nef	Negative factor
NELF-E	Negative elongation factor
NES	Nuclear export signal
NF-κB	Nuclear factor kappa-light-chain-enhancer of activated B cells
NIH	National Institutes of Health
NK cells	Natural killer cells
NLS	Nuclear localization signal
NS5A	Non-structural protein 5A

NTD	Amino-terminal domain
ORF	Open reading frames
p53	Tumor suppressor protein 53
PAMPs	Pathogen associated molecular patterns
PBMCs	Peripheral blood mononuclear cells
PBS	Phosphate-buffered saline
PBS	Primer binding site
PBST	PBS with 0.1% Tween 20
pDCs	Plasmacytoid cells
PEI	Polyethylenimine
PGCs	Primordial germ cells
PHA	Phytohemagglutinin
PIC	Pre-integration complex
Pol	Polymerase
Pol II	RNA polymerase II
PPT	Purine rich polypurine tract
PR	Protease
PRRs	Pathogen-recognition receptors

PRRSV	Porcine reproductive and respiratory syndrome virus
PtdIns(4,5)P2	Phosphoinositide phosphatidylinositol-4,5-bisphosphate
pTEFb	Positive transcription elongation factor b
PVDF	Polyvinylidene difluoride
RanBP	Ran binding protein
Rev	Regulator of expression of virion proteins
RIG-I	Retinoic acid-inducible gene I
RIPA	Radioimmunoprecipitation assay
RNA	Ribonucleic acid
RPMI	Roswell Park Memorial Institute 1640 medium
RRE	Rev-response element
RT	Reverse transcriptase
RTC	Reverse transcription complex
SAMHD1	Sterile alpha motif and histidine/aspartic acid domain-containing protein 1
sCD4	Soluble CD4
SDG	Sustainable development goals
SDS	Sodium dodecyl sulfate
SDSL	Site-directed spin labeling

SERINC5	Serine-incorporator 5
shRNA	Small hairpin RNA
SIV	Simian immunodeficiency virus
SIV_{agm}	Simian immunodeficiency virus of African green monkey
SIV_{cpz}	Simian immunodeficiency virus of chimpanzee
SIV_{mac}	Simian immunodeficiency virus of macaque
SIV_{sm}	Simian immunodeficiency virus of sooty mangabey
SLF11	Schlafen 11
SLX4com	SLX4-MUS81-EME1 protein complex
SNP	Single nucleotide polymorphism
SOCS	Suppressor of cytokine signaling
SP1	Spacer peptide 1
SP2	Spacer peptide 2
STAT	Signal transducers and to activate transcription
STING	Stimulator of interferon genes
SU	Surface subunit/gp120
T	Thymidine
TAF	TBP-associated factors

TAK	Transforming growth factor beta-activated kinase
TAR	Transactivation-response region
Tat	HIV trans-activator
TBK1	Serine/threonine protein kinase 1
TBS	Tris buffer saline
TCA	Trichloroacetic acid
TF	Transmitted founder
TFIID	Transcription factor II D
TFV	Transmitted founder viruses
TIM	The T-cell Ig and mucin domain protein
TIR	Toll/interleukin-1 receptor
TIRAP	TIR domain-containing adapter protein
TLRs	Toll-like receptors
TM	Transmembrane
TNF	Tumour necrosis factor
TRAF	TNF receptor associated factor
TRAM	TRIF-related adaptor molecule
TRIF	TIR domain-containing adaptor-inducing interferon-β

TRIM5α	Tripartite motif-containing protein 5α
TSG101	Tumour susceptibility gene 101
TYK2	Tyrosine kinase 2
U	Uridine
UNAID	United Nations Programme on HIV/AIDS
VAPA	Vesicle membrane protein associated protein A
Vif	Viral infectivity factor
Vpr	Viral protein R
VPS4	Vacuolar protein sorting 4
Vpu	Viral protein U
Vpx	Viral protein X
VSV	Vesicular stomatitis virus
VSV-G	Vesicular stomatitis virus glycoprotein
WB	Western blot
XMRV	Xenotropic MLV–related virus
ZIKV	Zika virus
Ψ	Viral RNA packaging signal sequence

Acknowledgements

It was a long and rough journey to be trained as a Ph.D. candidate. There were so many times that I collapsed because of the hurdles, failures and stresses. I was very blessed that I could not stand on my own feet at those times; there were always so many hands lend to me, helping me stand up, walk straight and move forward. As much as I feel sorry for causing trouble for those around me, I cannot express how much I appreciated their understandings. Here, I want to express my sincere gratitude to all those who supported me, encouraged me and walked along.

First and foremost is my thesis supervisor Dr. Chen Liang. I think I was probably the most challenging student you have ever had. I never knew that I have such a sensitive personality and a weak heart until I started my graduate program. I was easily defeated by failures, discouraged by criticism, and often lost in my thoughts. You were the high-efficiency flashlight that showed me the way out. Without you lighting up the environment, I would never find anything in the darkness. As a supervisor, you not only did your best to help me with my project; the thing I appreciate the most is your care for the mental health of the student. Everyone would agree that Ph.D. training is very stressful. Especially to me, I developed many anxiety issues to the point they affected the efficiency of my work and the quality of my life. You don't know how big of a deal it meant to me when you showed an understanding of the problems I had. The amount of effort and care you put in to support my mental wellbeing is something I will remember forever.

I would also like to thank my Ph.D. advisory committee members, Dr. Anne Gatignol, Dr. Miltiadis Paliouras and Dr. Andrés Finzi, for their insightful comments, constructive feedbacks and scientific advice to my project.

Of course, I cannot talk about my Ph.D. journey without mentioning my "bestie" Saina Beitari. I will never forget that time Dr. Liang called us best friend, you nodded, and I shook my head. We started our degrees at the same time and have spent the past six years growing up together. I will not forget your morning greeting, and you probably will remember my unhappy morning face. I will always remember how we both only wrote our names on the abstracts the first time attending a conference. We were shy, we had fun, we argued, we made mistakes, and we learnt. My Ph.D. life would be so much less colourful without you. Your tolerance to my never-ending anxiety, encouragement when I was sad, and comfort when I was distressed are all I always feel thankful.

Most of the help I received on experimental techniques was from our lab's mother, Qinghua Pan, and our lab's big sister Dr. Zhen Wang. There were times I acted childish and upset Qinghua, but she helped me immediately after that, nonetheless. I always look up to you for your mature personality and warm motherhood. The late-night accompanies of Zhen was comforting and made me feel safe and happy. As the only post-doc in our lab, you were easy to talk to and ask for help. Whenever something went wrong, you never blamed the surroundings but calmly looked for solutions. You were also very caring to me outside of work when we lived in the same building. Thank you for the fruits!

Our previous master student Kavita, I enjoyed having lunch with you. Your extraordinary patience saved me countless times when I was in panic mode. Thank you for accompanying me during those two years. Myles, it impressed me a lot that you always express your opinions in an easy to accept way. I'm not sure whether I can do the same, but I will work toward it. Thank you for proofreading the résumé of my thesis! The previous lab members, Dr. Shilei Ding, Dr.

Zhenlong Liu, and Jin Qian, provided mentorship. I'm grateful that we had a chance to interact at some point in our lives.

The members of McGill AIDS Center, Cesar, Maureen, Ilinca; thank you all very much for maintaining the BSL-3 facility and fun lunchtime conversation. Many thanks to the Lady Davis Institute for providing me with a supportive and warm environment to complete my training. A lot of thanks to Christian Young, the manager of the flow cytometry facility. Your help was precious, especially in times I could not find my cell population. I would also want to express my gratitude to the administrative staff of LDI and the Division of Experimental Medicine, who helped me with all the administrative issues. Last but not least, I appreciate McGill University and the funding agencies for providing me with this valuable experience.

Chapter I: Introduction

1.1 History and epidemiology of HIV

1.1.1 Discovery of HIV

In 1981, several intravenous drug users and homosexual men were admitted into hospitals in the U.S. due to severe opportunistic infections, including *pneumocystis carinii* pneumonia and mucosal candidiasis, which are two rare illnesses that often occur in immunosuppressed people [1,2]. In the subsequent months, some of these patients further developed Kaposi's sarcoma, cancer which rarely occurs in individuals with intact immune systems [1]. The United States Centers of Disease Control and Prevention (CDC) immediately announced the outbreak of this immunodeficiency disease of unknown causes in 1981. Later in 1982, the disease was given its current name - Acquired Immunodeficiency Syndrome (AIDS) [2-5]. Scientists from France and the U.S. independently isolated the etiological agent of AIDS, and the results were published in the same issue of *Science* in 1983 [6,7]. The French group, led by Dr. Luc Montagnier from Pasteur Institute, named the virus lymphadenopathy-associated virus (LAV), while the U.S. group, led by Dr. Robert Gallo from the National Cancer Institute, found the similarity of the virus causing AIDS to Human T-lymphotropic Virus (HTLV), and thus gave the name HTLV-III [6,7]. The name Human Immunodeficiency Virus (HIV) was officially designated to replace LAV and HTLV-III in 1986 [8].

1.1.2 Epidemiology of HIV

According to a report by the United Nations Programme on HIV/AIDS (UNAID), 37.9 million people were estimated to be living with HIV in 2018. Among the infected people, 23.3 million people were receiving antiretroviral treatment as of 2018, around 1.7 million were newly

infected, and 0.77 million died from AIDS-related diseases. With the increased availability of combination antiretroviral therapy (cART), HIV-infected individuals live longer, which also contributes to the increasing number of infected people worldwide. The disease is most prevalent in Sub-Saharan Africa, where 70% of total infected people and 66% of total newly infected people reside [9-11]. By 2018, 62% of total infected people had access to cART, which led to a 33% drop in AIDS-related deaths compared to 2010. The Middle East and North Africa remain the least affected regions, with only 0.6% of the global cases. The primary transmission mode of HIV in Sub-Saharan Africa is through unprotected heterosexual intercourse, whereas in Eastern Europe, Central Asia, the Middle East, North Africa, East Asia, and the Pacific regions, major routes of HIV transmission also include needle sharing during intravenous drug use, unprotected intercourse of sex workers, and unprotected homosexual intercourse. Thus, increases in drug abuse, low treatment coverage (<20%), and lack of protection during intercourse contribute to increased HIV infections in these regions [9-12].

Despite the lack of a cure for HIV, great effort has been made to increase the accessibility of cART to prevent the spread of HIV, which has had a remarkable impact on the HIV epidemic [10]. Compared to 2000, the percentage of newly infected HIV patients has decreased by 35% in adults and 58% in children. 73% of pregnant women infected with HIV received antiretroviral medicine, which effectively prevents the vertical transmission of HIV to the newborn. Moreover, 40% of the total infected population is covered by cART, a significant increase from 17.8% in 2009. It has been estimated that 30 million potential infections and 7.8 million AIDS-related deaths have been averted since 2000 [9,10]. As a part of the sustainable development goals (SDGs), UNAIDS is determined to end the AIDS epidemic by 2030. In order to attain this goal, UNAIDS has developed the Fast-Track approach, which aims to reach, by 2020, 90% of infected people

aware of their status, 90% of HIV-positive people with access to the antiretroviral therapy, and 90% of patients on the treatment to maintain suppressed viral load [9,10]. Although the disease symptoms and viral load can be suppressed by cART, infected individuals still harbour HIV reservoirs. If HIV develops resistant mutations to the current drug therapy or if drug therapy is unavailable, HIV-positive patients could potentially transmit HIV to others. Therefore, HIV still poses a tremendous danger to the wellbeing of people worldwide. Continuous international collaborations in disease prevention and sustained research efforts towards finding a cure to HIV/AIDs are still desperately needed.

1.2 HIV pathogenesis

1.2.1 Routes of HIV transmission

HIV transmission results from direct contact with an infected individual's bodily fluids, including blood, pre-seminal fluids, semen, rectal fluids, vaginal fluids, and breast milk [12-14]. Hence, the primary sources of HIV transmission are unprotected anal or vaginal sexual intercourse, mother-to-infant vertical transmission during pregnancy, labour or breastfeeding, needle sharing among intravenous drug users, blood transfusions, and organ transplantation. The last two transmission routes are extremely rare now in developed countries due to rigorous HIV screening of donated blood and organs. Other bodily fluids such as saliva, tears, and sweat do not harbour HIV unless the blood of the infected individual is present in these fluids. Therefore, close contact with the infected people through hugging, shaking hands, and sharing dishes and washrooms do not lead to new infections as long as both uninfected and infected individuals have intact skin. Although HIV is present in the blood of infected individuals, insect bites from mosquitoes and ticks do not transmit HIV [13].

1.2.2 Disease progression of HIV infection

HIV infection often initiates from a single virus called transmitted founder virus (TFV) [15]. Once the infection is established, there are four sequential phases of disease progression: Eclipse phase, acute phase, clinical latency phase, and AIDS phase (Fig. 1) [16]. The eclipse phase occurs 1 to 2 weeks after the initial infection. The patients remain asymptomatic with no detectable viral level or any immune response, however, the viruses replicate and circulate in the patient, searching for new tissues and organs to infect [16]. The acute phase is marked by a surge of viral load (up to 10^7 copies of HIV RNA/ml plasma) and arises 2 to 4 weeks after infection [16]. The viremia is likely the combined result of a slow initial immune response and an increase in activated CD4+ T cells in the later phase of the immune response. A radical decrease of blood, lymph node, and gastrointestinal CD4+ lymphocytes due to HIV infection can be observed, often with the concurrent manifestation of flu-like symptoms [16-20]. The CD4+ T cells start to be quickly depleted by the exponentially increasing virus [16]. The adaptive immune responses, including anti-HIV antibodies and the CD8+ T cell response, begin to mount around the peak of viremia, which helps to control the viral load and restores the blood's CD4+ T cell levels [16]. The HIV infection is then controlled by the adaptive immunity at the cost of the CD4+ T cell reservoir [16,18]. During the following 1~20 years, HIV infection lapses to the chronic state, the patient may not show much noticeable clinical manifestation. The viral load stays constant or gradually increases during this period, and a large amount of CD4+ T cells are killed directly by HIV and the bystander effect [16,21]. When the CD4+ T cell count decreases below 200 cells/ml, the immune system becomes so severely compromised that the viremia of HIV, the adventitious pathogens, and the cancerous cells go out of the control [16,18]. The infected individual eventually dies of HIV-related diseases such as tuberculosis, pneumonia and Kaposi's sarcoma [1,2,4,18]. HIV

also evades the blood-brain barrier and the kidney and causes dementia and nephropathy [22-24]. In general, an untreated HIV infection is almost uniformly lethal, with more than a 95% mortality rate [16].

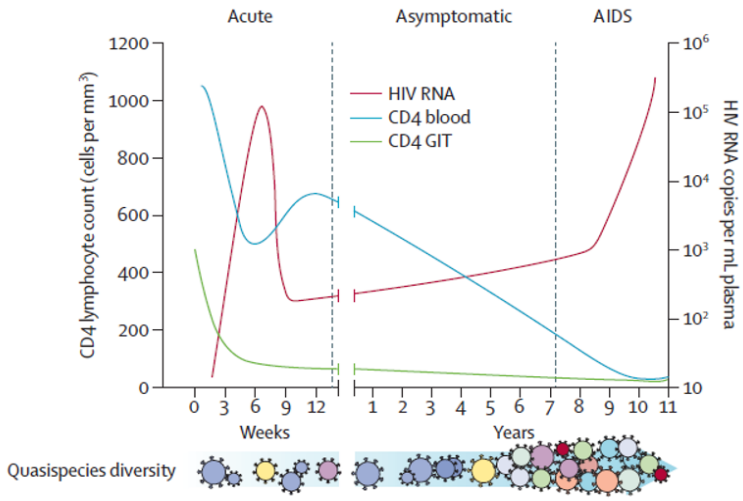

Figure 1: Disease progression of HIV infection [21]. The left y-axis represents CD4 lymphocytes count for the CD4 blood (blue line) and CD4 GIT (green line). The right y-axis represents HIV RNA copies/ml in plasma (red line). The x-axis shows the time after HIV infection, and the image at the bottom demonstrate an increase of HIV quasispecies over time [21].

1.3 Virology of HIV

1.3.1 HIV classification, origin and distribution

HIV belongs to the family of retroviruses [6,7]. The hallmark of a retrovirus is the reverse transcription of viral RNA into DNA, which is subsequently integrated into the host DNA genome [25-27]. There are two groups of retroviruses that are separated by the complexity of the genome: simple retroviruses which encode viral genes *gag*, *pol,* and *env*; and complex retroviruses which carry additional regulatory and accessory genes, such as *nef*, *rev*, *tat*, *vpu*, *vpr*, *vif,* and *vpx* [28]. Lentivirus is one of the genera in the category of the complex retrovirus, to which HIV, simian immunodeficiency virus (SIV) and other immunodeficiency viruses belong [29]. Two

types of HIV have been discovered, HIV-1 and HIV-2, which result from independent zoonotic transmission events of SIV from non-human primates [6,7,30-32].

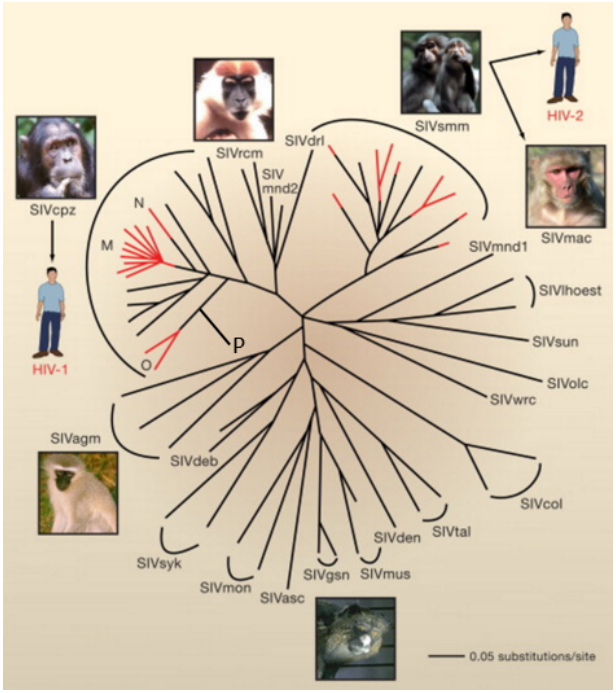

Figure 2: Phylogenetic analysis of HIV-1, HIV-2 and SIV (Adapted from Ho and Bieniasz, 2008) [33-35]. HIV-1 is the result of SIV transmission from chimpanzee to human. HIV-2 arose from SIV_{smm} transmission from sooty mangabey to humans.

The three groups of HIV-1, group M (main), group N (non-M, non-O), and group O (outlier), arose from three independent cross-species transmissions of SIVcpz circulating in chimpanzees, in particular, the *Pan troglodytes troglodytes* (*P. t. troglodytes*) from Central Africa (Figure 2) [32,36-39]. Group M accounts for the majority of HIV infections worldwide and can be further divided into nine subtypes: clade A, B, C, D, F, G, H, J and K [40-45]. The geographic distribution of each clade varies significantly (Figure 3). Clade B is the most prevalent strain in North America, South America and Europe, whereas Clade C is the dominant form in South Africa, East Africa, Southeast Asia, and Australia [31]. Central Africa is the epicenter of the global HIV epidemic, and also has a mixture of different HIV-1 strains [31]. HIV infection by Group N is confined to Cameroon, with only 14 infections identified as of 2010 and an estimated prevalence of 0.1% [46,47]. Group O infections are primarily found in Cameroon,

Gabon, and Equatorial Guinea, with low and stable prevalence [48,49]. Recently, an HIV-1 strain distinct from the previously discovered HIV-1 groups was identified in a Cameroonian woman living in France. The SIV circulating in gorillas (*Gorilla gorilla gorilla*), SIVgor, is the likely source of this new HIV-1 strain. Despite the rare incidence of infection by this new strain (0.06%), it is enough distant from the other circulating HIV-1 groups and has been designated as group P [31,34,35].

HIV-2 entered into humans via a cross-species transmission of SIVsmm from Sooty mangabey, namely *Cercocebus torquatus atys*. HIV-2 infections are primarily confined to West Africa [50,51]. There are eight subgroups of HIV-2, consisting of the epidemic groups (A and B), responsible for the epidemics in West Africa, and the non-epidemic groups (C, D, E, F, G and H), responsible for only a few reported infections. As of 2005, only one infected individual had been identified for each of the non-epidemic groups [50-58]. In addition to the difference in geographic distribution, HIV-2 also differs from HIV-1 in the natural course of disease progression [59]. The heterosexual and vertical transmission rates of HIV-2 are lower compared to HIV-1 [60,61]. Only groups A and B demonstrate some evidence of human transmission, whereas groups C to H failed to establish a chain of human infection [53,62]. HIV-2 infection has also been shown to exhibit longer latency in infected individuals and lower viral load, leading to slower disease progression, a lower rate of developing AIDS, and longer life expectancy than the HIV-1infection [60,63,64].

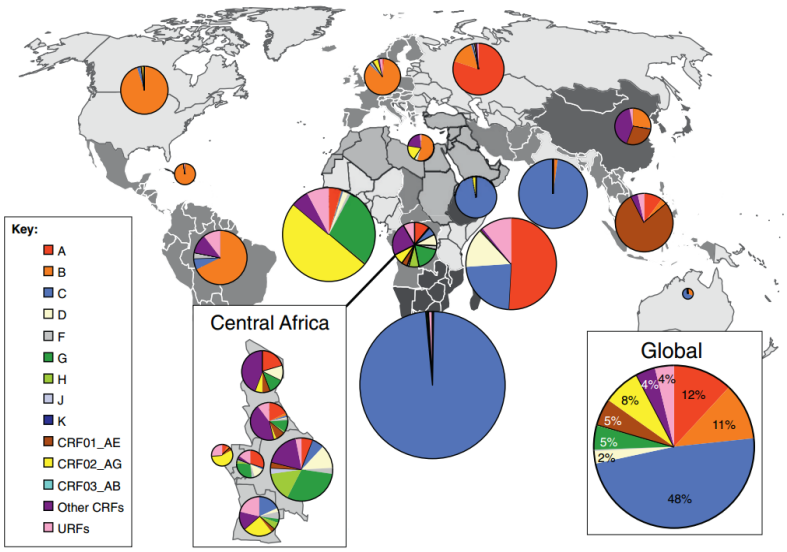

Figure 3: Global distribution of different subtypes and recombinant HIV-1 [31,65]. Clade A, B and C of HIV-1 accounts for almost three-quarters of HIV infection globally. The dominance of subgroups of HIV-1 differs geographically. For example, clade B dominates HIV-1 infection in North America, South America and Western Europe.

1.3.2 HIV genome and its structure

The HIV genome is about 9 kb long with two long terminal repeats (LTR) at both ends flanking nine genes that encode fifteen structural, regulatory, and accessory proteins (Figure 4) [66-69]. LTRs have a critical role in virus integration, as well as viral gene expression [70]. HIV-1 has three structural genes, including group-specific antigen (*gag*), polymerase (*pol*) and envelope (*env*) [69]. The structural proteins that form the viral core, specifically, matrix (MA or p17), capsid (CA or p24), and nucleocapsid (NC or p7), are encoded in the *gag* gene [66,67,69]. Two spacer sequences, spacer peptide 1 (SP1) and spacer peptide 2 (SP2), separate CA from NC and NC from p6, respectively; they play important roles in regulating virion assembly and capsid maturation [71-74]. The p6 peptide serves as the docking site for cellular factors that aid HIV budding [75,76]. The *pol* gene contains all the enzymes required for HIV replication, including

protease (PR), reverse transcriptase (RT), and integrase (IN) [66-69]. The virus envelope glycoprotein (Env), comprising the surface subunit (SU/gp120) and the transmembrane subunit (TM/gp41), is encoded by *env* [66-69]. In addition to the structural genes, HIV-1 also has two regulatory genes, transactivator of transcription (*tat*) and regulator of expression of virion (*rev*), which are essential for virus gene expression [68,77-82]. There are also four accessory genes, viral infectivity factor (*vif*), viral protein unique (*vpu*), viral protein R (*vpr*), and negative regulatory factor (*nef*). They assist HIV replication and modulate HIV pathogenesis *in vivo* [67,83-86]. The genomic structure of HIV-2 is similar to HIV-1 except that HIV-2 encodes the viral protein X (*vpx*) instead of *vpu* in HIV-1[66,68].

HIV is a spherically enveloped virus with an average diameter of 100 nm. The virus envelope originates from the host cell lipid bilayer and has about 10 Env glycoprotein trimers inserted in each virion. Each Env glycoprotein has the gp41 domain non-covalently linked to the gp120 domain facing the exterior surface of the envelope [87,88]. Three Env molecules form a trimer. The inner surface of the virus membrane is lined by MA, and the conical-shaped viral capsid core is located at the center of the virus particles. The core is constructed by ~ 250 CA hexamers and 12 CA pentamers. The HIV RNA genome is packed within the core as dimeric ssRNA protected by the NC proteins [87, 89,90]. Other viral proteins, including PR, RT, IN, Vpr, Vif and Nef are all incorporated into HIV particles [88]. The early gene products Tat and Rev are not found in HIV particles [88]. Vpu, the viral accessory protein that regulates the CD4 receptor and assists the release of newly formed HIV particles, does not get into HIV particles as well [91].

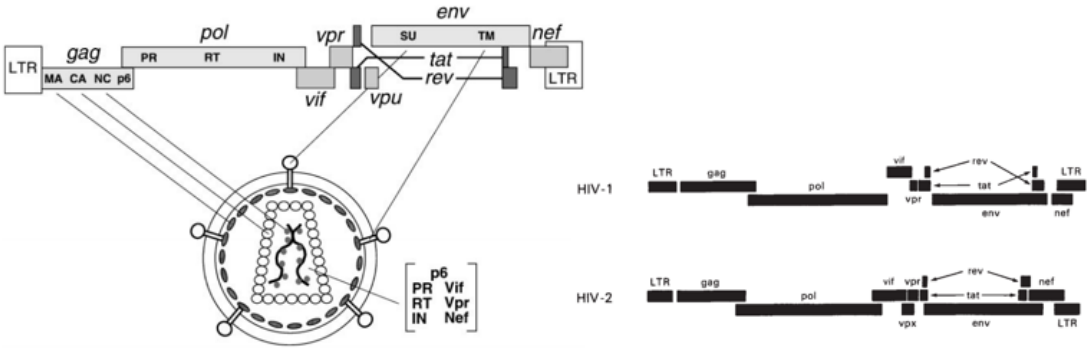

Figure 4: HIV genome and its virion structure [67,68]. The left illustrates the HIV-1 genome and the virion structure. The right depicts the difference between HIV-1 and HIV-2 genomes.

1.4 HIV replication cycle

In order to discover the efficient way of combatting HIV infection, it is critical to understand how the virus replicates in the host cells. Therefore, in the following section, I will introduce what we know about the HIV life cycle in detail.

1.4.1 HIV entry

HIV entry can be divided into four phases: non-specific interaction, CD4-gp120 binding, coreceptor-gp120 binding, and membrane fusion [92] (Fig. 5). The initial HIV attachment to the host cells can be mediated by the interaction between the viral Env protein with the non-specific host membrane proteins, such as negatively charged cell surface heparan sulfate proteoglycans [93], or by interacting specifically with cellular proteins, such as α4β7 integrin [94,95] and dendritic cell-specific intercellular adhesion molecular 3-grabbing non-integrin (DC-SIGN) [96]. In vitro, this attachment of the virus to the host cells via non-specific or specific mechanisms can bring Env proteins to proximity and augment the efficiency of Env-CD4 binding [97].

The second step – Env-CD4 binding – is absolutely required for HIV to enter the target cells and establish infection [98-100]. The Env spikes exist as a trimer of a heterodimer gp120-gp41. It has been reported that 1 to 8 Env spikes are required for a successful entry [101]. Gp120 is composed of 5 conserved domains (C1-C5) and 5 variable loops (V1-V5). The conserved domains are important in CD4 binding, and the V3 loop is the determinant element of the virus co-receptor tropism [102-106]. The binding of gp120 to CD4 causes a conformational change in gp120, leading to the exposure of the V3 loop via the rearrangement of the V1/V2 loops [107].

There are two co-receptors that HIV uses for entry, C-C chemokine receptor type 5 (CCR5 or R5) and C-X-C chemokine receptor type 4 (CXCR4 or X4) [108-112]. HIV that exclusively uses CCR5 is called R5 tropic, and similarly, HIV using CXCR4 for entry is called X4 tropic. A separate class is called R5X4 dual tropic because they use both CCR5 and CXCR4 as co-receptors [113]. Following the binding to both CD4 and the co-receptor, HIV is often observed to highjack the cellular transport machinery, and "surf" on the cellular membrane to the specific destination where the entry can be most efficiently carried out [114,115].

The binding of the co-receptor exposes the hydrophobic fusion peptide at the N-terminus of gp41, which is then inserted into the cell membrane [116,117]. The hinge of gp41 fusion peptide starts to fold and brings the N-terminus and C-terminus of gp41 closer together to form a 6-helix bundle [116,117]. Since the C-terminus of gp41 is the transmembrane domain incorporated in the virion membrane, the membrane of the target cell and the viral membrane can be brought to proximity, allowing hemifusion formation [118]. Subsequently, the fusion pore is formed between the virus and the cell membrane, resulting in the release of the virus core into the cytoplasm.

HIV fusion is pH-independent, as Env protein is sufficient to mediate the virus-cell fusion [119]. However, this property does not imply that HIV enters the cell exclusively at the cell membrane. It has been reported that HIV can also enter cells via endocytosis [120].

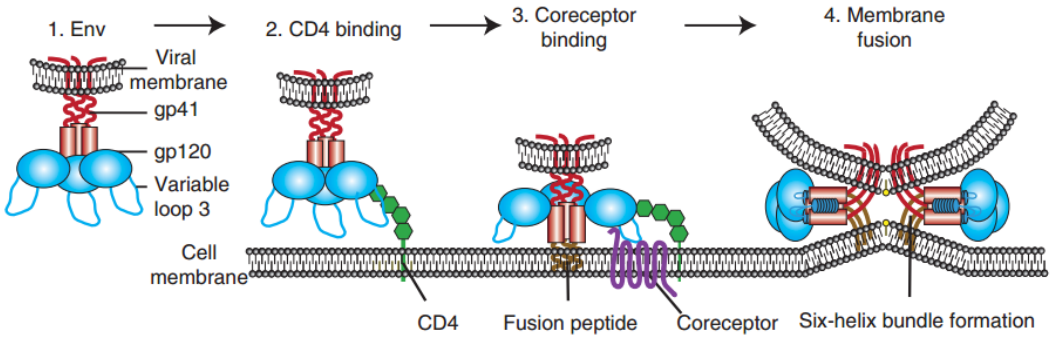

Figure 5: HIV entry [92]. The image illustrates the binding of HIV Env to CD4, and subsequently to CCR5/CXCR4. The conformational rearrangement of HIV Env during receptor binding is also shown.

1.4.2 HIV reverse transcription and integration

Following entry, HIV RT converts viral RNA into DNA [121]. HIV RT possesses two enzymatic activities, the DNA polymerase activity, which can use either RNA or DNA as the template, and the RNase H activity, which exclusively degrades RNA in the context of an RNA/DNA hybrid [122-126].

HIV-1 uses $tRNA^{Lys3}$ as the primer to bind to the primer binding site (PBS) located about 180 nucleotides away from the 5' end of HIV-1 RNA (Fig. 6). After adding 5 to 6 nucleotides to the 3' end of the primer, the speed of polymerization increases [127,128]. As the RT catalyzes the synthesis of viral DNA, the RNA/DNA hybrid serves as the substrate for the RNase H activity of the RT, which results in the degradation of the RNA and leaves the single-stranded DNA (ssDNA) intact [125,129,130]. The newly synthesized (-)ssDNA then hybridizes to the direct repeat (R) at the 3' end of the viral RNA, termed the first template switch. This (-)ssDNA serves as the

primer for RT to continue to copy viral RNA into DNA. Since each HIV particle carries two copies of genomic RNA, this first template switch can occur either in *cis* or *trans*, which accounts for the high recombination rate of HIV [125,131-134]. Along with reverse transcription, viral RNA is degraded except for the purine-rich polypurine tract (PPT) sequence, which serves as the primer for synthesizing the plus strand of viral DNA [125,129,130]. HIV-1 has two PPT sequences, with one located near the 3' end, which is essential for virus replication, and the other is located in the middle, which contributes to a more efficient synthesis of dsDNA [135,136]. The synthesis of (+)DNA proceeds until the first 18 nt of $tRNA^{Lys3}$ is copied [137,138-140]. This 18nt DNA then reanneals to the PBS, allowing the continuous synthesis of (+)DNA; this is called the second template switch.

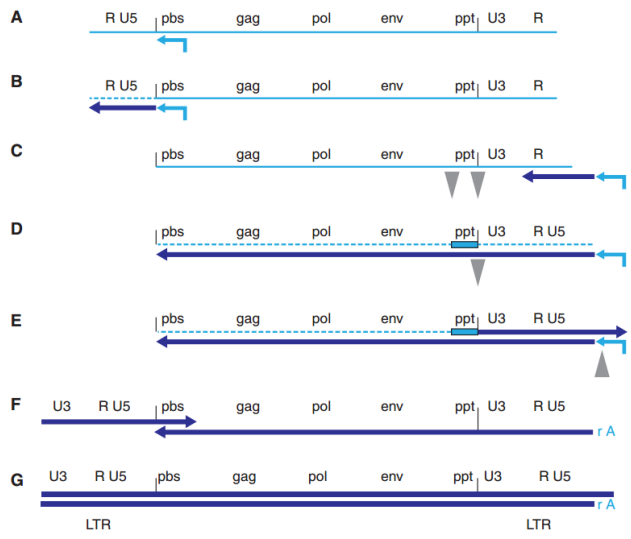

Figure 6: Reverse transcription of HIV genome [121]. This cartoon illustrates the process of reverse transcription of HIV RNA to DNA. The sequence of polymerization and strand transfers are depicted in the order from A to G.

In vivo, reverse transcription occurs in the reverse transcription complex (RTC), composed of MA, CA, NC, IN, and Vpr [141-143]. There are two hypotheses explaining the process of uncoating, which involves the conversion of the core structure to RTC, and eventually, to the pre-integration complex (PIC). The first set of evidence suggests a slow and continuous change of RTC to PIC, while reverse transcription proceeds [144,145]. The second hypothesis, which has been supported by many lines of evidence, proposes that RTCs have a "core-like" structure, in which reverse transcription occurs [146-156]. The core-like structure is transported to the perinuclear region and is converted into PIC before nuclear import.

Following reverse transcription, the newly synthesized viral DNA becomes tightly associated with IN and other high-molecular-weight nucleoproteins, forming PIC [157]. Due to its size (50 nm), PIC is imported into the cell nucleus with the help of nuclear transport receptors [158]. While the exact mechanism of PIC nuclear import has not been elucidated, MA, CA, IN, and the DNA flap are essential for this process. The nuclear pore proteins, such as Nup358 and the nuclear transport receptor Transportin-3, also participate in the PIC nuclear import. Therefore, both viral and cellular factors contribute to PIC nuclear import.

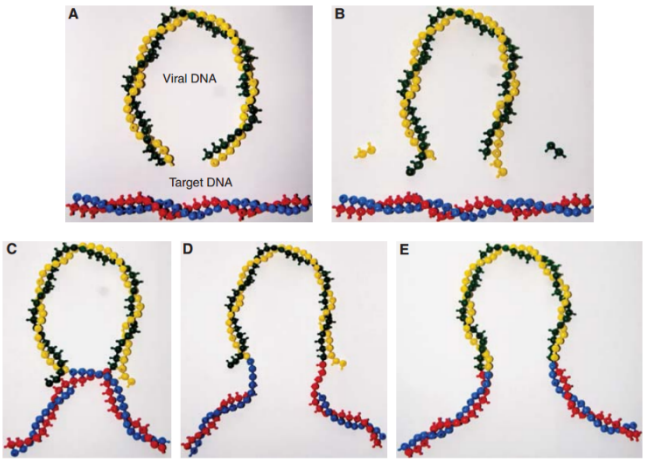

Figure 7: Integration of HIV DNA into the host DNA [159]. The illustrations depict the process of HIV DNA integration in the host DNA. The black and yellow strings of beads represent the dsDNA of HIV, and the blue and red strings of beads represent the host cell DNA.

Once entering the nucleus, HIV DNA is integrated into cellular DNA by viral IN [159-161]. The integration process is initiated by 3' end processing, in which the last two nucleotides are cleaved, leaving CA-3' conserved sequences at both ends (Fig. 7B). The 3' ends of the viral DNA attack the phosphodiester bound on the opposite strand of the target DNA in major grooves separated by 5 nucleotides, which form two covalent bonds with the target DNA. The single-strand break introduced by the viral DNA attack and the 5' two nucleotides overhanging on the viral DNA is subsequently repaired by the cellular DNA repair machinery, which marks the completion of integration.

The preferential site of integration has been intensively studied. It has been revealed that host DNA wrapped in nucleosomes is favoured by viral DNA integration both *in vitro* and *in vivo* [162-165]. In particular, distortion of the DNA structure, including the sharp DNA kink in the nucleosomes, likely facilitates viral DNA integration by lowering the activation energy [159,162,166-168]. The mapping of HIV integration sites in acute infections of many cell types in several whole genome-wide studies has further revealed that HIV strongly prefers transcription active sites [165,169-174]. The genetic features associated with HIV-1 insertion sites include the G/C content, DNase I cleavage density, and gene density, which are also characteristics of euchromatin [165,170]. The site-specificity of integration is affected by the types of IN. For example, the substitution of HIV IN with MLV IN alters the pattern of preferred sites of insertion [175]. In addition, the lens epithelium-derived growth factor (LEDGF/p75) is of particular importance in aiding site selection and in enhancing integration efficiency [176-179]. The N-terminus of LEDGF/p75 preferentially binds to euchromatins, and the C-terminus binds tightly to IN, which thereby tethers IN to euchromatin [180-184]. LEDGF/p75 can also boost integration efficiency by preventing the formation of 2-LTR circles, which is the form of a viral genome that cannot be integrated

into the host genome [185]. Recently, the host chromatin architecture has been proposed to determine the site of integration [186]. HIV-1 PIC preferentially attacks euchromatin that is located 1μm beneath the nuclear envelope near the nuclear pores [186]. Therefore, viral proteins and cellular factors together cooperate to accomplish HIV DNA integration.

1.4.3 HIV gene expression

The integrated HIV DNA contains its transcriptional promoter, LTR [187]. LTR consists of multiple DNA regulatory elements, including three tandem SP1 binding sites, an efficient TATA element, and a highly active initiator sequence that cooperatively recruits cellular transcription factors such as TFIID and TAF [188-191]. The viral proteins are produced sequentially and can be largely divided into two groups: viral proteins (Tat, Rev and Nef) that are produced from completely spliced transcripts, and those that are produced from incompletely spliced or unspliced transcripts (Fig. 8) [192,193].

Transcription from HIV-1 LTR is hindered by some cellular factors, namely the negative elongation factor (NELF-E) [194-196]. Therefore, the initial synthesis of viral genes can be inefficient. However, HIV Tat protein strongly stimulates transcription from HIV LTR, resulting in a positive feedback circuit [197]. If the level of Tat cannot reach the threshold due to the closure of the chromatin or other reasons, the transcription efficiency of the viral genes remains low, eventually leading to latency [198,199].

Tat accelerates transcriptional elongation by binding to the transactivation-response region (TAR) [80,81,200]. TAR is located downstream of the transcription initiation site and functions as a RNA regulatory signal with a nuclease-resistant stem-loop secondary structure [80,81,201,202]. The position at the 3' end of the promoter, the orientation of the sequence, and the secondary structures formed have been shown critical for the functionality of TAR [79,201,202]. Tat

binds to the uridine (U)-rich bulge near the apex of the TAR RNA stem [203,204]. The TAR RNA apical loop and the Tat protein together recruit cellular factors such as cyclin-dependent kinase 9 (CDK9) and Cyclin T1 (CycT1), which are components of a ubiquitous positive acting elongation factor P-TEFb [205-210]. Tat binding to CDK9 activates the kinase activity of P-TEFb, which subsequently phosphorylates cellular elongation factors [209,211,212]. NELF-E at its unphosphorylated state binds to TAR and blocks the movement of the elongation complex [194-196]. The activated P-TEFb phosphorylates NELF-E, which results in its detachment from TAR and removes the steric hindrance [213]. Tat:P-TEFb also hyper-phosphorylates the C-terminal repeats of Spt5, which are subunits of the 5,6-dichloro-1-beta-D-ribofuranosylbenzimidazole (DRB) sensitivity inducing factor (DSIF) [214,215]. While unphosphorylated DSIF serves as an elongation inhibitor, the phosphorylation of Spt5 converts DSIF into a transcription activator, which positively affects the elongation and stabilizes the transcription complex on the template [214,216,217]. Furthermore, Tat:P-TEFb hyper-phosphorylates the C-terminal domain (CTD) of the RNA polymerase II (Pol II) to enhance its polymerization efficiency [211,218].

HIV-1 RNA has 4 splice donors and 8 splice acceptors, which allow the production of more than 40 different viral mRNA variants. The incompletely spliced mRNA encodes for viral structural proteins and enzymes. However, the nuclear export of incompletely processed mRNA is prevented by cellular mechanisms. The primary role of Rev is to help the incompletely spliced or unspliced viral mRNA to circumvent the cellular surveillance system and be exported out of the nucleus [219]. The arginine-rich domain (ARD) of Rev binds to the viral mRNA at the Rev-response element (RRE), a highly structured 351-nucleotide long RNA stem-loop located in the *env* gene [220-223]. The initial Rev binding to the high-affinity site at the apex of RRE leads to the cooperative binding of additional Rev monomers, resulting in the oligomerization of Rev along

with the mRNA transcript [221,224-227]. The karyopherin family member Crm1, also known as exportin 1, interacts with a 10-amino acid leucine-rich nuclear export signal (NES) near the C-terminus of Rev in the presence of GTP-bound Ran GTPase. The cargo is then exported out of the nucleus through the nuclear pores. In the cytoplasm, Ran GTPase hydrolyzes GTP with the aid of Ran GTPase-activating proteins (GAP) and RanBP1, which causes the dissociation of the Rev complex and releases the viral mRNA [228]. Rev is imported back into the nucleus by binding to the nuclear import factor, importin-β and GDP-bound Ran [229].

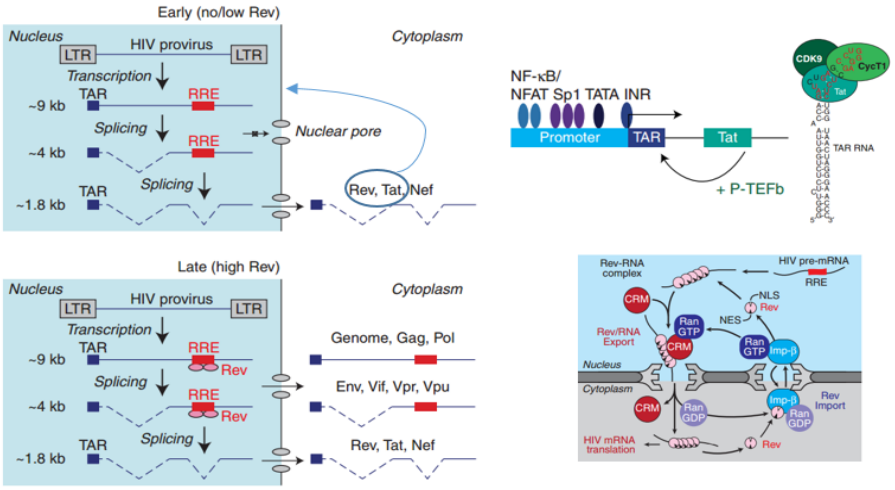

Figure 8: Transcriptional regulation of HIV-1 genome expression (Adapted from [187]). After the successful integration of HIV-1 DNA, Tat, Rev and Nef are produced from the completely spliced viral mRNA. Tat and Rev are imported back to the nucleus. Tat accelerates the rate of HIV-1 gene transcription, and Rev exports unspliced viral mRNA that produces HIV-1 structural proteins and other viral proteins.

As previously mentioned, HIV-1 has a small compact genome encoding many proteins required for its replication. This is achieved by having overlapping open reading frames (ORFs), which allows one RNA sequence to encode several proteins. In order to synthesize the proteins

in different ORFs, programmed frameshifting is used during translation [230,231]. One example of this frameshifting occurs in the *gag-pol* transcript, which is subsequently translated into the Gag or Gag-PR-RT-IN (Gag-Pol) polyproteins. In order to translate the *pol* gene that is located in a different ORF to *gag*, a -1 nt shift is required. The ribosomes move along the mRNA and encounter the heptanucleotide "slippery" sequence (UUUUUUA), located 200 nt upstream of the Gag termination codon. Then the ribosome slips into a stem-loop pseudoknot located adjacent to the 3' end of the heptanucleotide, which results in a -1 frameshift [187,232,233]. The frameshifting events occur at a 5% frequency, accounting for the 1:20 ratio between the produced Gag and the Gag-Pol precursors.

The membrane-associated Env protein is produced in the endoplasmic reticulum (ER) as a gp160 precursor. As the protein is transported outwards from the ER to the Golgi and trans-Golgi, Env becomes heavily glycosylated. gp160 is also cleaved by a cellular proteolytic enzyme, furin, and becomes a gp120/gp41 heterodimer [234-236].

1.4.4 HIV particle assembly, release and maturation

Gag protein plays a central role in HIV assembly [237,238] (Figure 9). The Gag is a 55 kilo Dalton (kDa) polyprotein, encompasses MA, CA, NC and p6. The MA domain is composed of five α-helices, one short 3_{10} helical stretch, and a three-stranded β-sheet, and targets Gag to the membrane [239]. The N-terminus of MA is covalently attached to a myristic acid moiety, which can be exposed following the electronic interaction of MA with a negatively-charged inositol head group of the phosphoinositide phosphatidylinositol-4,5-bisphosphate (PtdIns(4,5)P2), thereby facilitating its insertion into the membrane [240-242]. The Gag is often targeted to lipid raft and can also induce the coalescence of lipid raft in the virus assembly region [243]. The NC domain drives the packaging of viral genomic RNA dimers. NC is a nucleic acid chaperon, composed of two

zinc-finger-like domains that mediate the binding to viral RNA packaging signal sequence (Ψ) [244,245]. Viral RNA dimers can be actively recruited to the membrane by Gag and/or passive diffusion [246-248]. Following arrival to the plasma membrane, Gag multimerizes radially around the Gag-RNA center to generate the continuous hexameric lattice [247,249-252]. The multimerization of Gag is promoted by the CA domain, which has a N-terminal domain (NTD) and a C-terminal domain (CTD) separated by a flexible linker [253,254]. The proline-rich loop of CA NTD binds to host peptidyl isomerase cyclophilin A (CypA), contributing to the viral evasion of the host immune system [253,254]. The CA CTD mediates the multimerization of Gag [254,255]. Gag-Pol is recruited into the virion via the CA-mediated Gag multimerization. The mechanism of Env recruitment remains inconclusive. However, there are four non-exclusive theories proposed to explain the membrane targeting of Env: (1) passive transport by the cellular mechanism; (2) co-targeting of Gag and Env to the lipid raft microdomain; (3) direct recruitment by Gag; and (4) cooperative recruitment by Gag and cellular bridging proteins [256]. Several studies suggest an essential role of the direct or indirect interaction between the MA domain of Gag and the C-terminal tail of gp41 in the recruitment of Env to the assembly site [256,257]. In support of this mechanism, MA trimer formation has been shown to be important in recruiting Env to the virion [258].

Following the assembly of viral proteins, the membrane must undergo fission to release the HIV particle. The unstructured small p6 peptide domain at the C-terminal of Gag drives virion budding by hijacking the host endosomal sorting complex required for transport (ESCRT), which promotes the membrane scission [75,259,260]. There are two ESCRT recruiting motifs, P(T/S)AP and YPXL, in p6 [261,262]. P(T/S)AP directly interacts with a subunit of ESCRT-1 called tumour susceptibility gene 101 (TSG101), which has a dominant role in recruiting the ESCRT

machinery [263-266]. The second motif YPXL binds to ALG-interacting protein X (ALIX), which is an adaptor protein involved in ESCRT III-mediated membrane remodelling [261]. ESCRT III assembles to form a circular array or spiral at the neck of the budding vesicle and pinches the vesicle off with the energy supplied by vacuolar protein sorting 4 (VPS4) [267-269].

The maturation of the viral particle is characterized by the sequential processing of the Gag and Gag-Pol precursor by the dimeric aspartyl protease PR [74,270]. The cleavage of Gag releases individual MA, CA and NC proteins, which results in significant morphological rearrangement of HIV particle. The liberated MA forms a hexamer of its trimer underneath the lipid bilayer, CA forms hexamers and 12 pentamers to produce a fullerene-like conical-shaped closed-end viral core, while NC coats the viral genomic RNA with preferential binding sites in 5'UTR and RRE [251,258,271-274].

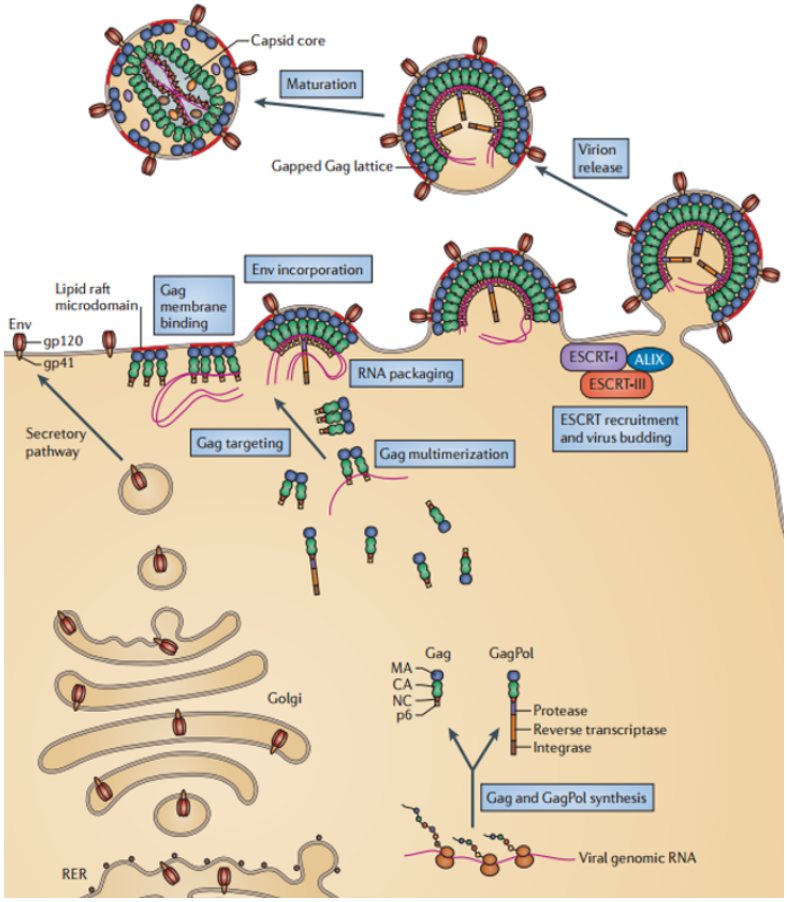

Figure 9: HIV assembly, release and maturation [237]. Gag and Gag-Pol assemble at the lipid raft of the plasma membrane together with Env. The virions bud by deploying cellular endosome fission system ESCRT. The maturation of the HIV virions occurs post-budding, characterized by viral protease cleavage of Gag and Gag-Pol.

1.5 Interferon response against HIV infection

Infection of cells by a pathogen often triggers the recognition of the pathogen-associated molecular patterns (PAMPs) by the cellular pathogen-recognition receptors (PRRs) [275]. For HIV-1 infection, the initial pathogen recognition process mainly occurs in CD4+ immune cells. This leads to the production of interferon (IFN) and other pro-inflammatory cytokines and chemokines, which work together to initiate a cell-intrinsic innate immune response and to recruit innate immune cells such as macrophages, dendritic cells and natural killer cells (NK cells) to the site of infection [276]. Previous studies have revealed the importance of IFN in establishing an antiviral state in both infected cells and surrounding non-infected cells by activating the interferon-stimulated genes (ISGs) [277,278].

Host cells deploy various mechanisms to inhibit HIV replication. However, HIV also develops mechanisms to evade cellular immunity, including the interference of signal transduction involved in PAMP detection, suppression of IFN production, and direct evasion of restriction factors [275]. There is much evidence suggesting that Vpu and Vpr disrupt the proper induction of IFN and ISGs. Vpu downregulates interferon regulatory transcription factor 3 (IRF3) through lysosome-mediated degradation or the caspase-mediated cleavage, whereas Vpr mediates ubiquitination of IRF3 and directs it to the proteasome for degradation [279-281]. In the dividing cells, Vpr is able to induce G2/M arrest by ectopically activating cellular kinases and the SLX4-MUS81-EME1 protein complex (SLX4com) [282]. Vpr association with SLX4com increases its nuclease activity and degrades the viral DNA accumulated in cells, thus avoiding detection by cellular DNA sensors and immune surveillance [282].

HIV has developed various strategies to counteract host restriction factors, such as mutating the targeted viral proteins to escape recognition [283-285] and using viral proteins to inhibit restriction factors.

1.5.1 Pattern recognition receptor sensing of HIV

Several PRRs have been reported to detect HIV-1 infection. In the early phase of HIV-1 replication, viral DNA is detected by two PRRs, interferon-inducible protein 16 (IFI16) and cyclic GMP-AMP synthase (cGAS) (Figure 10) [286-289]. IFI16 is a member of the PYHIN protein family, which binds to DNA via the hin domain and interacts with proteins through the pyrin domain [290]. IFI16 is expressed in both the nucleus and the cytoplasm. It directly binds to the LTR region of the reversely transcribed DNA products [287,291]. Upon binding to the HIV-1 DNA, IFI16 interacts with the adaptor protein stimulator of interferon genes (STING) and activates the serine/threonine protein kinase 1 (TBK1) and the transcription factors IRF3 and IRF7.

cGAS detects HIV-1 by binding to viral DNA [286]. cGAS is expressed in the cytosol and contains two functional domains, the N-terminal DNA-binding domain and the nucleotidyltransferase domain. After binding to dsDNA, cGAS produces a dinucleotide product cyclic GMP-AMP (cGAMP) [289,292]. cGAMP binds to STING, which subsequently activates TBK1, IRF3 and IRF7 [293]. Therefore, similar to IFI16, cGAS activates the IFN signalling and triggers the innate immune response. In addition, cGAMP can be transferred to the adjacent cells via gap junction, serve as a paracrine signalling agent, and establish the antiviral state in the neighbouring cells [294]. Remarkably, recognition of HIV-1 and HIV-2 by PRRs is differently regulated by host factors. The capsids of HIV-1 and HIV-2 bind to a cellular protein-folding chaperon, CypA, upon entry into the cells [295]. The interaction of CypA with the HIV-1 capsid prevents the detection of viral DNA from PRRs, while the CypA-HIV-2 capsid complex

facilitates the detection of dsDNA through cGAS in the cytosol [296,297]. This differential interaction of CypA-HIV-2 with cGAS may partially explain the less pathogenic nature of HIV-2 infection [296,298].

In addition to IFI16 and cGAS, toll-like receptors (TLRs) have also been reported to detect HIV infection [299]. There are nine members in the TLR family. They share a similar structure, including a transmembrane domain, an extracellular leucine-rich PAMP binding domain, and a cytosolic signal transduction domain [300]. HIV gp120 is recognized by TLR2 and TLR4, which are expressed on the surface of mucosal epithelial cells [301]. Although epithelial cells are not infected by HIV-1, the interaction of gp120 with TLR2 and TLR4 can trigger the production of IFN and other pro-inflammatory cytokines, which creates the antiviral state in the neighbouring HIV target cells. HIV-1 genomic RNA is reported to be recognized by TLR7 and TLR8 in the endosomes [302]. TLR7 and TLR9 are expressed in the major IFN producing cells, plasmacytoid cells (pDCs), at high level [303,304]. Although pDCs are not productively infected by HIV-1, they interact with and sense HIV-1 RNA or DNA by endocytosing HIV-1 particles and HIV-1 infected T cells [305,306]. Upon detecting HIV-1, TLR2 and TLR4 transmit signals using the adaptor proteins TIRAP/MyD88, whereas TLR7 and TL8 use MyD88 only. The signalling cascade eventually leads to the activation of the nuclear factor k-light-chain enhancer of activated B cells (NF-κB). In addition, TLR4 also passes down the signal via another route, in which TRIF/TRAM serves as the adaptor proteins that activate NF-κB via TRAF6, and IRF3 and IRF7 via TBK1 [300,307].

HIV RNA can also be recognized by RIG-I, a cytosolic RNA helicase [308-311]. Activated RIG-I relocates to the mitochondrial associated ER membrane. The caspase activation and recruitment domains (CARDs) of RIG-I interact with adaptor protein mitochondrial antiviral-

signaling protein (MAVS), which initiates the assembly of the signalling complex to activate NF-κB and IRF3/IRF7 [312,313].

Tetherin (also known as BST2 or CD137) is an IFN-induced protein, expresses on the cell surface to prevent the virus from detachment [314-316]. In addition to its prominent role as a restriction factor, tetherin also functions as a PRR [317-319]. Once tetherin is C-terminal linked to a Vpu-defective HIV-1, tetherin starts to cluster on the plasma membrane and detach from the cortical actin cytoskeleton. As a result, the two tyrosine (Y) residues located on the N-terminal cytoplasmic tail are exposed to the tyrosine kinase Syk for phosphorylation. The phosphorylated tetherin recruits the adaptor proteins tumor necrosis factor (TNF) receptor-associated factor 2 and 6 (TRAF2 and TRAF6) and the transforming growth factor beta-activated kinase 1 (TAK1) for activation of NF-κB [317,319]. The activated NF-κB relocates into the nucleus and promotes the expression of proinflammatory C-X-C motif chemokine 10 (CXCL10), IL-6 and type I IFN [317].

The IFN production in response to the PRR activation feeds into a positive feedback loop, where IFN-inducible PRR expression and IRF7 are increased and facilitate the establishment of an antiviral state.

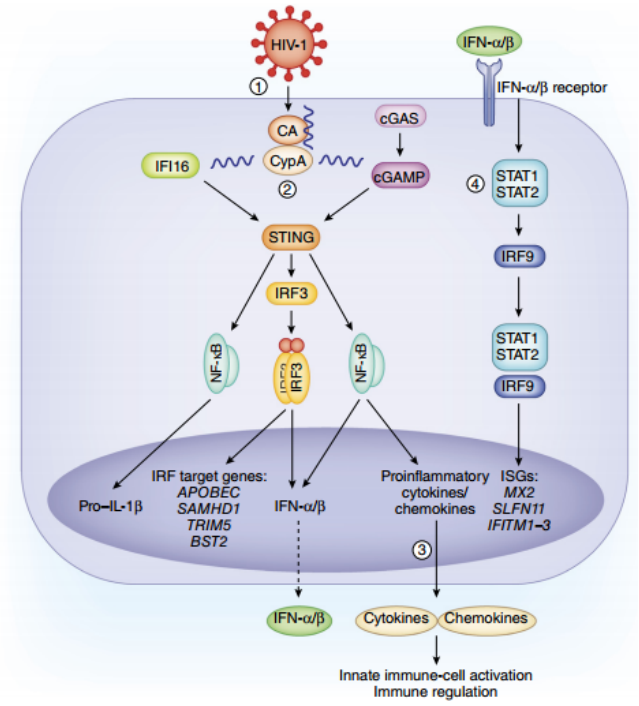

Figure 10: PRR signaling and IFN activation pathway. HIV components are recognized by PRRs, such as IFI16, RIG-I, tetherin and TLRs, triggering the production of IFN.

1.5.2 Restriction of HIV infection by ISGs and viral evasion

PRR signalling pathways converge to the upregulation of inflammatory cytokines and IFNs by activating NF-κB, IRF3 and IRF7 [320]. NF-κB and IRF3 are broadly and constitutively expressed, whereas IRF7 is only constitutively expressed in pDCs, T cells and other immune cells. The expression of IRF7 in most cell types must be induced by IFN [321]. NF-κB is activated by phosphorylation-induced degradation of its inhibitor IκB. IRF3 and IRF7 are activated by TBK1 or IKK-ε protein kinase-mediated phosphorylation of both factors. Activated NF-κB and homo- or heterodimer of IRF3, and/or IRF7 work together to activate the production of IFN-β [322]. The activation of IFN-α transcription only requires IRF3 and IRF7 [322].

IFN is categorized into three families, Type I IFN, Type II IFN, and Type III IFN. There are seven members of IFN in the Type I family, and all members of Type I IFN bind to IFNα receptors 1 and 2 (IFNAR1 and IFNAR2) [323]. Type II IFN binds to IFNGR1 and IFNGR2 receptors, and Type III IFN interacts with IFNLR1 and IL-10R2 receptors. After Type I and III

IFN binding, JAK1 and TYK2 kinases, associated with the receptors, phosphorylate each other for activation, and also phosphorylate the receptors to recruit signal transducers and to activate transcription factors (STAT1 and STAT2). The phosphorylation of STAT1 and STAT2 enables them to dimerize and associate with IRF9, forming an IFN stimulated gene factor 3 complex (ISGF3). In the case of Type II IFN, a homodimer complex IFNγ activation factor (GAF) is formed by the phosphorylated STAT1. Both complexes relocate into the nucleus, bind to the ISRE and GAS DNA motif respectively, and initiate transcription of ISGs. There are 10 ISGs that have been reported to inhibit HVI-1 infection at different steps of viral replication. These include APOBEC3G, TRIM5α, tetherin, SAMHD1, SLFN11, MxB, MARCH8, GBP5, CH25H and IFITMs. In addition to these ISGs, a constitutively expressed protein without IFN inducibility, SERINC5, has also been shown to inhibit HIV-1 infection. The anti-HIV activities of these host proteins will be introduced below.

1.5.2.1 Apolipoprotein B mRNA editing enzyme catalytic polypeptide-like 3G (APOBEC3G)

APOBEC3G, or A3G for short, is one of the seven members from a family of ssDNA deaminase expressed in a wide range of cell types, including CD4+ T cells and macrophages [324-327]. A3G interferes with reverse transcription of HIV-1. It is packed into the virions and manifests its antiviral activity in the subsequent round of infection [325,328]. During HIV-1 assembly at the plasma membrane, A3G interacts with the NC domain of Gag in a non-specific RNA-dependent manner to infiltrate the virions [329,330]. The incorporated A3G catalyzes the deamination of cytosine (C) and changes it to uridine (U) in the minus strand of viral DNA [328]. During reverse transcription, U is read as thymidine (T) by RT, and the newly synthesized DNA carries adenosine (A) instead of guanosine (G) if viral RNA is transcribed faithfully. Thereby,

A3G causes G→A mutations and detrimentally changes the viral genomic sequence by introducing nonsense and missense mutations [328,331]. The frequency of A3G-driven mutations is higher towards the 3' end of HIV-1 DNA due to the prolonged exposure of viral ssDNA to A3G [332]. A3G also preferentially targets the second C of a consecutive CC sequence, leading to a GG→GA mutation that often results in a termination codon (TGA) [333,334]. Consequently, the viral genome is either prematurely degraded in the cytosol or fails to produce viable progenies after being integrated into the host genome. Of note, A3G has been shown to prevent the accumulation of viral cDNA, likely by sterically hindering the elongation of HIV DNA during reverse transcription [335]. Although A3G has been the focus of the APOBEC3 family due to its potent anti-HIV activity, other APOBEC3 members such as A3B, A3D, A4F and A3H have also been shown to inhibit HIV-1 [333,334].

Nonetheless, the anti-HIV-1 activity of A3G is countered by Vif, an HIV-1 accessory protein that induces A3G degradation [336]. Vif directly interacts with APOBEC3G and recruits a cullin5-based E3 ubiquitin ligase-elongin B-elongin C-Rbx-1 complex to polyubiquitinate A3G, which leads to proteasomal degradation [337]. Vif is composed of two domains separated by a zinc-binding motif [338]. The zinc-binding motif of Vif directly binds to cullin5, the suppressor of cytokine signaling (SOCS) box. Cullin5 also interacts with the elongin B and C heterodimer and the discontinuous elements at the N-terminus of Vif, which are involved in recognizing specific species of A3G [339]. Subsequently, Vif recruits an additional cofactor Core Binding Factor β (CBFβ) to the E3 ligase complex and elicits the ubiquitination of A3G [340]. Vif has also been shown to be capable of recognizing A3F and A3H, and induce their degradation [341,342].

Despite the effort of HIV-1 to exclude A3G from the newly produced virions, some A3G may escape the Vif-mediated degradation and still find their way into the virus, which is

surprisingly beneficial to HIV-1 survival [343]. When small amounts of A3G are packed into the virions, sublethal levels of mutations are introduced via deamination, accelerating hypermutation and promoting HIV sequence diversity [344]. The incomplete degradation of APOBEC3 could result from Vif variants, which have less affinity to APOBEC3 proteins. The defective Vif has been associated with the failure of antiretroviral treatments *in vivo* [345].

1.5.2.2 Tripartite motif-containing protein 5α (TRIM5α)

TRIM5α was first identified in a screen for anti-HIV-1 rhesus macaque genes when expressed in human cells [153]. TRIM5α is a member of the TRIM containing protein family, which encompasses 70 members with similar domain structures [346]. TRIM5α is a cytoplasmic protein, bears N-terminal RING and B-box type 2 domains, a central coiled-coil domain that mediates the dimerization of TRIM5α, and a C-terminal PRYSPRY domain (also known as B30.2 domain) that determines the substrate specificity [347-349]. The hypervariable V1-V3 segments in the SPRY domain are likely involved in target recognition since mutations in the V1 segment of primate TRIM5α result in the alteration of their affinity to HIV-1 and SIV capsids [348,350-352].

The exact mechanism of the anti-retroviral function of TRIM5α has not been completely elucidated. There is evidence suggesting the direct interaction of TRIM5α with the HIV-1 capsid, and other studies revealing that their binding alters the structure of HIV-1 capsids, leading to premature uncoating [353]. Capsid degradation disrupts the architecture of RTC and abrogates reverse transcription. The two zinc-binding N-terminal domains are important for the full antiviral activity of TRIM5α. The B-box domain contributes to the formation of TRIM5α multimers [354]. The TRIM5α multimer interacts polyvalently with the hexagonal lattice of the HIV-1 capsid with high efficiency, and potentiates the anti-retroviral capacity of TRIM5α [355,356].

Despite the E3 ubiquitin ligase activity in the RING domain, ubiquitin-mediated degradation is not essential to the antiviral function of TRIM5α, as evidenced by the normal anti-HIV-1 function of TRIM5α in the presence of a proteasome inhibitor or inactive E3 [350]. Surprisingly, TRIM5α-driven premature uncoating and abrogated reverse transcription are rescued by a proteasome inhibitor, albeit that HIV-1 infection is still strongly inhibited [156,357]. There are two possible explanations to this seemingly conflicting observation, (1) there are redundant pathways that TRIM5α deploys to inhibit HIV-1, and (2) the proteasome inhibitor delays the normal activity of TRIM5α and allows reverse transcription to take place before the antiviral activity of TRIM5α kicks in [358]. Regardless, it is clear that capsid binding and multimerization are essential for the antiviral function of TRIM5α, which is exerted before the nuclear entry of PIC.

1.5.2.3 Bone marrow stromal antigen (BST-2/tetherin)

The BST2/CD317 has been identified in a microarray screening of IFN inducible membrane-associated proteins in the cells that are not permissive to infection of *vpu*-deleted HIV-1 [359]. The protein was subsequently renamed tetherin, due to its ability to tether the virions to the cell surface [314]. Tetherin is a homodimer connected by a disulfide bond. It has an N-terminal cytoplasmic tail, a transmembrane anchor, an extracellular coiled-coil α-helical domain, and a C-terminal glycosyl-phosphatidylinositol (GPI) linkage [360, 361]. Tetherin tethers the virions to the cell surface by inserting its C-terminus into the lipid bilayer of the virus envelope, and N-terminus into the cellular membrane. Although either orientation of tetherin is theoretically possible in linking virions to the membrane, the aforementioned model appears to be the predominant one.

To overcome the retention by tetherin, Vpu, a type I transmembrane protein, is encoded by HIV-1 [314,396]. Vpu is synthesized in the ER, as tetherin. Vpu directly binds to tetherin and

sequesters it in the perinuclear region to prevent its transportation to the cell surface [362]. Vpu has also been shown to cause internalization of the cell surface tetherin via endocytosis, which leads to its degradation [363,364]. Furthermore, Vpu has been shown to prevent tetherin-mediated activation of NF-κB by stabilizing IκB in the cytosol and preventing nuclear import of p65 [365]. Thus, Vpu inhibits both PRR function and anti-HIV-1 effector function of tetherin.

Vpu also interacts with CD4, which leads to the proteasomal degradation of CD4, allowing gp160 translocation to Golgi and cell surface. [366,367]. Without Vpu, CD4 sequesters gp160 in Golgi and prevents its translocation to the plasma membrane, resulting in fewer Env incorporated into the virions [366].

The viruses that do not encode Vpu have other ways to counter tetherin. HIV-2 has evolved to use the Env protein to overcome tetherin [368]. SIV do not contain Vpu, and uses Nef to target tetherin and induce tetherin endocytosis [369,370].

1.5.2.4 Sterile alpha motif and histidine/aspartic acid domain-containing protein 1 (SAMHD1)

SAMHD1 was first discovered by a mass spectrometry pull-down assay performed on viral protein Vpx in monocyte-derived macrophages (MDM) and myeloid cells [371-373]. As the name indicates, SAMHD1 has an N-terminal SAM domain, which contains a nuclear localization signal (NLS), and a C-terminal HD domain, which is shared by a class of phosphodiesterase, phosphatase and nuclease [374,375]. SAMHD1 possesses deoxyguanosine triphosphate (dGTP) dependent phosphohydrolase activity and catalyzes the removal of triphosphate from deoxynucleotide triphosphates (dNTP) [371,376,377]. This causes dNTP depletion, which blocks viral reverse transcription. Hence SAMHD1 inhibits a wide range of retroviruses, except foamy viruses, which usually complete the reverse transcription before entering the cells [378].

However, more recent mutagenesis studies suggest that the dNTPase activity may not be essential for the anti-HIV function of SAMHD1. The threonine (T) 592 to glutamic acid (E) mutation in SAMHD1 mimics its phosphorylated state and retains the dNTPase activity, but results in the loss of the virus restriction function [379-382]. The dissociation of the dNTPase activity of SAMHD1 and its antiviral activity suggests that depleting the dNTP pool may not be the only mechanism by which SAMHD1 restricts viruses. Interestingly, SAMHD1 has also been shown to have RNase and ssDNase activity [383]. The D137N SAMHD1 mutant, which retains its nuclease activity but not its dNTPase activity, inhibits HIV-1 [384]. In comparison, the Q548A mutation, which disables the nuclease activity without affecting dNTPase activity, hampered the anti-HIV activity of SAMHD1, suggesting the importance of nuclease activity in the antiviral function of SAMHD1. However, the differential localization of SAMHD1 (nucleus) and reverse transcription (cytoplasm) make it counterintuitive to think that the nuclease activity of SAMHD1 can affect HIV RNA. HIV infection can be rescued by degrading SAMHD1 or supplementing the infected cells with nucleoside several hours after virus entry [385]. Therefore, it remains an open question of how dNTPase and nuclease activities of SAMHD1 contribute to its anti-HIV activity.

Vpx is only present in HIV-2 and some SIVs from macaque, red-capped monkeys and sooty mangabeys. Vpx and Vpr evolved from gene duplication events [386]. The deletion of Vpx from SIV does not affect its infection in activated CD4+ T cells but disables the virus from infecting DCs and MDMs [387]. It has been previously shown that myeloid cells and resting CD4+ T cells do not support HIV-1 infection due to the restriction activity of SAMHD1 [388]. For HIV-2 and some SIVs, this block is alleviated by Vpx that is brought into infected cells with the virions. Vpx recruits cullin 4A-cased E3 ligase to SAMHD1 in the nucleus, leading to the ubiquitination

of SAMHD1 for proteasomal degradation [389]. Upon entering the cells, Vpx operates independently of capsid uncoating, causes the reduction of SAMHD1 within an hour and continuously suppresses SAMHD1 expression for several days [390,391].

1.5.2.5 Schlafen 11 (SLFN11)

SLFN11 has RNA helicase domains. It acts at the late stage of HIV replication [392]. SLFN11 inhibits the translation of viral mRNA by detecting viral RNA via viral codon bias and binding to cellular tRNAs, thus reducing the tRNAs available to viral protein synthesis. High expression of SLFN11 in CD4+ T cells is thought to contribute to the maintenance of the chronic infection and non-progressing state of HIV-1 infected patients known as elite controllers [393].

1.5.2.6 Myxovirus resistant protein 2 (Mx2/MxB)

MxB/Mx2 is a large GTPase from the dynamin superfamily, which inhibits HIV-1 infection by interfering with the nuclear import of viral DNA [283-285]. MxB binds to the HIV-1 capsid and disrupts viral uncoating [394]. The N-terminus of MxB is important for binding to viral capsid. Similar to TRIM5α, MxB recognizes the higher-order structure of the HIV capsid instead of individual capsid hexamer. In support of this notion, the length of the antiparallel MxB dimer matches the spacing between CA hexamer interfaces. The binding of MxB to the HIV core may potentially affect the binding affinity of CA to other cellular proteins, which ultimately reduces the replication efficiency. A study has shown that the conformation of the HIV-1 capsid determines the sensitivity to MxB inhibition [395]. Therefore, the change in the HIV-1 capsid is critical for the virus to evade capsid targeting restriction factors, including TRIM5α and MXB.

Recently, several studies expanded the antiviral spectrum of MxB beyond HIV-1. RNA replication of the Hepatitis C virus (HCV) depends on the host factor CypA. Yi and colleagues have shown that MxB inhibits HCV infection by interfering with the binding of HCV protein

NS5A to CypA [396]. They further showed that two other viruses, the Japanese encephalitic virus and Dengue virus, which also depend on CypA for efficient replication, are also susceptible to MxB inhibition. This study suggests a broad activity of MxB against CypA-dependent viruses. In addition to HCV, three recently published independent studies have reported potent inhibition of all three classes of herpesvirus by MxB [397-399]. Their data suggest that MxB uses different mechanisms to inhibit HIV-1 and herpesviruses.

1.5.2.7 Membrane-associated really interesting new gene C4HC3 8 (MARCH8)

MARCH8 is a RING-finger E3 ubiquitin ligase, which belongs to the MARCH family [400,401]. MARCH8 has two or more predicted transmembrane domains and contains a C4HC3 RING finger domain in the cytoplasmic N-terminus, which interacts with the E2 enzyme. MARCH8 is highly expressed in myeloid cells. Its expression can be slightly elevated by IFN stimulation in macrophages [402]. Overexpression of MARCH8 in virus-producing cells reduces the infectivity of HIV-1 reporter viruses pseudotyped with VSV-G, HIV-1 Env, HIV-2 Env, SIV Env, MLV Env and xenotropic MLV–related virus (XMRV) Env. In contrast, the expression of MARCH8 in target cells does not affect virus infection. The entry assay has shown that MARCH8 impedes virus entry into target cells. By further examining the Env incorporation in the virions using enzyme-linked immunosorbent assay (ELISA) and western blot (WB), it was found that MARCH8 reduces the level of gp120 in the viruses but does not affect the expression of Env in cells. Further studies revealed that MARCH8 downregulates viral Env from the cell surface and retain them in intracellular endosomes.

1.5.2.8 Guanylate binding protein 5 (GBP5)

GBP5 is a member of GTPases subfamily [403,404]. GBP5 interferes with the processing and incorporation of viral Env. Its localization in the Golgi is essential for its antiviral function. In

contrast, mutagenesis studies have shown that the GTPase activity of GBP5 is dispensable for its antiviral function. Strikingly, HIV-1 primary isolates, AD8 and YU-2, from brain macrophages have a *vpu* inactivating mutation and manifest resistance to GBP5 inhibition [404]. Since Vpu and Env are translated from the same viral mRNA, lack of Vpu synthesis increases the expression of Env, which overcomes the GBP5-mediated decrease in Env processing. Restoration of Vpu expression in AD8 and YU-2 decreases the level of Env, which sensitizes both viruses to GBP5. Therefore, the mutations at the start codon of *vpu* can be beneficial to the virus by escaping from GBP5 restriction, but it comes at the cost of becoming susceptible to tetherin. Whether the *vpu* mutation can provide an advantage to HIV-1 likely depends on the cellular environment in which HIV-1 replicates.

1.5.2.9 Cholesterol 25 Hydroxylase (CH25H) and 25-hydroxy cholesterol (25HC)

Oxysterols are a group of cholesterol oxidation derivatives emerging as a new class of restriction factor with broad antiviral properties. One of the members, 25-hydroxycholesterol (25HC), has been shown to inhibit the Zika virus (ZIKV), HCV, Ebola virus, Nipah virus, Rift Valley Fever virus and HIV-1 [405,406]. The conversion of cholesterol to 25HC is catalyzed by an ER-associated enzyme called cholesterol 25 hydroxylase (CH25H) [407]. CH25H is IFN-inducible, and its expression can be further upregulated by 25HC. The hydroxyl group on 25HC renders it water soluble and allows the secretion of 25HC to the extracellular space. Hence, the secreted 25HC enters the neighbouring cells and serves as a messenger that prepares the cells against viral infection. 25HC has been reported for its potential participation in the cholesterol biosynthesis pathway and maintaining cholesterol homeostasis [408] [409] [410]. However, these results have been challenged by *in vivo* experiments. A study on mice has demonstrated that the lack of the CH25H gene does not result in cholesterol dysregulation [410]. Moreover, patients who have

spastic paresis, a hereditary disease that causes an upregulated level of 25HC, have shown normal cholesterol homeostasis [411]. These *in vivo* studies provided opposing evidence on the role of 25HC in regulating cholesterol metabolism. Furthermore, a high level of 25HC has been observed in macrophages and dendritic cells during inflammation, suggesting an important function of 25HC as an immune modulator [412] [413] [414].

The anti-HIV-1 activity of 25HC has been well demonstrated in *in vitro* cell culture assay and *in vivo* rodent models [406]. It has been shown that the entry of HIV-1 was hindered by 25HC treatment, and it was proposed that 25HC inhibits the fusion of HIV-1 virions to the cells. A subsequent study using a biomembrane model system shed further light on the mechanism of the anti-HIV-1 function of 25HC [415]. Despite its soluble property, 25HC was found to be incorporated in the cell membrane and to impede fusion pore formation. Moreover, the structure of the HIV-1 Env fusion peptide may have also been directly altered by 25HC.

Another property of 25HC is its antiviral function in virus producer cells. Similar to IFITM proteins, 25HC was also shown to interfere with the function of the Lassa Virus glycoprotein by altering its glycosylation profiles [416]. More interestingly, 25HC has further been shown to prevent the uncoating of a non-enveloped virus, reovirus [417]. In addition, other non-enveloped viruses, human papillomavirus-15 (HPV-16), human rotavirus (HRoV) and human rhinovirus (HRhV), are also inhibited by 25HC [418]. Remarkably, CH25H, the enzyme that produces 25HC, has antiviral capacity independent of its enzymatic activity [419]. Chen and colleagues have shown that the CH25H mutant lacking its hydroxylase activity can still suppress HCV replication by sequestering NS5A[419]. The dimerization of NS5A is essential for viral replication. Another study on porcine reproductive and respiratory syndrome virus (PRRSV)

further highlighted that the CH25H mutant could restrict PRRSV replication by targeting the nonstructural protein 1 alpha for degradation [420].

1.5.3 Introduction to interferon-induced transmembrane proteins (IFITMs)

1.5.3.1 Members of the IFITM family and their biological functions

IFITM proteins were first identified in a cDNA library screening of genes that contain ISRE in IFN-treated T98G glioblastoma multiforme tumour cells [421]. Among up-regulated genes, a group of homologous genes, namely 9-27, 1-8D, and 1-9U, had the highest level of up-regulation by IFN. They were later renamed IFITM1, IFITM2, and IFITM3, respectively [422]. In humans, there are five members in the IFITM family, IFITM1, 2, 3, 5, and 10, which have arisen from gene duplication events during evolution [423]. The IFITM1, 2, 3, and 5 genes are located on the short arm of chromosome 11, and the IFITM10 gene resides near the centromere region.

Although named "interferon-inducible", IFITM5 does not have any ISRE in its promotor region. It was previously known as Bril, but was later renamed IFITM5 due to its sequence homology to the IFITM family [424]. IFITM5 is constitutively expressed in osteoblastoma cells and promotes bone mineralization. The C14T mutation in IFITM5 has been shown to cause varying degrees of osteogenesis imperfecta type V in humans [425]. There is not much known about the function of IFITM10.

IFITM1 has been shown to associate with CD81, carry out cell adhesion, and regulate cell growth in lymphocytes [426]. The IFITM1 interaction with CD81 is involved in β-integrin-mediated adhesion and the complement system in B-cells [427]. In mice, both IFITM1 and IFITM3 interact with CD81 and contribute to cell adhesion [428]. The IFITM3/CD81 complex has a critical role in mammary gland organization in rats and germ cell niche organization in mice [429,430].

Furthermore, IFITM3 has also been shown to play a role in epithelial cell differentiation, cell cycle control via an association with Fyn, hematopoietic stem cell homing, and migration via an association with osteopontin [430-432]. Transient knockdown experiments have shown that IFITM1 is required for the migration of primordial germ cells (PGCs) from the mesoderm to the endoderm in mice. IFITM3 is expressed in migratory primordial PGCs and contributes to PGCs homing to gonads [433,434]. However, the deletion of the entire *ifitm* locus does not affect the normal course of embryonic development, nor does it affect the fertility of the animals [435]. Therefore, the exact role of IFITM proteins in embryonic cell development of mice remains an open question.

IFITM1, 2, and 3 all possess antiproliferative and apoptosis-inducing features, which can be enhanced by IFN [436]. IFITM1 can induce G1-arrest by enhancing the tumor suppressor protein 53 (p53) regulated signalling cascade [437]. The activation of p53 results in the senescence of cells and programmed apoptosis [438]. IFITM2 expression also results in G1 and subG1 phase arrest, which leads to cell apoptosis independent of p53 [439]. Anti-proliferation activity by IFITM3 has been shown to inhibit the proliferation of IFN-sensitive melanoma cells, while IFITM3-expressing cells have shown a morphology similar to those undergoing senescence [440]. Interestingly, the anti-proliferation activity of IFITMs is only limited to pluripotent stem cell, as they do not interfere with the cell division of tumours and differentiated tissues [429,423].

IFITMs have also been identified as markers of malignancy and associated with the early phase of cancer progression [423]. The depletion of IFITMs is associated with a change in the adhesive property of cells and promotes cancer growth and metastasis. Hence, IFITM levels are downregulated in some tumour types, as exemplified by the reduced IFITM1 expression in astrocytoma, and the downregulation of IFITM1 and IFITM3 in metastatic melanoma cells

[441,442]. IFITM gene knockdown *in vivo* has been shown to promote cancer growth [437]. Interestingly, an elevated level of IFITMs has been observed in cytopenia, adenoma, colon carcinoma, gastric cancer cell line, and invasive stage breast carcinoma [443-446]. The overexpression of IFITM1 has even been shown to promote the invasiveness of head and neck tumoral cells *in vitro* [447]. It has been hypothesized that cancerous cells insensitive to the antiproliferative function of IFN are selected during extensive cell division, and the most invasive cells have an upregulated IFITM expression [423]. However, other evidence suggests the lack of association between IFITM expression levels and the IFN sensitivity of cancer cells [448,423]. Therefore, the association between high IFITM expression and IFN sensitivity is likely tumour type-specific [423].

The upregulated IFITMs are associated with many chronic inflammatory diseases, such as chronic HCV infection, ulcerative colitis, and inflammatory bowel disease, characterized by an increased IFN level [449-451].

1.5.3.2 IFITM gene sequences and protein structures

IFITM proteins contain C- and N-terminal variable regions, two membrane-associated domains, and a conserved intracellular loop (CIL) [422] (Fig. 13). The IFITM family belongs to a larger membrane-associated CD225/pfam04505 protein superfamily, sharing homology with the first membrane-associated domain and the CIL. The highly conserved CIL domain has also been shown to have motifs for potential protein kinase C and casein kinase II binding [422]. There have been three models of IFITM topology proposed previously. However, the Type II transmembrane topology with a cytoplasmic N-terminus and extracellular C-terminus has been supported by many lines of evidence including surface staining, fluorescence microscopy, mutagenesis assay, lysosomal degradation assay, and post-translational modifications analysis

[452]. Recently, systematic site-directed spin labeling (SDSL) and electron paramagnetic resonance (EPR) studies performed on IFITM3 have revealed that IFITM3 has a cytosolic localization of the N-terminal that is followed by an intramembranous region, a single transmembrane domain, and an extracellular C-terminal domain [453]. This result confirms the type II transmembrane topology of IFITM proteins [453].

IFITM proteins are ubiquitously expressed in different cells at basal levels, and the subcellular localization varies in different cell types and tissues [423]. IFITMs are synthesized in the ER, processed in the Golgi, and further translocated to the plasma membrane before reaching their final destination [423,437]. Therefore, there are always some IFITMs detected in the ER and the Golgi apparatus. IFITM1 is primarily found on the plasma membrane and the early endosomes, whereas IFITM2 and 3 are mainly located in the late endosomes and lysosomes [452,454,455]. IFITM2 and 3 have extended N-terminal regions of 21 amino acids, which have endocytic trafficking signals regulating their endosomal localization [422,454,455].

Interestingly, IFITM3 can be transported between cells via exosome, which transfers the antiproliferative functions to the neighbouring IFN-sensitive cells and the antiviral functions to the exosome accepting cells [440,456].

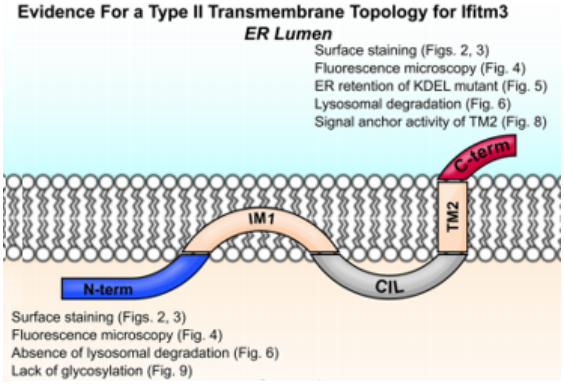

Figure 11: The membrane topology of IFITMs [452]. IFITM contains five domains, including the N-terminal cytoplasmic domain, intramembrane domain, CIL, transmembrane domain and the C-terminal extracellular domain.

1.5.3.3 Pathogen restriction activity of IFITM1, 2 and 3

In a 1996 study, the antiviral function of IFITM proteins was first reported. It was shown that the overexpression of IFITM1 partially inhibits vesicular stomatitis virus (VSV) infections in both cell lines and mice [457]. However, it was not until 2009 that IFITM proteins started being widely recognized as potent antiviral restriction factors. A study showed that IFITM3 strongly inhibits infection by West Nile virus, Dengue virus, and Influenza A virus (IAV) [458]. Subsequent studies rapidly increased the repertoire of viruses inhibited by IFITM proteins. Influenza B virus (IBV), the yellow fever virus, Omsk hemorrhagic fever virus, HCV, VSV, rabies virus, Lagos bat virus, Marburg virus, Ebola virus, SARS-CoV-1, HIV-1, jaagsiekte sheep retrovirus, Semliki Forest virus, La Crosse virus, hantavirus, Andes virus, Rift Valley fever virus were all reported to be sensitive to the inhibition by IFITMs [459-469]. Most of these viruses are enveloped RNA virus, but the non-enveloped dsRNA virus Reovirus is also inhibited by IFITM3 [470].

Interestingly, different viruses have varying degrees of susceptibility to the antiviral activity of IFITM proteins. The infection of influenza viruses is more severely hampered by IFITM3 than by IFITM1 or by IFITM2, whereas the HCV is sensitive to IFITM1 but not to IFITM3 inhibition [458]. It has been previously proposed that the subcellular location of each IFITM and the site of virus entry correlate with viral sensitivity to each IFITM. However, the

Bunyaviridae viruses have provided evidence against such a general mechanism of action. Despite the similarity in their morphology and glycoproteins, the La Crosse virus, the Hantaan virus, and the Andes virus are inhibited by all IFITMs, whereas the yellow fever virus is only restricted by IFITM2 and IFITM3 [464]. Crimean-Congo hemorrhagic defer virus has been shown to be completely resistant to IFITM restriction [464]. Furthermore, the same virus can exhibit differential sensitivity to the same IFITM in different cell types. For example, the Marburg virus is more sensitive to IFITM3 inhibition in A549, HUVEC, and 293T cells, but is more sensitive to IFITM1 in Vero E6 cells [460]. Similar differences in IFITM sensitivity in different cell lines were also observed for the Ebola virus and the SARS-CoV-1 [460]. Therefore, factors determining the range and the extent of virus inhibition by each IFITM need further investigation.

Some viruses are completely resistant to IFITM proteins, including murine leukemia virus (MLV), Lassa virus, Machupo virus, lymphocytic choriomeningitis virus, Crimean-Congo hemorrhagic fever virus, human cytomegalovirus, and adenovirus type 5 [458,464,471]. Interestingly, infection by HPV and human coronavirus OC43 are even enhanced by IFITM3 [471,472]. IFITM proteins not only inhibit viruses. Mycobacterium tuberculosis (MTb), an intracellular bacteria, is inhibited by IFITM3 [473]. IFITM3 restricts MTb infection by preventing entry into the cytosol and enhancing the acidification of late phagosomes, leading to the destruction of the bacteria. This observation suggests that IFITM3 has broad antimicrobial activity and the mechanism behind its pathogen restriction activity is likely not specific to each pathogen.

IFITMs undergo post-translation modifications. Cysteines at positions 71, 72 and 105 in IFITM1, 2, and 3 are palmitoylated. This modification has been shown to increase the clustering of IFITM3 and augment its antiviral function against IAV [474]. The rate of IFITM3 turnover is regulated by four lysine residues at positions 24, 83, 88 and 104, which are ubiquitinated and

increase protein turnover [475]. A mutagenesis study has shown that mutating these four lysine residues to stop ubiquitination stabilizes IFITM3 expression, increasing its antiviral activity [475]. As previously noted, the N-terminus of IFITM2 and 3 guides their subcellular translocations [454]. The single tyrosine residue at position 20 (Y20) is a part of a YxxØ-type sorting signal for clathrin-mediated trafficking. This short peptide binds to the μ2 subunit of the AP-2 complex and directs IFITM3 to the endosomal compartments[454,476]. Phosphorylation of Y20 by the kinase Fyn regulates IFITM3 endosomal translocation, which is critical for its antiviral function. Recently, IFITM proteins have been shown to form homo- and hetero-oligomers [477]. Two phenylalanines, F75 and F78, are required for the inter-monomer interaction. Loss of the oligomerization reduces IFITM3 restriction potency against IAV and the Dengue virus [477]. The exact role of IFITM oligomerization is still not well understood, but likely affects both IFITM distribution and antiviral function [478].

1.5.3.4 Antiviral mechanisms of IFITM3

IFITM3 has been shown to interfere with incorporating cholesterol into endosomal membranes by interacting with vesicle membrane protein-associated protein A (VAPA). This prevents the association of VAPA with an oxysterol binding protein, which regulates cholesterol trafficking [479]. Overexpression of IFITM3 increases cholesterol levels in the endosomal membrane, which reduces endosomal membrane fluidity and impedes viral fusion. However, a separate study reported that simply increasing cholesterol in endosomes with chemical treatment did not block IAV entry [480]. It is thus unknown whether IFITM3 inhibits viruses solely by modulating cholesterol levels in cellular membranes.

Li and colleagues have shown that IFITM3 inhibits viruses by hampering membrane hemifusion [462]. They conducted a membrane fusion assay to evaluate the membrane fusion

function of class I, II and III viral envelope proteins. IAV HA, SFV E1/E2 and VSV-G, which represent class I, II and III, respectively, were studied. The results showed that the expression of IFITM3 does not affect the binding efficiency and the pH-induced conformational change of these viral envelope proteins. Instead, IFITM3 inhibits the formation of hemifusion. This inhibition can be reverted by negative curvature-promoting oleic acid. Further experiments have revealed a reduction of membrane fluidity and an increase in the positive curvature of the outer leaflet of the plasma membrane as a result of IFITM3 expression. These findings support the previously proposed "tough-membrane" model [481]. However, this membrane fusion assay does not faithfully reflect the actual viral entry process, since the contact surface area differs between cell-cell fusion and virus-cell fusion [482]. Another study showed that IFITM3 does not affect the membrane mixing between the virus envelope and the endosomal membrane, but instead prevents fusion pore formation [480]. It has been proposed that IFITM3 stabilizes the outer leaflet of endosomes without affecting the luminal side of the membrane, and thus prevents the completion of the membrane fusion.

While it is unclear how IFITMs reduce membrane fluidity, the rigidity of the membrane could underpin the broad antiviral activity of IFITMs by impeding membrane fusion and inhibiting the lateral movements of membrane-associated proteins. As in the cases of HIV-1 and HCV, the latter could potentially interfere with the clustering of host receptors [481].

1.5.3.5 Anti-HIV function of IFITMs

Similar to the Marburg virus, HIV-1 inhibition by IFITMs is cell type-dependent [482]. Brass and the colleagues showed that overexpression of IFITM1, 2, and 3 does not affect HIV-1 entry in TZM-bl cells and GHOST-CCR5 reporter-cell lines [458]. Our group observed that IFITMs inhibit HIV-1 infection in CD4+ T cells [463]. During the shRNA knockdown screen of anti-HIV-1

ISGs in SupT1 cells, IFITM2 and IFITM3 were identified to inhibit HIV-1 infection. This was confirmed by IFITM overexpression experiments showing that IFITM proteins strongly suppress HIV-1 infection with IFITM2 and IFITM3, but not IFITM1, by inhibiting HIV-1 entry [454,483]. Interestingly, a reduction in the Gag protein has been observed with the expression of IFITM1 [484], suggesting that IFITM1 does not interfere with HIV-1 entry, but instead, works at an early stage of the virus replication cycle, and possibly between the integration of DNA and the expression of Gag. These studies suggest that IFITM proteins restrict HIV-1 infections by two mechanisms, i.e. interfering with virus entry and suppressing viral protein synthesis.

In 2014, a new mode of antiviral activity by IFITM proteins was reported [485-487]. Previous studies on IFITMs focused on their role in the virus target cells. Compton and colleagues examined the antiviral function of IFITM3 protein in HIV-1 producer cells. They found that IFITM3 in virus producer cells inhibits HIV-1 more strongly than IFITM3 expressed in target cells [485]. IFITM3 does so by incorporating into HIV-1 particles and blocks viral entry. Moreover, IFITM3 can significantly decrease the cell-to-cell transmission of HIV-1, which is the major route of HIV-1 spread between cells [485]. The amount of IFITM3 incorporated into HIV-1 is viral strain-dependent and is directly correlated with the degree of inhibition imposed by IFITM3. In addition, IFITM3 expression in the producer cells has also been shown to reduce the infectivity of pseudotyped HIV-1 viruses that carry envelopes of Gibbon ape leukemia virus or feline leukemia virus RD114 [486]. However, a subsequent study done by Foster and the colleagues could not reproduce the anti-HIV-1 activity of IFITM3 demonstrated in the virus producer cells [485,487]. Foster et al. used U87 glioblastoma cells in their study, and instead of overexpressing IFITM3 they knocked down IFITM3 by shRNA, which contribute to a lower level of IFITM3 in the virus-producing cells. The possibility that IFITM3 deploys a tetherin-like mechanism to manifest

its antiviral activity has been rejected based on the observation that IFITM3 does not tether virions on the cell surface [486].

Mechanistically, IFITM2 and IFITM3 in virus-producing cells were shown to disrupt HIV-1 gp160 maturation, which results in fewer mature gp120/gp41 incorporated into the virions. The Env processing of HIV-2 and SIV are also abrogated by IFITM3. Moreover, IFITM3 was also shown to induce gp120 shedding in virus-producing cells. Hence, IFITM3 impairs HIV-1 infectivity by disrupting Env processing and incorporation into virus particles [487]. However, a study by Neil lab does not support the inhibition of Env protein processing by IFITM3 [488]. This study showed that knocking out IFITM3 in U87 cells did not affect the Env processing of both X4 and R5 viruses.

It has been shown that subcellular localization of IFITM3 is critical for inhibition of either X4-tropic or R5-tropic HIV-1. While the X4-tropic HIV-1 is more inhibited by IFITM3 than the R5-tropic HIV-1, the Y20F IFITM3 mutant, which is located to the cell surface, inhibits as much the R5-tropic HIV-1 as the X4-tropic virus. More intriguingly, Foster et al. discovered that transmitted founder (TF) viruses are resistant to IFITM3, whereas HIV-1 from chronically infected patients are IFITM3-sensitive. They proposed that HIV-1 Env is initially resistant to IFITM3 to establish a successful infection. However, pressure from the neutralization antibodies drives the Env to change in order to escape from neutralization antibodies, albeit at the cost of becoming sensitive to IFITM3 inhibition. Thus, IFITM3 plays an important role in deterring HIV-1 transmission.

Interestingly, IFITM3 serves a role in adaptive immunity as well. A recent study showed that IFITM3 KO mice exacerbated disease progression upon infection by murine cytomegalovirus (MCMV) [489]. IFITM3 does not inhibit MCMV but helps to control MCMV

infection in mice by promoting cellular immunity and preventing virus-induced lymphopenia and the apoptosis of natural killer cells and T-cells. IFITM3 inhibits IL-6 expression, which results in the loss of NK cells if left uncontrolled. Another study on influenza virus showed that IFITM3 increases the lifespan of CD8+ T cells [490]. Therefore, in addition to directly restricting viral replication, IFITM3 also indirectly promotes the adaptive immune response. Both activities together assist the control and clearance of virus infections.

1.5.3.6 HIV-1 resistance to IFITMs

Not only do IFITMs inhibit different viruses to various extents, but different HIV-1 strains also showed varying degrees of sensitivity to IFITM proteins [491]. The IFITM-resistant phenotype can be attributed to natural selection during the virus-host interaction [483]. The X4-tropic HIV-1 strain BH10 is sensitive to IFITM1 restriction in SupT1 cells. Not surprisingly, long-term replication of the BH10 virus in IFITM1-expressing SupT1 cells led to the emergence of IFITM1-resistant BH10 mutants. Sequencing of escape viruses revealed mutations in the Vpu and Env proteins. Further studies showed that the Vpu34 and Env G367E mutations together enable efficient replication of BH10 in IFITM1-expressing SupT1 cells. The Vpu34 mutation introduces a stop codon at position 35 of Vpu, and the EnvG367E mutant changes Glycine at 367 to a negatively charged glutamic acid at the CD4 binding site of gp120. These two mutations enhance cell-to-cell transmission of BH10, which may enhance virus replication and indirectly overcome IFITM1 inhibition. To determine the viral protein involved in aiding the virus to escape from IFITM1, a panel of chimeric viruses were generated between BH10 and the IFITM1-resistant HIV-1 strain NL4-3 [492]. After assessing the infectivity of each chimeric virus, the results demonstrated that, when Env (excluding the segment overlapping with the Vpu gene) is interchanged between BH10 and NL4-3, BH10 is rendered resistant to IFITM1, whereas NL4-

3 becomes susceptible to IFITM1 restriction. Therefore, these two studies suggest that the Env protein of HIV-1 regulates virus susceptibility towards IFITM1 inhibition. It remains to be determined how Env is capable in evading restriction by other IFITMs.

1.5.3.7 Regulation of IFITM3 antiviral activity by its single nucleotide polymorphism (SNP)

The importance of IFITM proteins in inhibiting pathogens has been supported by *in vivo* studies. The *ifitm3* knockout mice show poor disease progression in morbidity and mortality when infected by a non-lethal strain of IAV [459,493]. More importantly, a SNP of IFITM3 in humans (rs12252) is associated with severe cases of H1N1 IAV or influenza B virus infection in Caucasian and Han Chinese cohorts [459,494,495]. Recently, the SNP rs12252-C (also known as minor C allele) in IFITM3 was shown to associate with the rapid progression of HIV-1 infections in Han Chinese cohorts [496]. It has been proposed that the minor C allele mutation causes an alteration in the splice acceptor in the *ifitm3* gene, leading to the loss of 21 amino acids from the N-terminus [459]. Since the N-terminus of IFITM3 is critical for its endosomal localization, the lack of the N-terminus results in plasma membrane localization of the IFITM3 mutant and abrogates its antiviral function against viruses that enter cells via the endosomal pathway [454]. However, the endogenous expression of such a truncated IFITM3 has not been identified [497]. Another SNP (rs38881888) in the core promoter region of the *ifitm3* has been shown to increase the susceptibility towards infection by TB in Han Chinese cohorts, possibly through reduced expression of IFITM3 [498]. These findings collectively suggest the importance of SNPs in regulating IFITM3 expression and localization, which are critical in determining IFITM3 antiviral activity.

More recently, another SNP rs34481144 in the core promoter region of *ifitm3* has also been identified as an important transcription regulator of IFITM3 expression [490]. The

rs34481144-A has been identified as a risk allele enriched in patients with severe illness upon influenza infection. It has been shown that rs34481144 is located in the core binding site of the CCCTC-binding factor (CTCF). The rs34481144-A provides a binding site with a higher affinity to CTCF, and thereby reduces the expression of IFITM3. Since IFITM3 also has anti-HIV-1 activity, I hypothesize that the A allele at rs34481144 SNP may also be enriched in HIV-1-infected population and negatively affect HIV-1 infection and/or disease progression.

1.6 Research objectives

Inhibiting viral entry is an important strategy for preventing HIV-1 infection. Two drugs have been developed against HIV-1 entry and approved by the FDA to treat patients, namely enfuvirtide and maraviroc. Both drugs are used as the last resort of medication in restricted cases with multi-drug resistant HIV-1. Therefore, it is very important to discover new therapeutical approaches to inhibit viral entry and develop new anti-HIV-1 drugs.

When I started my Ph.D. project in 2014, it was unknown how HIV-1 resists IFITM inhibition, and whether SNPs in the *ifitm* genes are associated with HIV-1 infection and disease progression. IFITM proteins are not the only ISGs that inhibit virus entry. 25HC was reported to impair the entry of several important pathogenic viruses, including HIV-1. It was unknown whether IFITM proteins and 25HC together pose a stronger barrier to HIV-1 entry. To answer these questions, I have pursued the following aims:

AIM 1: Determine how HIV-1 Env confers resistance to IFITM3.

I first screened a group of primary HIV-1 strains for their sensitivity to IFITM proteins and discovered that that HIV-1 strains AD8-1 and YU-2 were completely refractory to IFITM3 inhibition. Through mutagenesis analysis, I found that the viral Env protein determines viral susceptibility to IFITM3 and that the V3 loop underpins this important function of Env protein.

AIM 2: Investigate the effect of SNP in the *ifitm3* gene on the antiviral activity of IFITM3.

The SNP rs34481144 in *ifitm3* gene has been shown to associate with the severity of the influenza A virus infection. I hypothesized that the rs34481144 SNP might also be enriched in HIV-1 infected individuals and correlate with HIV-1 acquisition and/or disease progression. I tested how rs34481144-A and -G in PBMCs affect the cell susceptibility to NL4-3 infection, as well as the frequency of rs34481144-A in the HIV-1 patients.

AIM 3: Investigate the combined activity of IFITM3 and 25HC.

Since both 25HC and IFITM3 were shown to inhibit viral entry by modifying cell membrane composition [462,499], I hypothesized that 25HC and IFITM3 might function in an additive or synergistic manner. I tested the susceptibility of the cells to NL4-3 and AD8-1 infection under different conditions and found that 25HC potentiates the antiviral activity of IFITM3 against NL4-3, but not AD8-1.

Chapter II: Materials and Methods

2.1 Cell Culture

2.1.1 Cell propagation

HEK293T is a human embryonic kidney cell line. TZM-bl luciferase reporter cells are a HeLa-derived cell line that expresses CD4, CXCR4 and CCR5, and contains the HIV-LTR driven firefly luciferase reporter gene. MT4 cells are human leukemic T cells. MT4-R5 is a cell line that was engineered to express the R5 coreceptor, through puromycin selection. Constitutive expression of IFITM3 in MT4-R5 cells was achieved by transducing the cell line with the pQCXIH-IFITM3 vector and selecting with 500μM hygromycin. HEK293T (catalogue number 103), TZM-bl (catalogue number 8129), MT4 (catalogue number 120) were obtained from the NIH AIDS Reagent program. C8166-R5 cells are human umbilical cord blood T lymphocytes immortalized by human T cell leukemia virus, and were derived from the parental C8166-45 cell line to stably express CCR5. HEK293T cells and TZM-bl cells were propagated in Dulbecco's Modified Eagle Medium (DMEM) supplemented with 10% Fetal Bovine Serum (FBS), 100 units/ml penicillin and 100 μg/ml Streptomycin (P/S) at 37 ºC and 5% CO_2. C8166 cells were maintained in Roswell Park Memorial Institute (RPMI) 1640 medium, supplemented with 10% FBS, 100 units/ml penicillin and 100 μg/ml Streptomycin, and 1μl/ml of puromycin at 37 ºC and 5% CO_2. MT4/R5 cells were cultured in RPMI 1640 medium containing 10% FBS, 100 U/ml penicillin, 100 μg/ml streptomycin, and 500 μg/ml G418. DMEM (catalogue number 11965-092), RPMI 1640 (catalogue number 11875-093), FBS (catalogue number 11875-093), and penicillin-streptomycin (catalogue number 15140-122) were purchased from Life Technologies. Puromycin (catalogue number P8833) and G418 (catalogue number A1720) were obtained from Sigma-Aldrich.

2.1.2 Peripheral blood mononuclear cells (PBMCs) and Cord blood-derived mononuclear cells (CBMCs)

PBMCs were isolated from the blood (4 ml) donated from the Jewish General Hospital (JGH) authorized by ethic committee. CBMCs were isolated from cord blood donated from JGH. Blood samples were first mixed with an equal volume of sterile PBS. The diluted blood was gently loaded onto the pre-seeded 4 ml of Ficoll-Plaque solution in a 15 ml Falcon tube. The blood was then separated into three layers (plasma, PBMCs/CBMCs, Ficoll solution and erythrocytes) by centrifuging the Falcon tube at 1000 rpm for 30 min (CS-6R; Backman Coulter). The first layer of plasma was carefully removed without disturbing the PBMCs/CBMCs layer. Then the second layer was carefully collected and transferred to a new Falcon tube, and subsequently washed by 10 ml of PBS (2X). The cells were then resuspended in the RPMI 1640 growth medium containing phytohemagglutinin (PHA). The cells were left over night, and an aliquot was used for genotyping. Cells were then plated in 24-well plate for IFN treatment and HIV-1 infection.

2.1.3 PBMCs and CBMCs DNA extraction

The total DNA was extracted from PBMCs and CBMCs using DNeasy Blood & Tissue Kits (catalogue number 69504; QIAGEN). The PBMCs/CBMCs were washed with PBS twice and suspended in 200 μl of PBS. 20 μl of protein kinase K and 200 μl of lysis buffer AL were added into each tube. The Eppendorf (EP) tubes were then vortexed immediately, and the mixture was further incubated at 56^{o}C for 10 minutes. A volume of 200 μl of ethanol was added to the sample immediately, followed by vortexing. The lysate was transferred into the DNeasy Mini spin column and centrifuged at 8000 rpm (Eppendorf 5415d centrifuge) for 1 minute. The flow-through was discarded, and the column was inserted into a new collection tube. Columns

were washed with 500 μl AW1 buffer and 500 μl AW2 buffer. The excess liquid was eliminated by centrifuging the empty tubes for 2 minutes at 13200 rpm (Eppendorf 5415d centrifuge). After transferring columns into clean EP tubes, columns were further air-dried for 2 minutes. DNA was eluted by overlaying with the 30 μl of ddH2O for 2 minutes, followed by centrifugation at 13200 rpm (Eppendorf 5415d centrifuge). The concentration of DNA was measured by Nanodrop.

2.1.4 PCR and genotyping

The desired fragment of DNA was amplified using Q5® High-Fidelity PCR Kit (catalogue number E0555; NEB). The primers used for amplifying and genotyping rs34481144 SNP were 5'-GTTGAACAGGGACCAGACGA-3' and 5'-AGGGCGGAACAAATTCCTGAG-3'. PCR products were analysed in a 1.5% agarose gel, and DNA fragments were purified using the E.Z.N.A. ® gel extraction kit (catalogue number D2500; OMEGA bio-tek). The concentration of the DNA extracted was measured using Nanodrop, and subsequently sent to Eurofins Scientific for sequencing.

2.2 HIV-1 Production

2.2.1 Plasmid DNA constructs

pNL4-3 (catalogue number 114), p89.6 (catalogue number 3552), pYU-2 (catalogue number 1350), pWITO (catalogue number 11739), pTHRO (catalogue number 11745), and pRHPA (catalogue number 11744) were obtained from NIH AIDS Reagent Program. pAD8-1 and pNL(AD8) were kindly provided by Dr. Eric O. Freed [500]. N-terminal FLAG labelled IFITM1, 2 or 3 were cloned into pQCXIP as previously described [463]. pQCXIP (catalogue number 631516) was purchased from Clontech. NL4-3 *env* cDNA flanked by SalI and NheI that

contain the V3-loop sequence of AD8-1, YU-2, WITO, THRO or RHPA were synthesized by Invitrogen. The synthesized sequences were cloned into pNL4-3 via restriction enzyme digestion of SalI and NheI, followed by ligation. SalI-HF (catalogue number R3138S) and NheI-HF (catalogue number R3131S) were obtained from New England Biolabs (NEB). The clone constructs were transformed into DH-5α competent cells (catalogue number 18265-017) purchased from Invitrogen. The successful clones were selected out, and sent for sequencing at Genome Quebec. The correct clones were maxi-prepped using E.Z.N.A. Plasmid Maxi Kit (catalogue number D6922-02) purchased from OMEGA bio-tek.

2.2.2 Virus Production

HEK293T cells were seeded in a 6-well plate at 0.6×10^6 cells/well 20 hours prior to transfection. Proviral DNA (500 ng), 0, 25, 50, 100 and 200 ng of IFITM1, 2 or 3 plasmids, and 500, 475, 450, 400 and 300ng of pQCXIP empty vector were transfected into HEK293T cells using polyethyleneimine (PEI). The ratio of DNA to PEI used was 1:3. The medium was changed 6 hours post-transfection. The supernatant and the cells were harvested 48 hours post-transfection. The supernatant was centrifuged at 3000 rpm (CS-6R; Beckman Coulter) for 20 minutes at 4 ^{o}C to eliminate cell debris. Viruses were then aliquoted into 1ml and stored at -80 ^{o}C. The total virus production was quantified by measuring viral RT activity.

2.2.3 RT Assay

A volume of 10 μl of the virus was mixed with 40 μl of the reaction cocktail that contains Triton-X, poly-adenosine RNA template, and tritium labelled deoxy tritium nucleotide triphosphate (dTTP) (Perkin Elmer). The mixture was then incubated at 37^{o}C and 5% CO_2 for 3 hours. The synthesized nucleic acids were precipitated by adding 150 μl of cold 10% trichloroacetic acid (TCA) (Millipore) into each well. The mixture was further incubated at 4^{o}C

for 30 minutes. The sample mixtures were subsequently transferred into the MultiScreen filter plate (Millipore). The solvent was drained by vacuuming the filter plate, and the tritium labelled DNA was left on the membranes of the filter plate. The membranes were washed twice with 200 μl of 10% TCA, followed by another wash with 200 μl of 95% ethanol. Each membrane was transferred into scintillation vials (Diamed), and 3 ml of liquid scintillation cocktail (MP Biomedicals) was added into each vial. The amount of radioactivity released from each membrane was measured by detecting β decay using the liquid scintillation counter Wallac 1410 (PerkinElmer).

2.2.4 Purification of HIV-1 particles

HEK293T cells were seeded in 10 cm cell culture plates at 4×10^6 cells/plate. Twenty hours after seeding, 5 μg of proviral DNA, 1 μg of IFITM3 DNA or 1 μg of pQCXIP DNA were transfected into each dish using PEI. The ratio of HIV-1 DNA to IFITM3/pQCXIP DNA (5 μg :1 μg) was kept the same as the transfection experiments described in section 2.2.2 (500 ng: 100 ng). The medium was changed 6 hours post-transfection, and the viruses were harvested 48h post-transfection. The harvested viruses were filtered through 0.2 μm sterile polyethersulfone membrane syringe filter (catalogue number 28145-501; VWR International) to eliminate cell debris and extracellular matrix. The harvested viruses were slowly transferred ultracentrifugation tubes (catalogue number 344059; Beckman Coulter) that were pre-loaded with 2 ml of 20 % sucrose cushion. Sucrose (catalogue number SUC507.1; BioShop) was dissolved in PBS (Gibco). The virus was pelleted at 35000 rpm for 1 hour at 4 ^{o}C by ultracentrifugation (Optima L-100XP Ultracentrifuge Beckman Coulter). The pelleted viruses were resuspended in 100 μl of 10% FBS DMEM.

2.3 HIV-1 Infection

2.3.1 Luciferase Assay

Each well of a 24-well plate was seeded with 5.0×10^4 TZM-bl cells 20 hours prior to infection. Viruses with an equal amount of RT activity were used for infecting TZM-bl cells. At 40 hours post-infection, TZM-bl cells were washed once with cold 1X Dulbecco's phosphate-buffered saline (DPBS) (catalogue number14190-144; Gibco by life technology) and lysed with 100 μl of 1X passive lysis buffer (catalogue number E1941; Promega). Of each sample, 10 μl was mixed with 40 μl of the luciferase substrate (catalogue number E4530; Promega). Luciferase activity was measured using Glomax 20/20 luminometer.

2.3.2 BlaM-Vpr viral entry assay

HIV-1 entry was assessed by BlaM-Vpr viral entry assay as described previously [501,502]. The BlaM-Vpr-containing viruses were produced by co-transfection of 5 μg of HIV-1 DNA, 1μg of pCMV-BlaM-Vpr DNA and 1μg of IFITM3 or pQCXIP vector into HEK293T cells. The supernatant was filtered through the 0.2-μm filters and pelleted at 35000 rpm for 1h at 4 ^oC. The viruses were re-suspended in 10% FBS RPMI 1640 medium. Of each sample, 5 μl was used for RT activity. The rest of the viruses were aliquoted and stored at -80 ^oC. C8166-R5 cells were used for viral entry assay. A total of 1×10^6 C8166 cells were plated with 400 μl of 10% FBS RPMI 1640 in each well of a 24 well plate. Concentration of 5 μg/ml of polybrene (catalogue number 107689; SIGMA-ALDRICH) was included, followed by a 45-minute spinoculation at 1800 rpm (CS-6R, Beckman Coulter) and a subsequent 2 hours of incubation at 37 ^oC 5% CO_2. The cells were then transferred to EP tubes and the viruses that did not succeed in the entry were washed off by CO_2 independent medium (catalogue number18045-088; Gibco by life technology). The cells were loaded with CCF2-AM (catalogue number1032; Invitrogen) and

incubated in the dark at room temperature for 1 hour. The cells were washed with the developing solution, transferred into a V-bottom 96 well cell culture plate (catalogue number 651180; Greiner Bio-One International), and bathed in the developing solution overnight (16 h) at room temperature in the dark. Next, cells were washed twice with cold DPBS containing 2% FBS, fixed with 2% paraformaldehyde (catalogue number PAR070; BioShop) containing 2%FBS DPBS, and analyzed by flow cytometry (BD LSR Fortessa Analyser; BD Biosciences). Results were analyzed with the FlowJo software.

2.3.3 Assay of HIV-1 inhibition by AMD3100 and maraviroc

A total of 1.2×10^6 TZM-bl cells were seeded in a 24-well plate 20 hours before infection. The TZM-bl cells were then incubated with 0, 5.14×10^{-5}, 2.67×10^{-4}, 1.28×10^{-3}, 5.14×10^{-3}, 0.01 μg/ml of X4 inhibitor AMD3100 or R5 inhibitor Maraviroc for 1 hour. The TF viruses and V3-loop NL4-3 mutant viruses (normalized for RT activity) were used to infect TZM-bl cells. The cells were harvested 40-hour post-infection and luciferase activity was measured. AMD3100 (catalogue number 8128) and Maraviroc (catalogue number 11580) were both obtained from the NIH AIDS reagent program.

The duo-tropic 89.6 bearing IFITM1, 2 or 3 were produced by co-transfection of the 89.6 HIV-1 DNA and IFITM expression vector into HEK293T cells. The viruses were quantified by measuring the RT activity. Twenty hours after plating TZM-bl cells in 24-well plates, the cells were incubated with fresh 10% FBS DMEM P/S medium containing no drug, 0.02 μg/ml AMD3100 or 0.02 μg/ml Maraviroc for 1 hour. Subsequently, the cells were infected by 89.6, 89.6-IFITM1, 89.6-IFITM2 or 89.6-IFITM3 of an equal amount of RT activity. NL4-3 and AD8-1 were included as positive controls. The cells were incubated for another 40 hours before harvesting, and the luciferase activity was measured.

2.3.4 Neutralization assay with antibodies and soluble CD4 (sCD4)

Monoclonal neutralizing antibodies, VRC03 (catalogue number12032), 17b (catalogue number 4091), 7H6 (catalogue number12295), 10E8 (catalogue number 1294), 447-52D (catalogue number 4020), 10-1074 (catalogue number 12477), PG16 (catalogue number 12150) and CH01 (catalogue number 12561), and sCD4 (catalogue number 4615) were obtained from NIH AIDS reagent program. Viruses were adjusted according to their RT activity, in a final infection volume of 100 µl. The viruses were then incubated with each of the antibody or sCD4 at the concentration indicated in Table 1 for 1 hour at 37 ^{o}C, 5%CO_2.

Table 1: Concentrations of antibodies and sCD4 for neutralization assay

Neutralizing antibodies	Concentration (µg/ml)				
VRC03	0	0.125	0.25	0.5	1.0
17b	0	0.25	0.5	1.0	2.0
7H6	0	0.1	0.2	0.5	1.0
10E8	0	0.1	0.2	0.5	1.0
447-52D	0	0.1	0.2	0.5	2.0
10-1074	0	0.1	0.2	0.5	1.0
PG16	0	0.02	0.05	0.1	0.2
CH01	0	0.25	0.5	1.0	2.0
sCD4	0	0.025	0.05	0.1	0.2	0.5

TZM-bl were pre-seeded in 24-well plate 20 hours prior and were then infected with the pre-incubated virus mixture. The fresh medium was added into each well to achieve a final volume of 1 ml and incubated for 40 hours prior to measurement of luciferase activity.

2.4 Protein Analysis

2.4.1 Co-immunoprecipitation (Co-IP)

HEK293T were seeded and transfected as described in 2.2.2. Cells were gently washed with 5 ml of cold PBS three times in the cell culture plate (10 cm). Cold PBS (5 ml) was added into each plate and cells were harvested using a cell lifter (Fisher Scientific) into 15 ml Falcon tubes. The cells were pelleted at 1500 rpm (CS-6R; Beckman Coulter) for 5 minutes, and then lysed in 500 μl of the cell lysis buffer followed by incubation on ice for 40 minutes. The cell lysis buffer used for Co-IP consisted of 50 mM Tris-HCl (pH 8.0), 100 mM NaCl, 1 mM EDTA, 1% Triton X-100, and protease inhibitors. Lysed cells were transferred into EP tubes and centrifuged at 13200 rpm (Microfuge 16; Beckman Coulter) for 15 minutes. Affinity gel with FLAG antibody (Sigma-Aldrich) was used for precipitating FLAG-tagged IFITMs and FLAG-tagged transferrin. The beads were washed once with 1 ml of the RIPA lysis buffer (without protease inhibitor), and were incubated on ice for 5 minutes. The cell lysates and beads were then incubated overnight (16 hours) on an orbital shaker at 4^{o}C. Beads were then pelleted at 2500 rpm for 5 minutes at 4^{o}C. The supernatants were transferred to fresh EP tubes and stored at -80 ^{o}C. The beads were washed with 1 ml protease-free cell lysis buffer twice using the orbital shaker and were further washed twice with 1 ml of Tris buffer saline (TBS: 50 mM Tris-HCl at pH7.4 and 150 mM of NaCl). After the last wash, 50 μl of 3× Flag peptide elution solution was added and gently mixed by tapping the tubes every 5 minutes during the 30 minutes incubation on ice. The beads were then pelleted at 6000 rpm for 6 minutes in the cold room. The eluates were carefully transferred into fresh EP tubes. The eluates were prepared and analyzed by western blot.

2.4.2 Western blot

The cells were harvested and lysed with Cytobuster protein extraction reagent (catalogue number 71009; EMD Millipore Novagen) containing protease inhibitor (catalogue number 11836153001; Roche) on ice for 1 hour. The cell debris ware removed by centrifuging cell lysates at 13200 rpm (Microfuge 16; Beckman Coulter) for 20 minutes at 4 ^{o}C. The lysates were then denatured by adding the 4X protein loading buffer followed by 5-minute boiling. The protein samples were loaded onto 1% sodium dodecyl sulfate (SDS) (catalogue number SDS001; BioShop) - 12% polyacrylamide (catalogue number ACR009; BioShop) gels for the detection of tubulin, Gag and FLAG-IFITM3, and onto 1% SDS 8% polyacrylamide gels for the detection of Env. The protein was separated by electrophoresis at 100 V for 2~3 hours, and then transferred onto polyvinylidene difluoride (PVDF) membrane (catalogue number 3010040; Roche). The membrane was blocked in 5% skim milk dissolved in 1X PBS with 0.1% Tween 20 (catalogue number TWN510; BioShop) (PBST) for 1 hour, followed by incubation with a 1:5,000 dilution of primary antibodies for 2 hours at room temperature. After washing with PBST, the membranes were further incubated with a 1:10,000 dilution of secondary antibodies for 1 hour at room temperature. The primary antibodies included: monoclonal mouse α-tubulin antibody (B-5-1-2) (catalogue number sc-23948; Santa Cruz Biotechnology), monoclonal mouse α-flag antibody (catalogue number F1804-1MG; SIGMA-ALDRICH), polyclonal rabbit α-p24 antibody (catalogue number SAB3500946; SIGMA-ALDRICH), monoclonal mouse α-gp41 antibody (catalogue number 526; NIH AIDS reagent program), and sheep α-gp120 antiserum (catalogue number 288; NIH AIDS Reagent program). The secondary antibodies included enhanced chemiluminescence (ECL) rabbit IgG Horseradish peroxidase (HRP)-linked whole antibody from donkey (catalogue number NA934V; GE Health Care Life Science), ECL Mouse HRP-

linked IgG whole antibody from sheep (catalogue number NA931; GE Health Care Life Science), and HRP-rabbit anti-Sheep IgG (catalogue number 618620; Invitrogen). The membranes were treated with Western Lightening Plus-ECL Enhanced Chemiluminescence Substrate (catalogue number NEL105001EA; PerkinElmer), and the chemiluminescent signals were detected by exposure to X-ray film (catalogue number 6041768; Carestream).

2.4.3 Quantification of Western blot signals

The intensity of protein bands was quantified using the ImageJ software. Since only relative band intensity is measured via ImageJ, protein bands from gp120 and gp160 of the same virus sample (two bands of the same lane) were quantified together at the same time. The degree of Env processing from each virus sample was calculated using the following formula: band intensity of gp120/(band intensity of (gp120+gp160)).

2.4.4 HIV-1 Env stability assay

HEK293T cells were transfected with proviral DNA [503]. Twenty-four hours after transfection, cells were metabolically labelled with 100 μCi/ml of [^{35}S]methionine-cysteine (catalogue number NEG772007MC; PerkinElmer) dissolved in 5% dialyzed FBS-supplemented methionine- and cysteine-negative DMEM for 16 hours. The cells were then lysed in RIPA buffer containing 140 mM NaCl, 8 mM Na_2HPO_4, 2 mM NaH_2PO_4, 1% NP-40, and 0.05% SDS. The radiolabelled Env proteins in the cell lysates or supernatants were precipitated using serum from HIV-1 patients for 1 hour at 37 °C. The immunoprecipitated samples were separated by migration on a polyacrylamide gels and analyzed using a PhosphorImager (Molecular Dynamics). The association index measures the relative ability of the gp120 domain to stay on the Env trimer on virus-producing cells. The association index values thus describe the intrinsic stability of the association between gp120 to gp41. A low association index is a good

indicator of decreased levels of gp120 in virus particles [504,505]. The association index of NL4-3 was arbitrarily set to a value of 1, and the values for other viruses were calculated relative to the value for NL4-3 association index = [(target gp120) $_{\text{cell lysate}}$ × (NL4-3 gp120) $_{\text{supernatant}}$]/[(target gp120) $_{\text{supernatant}}$ × (NL4-3 gp120) $_{\text{cell lysate}}$]. The processing index measures the relative efficiency of Env maturation from the gp160 precursor to gp120. The processing index of NL4-3 was arbitrarily set to a value of 1, and the values for other viruses were calculated relative to the value for NL4-3 processing index = [(total gp120) $_{\text{target}}$ × (gp160) $_{\text{NL4-3}}$]/[(gp160) $_{\text{target}}$ × (total gp120) $_{\text{NL4-3}}$].

2.4.5 Statistical analysis

The *P* values were calculated based on the unpaired two-tailed t-test. A *P* value that is smaller than 0.05 was deemed statistically significant. The R^2 values and the *P* values in the correlation graphs were calculated based on the linear regression module implemented in the Excel program.

Chapter III: Results

3.1 HIV-1 Env confers resistance to IFITM3

3.1.1 HIV-1 strains have differential responses to IFITM1, 2 or 3 inhibition, and the V3 loop of Env determines the viral sensitivity to IFITMs.

The studies by Compton's and Tartour's group on IFITMs [506,507], when expressed on the virus producer cells, unveiled another potent role of IFITM proteins in inhibiting HIV-1, which prompted me to study the mechanism of IFITM inhibition in virus producer cells. I first investigated the sensitivity of different HIV-1 strains to IFITM 1, 2, or 3 expressed in virus producer cells. A laboratory-adapted strain X4-tropic NL4-3, a duo-tropic primary isolate 89.6, and two R5-tropic primary isolates YU-2 and AD8-1 were tested for their susceptibility to IFITMs. In this system, I produced the viruses by transfecting the DNA of each HIV-1 strain together with either IFITM1, 2 or 3 DNA into HEK293T cells. The viruses harvested (normalized for RT activity) were then used to infect TZM-bl luciferase reporter cells. The luciferase gene in TZM-bl cells has HIV LTR as its promoter, and therefore, can be activated by Tat. The amount of luciferase is thereby regulated by the amount of Tat following virus infection.

IFITM1, 2 or 3 expressed in the virus-producing cells demonstrated differential inhibitory potency on the tested strains in a dose-dependent manner (Figure 12). Consistent with the previous paper from our lab, NL4-3 was resistant to IFITM1[483]. In contrast, IFITM1 inhibited 89.6 and AD8-1. In the case of YU-2, its infectivity was increased by up to 4.5-fold by IFITM1. All the HIV-1 strains except AD8-1 were inhibited by IFITM2 to different degrees. The 89.6 was

the most sensitive HIV-1 strain to IFITM2 inhibition, with a 5-fold decrease in its infectivity. YU-2 and NL4-3 were moderately inhibited by IFITM2 to 2- and 2.5-fold, respectively, when 200 ng of IFITM2 was co-transfected, whereas AD8-1 was completely resistant to IFITM2. Differential inhibition was also observed for IFITM3. The infectivity of NL4-3 was inhibited by 5-fold when IFITM3 was expressed in the virus-producing cells. Compared to IFITM2, 89.6 and YU-2 were more resistant to IFITM3 inhibition, with a 3- and 1.7-fold reduction in their infectivity. AD8-1 was refractory to IFITM3 inhibition, as in the cases for IFITM1 and 2. It is interesting to note that the expression of IFITM1 or IFITM2 in the producer cells reduced the production of NL4-3, 89.6, YU-2, but not AD8-1 (Figure 12). In contrast, IFITM3 exerted a minimal effect on virus production, consistent with our previous reports [463,508]. In summary, NL4-3, 89.6 and YU-2 are subject to differential inhibitory potency by IFITM proteins, whereas the AD8-1 is completely resistant to all three IFITMs.

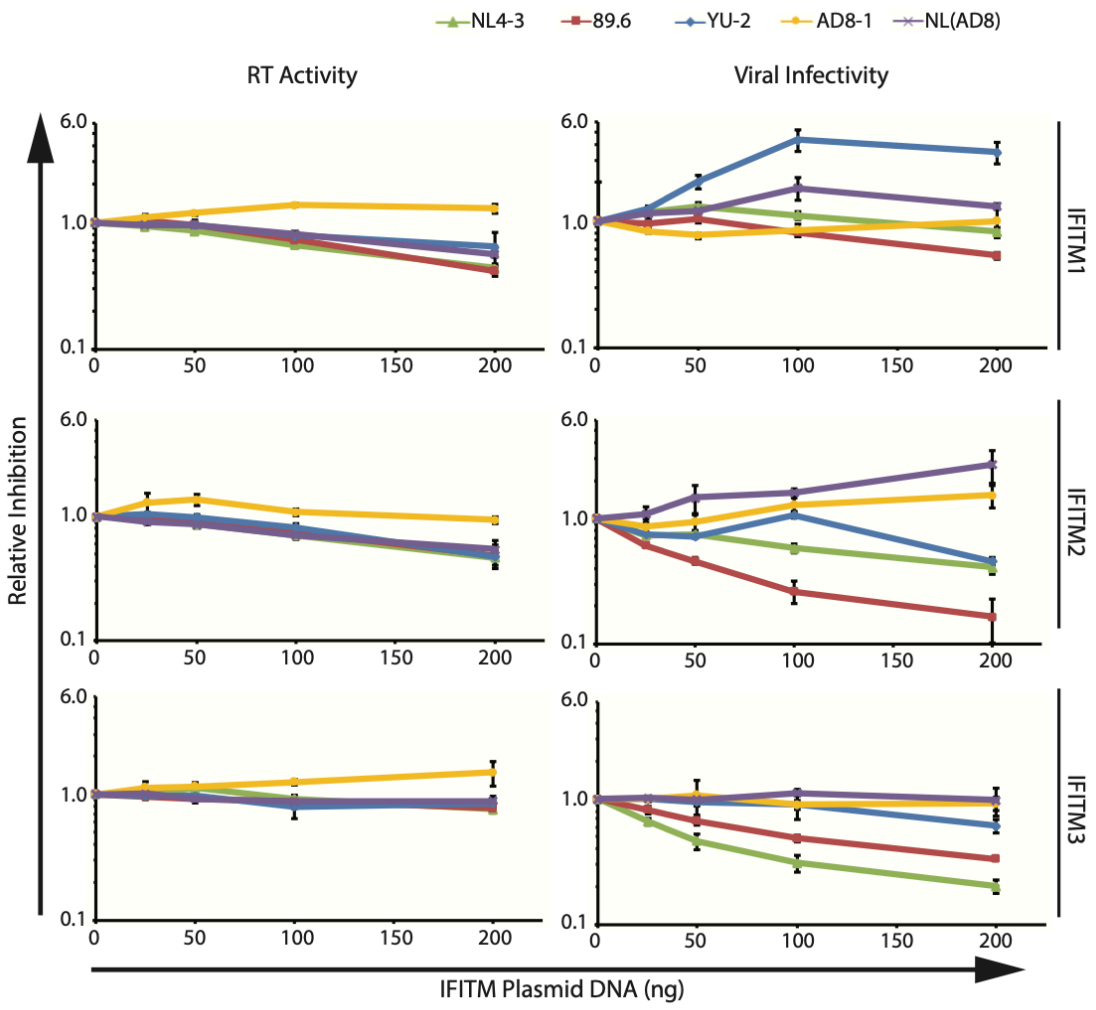

Figure 12: Susceptibility of NL4-3, 89.6, YU-2, AD8-1 and NL(AD8) to different doses of IFITM1, 2 and 3. The proviral DNA was transfected into HEK293T cells with the empty pQCXIP vector, or IFITM1, IFITM2 or IFITM3 expressing vector. The level of virus production was quantified by measuring the RT activity of the supernatants. HIV-1 infectivity was assessed by infecting TZM-bl cells. The x-axis represents the amount of IFITM DNA used for transfections. The levels of RT activity or viral infectivity of each virus in the absence of IFITMs are arbitrarily set to a value of 1. The y-axis represents relative inhibition by individual IFITMs.

The values were calculated by comparing the RT activity or infectivity of IFITM-bearing viruses to the IFITM-free controls. The experiments have been repeated six times, and the error bars were plotted based on the SEMs.

Next, I sought to determine which viral protein in AD8-1 helps the virus escape the antiviral activity of IFITM3. From a previous study done by our lab, IFITMs inhibit virus entry. Since we have previously shown that HIV-1 strain BH10 mutated its viral Env protein to escape from IFITM1 inhibition [483], I suspected that Env might be behind the IFITM3-resistant property of AD8-1. Therefore, I tested NL(AD8), a NL4-3 mutant which *env* sequence was replaced by the AD8-1 *env* [500] (Figure 13A). In support of our hypothesis, NL(AD8) produced from IFITM1, 2 or 3 expressing HEK293T cells showed robust resistance to all three IFITMs (Figure 12 and 13B). Of note, virus production of NL(AD8) was reduced by IFITM1 and IFITM2 to the same level of NL4-3, because NL(AD8) expressed NL4-3 genes except for the *env* (Figure 12 and 14). To evaluate Gag and IFITM3 expression for each strain, virus-producing cells and viruses were subject to WB analysis (Figure 13C). The WB results confirmed that NL(AD8) Gag expression was reduced with IFITM1 or 2 but not IFITM3, which was in agreement with results of RT assays (Figure 12, 13C and 14).

Collectively, these data suggest that by substituting Env of NL4-3 with that of AD8-1, the mutant NL4-3 becomes resistant to IFITMs. Therefore, Env is the viral protein that determines the viral sensitivity to IFITMs inhibition. Across strains that have demonstrated differential sensitivities to IFITM3, the amount of IFITM3 protein expressed in the virus producer cells, as well as the amount of IFITM3 incorporated in the virions, were not correlated with the viral susceptibility to IFITM3 (Figure 13C).

Nonetheless, I observed that an increase in the IFITM expression resulted in a more potent inhibition in IFITM-susceptible strains (Figure 12 and 14). The amount of Env and Gag showed a gradual decrease concurrent with the increase in the level of IFITM1 and IFITM2 for NL4-3, 89.6, YU-2 and NL(AD8). In contrast, AD8-1 Env and Gag levels were not reduced by IFITM1 or 2. Consistent with the results of RT activity, IFITM3 expression did not reduce Gag levels in all tested viruses (Figure 12 and 14). Therefore, IFITM3 inhibits HIV-1 infection by means other than interfering with viral production.

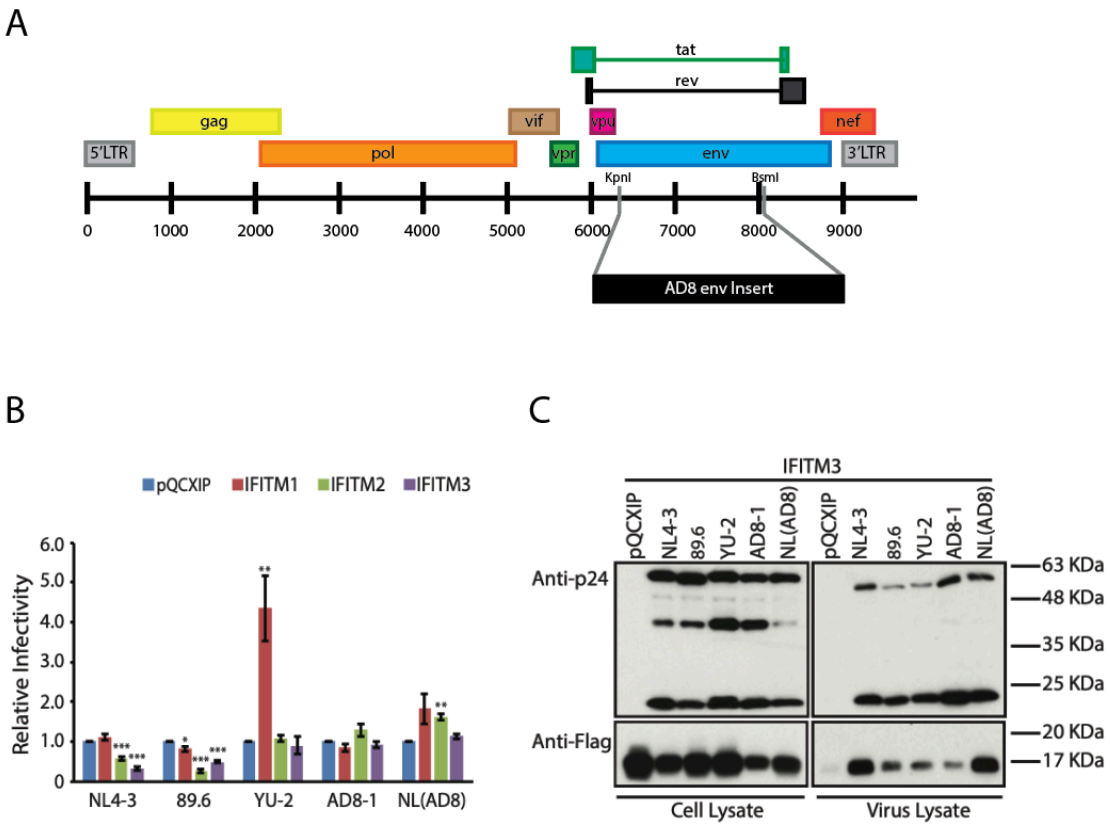

Figure 13: Env modulates the HIV-1 sensitivity to IFITMs. (A) The gene map of the NL(AD8) construct. On the NL4-3 backbone, a major fragment of the *env* gene has been substituted by the AD8 *env* gene. As such, the construct produces NL4-3 virions that carry AD8 Env. (B) The relative infectivity of different HIV-1 strains produced from HEK293T cells

transfected with 100 ng of IFITM DNA. The volumes of viruses with the same amount of RT activity were used to infect TZM-bl cells. Viral infectivity was measured by conducting the luciferase assay. The relative infectivity was obtained by comparing the infectivity of IFITM-bearing viruses to that of the IFITM-free controls, which are arbitrarily set to a value of 1. The experiments were performed six times independently, and the average is shown in (B) together with the SEM. Student t-test has been done to assess the statistical significance of the difference in relative infectivity (*, $P < 0.05$; **, $P < 0.01$; ***, $P < 0.001$). (C) The WB images of the virus-producing cells and the virus lysates were shown. Anti-p24 and anti-FLAG antibodies were used to probe Gag and IFITM3.

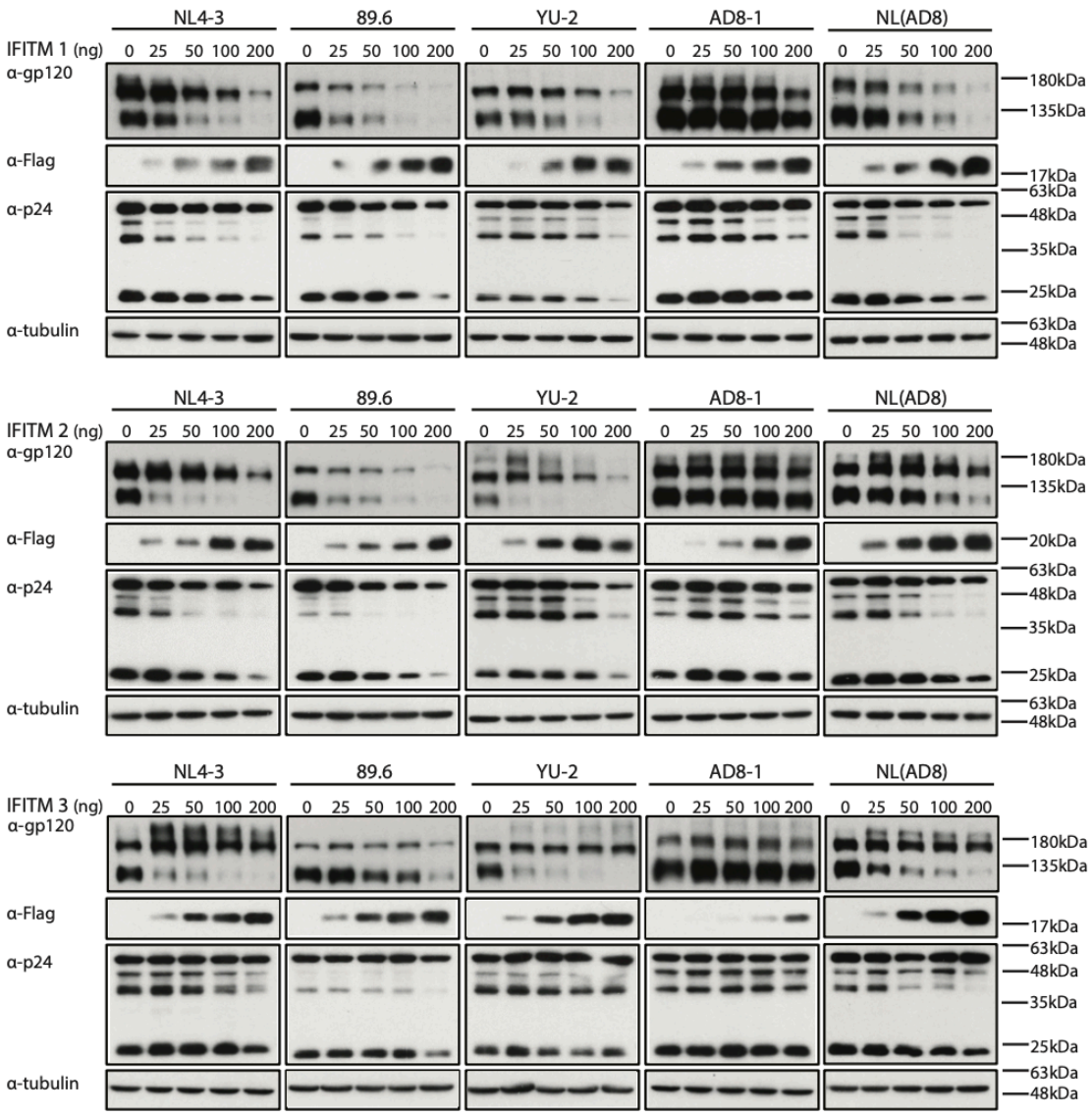

Figure 14: Western blot of the virus-producing HEK293T cells transfected with different doses of IFITM DNA. The virus-producing cells were harvested, and western blot was performed on the cell lysates to assess IFITM expression and the production of viral proteins. Tubulin was used as the loading control. The anti-gp120 and anti-p24 antibodies were used for Env and Gag detection. All the IFITM proteins were detected by anti-FLAG antibody.

From the previous observation that the Env is sufficient to alter IFITM sensitivity of HIV-1, I was prompted to map IFITM3-resistance to a specific domain of Env. AD8-1 differs from NL4-3 for the co-receptor usage, and V1, V2, and V3 loop have been shown to make a major contribution to co-receptor selection [509,510]. Therefore, I tried to construct NL4-3 mutants by replacing the V1, V2, or V3 loop of NL4-3 with the corresponding sequence from AD8-1. In order to achieve precise replacement of the desired sequence, NL4-3 *env* inserts that contain either V1, V2, or V3 loop from AD8-1were synthesized (Figure 15A). NL4-3-AD8V1, -AD8V2, -AD8V3 mutant *env* were inserted into the pNL4-3 construct to generate three mutants, namely NL(AD8V1), NL(AD8V2) and NL(AD8V3). The NL(AD8V1), NL(AD8V2), and NL(AD8V3) viruses were then produced from IFITM3-expressing or control HEK 293T cells. The level of virus production was quantified by measuring RT activity, and the same amount of viruses were used to infect TZM-bl cells. As shown in Figure 15, there is no significant variation in virus production among different mutant strains (Figure 15B). In agreement with my previous observation, IFITM3 did not affect virus production. However, two of these mutant viruses, pNL(AD8V1) and pNL(AD8V2), failed to produce viable virions (Figure 15C). The incompatibility of variable domains from different HIV-1 strains has been reported in other studies as well [511]. Only NL(AD8V3) virus was viable and also showed resistance to IFITM3. Together, these results suggest that the V3 loop of an IFITM3-resistant HIV-1 is sufficient to render IFITM3 resistance to a previously IFITM3-sensitive strain.

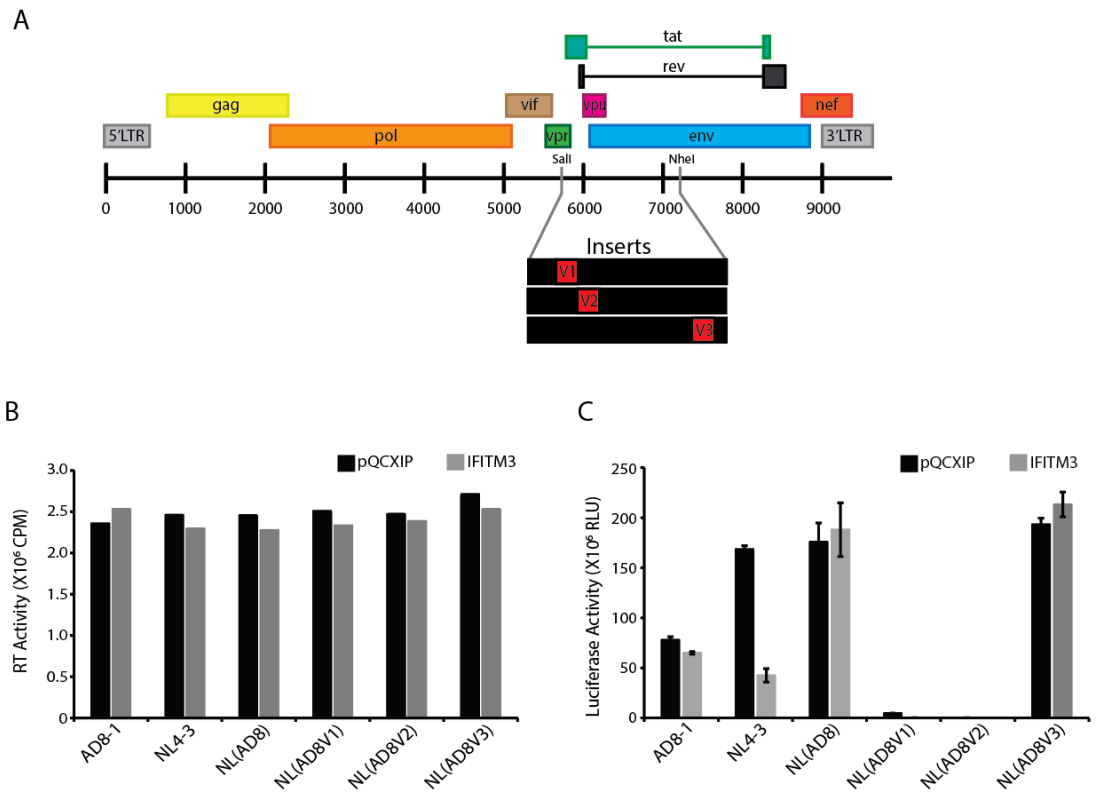

Figure 15: V3 loop of the Env is sufficient to render resistance to the otherwise IFITM3 sensitive NL4-3. (A) Illustration of the V1, V2, V3 loops of NL4-3 Env replaced with the counterparts of AD8 Env. Each NL4-3 mutant expresses either AD8V1, AD8V2 or AD8V3 in the context of NL4-3 Env. (B) Virus production is assessed by the RT activity of the supernatant. 100 ng of IFITM3 DNA was transfected into HEK293T cells to produce IFITM3-bearing viruses. The RT activity showed that IFITM3 expression in the virus-producing cells did not affect the total amount of produced virus. (C) The infectivity of the viruses was evaluated by infecting TZM-bl cells. The luciferase activity data showed that only the NL(AD8V3) mutant established successful infection in TZM-bl cells and demonstrated a robust resistance to IFITM3 inhibition. The average of three data points is shown in the graph, and the error bars are plotted based on calculated SEM.

3.1.2 The V3 loop of Env governs the viral sensitivity of TF viruses to IFITM3.

To determine the prevalence of IFITM3 resistance in the TF viruses, I tested ten TF viruses for their sensitivity to IFITMs. TF viruses were produced from HEK293T cells that ectopically expressed IFITM1, IFITM2 or IFITM3. The level of viral production was assessed by their RT activities, and the infectivity was measured by infecting TZM-bl cells. Similar to what I observed in Figure 1 and 2, IFITM1 diminished virus production of tested TF viruses to varying degrees (1.2- to 1.65-fold reduced RT activity) (Fig.16A). To a lesser extent, IFITM2 also reduced virus production. IFITM3 showed no effect on virus production of TF viruses THRO, ZM246F and ZM247F. For the TF viruses, including CH040, CH058, CH077, CH106, REJO and WITO, there was in fact a 1.1- to 1.3-fold increase in virus production, which has also been observed for AD8-1 (Figure 12 and 16A). Interestingly, IFITM1 appeared to increase the infectivity of CH058, CH106, REJO, RHPA, THRO, WITO and ZM247F by 1.7 to 3-fold (Figure 16B). The remaining strains, CH040, CH077 and ZM246F, showed complete resistance to IFITM1 restriction. Most of TF viruses were sensitive to IFITM2 restriction, except CH058, THRO, WITO and ZM247F (Figure 16B). Among the IFITM2 resistant strains, CH058 was sensitive to IFITM3 inhibition along with CH077, CH106, REJO and RHPA. Therefore, among all the tested TF viruses, THRO, WITO and ZM247F demonstrated resistance to all three IFITM proteins.

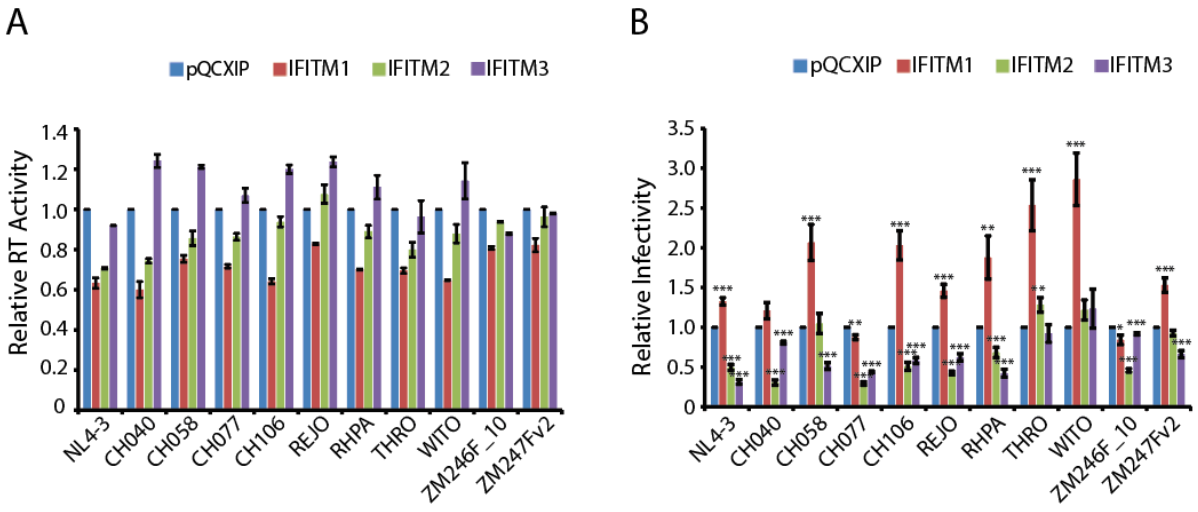

Figure 16: Susceptibility of the TF viruses to IFITM1, 2 or 3. (A) The level of virus production was assessed by measuring RT activity of the supernatants. (B) Viral infectivity was measured by infecting TZM-bl luciferase reporter cells. The values of relative inhibition/relative RT activity were calculated by comparing the RT or luciferase activity of IFITM-bearing viruses to that of the IFITM-free control. The control RT and luciferase activity were arbitrarily assigned a value of 1. The experiments were repeated four times, and the error bars were plotted based on the SEMs. Student t-test was run to assess the statistical significance of the difference in the fold of inhibition (*, $P < 0.05$; **, $P < 0.01$; ***, $P < 0.0001$).

Next, I investigated whether the V3 loop of other HIV-1 strains can alter NL4-3's response to IFITM3. The V3 loop of YU-2, WITO, THRO and RHPA were inserted into the pNL4-3 plasmid to construct NL4-3 mutants, namely NL(YU-2V3), NL(WITOV3), NL(THROV3) and NL(RHPAV3) (Figure 17A). The IFITM3-bearing V3-loop mutant viruses were produced and used to infect TZM-bl cells. The viruses were produced at a larger scale compared to those produced in previous experiments. Although the ratios of the viral plasmid

and the IFITM3 DNA used in transfection were kept constant, the increase in the net amount of IFITM3 DNA may have led to a more pronounced anti-HIV-1 inhibitory activity of IFITM3 (Figure 17B). Nevertheless, AD8-1 and NL(AD8) remained IFITM3-resistant (Figure 17B). Therefore, IFITM3-resistant HIV-1 does not become susceptible to IFITM3 inhibition despite the increased expression of IFITM3.

The results showed that NL(AD8V3) was resistant to IFITM3, as I have previously observed (Figure 15C and 17C). NL(WITOV3) was completely resistant to IFITM3 inhibition, recapitulating the IFITM3-resistant phenotype exhibited by WITO. NL(YU-2V3) and NL(THROV3) were inhibited by IFITM3 to 5.4- and 4.5-fold, respectively. However, compared to the degree of inhibition experienced by NL4-3, 13-fold decrease, NL(YU-2V3) and NL(THROV3) were 2.4- and 2.8-fold more resistant to IFITM3 inhibition, respectively. The increase in resistance to IFITM3 was comparable to what has been observed in YU-2 and THRO, which were 2.9- and 2.6-fold more resistant to IFITM3 inhibition compared to NL4-3 (Figure 17C and 16B). By substituting the V3 loop of NL4-3 for that of YU-2 and THRO, the mutated viruses responded to IFITM3 inhibition in similar manners to the V3 loop donor viruses. Therefore, the V3 loop of Env is the determinant in the HIV-1 sensitivity to IFITM3 inhibition and IFITM3-resistant V3 loop alone is sufficient to confer resistance to IFITM3 in the context of NL4-3. One interesting observation in NL(RHPAV3) was its IFITM3 resistant property despite the modest IFITM3 sensitivity of RHPA. This result suggests that although the V3 loop has an essential role in governing the viral sensitivity to IFITM3, other viral factors are also involved.

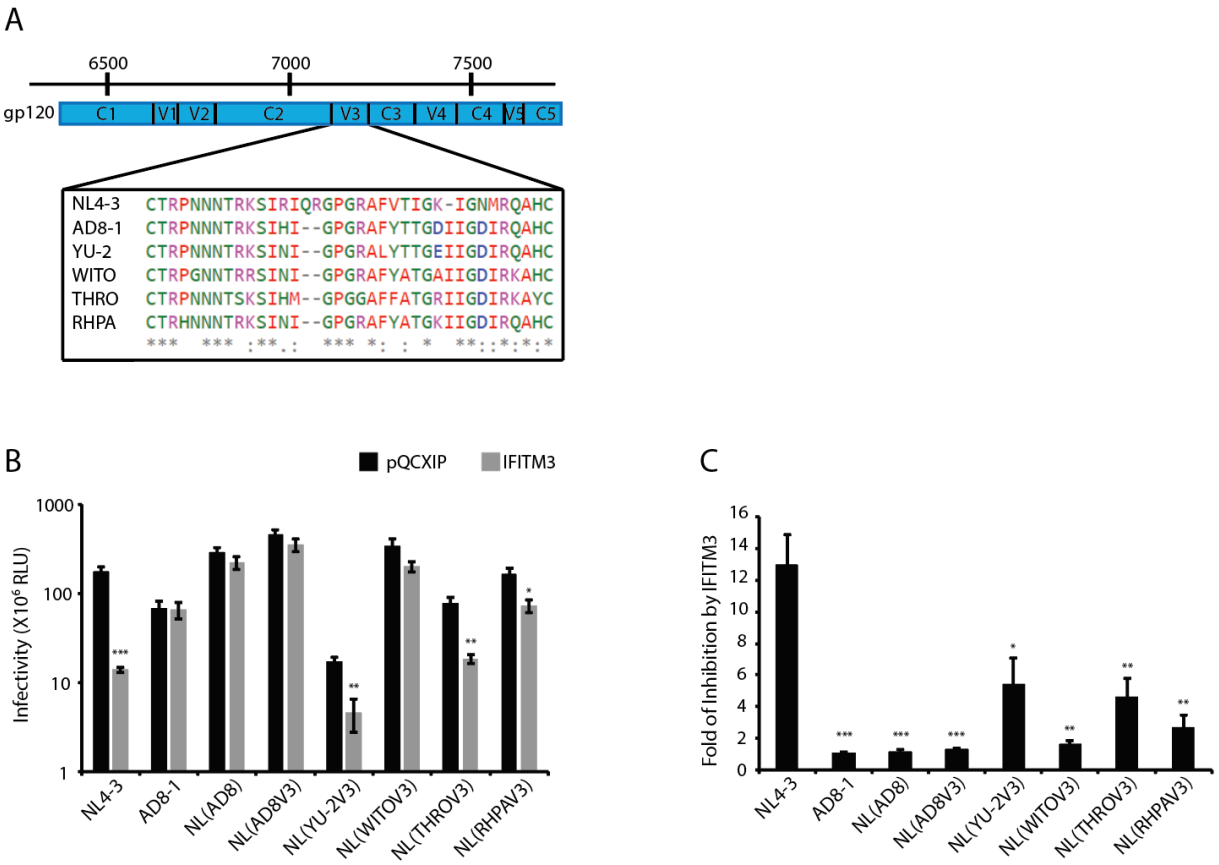

Figure 17: The V3 loop of Env is sufficient to determine HIV-1 sensitivity to IFITM3. (A) Illustration of the domain of gp120. The NL4-3 mutants express the V3 loop from different primary isolates, including from TF viruses. (B) Viruses normalized for RT activity were used to infect TZM-bl cells. Experiments were conducted three times in triplicates. The average luciferase activity is shown in the graph, and the SEMs are displayed as the error bars. (C) Fold inhibition of viral infection by IFITM3 was calculated by dividing the infectivity of the IFITM3-bearing viruses with that of the IFITM3-free controls. Student t-test was performed to determine whether the difference in the relative infectivity was statistically significant (*, $P < 0.05$; **, $P < 0.01$; ***, $P < 0.001$).

3.1.3 Virion-associated IFITM3 impedes HIV-1 entry to the target cells.

IFITM3 expressed in the virus target cells has previously been shown to inhibit HIV-1 entry to the cells. This finding prompted me to verify whether the IFITM3 expressed in the virus-producing cells also exerts its inhibitory effect at the viral entry stage. To assess the impact of IFITM3 on virion fusion, the BlaM-Vpr entry assay was performed. The BlaM-Vpr containing HIV-1 viruses were produced from IFITM3-expressing or control HEK293T cells. Equal amount of viruses were used to infect C8166-R5 cells. The percentage of infected cells was quantified by flow cytometry (Figure 18A). The occurrence of fusion is detected by the change in fluorescent colour from AmCyan to Pacific Blue, resulting from successful cleavages of CCF2 by beta-lactamase.

The entry efficiency of the IFITM3-bearing and IFITMs-free viruses was assessed (Figure 18A and 18B). The expression of IFITM3 in the virus-producing cells diminished the entry of NL4-3, NL(YU-2V3) and NL(THROV3) to C8166-R5 cells with 5-, 4- and 3-fold, respectively (Figure 18C). The IFITM3 resistant viruses AD8-1, NL(AD8V3), NL(WITOV3), and NL(RHPAV3) were all refractory to the IFITM3 inhibition of virus entry, which is in agreement with results presented in Figure 17. Together, these results suggest that the expression of IFITM3 in virus-producing cells hampers the HIV-1 infection at the viral entry step.

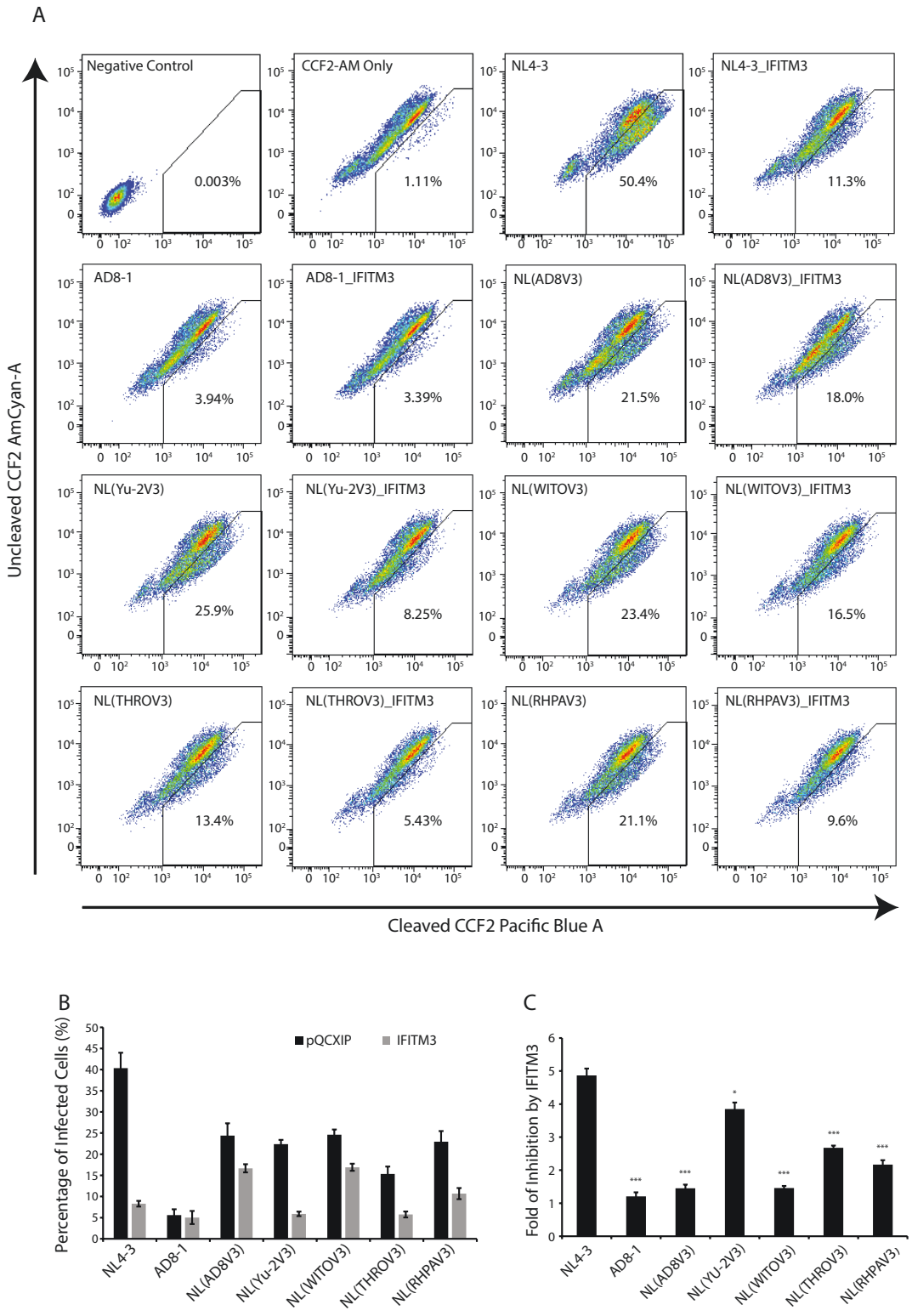
A
Negative Control
0.003%
CCF2-AM Only
1.11%
NL4-3
50.4%
NL4-3_IFITM3
11.3%
AD8-1
3.94%
AD8-1_IFITM3
3.39%
NL(AD8V3)
21.5%
NL(AD8V3)_IFITM3
18.0%
NL(Yu-2V3)
25.9%
NL(Yu-2V3)_IFITM3
8.25%
NL(WITOV3)
23.4%
NL(WITOV3)_IFITM3
16.5%
NL(THROV3)
13.4%
NL(THROV3)_IFITM3
5.43%
NL(RHPAV3)
21.1%
NL(RHPAV3)_IFITM3
9.6%
Uncleaved CCF2 AmCyan-A
Cleaved CCF2 Pacific Blue A
B
Percentage of Infected Cells (%)
pQCXIP
IFITM3
NL4-3
AD8-1
NL(AD8V3)
NL(Yu-2V3)
NL(WITOV3)
NL(THROV3)
NL(RHPAV3)
C
Fold of Inhibition by IFITM3
NL4-3
AD8-1
NL(AD8V3)
NL(YU-2V3)
NL(WITOV3)
NL(THROV3)
NL(RHPAV3)

Figure 18: IFITM3 impedes the entry of HIV-1. The BlaM-Vpr assay was performed to assess the efficiency of IFITM3-bearing HIV-1 and IFITM3-free HIV-1 (control viruses) entry to the cells. IFITM3-bearing and control viruses were used to infect C8166-R5 cells. The infected cells were quantified by detecting the Pacific Blue A signal, which is produced upon the cleavage of CCF2. (A) Results of one representative BlaM-Vpr assay. (B) The percentage of infected C8166-R5 cells with either IFITM3-bearing or the control HIV-1 viruses. The experiments were performed two times independently in triplicates. The average of one set of triplicated experiments are shown, and the SEM is shown as the error bars. (C) Fold inhibition of viral infection by IFITM3 was obtained by comparing the percentage of control virus-infected cells to that of the IFITM3-bearing viruses. The percentage of control viruses infected C8166-R5 cells is arbitrarily assigned a value of 1. The average fold inhibitions by IFITM3 from two independent experiments are presented. The values of SEM are calculated for each HIV-1 strain and are displayed as the error bars. Student t-test was run to determine the significance of differences (*, $P < 0.05$; *, $P < 0.01$; ***, $P < 0.001$).

Since IFITM3 is also expressed on HIV-1 target cells [506], I investigated whether HIV-1 strains resistant to IFITM3 when expressed in the virus-producing cells are also resistant to IFITM3 expressed on target cells. A derivative of the MT4-R5 cell line was tested, i.e. MT4-R5-IFITM3 cell line constitutively expressing IFITM3 was used as the target cells. NL4-3 and selected IFITM3-resistant primary strains were hence used to infect MT4-R5 or MT4-R5-IFITM3 cells. The infected MT4-R5 cells were then analyzed by flow cytometry (Figure 19A). The results showed that NL4-3 was also sensitive to IFITM3 expressed in the target cells with a 7.5-fold decrease in infection (Figure 19B). AD8-1, on the other hand, was less inhibited by

IFITM3 in the target cells with a 4-fold decrease in infection. The TF viruses, WITO, THRO, and ZM246F_10, were all resistant to IFITM3 in the target cells. In summary, NL4-3 is potently inhibited by IFITM3, and the TF strains are all resistant to IFITM3, whether it is expressed by producer or target cells. Despite the complete resistance to IFITM3 expressed in the producer cells, AD8-1 showed moderate sensitivity to the IFITM3 expressed in the target cells.

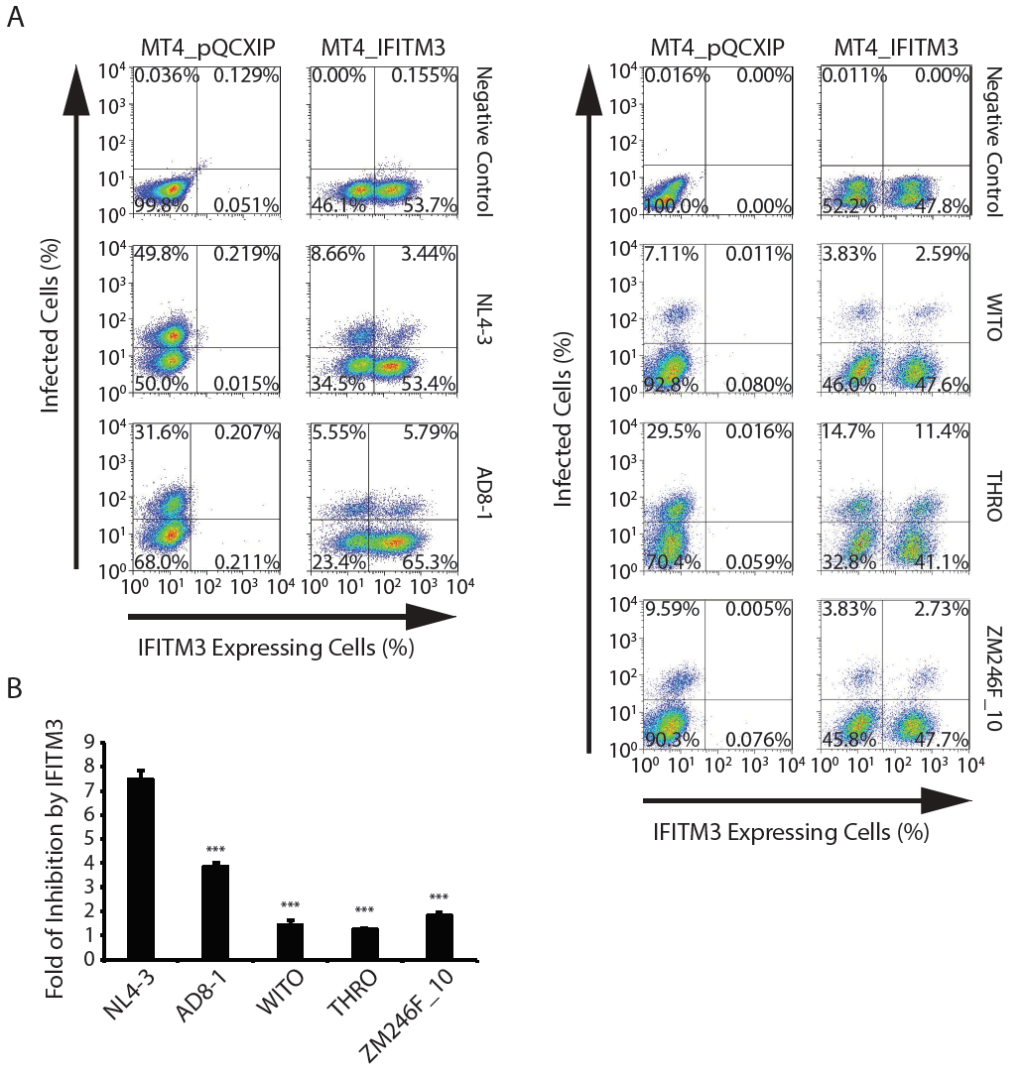

Figure 19: The inhibitory effects of IFITM3 in target cells on different HIV-1 strains. NL4-3, AD8-1, WITO, THRO and ZM246F_10 were used to infect MT4-R5 cells (termed MT4_pQCXIP in the figure) and MT4-R5-IFITM3 cells (termed MT4_IFITM3 in the figure).

The infected cells were quantified by measuring HIV-1 p24-positive cells using flow cytometry. (A) Results of the representative experiments. Anti-p24-FITC antibodies were used to label the infected cells, and anti-FLAG-DyLight 650 antibodies were used to assess the expression of IFITM3 in the MT4-R5 cells. (B) The fold inhibition by IFITM3 was calculated by dividing the percentage of infected MT4-R5 cells to that of MT4-R5-IFITM3 cells. Results from the three experiments are summarized, and the average is shown here. The error bars represent the SEMs. Student t-test was run to assess the statistical significance of the difference in the fold of inhibition (*, $P < 0.05$; **, $P < 0.01$; ***, $P < 0.0001$).

3.1.4 IFITM3 does not interfere with Env binding to its coreceptors.

Next, I investigated how the V3 loop modulates HIV-1 sensitivity to IFITM3. It has been known that the V3 loop determines HIV-1 coreceptor usage [509,510]. Therefore, the V3 loop from different HIV-1 strains could modulate the affinity of Env to the coreceptor. An increase in the binding strength of Env to its coreceptor may therefore offset the inhibitory effect exerted by IFITM3. To test this possibility, I looked for a correlation between the affinity of Env binding to its coreceptor and the sensitivity of such Env toward IFITM3 inhibition. Small-molecule inhibitors, AMD3100 and maraviroc were used to inhibit the binding of Env to its coreceptors. AMD3100 is a well-defined X4 antagonist, which binds to the X4 receptor and prevents the binding of its natural ligand SDF-1 as well as HIV-1 Env [512]. Maraviroc is a negative allosteric modulator of R5 receptor [513]. The binding of maraviroc to the R5 receptor prevents its interaction with the co-receptor binding sites of gp120. TZM-bl cells were incubated with AMD3100 or maraviroc at different concentrations for 1 hour prior to HIV-1 infection. YU-2, WITO, THRO and RHPA were used to infect TZM-bl cells to test for their affinity toward the coreceptors.

NL4-3, AD8-1 and 89.6 were used as positive controls for X4-, R5- and X4/R5-tropism, respectively. As expected, the infectivity of NL4-3 decreased with an increase in the concentration of AMD3100, while the virus was refractory to maraviroc inhibition (Figure 20A).

In contrast, AD8-1 demonstrated an exponential decrease in infectivity with an increase in maraviroc concentration but did not respond to AMD3100 inhibition. The infection of 89.6 was not affected by AMD3100 or Maraviroc treatment. Infections by YU-2, WITO, THRO and RHPA was not affected by ADM3100, while exponential reductions in their infectivity was observed under maraviroc treatment at a concentration of 0.00026 μg/ml (Figure 20A). The same experiments were performed on the NL4-3 mutants and NL4-3 wild type. The results showed that all the NL4-3 mutants were attenuated by maraviroc but not AMD3100, confirming the conversion of X4-tropic NL4-3 Env to R5-tropic mutant Env (Figure 20B). More importantly, the NL4-3 mutants exhibited differential sensitivity to maraviroc at the concentration of 0.00026 μg/ml, suggesting a difference in the affinity of Env to R5 among V3 loop mutant viruses. NL(AD8), NL(YU-2V3) and NL(THROV3) displayed more resistance to maraviroc, whereas NL(AD8V3) and NL(RHPAV3) were the most sensitive viruses. By plotting the correlation graph between the viral sensitivity to maraviroc and IFITM3 inhibition, I found that these two properties of the NL4-3 mutants did not correlate (Figure 20D). Therefore, these results reveal that the change in Env affinity to the coreceptors does not modulate the Env sensitivity to IFITM3 inhibition.

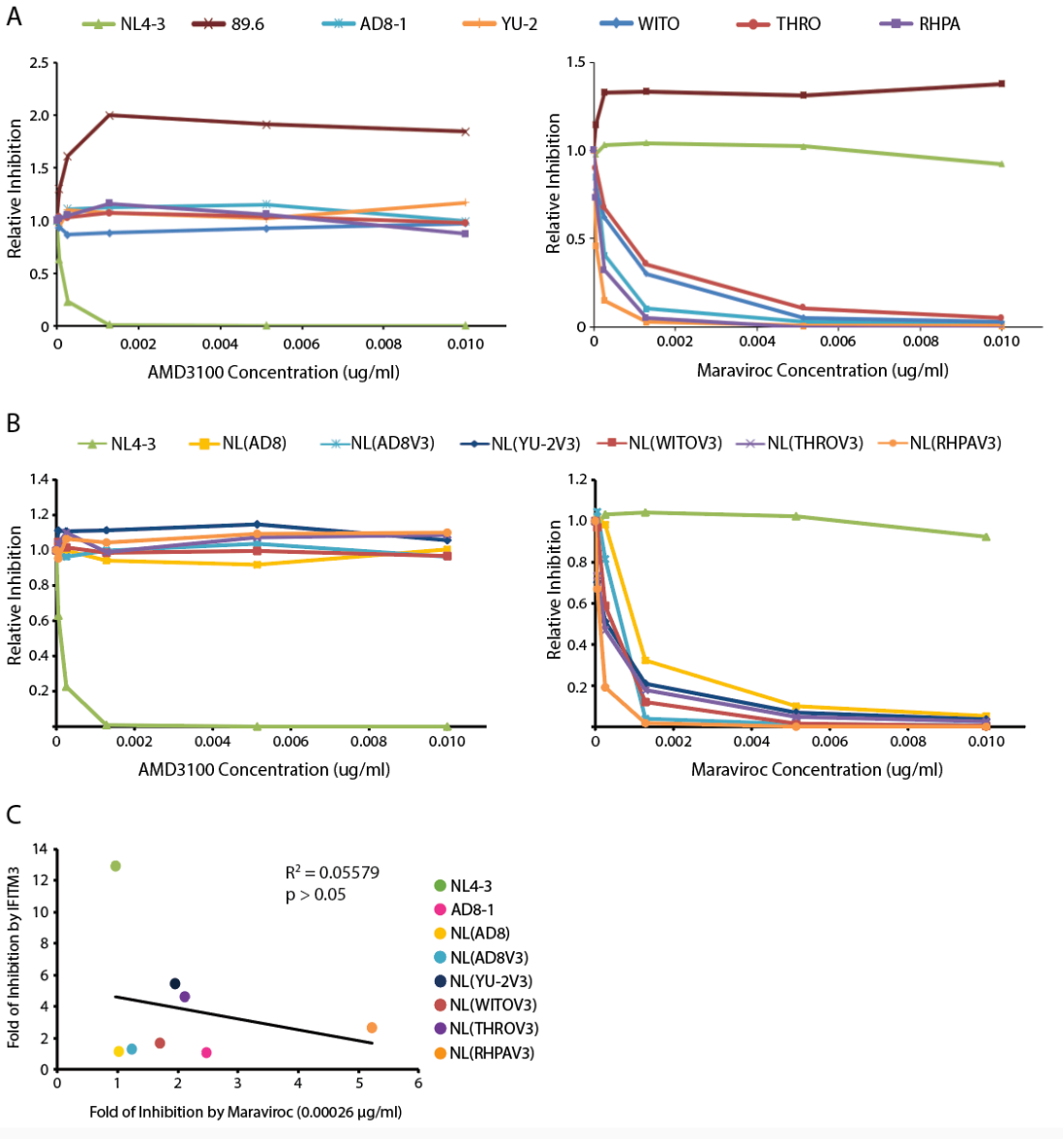

Figure 20: Effects of V3 loop on HIV-1 sensitivity to coreceptor inhibitors. TZM-bl cells were pre-incubated with AMD3100 or maraviroc of different concentrations for 1 hour prior to infection. HIV-1 were then used to infect TZM-bl cells. The TZM-bl cells were harvested 40 hours after infection for luciferase activity. The luciferase activities of individual infection without drug treatment were arbitrarily set a value of 1. The relative inhibitions were calculated by comparing the luciferase activities of virus infection with the drug treatments to the infection without drug treatment. (A) The effect of drug treatments on wild type HIV-1. (B) The effect of

changing the V3 loop of NL4-3 on the coreceptor selection and affinity of chimeric mutants. (C) Correlation between HIV-1 sensitivity to IFITM3 (data from Figure 17C) and 0.00026 μg/ml of maraviroc. Both R^2 and p-value suggest no significant correlation between the two parameters.

Since the IFITM3-resistant HIV-1 strains are R5-tropic and the sensitive strain uses X4 to enter the cells, I next tried to study whether the viral sensitivity to IFITM3 is related to its coreceptor tropism. I took advantage of the dual-tropic property of 89.6 and produced control 89.6, IFITM1-, IFITM2, and IFITM3-bearing 89.6 viruses. The viruses were then used to infect TZM-bl cells that were untreated or preincubated with AMD3100 or maraviroc for 1 hour. As one of the coreceptors is inhibited by the drug, the viral entry is mediated via the other available coreceptor. Comparing how 89.6 responds to IFITM inhibition in X4- or R5-dependent entry allows determining whether IFITMs preferentially inhibit HIV-1 of certain coreceptor tropism. The results revealed no statistically significant difference in the 89.6 sensitivity to IFITM inhibition regardless of the coreceptor used for viral entry (Figure 21). Therefore, IFITM proteins do not preferentially inhibit HIV-1 based on coreceptor tropism. This conclusion is further supported by the moderate inhibition of YU-2, RHPA, THRO, NL(YU-2V3) and NL(THROV3) infection by IFITM3 (Figure 16B and 18C).

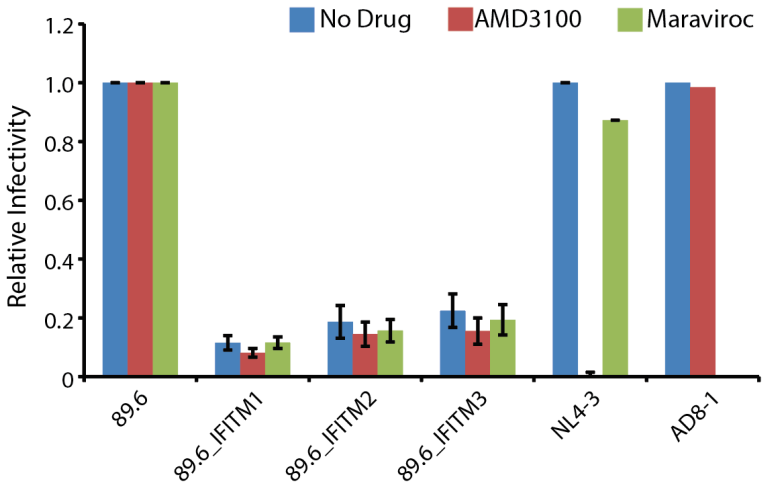

Figure 21: The sensitivity of X4/R5-tropic 89.6 to IFITM1, 2 or 3 under X4- or R5-dependent viral entry. The 89.6 plasmid DNA was transfected into HEK293T cells with 100 ng of empty vector, IFITM1, 2 or 3 DNA. Levels of viral production were determined by RT activity. TZM-bl cells were pre-incubated with AMD3100 or maraviroc containing DMEM. Viruses were then used to infect TZM-bl cells. At 40-hour post-infection, TZM-bl cells were harvested. Levels of luciferase activity of control 89.6 infections under each treatment were individually set at a value of 1. The relative infectivity was obtained by comparing the luciferase activity of IFITM-bearing 89.6 under each treatment to that of the control 89.6. Two independent experiments were done, each in duplicates. Averages of the relative infectivity are shown in the bar graph. SEMs were plotted as the error bars. A student t-test was used to evaluate the statistical significance of the difference.

3.1.5 IFITM3 impairs gp160 maturation in virus-producing cells.

I then questioned whether IFITM3 affects HIV-1 Env expression and processing. Env expression profile of both virus-producing cells and the purified viral particles were analyzed by

western blot (Figure 22A). IFITM3 was detected in the virus lysate, indicating the incorporation of IFITM3 into the virions. The intensity of gp120 and gp160 signals were measured, and the ratios of gp120 over the total amount of Env were calculated to represent gp160 processing efficiency. The results showed a decrease in the relative level of gp120 vs gp160 in the IFITM3-bearing viruses, suggesting a compromised gp160 processing (Figure 22B). However, for AD8-1 gp160 processing was not affected by IFITM3, and the amount of gp120 incorporated in IFITM3-bearing and control viruses were comparable. Therefore, the ability to resist IFITM3-mediated inhibition of gp160 processing likely contributes to AD8-1 resistance to IFITM3. In support of this notion, the gp120/total Env ratios in the V3-loop mutant viruses were higher than those of NL4-3. The results from the correlation analysis showed that IFITM3 sensitivity of HIV-1 is directly correlated with the degree of IFITM3-mediated defect in gp160 processing (Figure 22C). Thus, the data jointly suggest that IFITM3 undermines the infectivity of sensitive HIV-1 by decreasing the efficiency of gp160 processing. Combined with our findings described earlier, the V3 loop plays a key role in ensuring efficient gp160 processing in the presence of IFITM3.

The protein expression profiles of Env, Gag and IFITM3 in the virus-producing cells were also analyzed (Figure 22D). The ratios of gp120/total Env were calculated for each strain (Figure 22E). Except for AD8-1, gp160 processing of all the other strains were impaired by IFITM3 expression in the virus-producing cells. The difference between the efficiency of gp160 processing with IFITM3 expression to that without IFITM3 was statistically significant. However, the impairment of gp160 processing in the virus-producing cells did not show a significant correlation to viral sensitivity to IFITM3 (Figure 22F). This may result from the presence of unprocessed gp160 proteins in the ER, which can increase the background noise and

interfere with the results. Together, our data support the impairment of gp160 processing as one of the mechanisms that underlie the anti-HIV-1 activity of IFITM3.

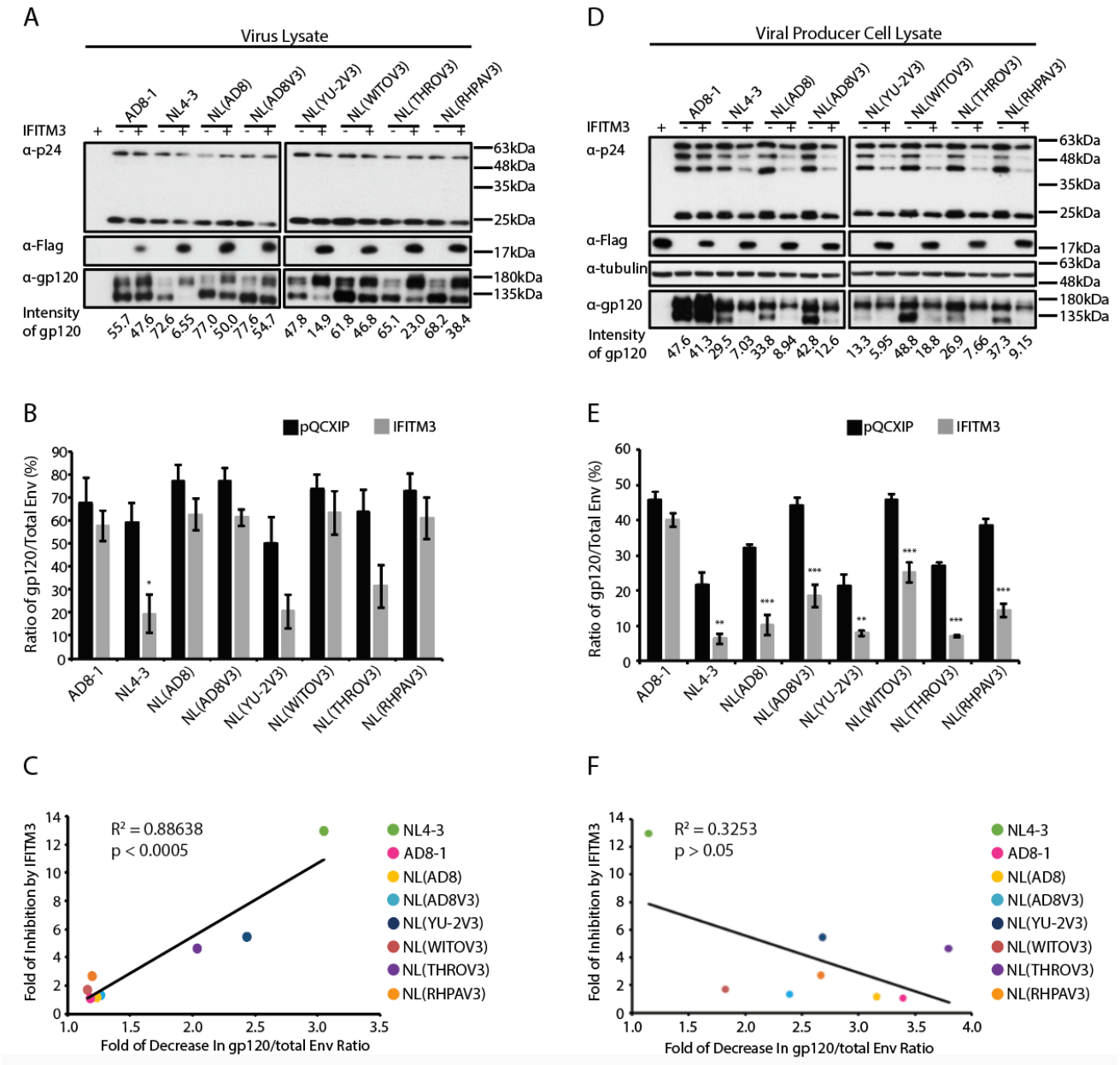

Figure 22: The effect of IFITM3 on HIV-1 Env maturation. HIV-1 particles were purified and pelleted by ultracentrifugation. The concentrated viruses and the corresponding virus-producing cells were examined in Western blot. (A) and (D) The representative Western blots of

four independent experiments. The intensities of gp120 and gp160 signals were quantified using ImageJ (NIH). The total Env level was calculated by combining the signals of gp120 and gp160 protein bands. The ratios of gp120/total Env are labelled as "intensity of gp120" in the Western blot data. (B) The graph shows the ratio of gp120/total Env for IFITM3-bearing and the IFITM-free control viruses. The averages of the four experiments are displayed in the bar graphs. SEMs were calculated to plot the error bars. The student t-test was performed to evaluate the statistical significance of the difference between the control and IFITM3-bearing groups (*, $P < 0.05$; **, $P < 0.01$; ***, $P < 0.001$). (E) The graph shows the ratio of gp120/total Env of the virus-producing cells that express IFITM3 or without IFITM3. (C) The correlation analysis was performed between the fold of inhibition by IFITM3 and the fold of decrease in gp120/total Env ratios in the virions. (F) The correlation analysis was also performed between the fold of inhibition by IFITM3 and the fold of decrease in cellular gp120/total Env ratios.

Due to the non-covalent association between gp120 and gp41, gp120 is prone to shed from the virus surface. To validate whether the stability of mature gp120 on the virion is correlated with the viral sensitivity to IFITM3, the association index and processing index were determined for NL4-3, AD8-1, NL(AD8) and NL(AD8V3) (Figure 23). The processing efficiency of gp160, which was inferred from the processing index, showed that all tested strains did not differ significantly in their processing efficiency (Figure 23B). The results are in agreement with our earlier findings from the Western blot analysis of the virus-producing cell lysates (Figure 22E and 23B). Next, the stability of gp120 on the virion surface was evaluated by referring to the association index of each virus (Figure 23C). The results showed that the gp120 of IFITM3-sensitive NL4-3 had a significantly unstable attachment to gp41 than the other three

IFITM3-resistant strains. More importantly, the V3 loop of AD8-1 alone was sufficient to restore the stability of gp120 of NL(AD8V3). Together, the data suggest that the V3 loop from AD8-1 confers resistance to IFITM3 by stabilizing the gp120/gp41 complex on the virions.

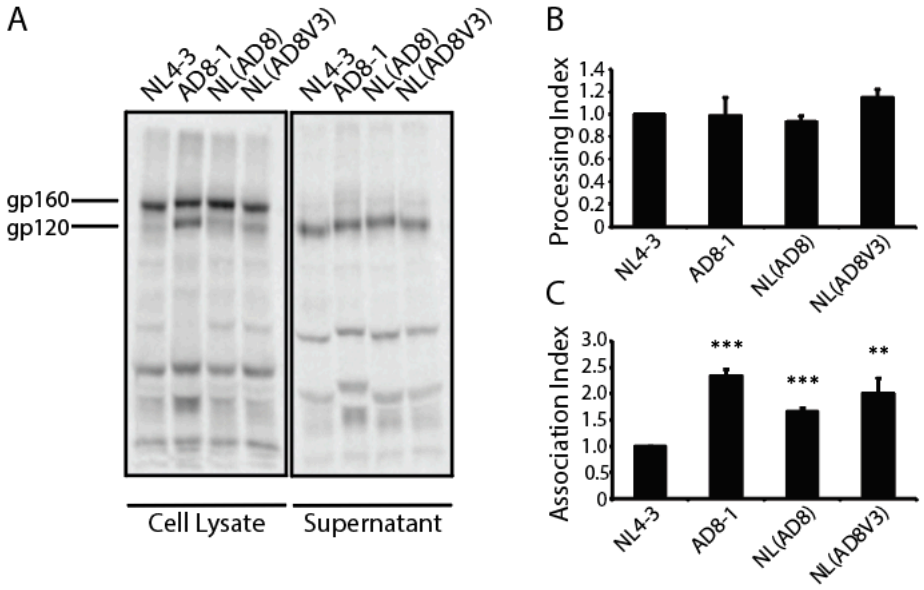

Figure 23: The efficiency of Env processing and gp120 stability from different HIV-1 strains. HIV-1 was produced by transfecting HEK293T cells with proviral DNA of NL4-3, AD8-1, NL(AD8) or NL(AD8V3). The Env was metabolically labelled with [^{35}S]methionine-cysteine. The Env of the tested viruses and the virus-producing cells were immunoprecipitated. The cell and viral lysates were then subject to SDS-PAGE and followed by Phosphorlmager analysis. (A) The Western blots of one representative experiment from three independent experiments are shown. (B and C) The gp160 processing index and the association values of NL4-3, AD8-1, NL(AD8) and NL(AD8V3) were obtained from three independent experiments. The average values are shown in the graph, with the SEM displayed as the error bars. The values for NL4-3 were arbitrarily given a value of 1. **, $P < 0.01$; ***, $P < 0.001$.

3.1.6 IFITM3 and gp160 are associated with each other.

The impairment of gp160 processing by IFITM3 raised the possibility that IFITM3 may associate with Env. This led me to question whether the amount of Env associated with IFITM3 modulates the viral sensitivity to IFITM3. Therefore, I analyzed the degree of interaction between IFITM3 and Env by performing co-immunoprecipitation. The proviral plasmids of different HIV-1 were transfected into HEK293T cells together with IFITM3, IFITM1 or CD71 (transferrin). As IFITM1 and CD71 served as two controls for possible non-specific membrane-mediated binding. IFITM3, IFITM1 and CD71 are FLAG-tagged, cell lysates were immunoprecipitated with anti-Flag antibodies. The inputs and the eluates of co-IP assays were analyzed by Western blots. The results showed that gp160 was detected in all eluates, most likely due to the membrane-mediated association of gp41 with IFITM3, IFITM1 and CD71. Interestingly, the heavily glycosylated gp160 proteins were only detected from the eluate of the IFITM3 group, suggesting a specific association between IFITM3 and glycosylated gp160 (Figure 24). Since gp160, IFITM3, IFITM1 and CD71 are produced in the endoplasmic reticulum, association with unprocessed gp160 is likely the results of the membrane-mediated nonspecific binding. The gp160 proteins are then subject to further modification and processing in Golgi, where they are heavily glycosylated and cleaved by furin. Since this more processed form of gp160 only showed association with IFITM3, their interaction can be deemed specific. Together with my previous results, I concluded that the interaction of glycosylated gp160 with IFITM3 impairs the maturation of gp160 in the Golgi. My results are in agreement with the study of Yu and colleagues [508], in which the association of IFITM3 with Env was shown to correlate with the disruption of Env processing.

I further evaluated the interaction between IFITM3 and Env of other mutant viruses (Figure 25). HEK293T cells were transfected with the proviral DNA of mutant NL4-3 and IFITM3 DNA. The cell lysates were immunoprecipitated, and the eluates were analyzed by Western blot. Anti-gp120 and anti-gp41 antibodies were used to detect Env associated with IFITM3 in the eluates and the inputs (Figure 25). In support of what I have observed earlier, the glycosylated gp160 proteins were detected in IFITM3-expressing cells. However, the amount of Env associated with IFITM3 did not correlate with the level of corresponding viral sensitivity to IFITM3. Collectively, these results suggest that gp160 processing in virus-producing cells is hampered by IFITM3 via a direct interaction with glycosylated gp160 in the Golgi. However, the amount of Env proteins associated with IFITM3 does not correlate with the degree of viral sensitivity to IFITM3. Therefore, other factors are likely contributing to the modulation of HIV-1 responsiveness to IFITM3 inhibition.

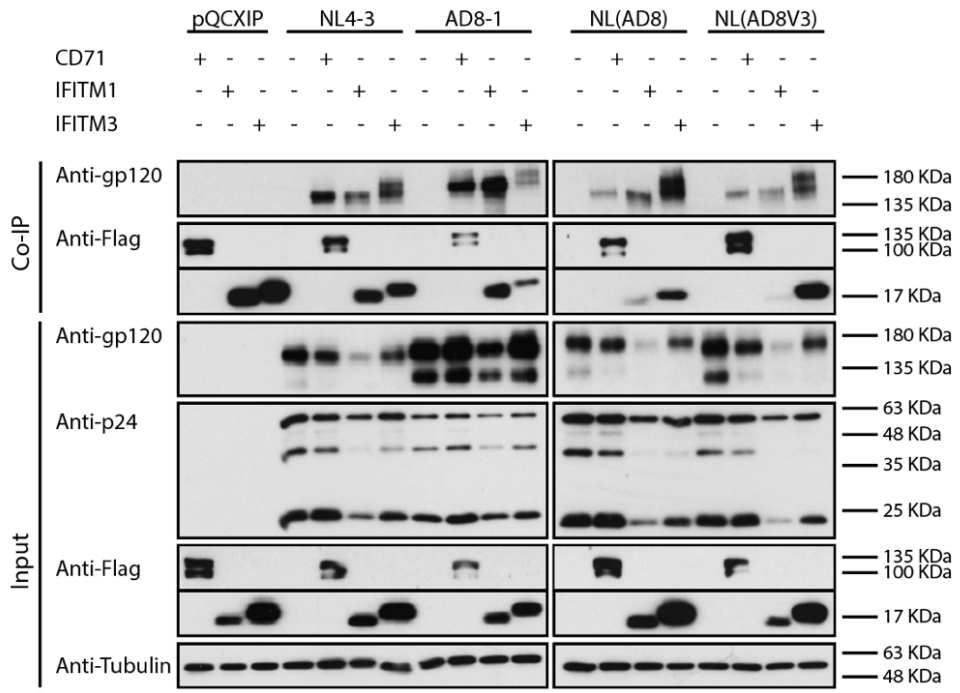

Figure 24: Co-IP of IFITM3, IFITM1 or CD71 with Env. HEK293T cells were transfected with the proviral DNA of different HIV-1 strains together with either IFITM1-FLAG, IFITM3-FLAG or CD71-FLAG DNA. The transfection of FLAG-tagged protein DNA or proviral plasmids alone was included as negative controls. The cells were harvested 48 hours post-transfection, and the lysates (input) were used for the immunoprecipitation with anti-FLAG antibodies linked to agarose beads. FLAG-tagged proteins and their associated proteins were eluted, and HIV-1 Env and FLAG-tagged proteins were detected by anti-gp120 and anti-FLAG antibodies, respectively. Gag and tubulin in the input solutions were detected using anti-p24 and anti-tubulin antibodies, respectively.

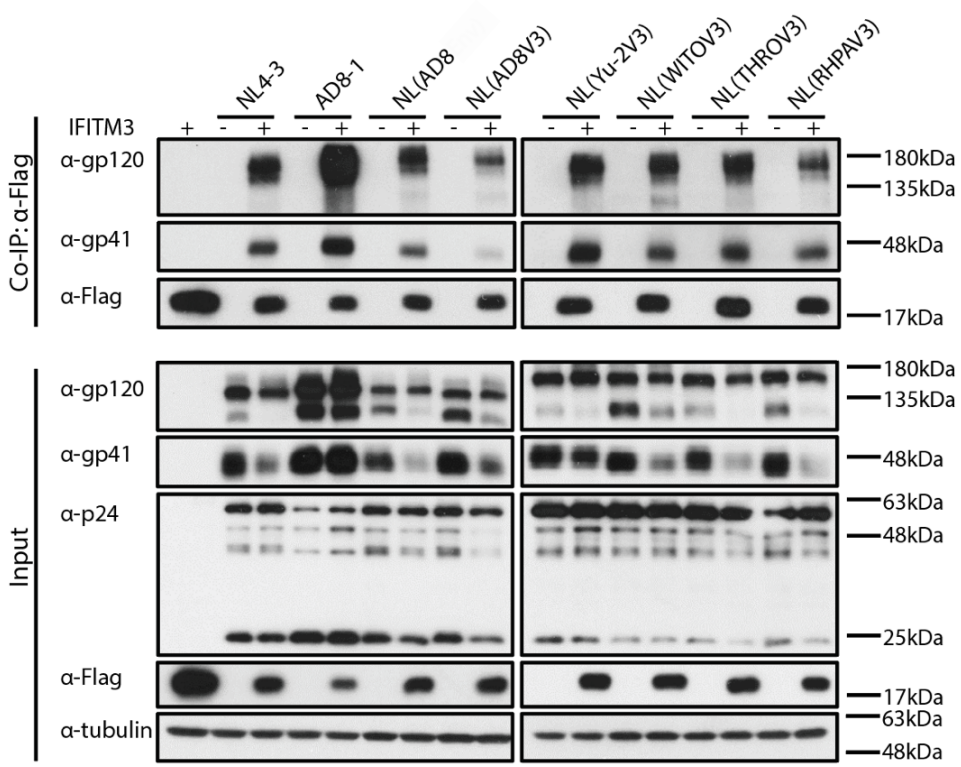

Figure 25: Co-IP of IFITM3 and Env of other NL4-3 mutant viruses. The proviral DNAs of NL4-3, AD8-1 and NL4-3 V3 loop mutants were transfected into HEK 293T cells with either the empty vector or IFITM3-FLAG DNA. The cells transfected with IFITM3 or proviral plasmid alone were included as negative controls. The cells were harvested 48 hours post-transfection, and the lysates were subjected to immunoprecipitation with anti-FLAG antibodies. The inputs and eluates were analyzed by Western blot. Env proteins were detected by anti-gp120 and anti-gp41 antibodies, and IFITM3 proteins were detected by anti-FLAG antibodies. The inputs were also analyzed for the expression of Gag and tubulin using anti-p24 and anti-tubulin antibodies, respectively.

3.1.7 The IFITM3-resistant Env shows resistance to sCD4 and the 17b antibody.

In section 3.1.4, we evaluated the role of co-receptor usage in modulating viral sensitivity to IFITM3. This prompted us to question whether the interaction between Env and CD4 also has a role in modulating HIV-1 response to IFITM3.

To directly evaluate the Env and CD4 receptor binding, I performed neutralization assays of HIV-1 viruses with soluble CD4 (sCD4). It has been reported that the binding of sCD4 reduces viral infectivity by inducing gp120 shedding [514]. The Env with CD4-bound conformation has been shown to more readily bind to sCD4, attesting a higher sensitivity to sCD4 neutralization [515,516]. Therefore, the changes in Env conformation can be detected by evaluating its sensitivity to sCD4 neutralization. HIV-1 was incubated with different concentrations of sCD4 at 37 ºC for 1 hour before infection of TZM-bl cells. The results showed that NL4-3 was very sensitive toward sCD4 neutralization, with 50% inhibitory concentration (IC_{50}) of 62 ng/ml (Table 2). In contrast, the IFITM3-resistant strains AD8-1, NL(AD8V3) and NL(WITOV3) showed no reduction of infectivity upon sCD4 treatment. NL(YU-2V3), NL(THROV3) and NL(RHPAV3) exhibited different levels of sensitivity to sCD4, with IC_{50} of 72 ng/ml, 227 ng/ml, and 388 ng/ml, respectively (Table 2). The sensitivity of the tested viruses to sCD4 neutralization was directly correlated with their sensitivity to IFITM3 (Figure 30B). As the binding of Env to sCD4 closely relates to the ligand-free conformation of Env, I concluded that the conformation of CD4 binding sites of Env modulates the viral response to IFITM3 inhibition.

IFITM3 has been previously shown to interact with Env from co-IP assay (Figure 24 and Figure 25). Therefore, I questioned whether IFITM3 modulates the ligand-free conformation of Env. To answer this question, IFITM3-bearing NL4-3, AD8-1 and other V3 loop mutant viruses were tested for their sensitivity to sCD4 neutralization. If IFITM3 modifies the conformation of

Env to one with stronger affinity to CD4, the infection of IFITM3-bearing viruses will experience more potent sCD4 inhibition. However, the results showed that the viruses responded similarly to sCD4 neutralization regardless of the presence of IFITM3 (Figure 26). These data suggest that IFITM3 does not affect the conformation of Env. Collectively, these results suggest that the ligand-free conformation of Env with a higher affinity to the CD4 receptor is more sensitive to IFITM3 inhibition. Nevertheless, IFITM3 does not sensitize Env to sCD4 neutralization (Figure 26).

Table 2: 50% inhibitory concentrations (IC50) of sCD4

		NL4-3	NL(YU-2V3)	NL(THROV3)	NL(RHPAV3)
pQCXIP	Function	$y=0.9714e^{(-10.72x)}$	$y=0.851e^{(-7.344x)}$	$y=0.929e^{(-2.735x)}$	$y=0.9901e^{(-1.763x)}$
	IC_{50} (ng/ml)	61.95	72.41	226.5	387.5
IFITM3	Function	$y=1.0151e^{(-11.66x)}$	$y=0.8517e^{(-6.873x)}$	$y=1.068e^{(-3.107x)}$	$y=0.911e^{(-1.727x)}$
	IC_{50} (ng/ml)	60.73	77.50	244.4	347.4

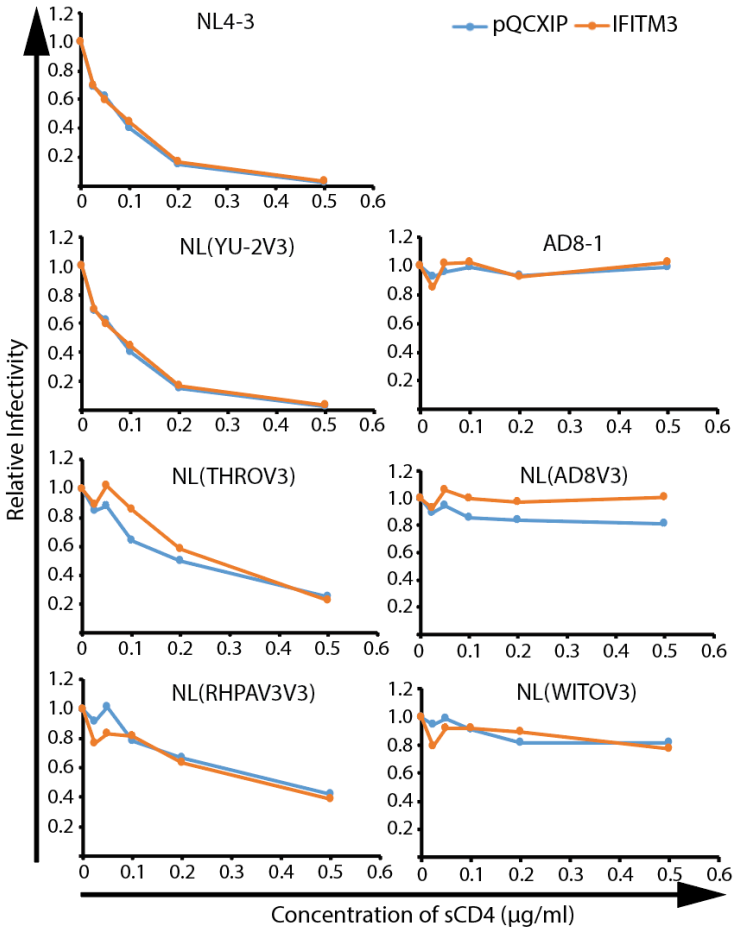

Figure 26: Inhibition of IFITM3-bearing and IFITM3-free HIV-1 with sCD4. The proviral plasmid DNA was transfected into HEK293T cells together with the empty pQCXIP vector or IFITM3 expression vector. The viruses were incubated with different concentrations of sCD4 (0.025, 0.05, 0.1, 0.2 and 0.5 µg/ml) for 1 hour at 37 ºC and were subsequently used for infecting TZM-bl cells. The viruses incubated with DMEM served as the negative controls. At 40-hour post-infection, the TZM-bl cells were harvested, and the luciferase activity was measured. The values of relative infectivity were obtained by comparing the luciferase activity of sCD4-treated viruses to that of the control infection. The luciferase activities for each virus infection without sCD4 treatment (i.e. DMEM only) were arbitrarily set at a value of 1.

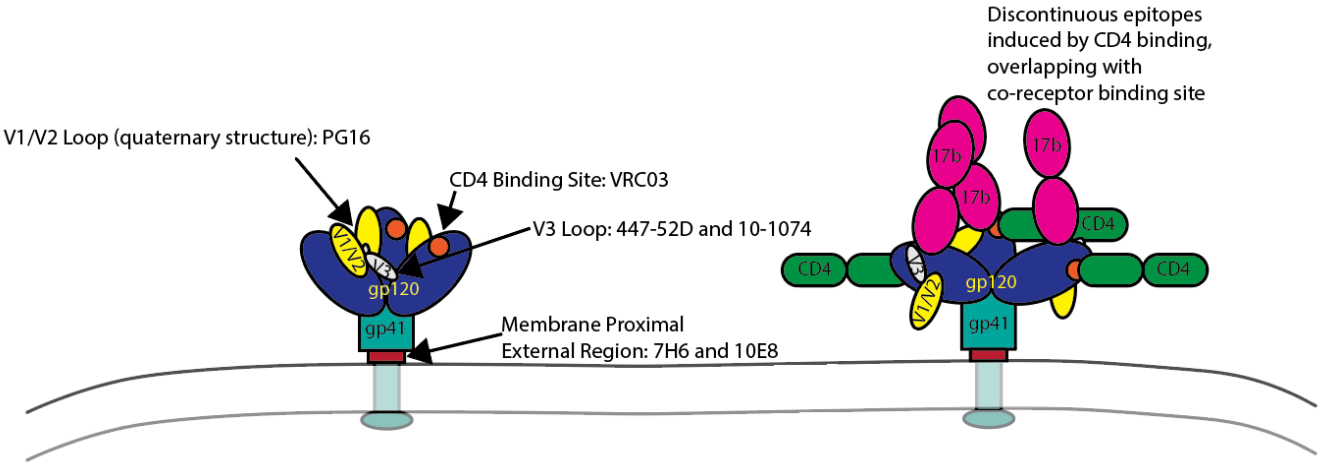

Figure 27: The epitopes of selected antibodies specific to HIV-1 gp120/gp41. Seven neutralization antibodies were selected for blocking HIV-1. The epitopes of the antibodies spread across different domains of the Env. VCR03 binds to the CD4 binding site; PG16 targets the quaternary structure of V1/V2 loops; 44752D and 10-1074 target different segments of the V3 loop; 7H6 and 10E8 bind to the membrane proximal external region (MPER); 17b targets discontinuous epitopes that are induced by CD4 binding and partially overlap with the co-receptor binding site.

Since the change in the V3 loop was shown to alter the conformation of Env, I attempted to further verify this finding by conducting antibody neutralization assays. Seven antibodies that target different epitopes on the Env protein were selected for the neutralization assay (Figure 27). HIV-1 was incubated with different concentrations of each antibody for 1 hour at 37^{o}C prior to infecting TZM-bl cells. Results demonstrated differential sensitivity between NL4-3 and other V3 loop chimeric viruses to 447-52D and 10-1074 (Figure 28). NL4-3 was barely affected by 10-1074 but was potently inhibited by 447-52D. Similar to previous observations, the infectivity of

the IFITM3-sensitive HIV-1 NL4-3 and NL(YU-2V3) were both potently inhibited by 447-52D, whereas the IFITM3-resistant HIV-1 strains were less inhibited. The sensitivity of NL(WITOV3), NL(AD8V3) and NL(RHPAV3) to 447-52D correlated with their ability to escape IFITM3.

A clearer correlation is observed between the virus sensitivity to the 17b antibody and its ability to escape from IFITM3. 17b targets CD4 induced discontinuous epitope overlapping with co-receptor binding site, and therefore, can act as the surrogate of the co-receptor ligand. Although the co-receptor tropism of NL4-3 and other V3-loop chimeric viruses varies, 17b binds to the common epitope between the two co-receptor binding sites. The infectivity result has shown that NL4-3 was the most potently inhibited virus, followed by NL(YU-2V3), NL(THROV3), NL(RHPAV3) in terms of susceptibility to 17b mediated inhibition. NL(AD8V3) and NL(WITOV3) were barely inhibited by 17b. Combining with the infection data obtained from viruses +/- IFITM3 (Figure 17C), I can correlate the virus sensitivity to 17b to the virus capability of escaping IFITM3, suggesting the more 17b resistant strains are also more resistant to IFITM3 inhibition.

In summary, the difference in virus response to the neutralizing antibodies suggests a variation in the accessibility of the epitope for each virus. This variation implies that the substitution of the V3 loop changes the conformation of Env. Among these antibodies, the virus sensitivity to 17b neutralization showed a direct correlation with their ability to overcome IFITM3 restriction (Figure 30B). Since 17b targets the CD4-induced epitopes on gp120, IFITM3 sensitive strains have a more “open” Env resting conformation.

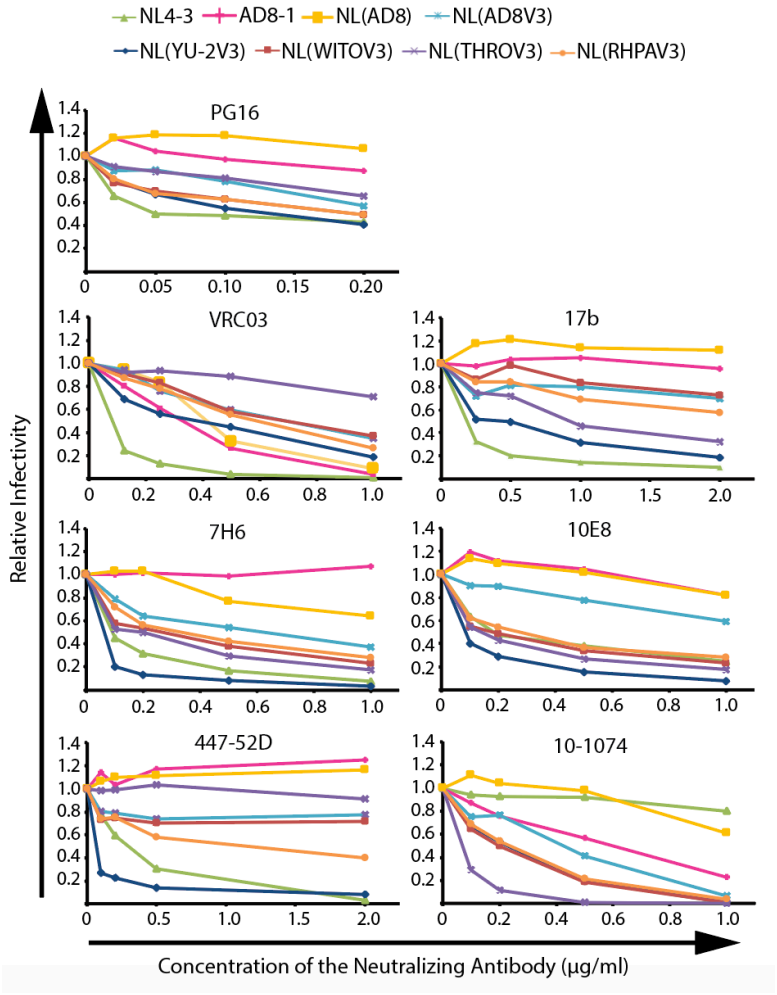

Figure 28: Inhibition of different HIV-1 strains with neutralization antibodies. NL4-3, AD8-1 and other NL4-3 mutants were incubated with either DMEM or different doses of neutralization antibodies for 1 hour prior to infecting TZM-bl cells. The DMEM incubated viruses served as the negative control and were arbitrarily set as 1 in the relative infectivity analysis. The infected TZM-bl cells were harvested 36 hours after infection, and luciferase activity was measured. Results were represented as relative infectivity, which was calculated by dividing the luciferase activity of the antibody-treated virus-infected TZM-bl cells to that of the negative control. The experiment was performed in duplicates. The concentrations of antibodies are displayed on the x-axis.

Our previous results have shown that virion incorporated IFITM3 does not potentiate the sensitivity of the virus to sCD4, which led us to examine whether the same applies to the neutralization antibody inhibition. To assess whether IFITM3 in the virus-producing cells modulates viral sensitivity towards neutralization antibodies, I selected IFITM3-bearing NL4-3 and NL(AD8V3) for the neutralization assay. The IFITM3-bearing and control NL4-3 and NL(AD8V3) were incubated with the neutralization antibodies for 1 hour at 37 ^{o}C before infecting TZM-bl cells. The results showed that the IFITM3-bearing NL4-3 and NL(AD8V3) exhibited the same level of sensitivity to the neutralization antibodies as their control counterparts (Figure 29). Therefore, IFITM3 of virus-producing cells does not affect the conformation of Env, nor does it make Env more sensitive to antibody neutralization.

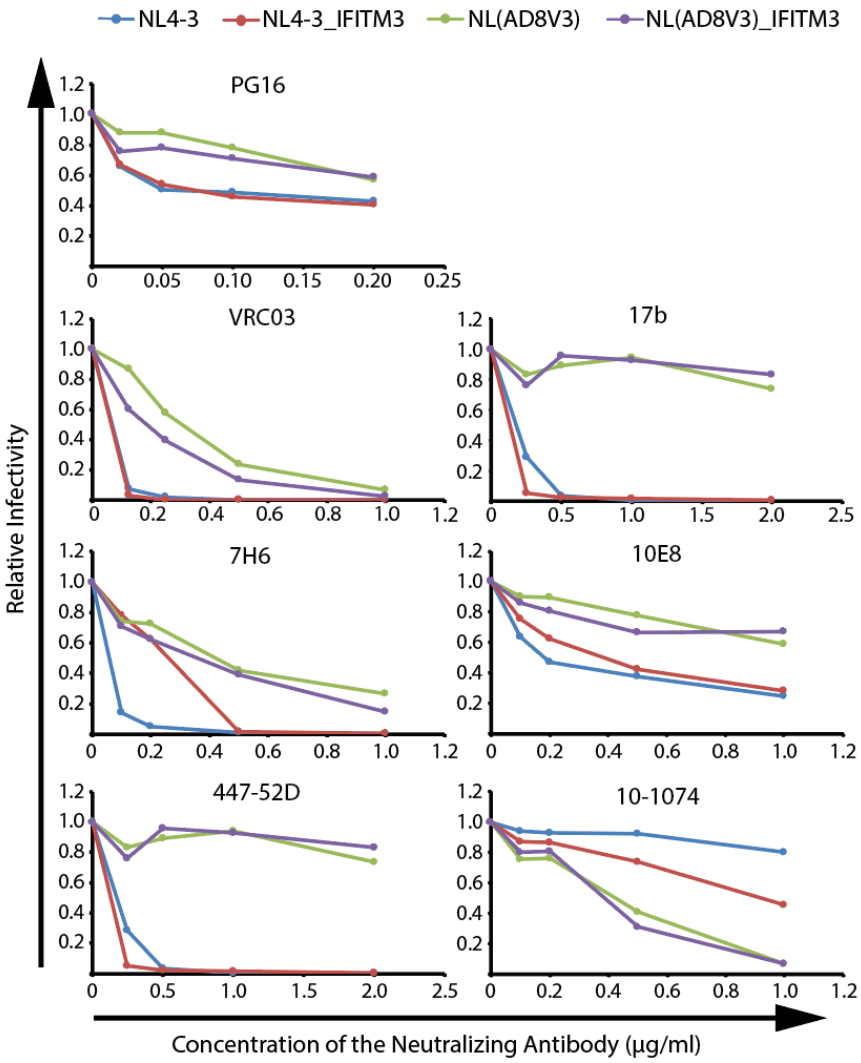

Figure 29: IFITM3 expressed in viral producer cells does not sensitize the viruses to neutralizing antibodies. IFITM3-bearing and the control NL4-3 and NL(AD8V3) were incubated with antibodies at different concentrations or only DMEM for 1 hour prior to infecting TZM-bl cells. The DMEM-treated viruses served as the negative control and was arbitrarily set as 1 in the calculation of relative infectivity. The TZM-bl cells were harvested 36-hour post-infection, and luciferase activity was measured. The relative infectivity (y-axis) was obtained by comparing the luciferase activity of antibody-treated viruses infected TZM-bl cells to that of the

antibody-free negative controls. The concentrations of the antibodies are indicated on the x-axis. The experiment has been performed in duplicates.

The differential response to 17b and sCD4 is caused by the variation in the ground state conformation of prefusion Env. My results showed that this conformation could be altered by replacing the V3 loop sequence. The binding of IFITM3 to Env does not contribute to any further change in conformation. However, it was observed that 17b- and sCD4-sensitive HIV-1 were more susceptible to IFITM3 inhibition (Figure 30). Together, these data suggest that the prefusion Env with a "closed" conformation can more efficiently resist sCD4 and 17b neutralization, which is also directly correlated with their ability to overcome IFITM3 inhibition.

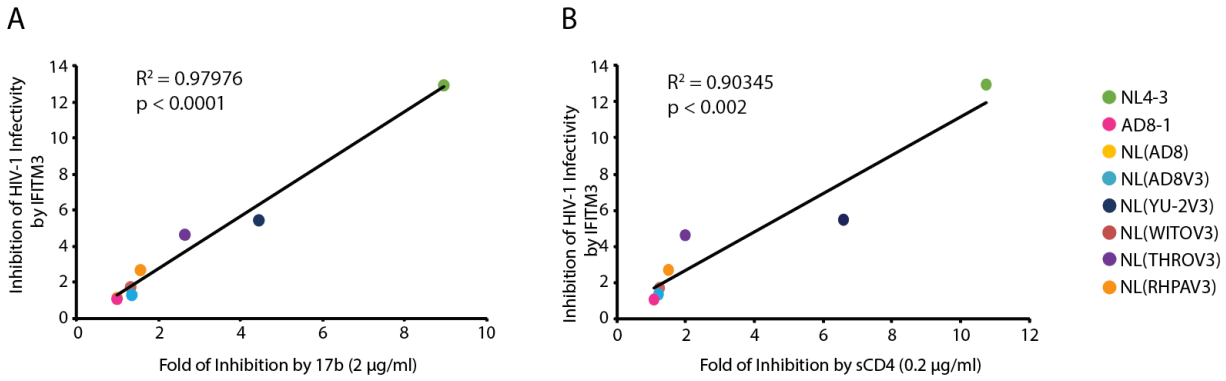

Figure 30: Correlation curve between the inhibitory properties of IFITM3 and those of 2ug/ml 17b and 0.2ug/ml of sCD4. The y-axis represents the fold inhibition by IFITM3, and the x-axis is the fold inhibition by 17b of 2ug/ml (A) and sCD4 of 0.2ug/ml (B). Correlation was analyzed by linear regression. Both R^2 and the p-value suggest strong correlations between the viral sensitivity to IFITM3 and to 17b and sCD4.

3.1.8 The single amino acid mutation of JRFL Env alters its sensitivity to IFITM3.

To further verify the correlation between the Env conformation and its IFITM3 resistance property, I tested JRFL WT and eight Env mutants for their sensitivity to IFITM3 (Figure 31). These mutated JRFL Env proteins were designed to change Env ligand-free conformations [517,518], and have been tested for the "openness" of their ground state conformation by examining their sensitivity to CD4 mimetics (DMJ-II-121) and conformation blocker (DMS806) [518]. If the correlation between Env conformation and Env sensitivity to IFITM3 holds, I expect to observe L193A being more potently inhibited by IFITM3 than I184A (Figure 31).

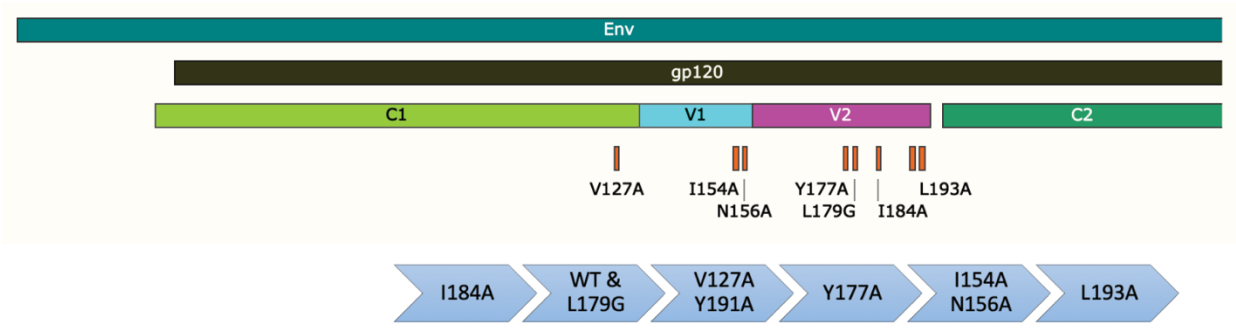

Figure 31: The "openness" of JRFL mutants in increasing order. The eight mutants were kindly provided by Dr. Finzi lab. All the mutations, except V127A, are mapped to V1 and V2 regions. The V127A mutation is mapped to the C1 region of Env. These three regions are important in determining the ground state conformation of Env, and therefore, the efficiency of Env binding to CD4. Based on the IC50 of each mutant to DMJ-II-121 and BMS-806, the Env mutants were ranked in increasing order of "openness" of the ground state conformation.

To test the JRFL WT and mutants for their sensitivity to IFITM3 inhibition, I produced IFITM3-bearing and IFITM3-free JRFL Env pseudotyped NL4-3ΔEnv viruses from HEK293T

cells. The level of viruses produced was determined by measuring the RT activity of each virus. The results showed no significant difference in the amount of virus production regardless of the expression of IFITM3 (Figure 32).

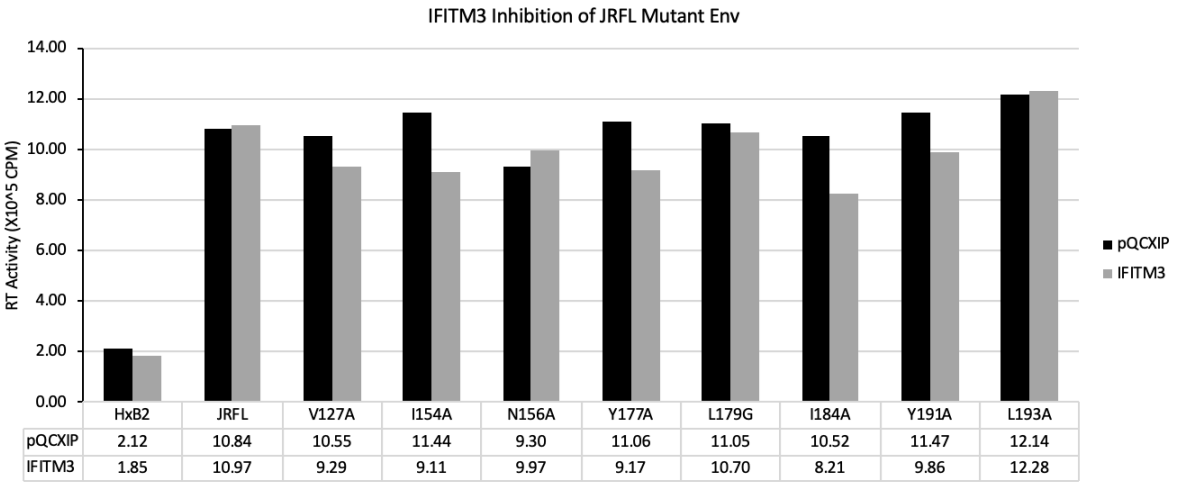

	HxB2	JRFL	V127A	I154A	N156A	Y177A	L179G	I184A	Y191A	L193A
pQCXIP	2.12	10.84	10.55	11.44	9.30	11.06	11.05	10.52	11.47	12.14
IFITM3	1.85	10.97	9.29	9.11	9.97	9.17	10.70	8.21	9.86	12.28

Figure 32: IFITM3 expression in the HIV-1 producer cells does not affect viral production. The pseudotyped HIV-1 was produced by co-transfecting HEK293T cells with HxB2 Env DNA, JRFL WT Env, or each of the JRFL mutated Envs with NL4-3ΔEnv plasmid. IFITM3-bearing viruses were produced by transfecting IFITM3 DNA. Control viruses were produced by transfecting pQCXIP empty vectors. The viruses were then quantified by measuring the RT activity. HxB2 Env was used as a positive control for the anti-HIV-1 activity of IFITM3.

The infectivity of JRFL Env pseudotyped viruses was tested by infecting TZM-bl reporter cells. The fold of inhibition by IFITM3 was calculated for each pseudotyped viruses. The *P* values were obtained by comparing the fold of inhibition of the mutants to that of the wild type JRFL Env (Figure 33A). Results showed that the fold inhibition of JRFL mutants by

IFITM3 differs significantly from that of the wild type JRFL Env, except for Y177A and I184A (Figure 33A).

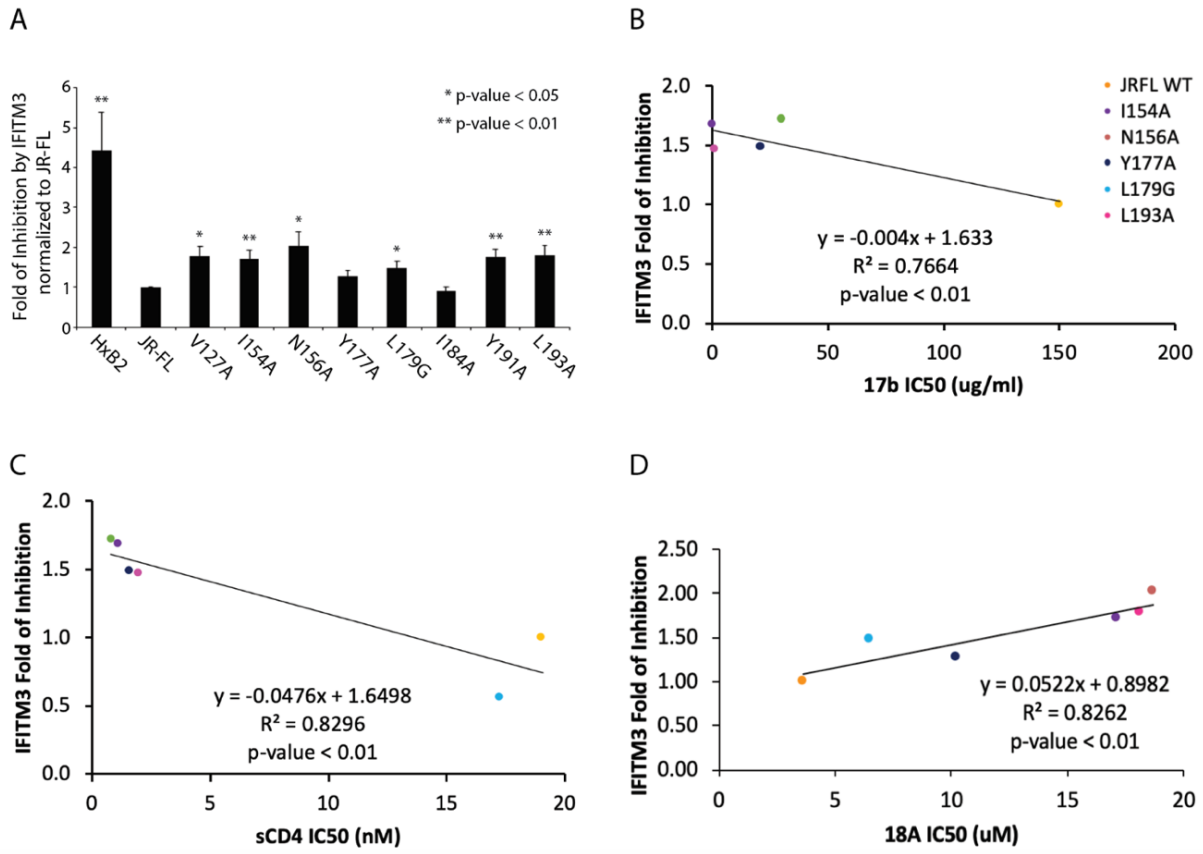

Figure 33: The susceptibility of JRFL mutants to IFITM3 is correlated with their sensitivity to sCD4, the 17b antibody, and a small conformation locking molecule 18A. (A) HIV-1 was used to infect TZM-bl cells. The cells were harvested 40 hours post-infection, and the luciferase activity was measured. The fold of inhibition by IFITM3 for each Env was calculated by individually setting the luciferase activity of IFITM3-bearing viruses to a value of 1. The fold inhibition mediated IFITM3 on HxB2 and JRFL mutants were all normalized to that of JRFL WT, which was arbitrarily set to a value of 1. The statistical significance of the differences was calculated by student t-test (*, $P < 0.05$; **, $P < 0.01$). (B and C) Correlation between viral

sensitivity to IFITM3 inhibition and the IC_{50} of 17b and sCD4, respectively. The values of IC_{50} are provided by Dr. Andres Finzi's lab. A linear regression was drawn for each correlation curve, and the degree of the fitness of the curve was displayed as R^2. The statistical significance was demonstrated by p values.

From the correlation study, I further found that the sensitivity of mutant JRFL Env to 18A and the cold inactivation assay correlates with its sensitivity to IFITM3. The conformation of the JRFL Env mutant can be inferred from the value of IC_{50} to 18A and their response to the cold inactivation treatment [517]. 18A is a conformation locker with a higher affinity to the Env of "closed" conformation, whereas the "open" Env is more sensitive to the cold inactivation treatment [517]. The results showed that the IFITM3-sensitive JRFL Env mutants were also sensitive to the cold inactivation treatment but were more resistant to the 18A neutralization. Together the evidence suggests that the Env with CD4-induced "open" conformation is more potently inhibited by IFITM3.

Since IFITM3 is also expressed in virus target cells, I tested the JRFL Env mutants for their sensitivity to the target cell-associated IFITM3. MT4-R5-QCXIN and MT4-R5-IFITM3 cells were infected by IFITM3-bearing or -free JRFL Env pseudotyped viruses. HIV-1-infected MT4 cells were quantified by p24 expression levels by flow cytometry. The results showed that IFITM3 in viral target cells more potently inhibited mutant JRFL Env compared to the virion-associated IFITM3. However, there was no significant difference in the sensitivity of the JRFL mutants to the target cell IFITM3. Interestingly, when IFITM3 on the virions and the target cells acted together, a synergistic inhibition against all viruses was observed. The difference in JRFL

mutant sensitivity to IFITM3 synergistic inhibition was much more pronounced, with the strongest inhibition observed for mutants I154A and V127A and Y177A.

I then calculated the correlation between the values of IC_{50} of the various inhibitory treatments to JRFL Env to the fold of inhibition by the synergistic effect of IFITM3. The correlation studies showed a significant linear relationship between the IC_{50} of particular treatments and the viral sensitivity to IFITM3. I observed that the sensitivity of JRFL mutants to 17b, 19b, sCD4 is linearly correlated with the fold inhibition imposed by IFITM3. The IC_{50} values of BMS-II to JRFL mutants were inversely correlated with their sensitivity to IFITM3 synergistic inhibitory effect. As previously mentioned, 17b and sCD4 neutralize Env with "open" conformation more efficiently. The antibody 19b targets the V3 loop of Env, which has also been shown to exhibit a higher affinity to Env with "open" conformation [517,519]. BMS-II is another conformation locker that more potently inhibits Env with "close" conformation [517]. Therefore, these findings together support my previous observation that Env with a more CD4-binding induced conformation (i.e. "open" conformation) is more sensitive to IFITM3 inhibition.

To verify that the "openness" determines the Env sensitivity to IFITM3, I used another JRFL mutant L193R, which was also kindly provided by Dr. Finzi. This mutant allows the Env to assume a more "open" conformation at the ligand-free state. The previous paper has shown that L193R was more sensitive to sCD4 treatment compared to L193A [518]. Therefore, I tested JRFL WT, L193A and L193R mutants for their response to IFITM3. The results, however, did not show a significant increase in sensitivity of L193R to IFITM3 compared to other Envs. The possible explanation is that the decreased viral infectivity caused by the single amino acid mutation may have masked the difference.

In section 3.1, I characterized the IFITM3-resistant activity of HIV-1 Env. I found that the V3 loop of Env affects resistance to IFITM3 inhibition by modulating the ligand-free conformation of Env. The Env with an "open" conformation at the CD4-free state shows higher sensitivity to IFITM3 inhibition. Interestingly, the incorporation of IFITM3 into HIV-1 particles does not enhance the viral sensitivity to sCD4 or 17b, suggesting that IFITM3 does not modify the Env conformation in the virions. My results also revealed that IFITM3 expressed in the virus-producing cells reduces the viral infectivity by interrupting the maturation of gp160. The V3 loop that confers resistance to IFITM3 inhibition also demonstrates resistance to IFITM3-mediated obstruction of gp120 production. Collectively, these findings highlight the multifaceted mechanism of IFITM3 in inhibiting HIV-1. The development of resistance to IFITM3 is shown to be critical for an efficient HIV-1 infection, which underlines the important role of IFITM3 in shaping HIV-1 evolution.

3.2 There is no correlation between the rs34481144 SNP in the *ifitm3* gene and HIV-1 acquisition and disease progression.

A previous study has shown that a single nucleotide polymorphism (SNP) rs34481144 in the core promoter of the *ifitm3* gene regulates the expression level of IFITM3 proteins [490]. Accordingly, this rs34481144-A SNP has been identified as a risk allele enriched in influenza patients with severe illness. The rs34481144 is located in the core binding site of CTCF, which has a higher affinity to CTCF with A allele than the dominant genotype G. CTCF is an insulator, which then reduces the expression of IFITM3 and the neighbouring genes. Since IFITM3 also has anti-HIV-1 activity, I hypothesize that the A-allele at rs34481144 SNP, through diminishing

IFITM3 expression, could be enriched in the HIV-1 infected individuals and promote HIV-1 infection and disease progression.

In support of this hypothesis, an earlier study done on SNP rs12252 has shown that HIV-1 patients with the risk allele rs12252-C display a more rapid disease progression compared to those with the protective allele rs12252-T [520], thus supporting the association of *ifitm3* SNPs with HIV-1 disease progression. Although rs12252 has not been shown to affect HIV-1 acquisition, I also genotyped rs12252 together with rs34481144 to verify the finding.

3.2.1 rs34481144-A does not increase the susceptibility of PBMCs to NL4-3 infection.

Allen and colleagues have shown that rs34481144-A leads to lower IFITM3 expression upon IFN stimulation. Therefore, I first studied the effects of rs34481144 on the potency of IFN-induced immunity against HIV-1 in PBMCs. To test the impact of rs34481144-A on HIV-1 infection, I infected IFN-stimulated and untreated PBMCs with NL4-3. By categorizing the fold of inhibition of each donor PBMCs based on the genotypes at rs34481144 (A/A, A/G and G/G), I examined the possible correlation between the magnitude of IFN inhibition and the genotype at rs34481144.

PBMCs were isolated from the blood of sixty healthy donors, which were then genotyped for rs34481144 and rs12252. The frequency of rs34481144-A in this sample group was 0.442, with 5 homozygous A/A, 41 heterozygous A/G genotype, and 14 homozygous G/G (Figure 34A). The frequency of rs12252-C was 0.408, with 3 C/C homozygous, 43 C/T heterozygous and 14 T/T homozygous individuals (Figure 34D). The individual donor PBMCs were separated into two groups, with one group stimulated with IFN for 24 hours and the other one not stimulated. Both groups were then infected with NL4-3. Since rs34481144 has been shown to

reduce IFITM3 expression upon IFN stimulation, I expected to see less inhibition of NL4-3 infection in PBMCs with the rs34481144-A. Surprisingly, the fold of inhibition of NL4-3 by IFN-treatment showed no difference among PBMCs with A/A, A/G or G/G genotypes (Figure 34B). However, Donor 42 displayed significantly different inhibition profiles compared to the rest of the four rs34481144-A/A PBMCs. When this outlier is excluded from the analysis, PBMCs with G/G genotype showed a 2-fold higher inhibition to NL4-3 infection than the A/A genotypes (Figure 34C). Therefore, individual genetic variation mitigates the effect of rs34481144 in controlling the HIV-1 infection. To increase the accuracy of the results, a larger sample group needs to be studied.

Interestingly, the previously identified risk allele rs12252-C was shown to be associated with reduced resistance to NL4-3 infection when one outlier was removed from C/C (Figure 34 F). Although an increase in the fold inhibition can be observed from C/C to T/T, the differences between each genotype were statistically insignificant (Figure 34E).

The IFITM3 expression level of individual PBMCs was analyzed by Western blots (not shown). The results showed a wide variation in the constitutive expression of IFITM3 and the inducibility of IFITM3 by IFN treatment among different individuals. Therefore, the correlation between the IFITM3 expression and the genotype at rs34481144 was not established based on this data.

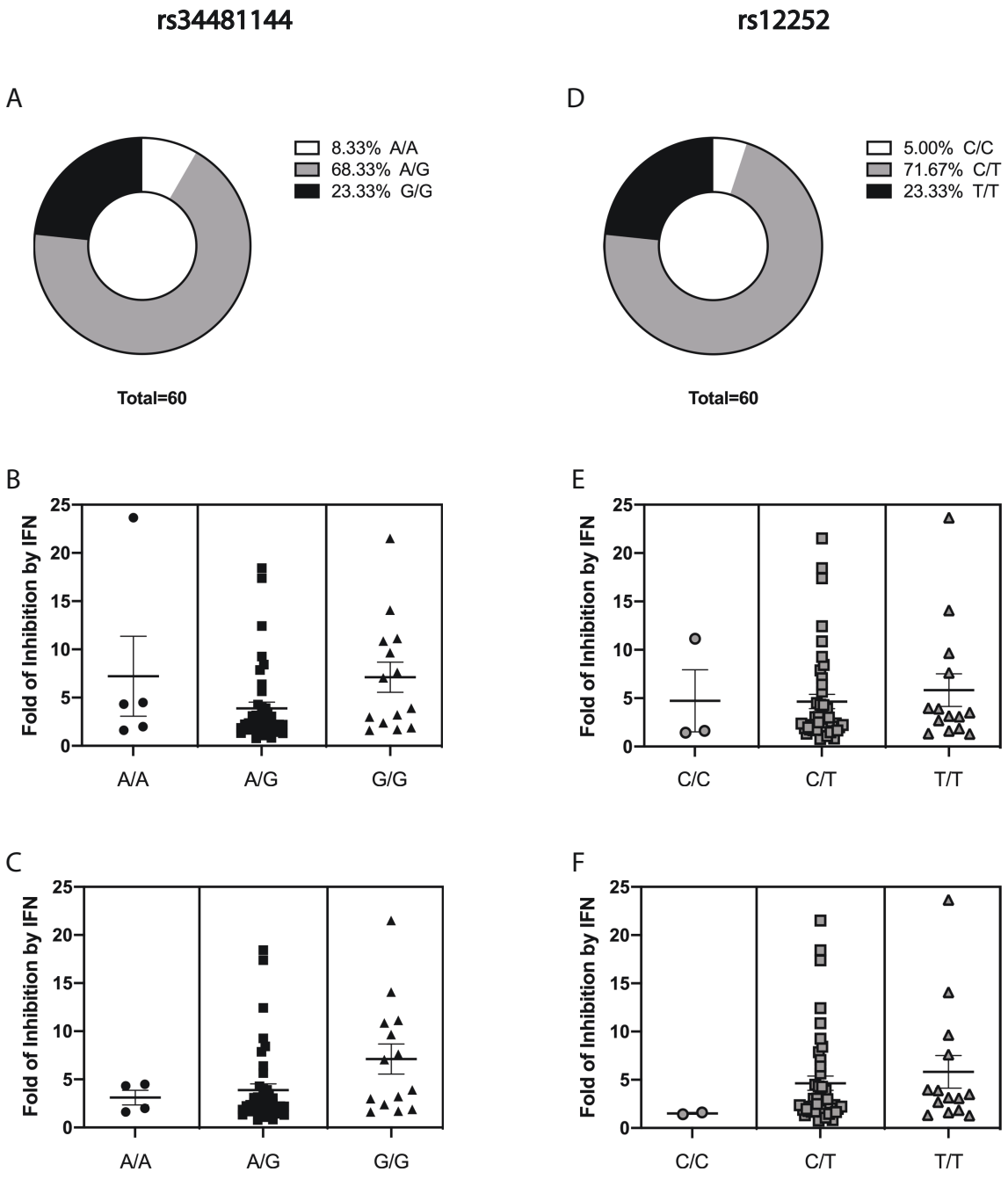

Figure 34: Effect of *ifitm3* SNPs on infection of PBMCs by NL4-3. (A) PBMCs isolated from 60 healthy donors were genotyped for rs34481144. The frequency of rs34481144-A is 0.442. (B) The PBMCs from each donor were divided into the IFN-treated group and the non-treated control group. After 24 hours of each treatment, PBMCs were infected by NL4-3. The infectivity

of the progeny viruses was used to infer the efficiency of the primary infection of PBMCs with NL4-3. Progeny viruses produced by PBMCs were collected and were used to infect TZM-bl cells. The TZM-bl cells were harvested 40 hours post-infection, and the luciferase activity was measured. The luciferase values from the control group were compared to the IFN-treated group, which provides us with the fold inhibition by IFN treatment. Folds IFN inhibition obtained for PBMCs of different individuals were categorized based on their rs34481144 genotypes. The average of the fold inhibition by IFN was calculated for each genotype. The error bars were plotted based on the SEM. The student t-test was performed to assess the statistical significance of the difference among the three genotypes (*, $P < 0.05$; **, $P < 0.01$). The same analysis was performed for rs12252.

3.2.2 An enrichment of rs34481144-A is observed in patients of African descent.

In parallel to section 3.2.1, I also examined a correlation between the rs34481144-A in HIV-1 infection using PBMCs isolated from HIV-1 patients. A total of 21 HIV-1 patients PBMCs were genotyped, and the level of IFITM3 induction by IFN was assessed. Eight of the samples were composed of PBMCs of the non-Hispanic/Latino white descendants. From the 1000 Genome Project data, the frequency of rs34481144-A is the highest for non-Hispanic/Latino white descendants with 0.46 prevalence. The results from genotyping samples of these eight patients showed that the allele frequency of rs34481144-A in the samples was 0.4 (Figure 35A). Compared to the frequency of rs34481144-A in the healthy population, the HIV-1 infected patients did not show any enrichment of this allele.

There were eleven samples from Haiti of African origins, with three patients carrying A/G and eight patients carrying G/G (Figure 35C). The data from the 1000 genome project has

shown that the frequency of rs34481144-A in African descendants is 0.04. Interestingly, the results from our genotyping of these samples showed a 5.8-fold increase in the frequency of A allele, with a value of 0.23. The patient samples were separated into two groups, the group treated with IFN for 24 hours and the control group that was not treated. The cells were then lysed, and I assessed the levels of IFITM3 expression among these eleven samples via WB (not shown). However, no correlation between IFITM3 expression and genotype was observed. The viral load of each individual at the time of sample collection was kindly provided by Dr. Bluma Brenner (Lady Davis Institute, Jewish General Hospital). The correlation analysis showed no significant association between viral load and the genotype rs34481144. The data were analyzed in the same fashion for rs12252. I did not observe any enrichment of rs12252-C, nor any correlation between the viral load and the genotype at rs12252 (Figure 35B and D).

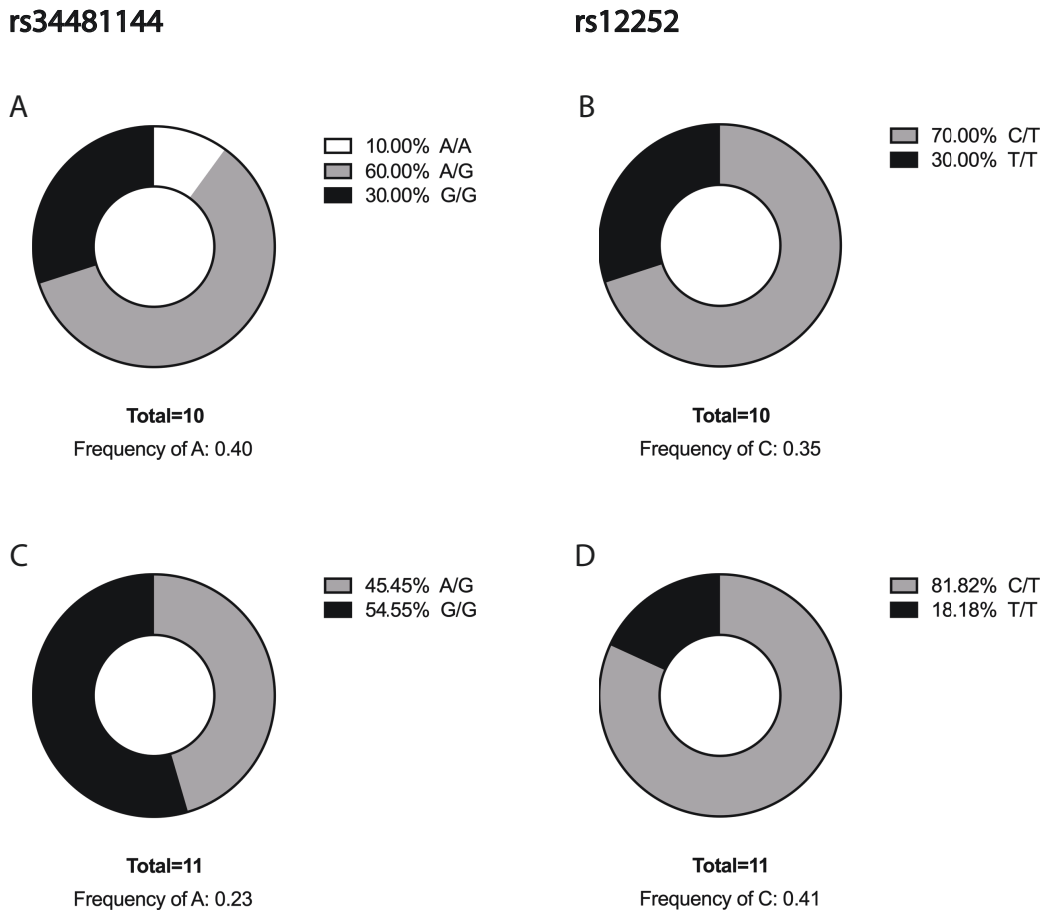

Figure 35: The results of genotyping PBMCs from 21 HIV-1 patients. (A) and (B): The PBMCs from non-Hispanic European origin were genotyped for rs34481144 and rs12252. Each genotype is colour coded with the corresponding percentages in the samples indicated on the right side of each image. (C) and (D): The PBMCs of African descendants were also genotyped for rs34481144 and rs12252. The percentage of each genotype is indicated, and the frequency of the risk allele for each SNP is shown at the bottom.

3.2.3 rs34481144-A is not enriched in HIV-1 infected Han Chinese patients regardless of the route of transmission.

The results from Figure 35 suggested that the genetic background of different ethnicities could potentially influence rs34481144 and rs12252 on the anti-HIV-1 activity of IFITM3. The 4.5-fold increase in rs34481144-A in the patient samples of African origin further raised a possibility that the risk allele may impose a more significant impact on the population with a naturally low frequency of this allele. Since the Han Chinese population has shown the lowest population frequency of rs34481144-A (0.01), I then examined whether there is an enrichment of rs34481144-A in the HIV-1 positive individuals compared to the healthy people. An earlier study has shown the SNP rs12252-C contributes to disease progression in patients of the Han Chinese population. Therefore, I also looked into the frequency of rs12252-C as well [520]. To include the impact of the transmission route on the susceptibility of HIV-1 infection, I genotyped three cohorts of the Han Chinese population, blood transmission, heterosexual transmission and MSM transmission.

rs34481144

A Blood Transfusion

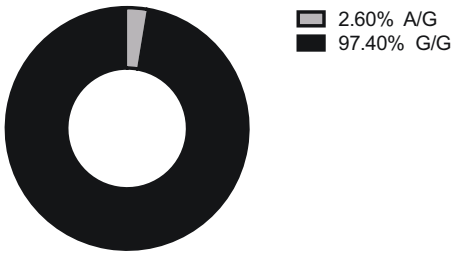

Total=77

Frequency of A: 0.01

C Heterosexually

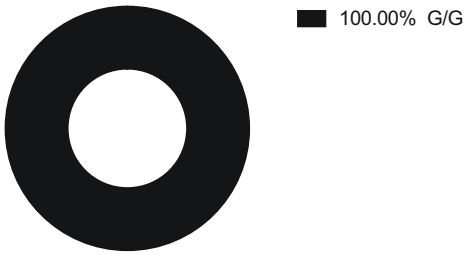

Total=186

Frequency of A: 0

E MSM

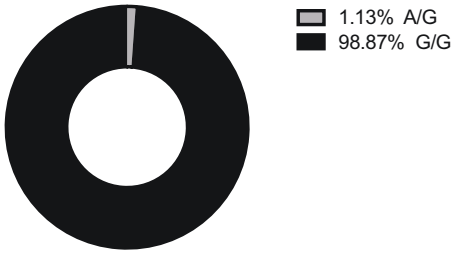

Total=177

Frequency of A: 0.01

G Han Chinese Cohort

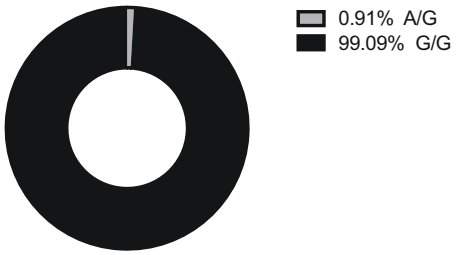

Total=440

Frequency of A: 0.005

rs12252

B Blood Transfusion

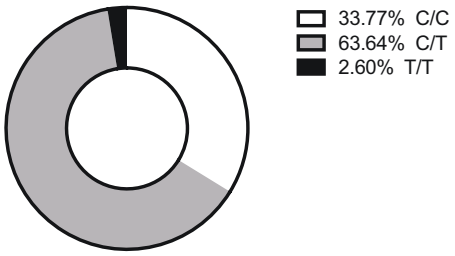

Total=77

Frequency of C: 0.66

D Heterosexually

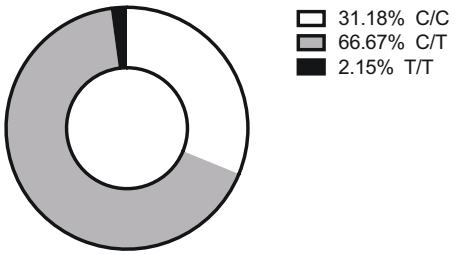

Total=186

Frequency of C: 0.65

F MSM

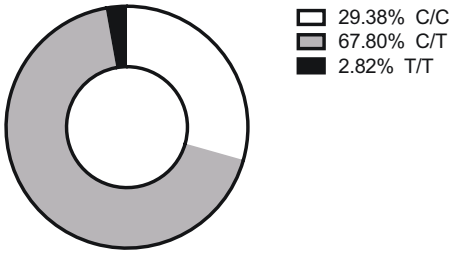

Total=177

Frequency of C: 0.63

H Han Chinese Cohort

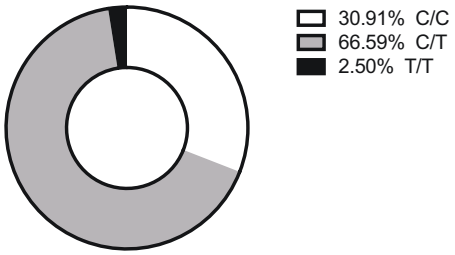

Total=440

Frequency of C: 0.64

Figure 36: The results of genotyping the Han Chinese HIV Cohort. (A) and (B): Blood samples of 77 patients infected by blood transfusion were genotyped for the SNPs rs34481144 and rs12252. (C) and (D): Blood samples of 91 female and 95 male patients who were infected via heterosexual transmission were genotyped for rs34481144 and rs12252. (E) and (F): 177 blood samples of patients infected via MSM were genotyped for rs34481144 and rs12252. (G) and (H): Results from the three cohorts are summarized. A total of 440 patient samples were genotyped for rs34481144 and rs12252. The homozygous risk genotype is labelled in white, heterozygotes are labelled in gray, and the homozygous protective genotype is labelled in black. The percentage of each genotype is presented, and the frequency of the risk allele is indicated at the bottom of each graph.

Among 77 samples of blood transmission caused infections, there was a 1.26-fold increase in rs12252-C and a 1.3-fold increase in rs34481144-A (Figure 36A and B). The patients were not pre-treated with antiretroviral drugs, and the CD4+, CD8+ cell count and the viral load were measured at the time of sample collection. The measurements were classified in terms of rs34481144 or rs12252 genotypes, respectively (Figure 37). The results showed no correlation between the CD4+ or CD8+ cell count to any genotypes. Interestingly, the rs12252 T/T and rs34481144 G/G carriers had a significantly lower viral load than other patients (Figure 37C and F). However, with only two samples carrying rs12252 T/T and two rs34481144 A/G, the statistical significance of the correlation is inconclusive.

Among the 177 MSM patients, there was no increase in the occurrence of the risk allele at both rs12252 and rs34481144 (Figure 36C and D). However, a 1.2-fold increase in rs12252-C and a reduction in the frequency of rs12252 T/T genotype was observed (Figure 36D).

According to the 1000 genome project database, the frequency of rs12252 T/T in the Han Chinese population is 18.4%. Compared to the healthy population, the MSM patients showed a 6.5-fold decrease in T/T frequency. Among 186 heterosexually transmitted patients (91 females and 95 males), the results showed no enrichment of rs34481144-A and a 1.2-fold increase in the rs12252-C allele. I observed an 8.6-fold decrease in rs12252 T/T genotype frequency, which coincides with the data obtained from the MSM group (Figure 36D and F). Since the patient history of treatment cannot be tracked for all samples collected from MSM and heterosexually transmitted cohorts, CD4+, CD8+ cell count and the viral load were not measured at the time of sample collection.

In conclusion, the risk allele A at rs34481144 was not enriched to a statistically significant level in the Han Chinese HIV-1 patients regardless of the transmission route. Interestingly, an increase in C allele frequency at rs12252 and the concurrent reduction of the protective T/T genotype was observed. The protective T/T genotype showed a possible correlation to reduced viral load, implicating that rs12252 SNP may be involved in preventing the disease progression. This result is in agreement with previous findings made by Zhang and colleagues [520].

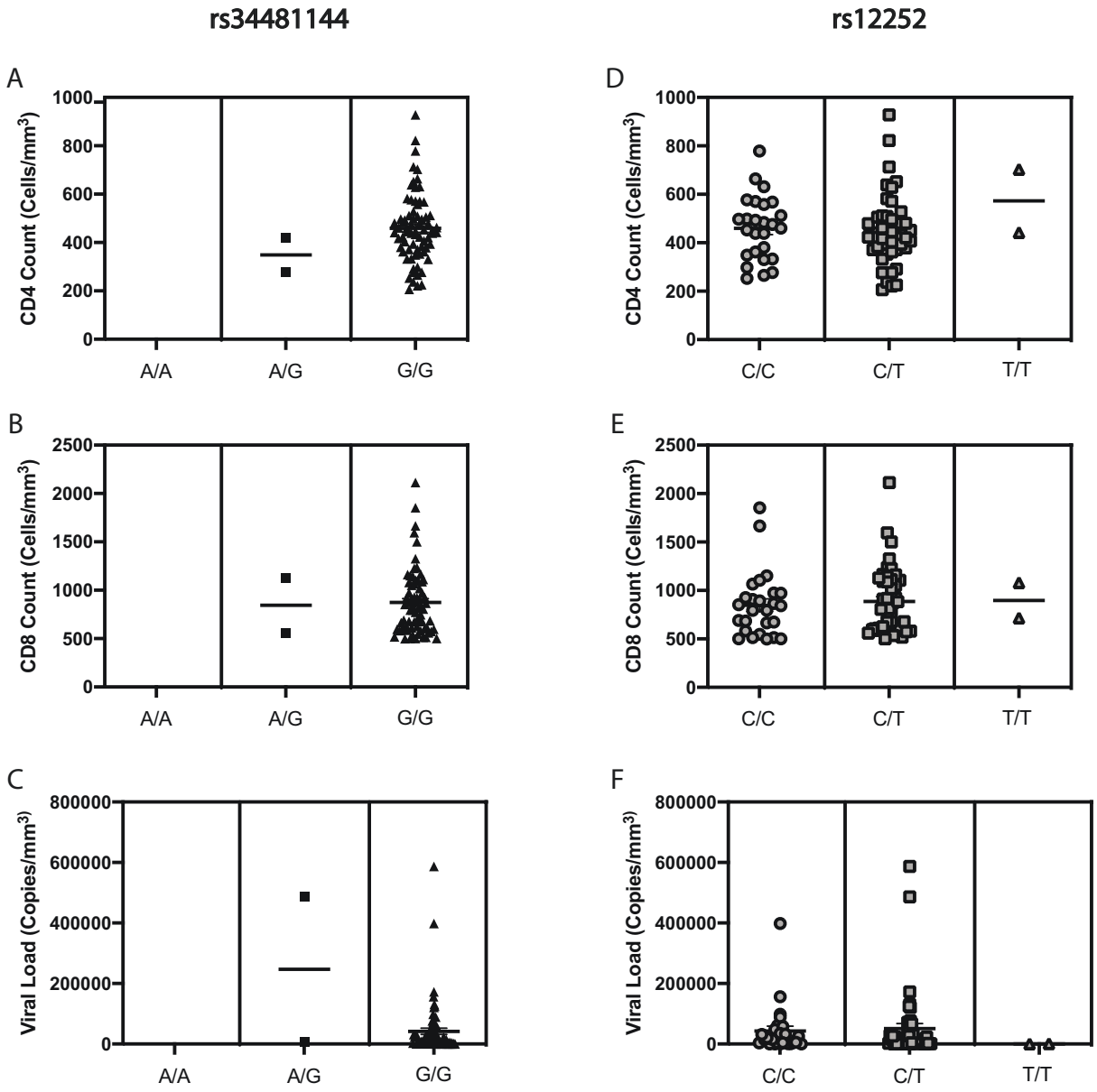

Figure 37: The effects of *ifitm3* SNPs on lymphocyte count and HIV-1 viral load. (A) – (C): The numbers of CD4+ T cells, CD8+ T cells and the values of the viral load at the time of blood collection were catalogued based on the genotype. There were no rs34481144 A/A. The mean was obtained from two A/G genotype carrying samples without SEM. The average was obtained for G/G homozygotes, and the SEM is shown as the error bars. (D) – (F): The numbers of CD4+ T cells, CD8+ T cells and the viral load at the time of blood collection were classified based on the rs12252 genotype. The mean and the SEM were obtained for both C/C and C/T genotypes

carrying samples. The mean was calculated and was shown for the two T/T homozygotes without SEM.

I obtained PBMCs of sixteen individuals from the blood transfusion cohorts to assess the expression level of IFITM3 mRNA. The mRNA level of GAPDH was also quantified as the internal control and used to normalize the cycle numbers of IFITM3. The normalized cycle numbers of the IFITM3 mRNA were categorized based on the genotypes at rs34481144 or rs12252 (Figure 38A and B). According to the results of Allen and colleagues, the *ifitm3* should be more in rs34481144 G/G carrying individual, and less expressed in A/A homozygotes. However, I did not observe the same result (Figure 38A), most likely due to the limitation in the sample numbers. The effect of the rs12252 genotype on IFITM3 expression was also assessed (Figure 38B). There is a general reduction in IFITM3 expression associated with rs12252-T. However, the small sample numbers limit the statistical analysis of this observation. Therefore, a significant correlation between the rs34481144 and rs12252 genotypes to IFITM3 expression level was not concluded.

Next, I investigated the correlation between the expression level of IFITM3 versus CD4+ T cell, CD8+ T cell count, and the values of viral load. The correlation was calculated between PCR cycle numbers of IFITM3 mRNA and the CD4+T cell, CD8+ cell count, and viral loads (Figure 38C - E). The results, however, showed that the level of IFITM3 was not related to the number of CD4+/CD8+ T cells nor the viral load. The IFITM3 level was also measured for the same set of samples after 24 hours of IFN-treatment. Correlations studied between the fold increase in IFITM3 expression after IFN-treatment (i.e. IFITM3 inducibility), T cell count and the level of viruses for each individual were examined (not shown). Again, no evident increase in

IFITM3 expression nor any correlation to T cell count and the viral load was observed. Since the patients were not treated with antiretroviral drugs at the time of blood harvesting, the active infection could have already caused a high level of IFN in patients, which would explain the limited to absence of increase in IFITM3 in PBMCs. Therefore, my results did not reveal any impact of rs34481144 and rs12252 genotypes on IFITM3 expression, stimulation by IFN, lymphocyte number, or the ability to control HIV-1 infection.

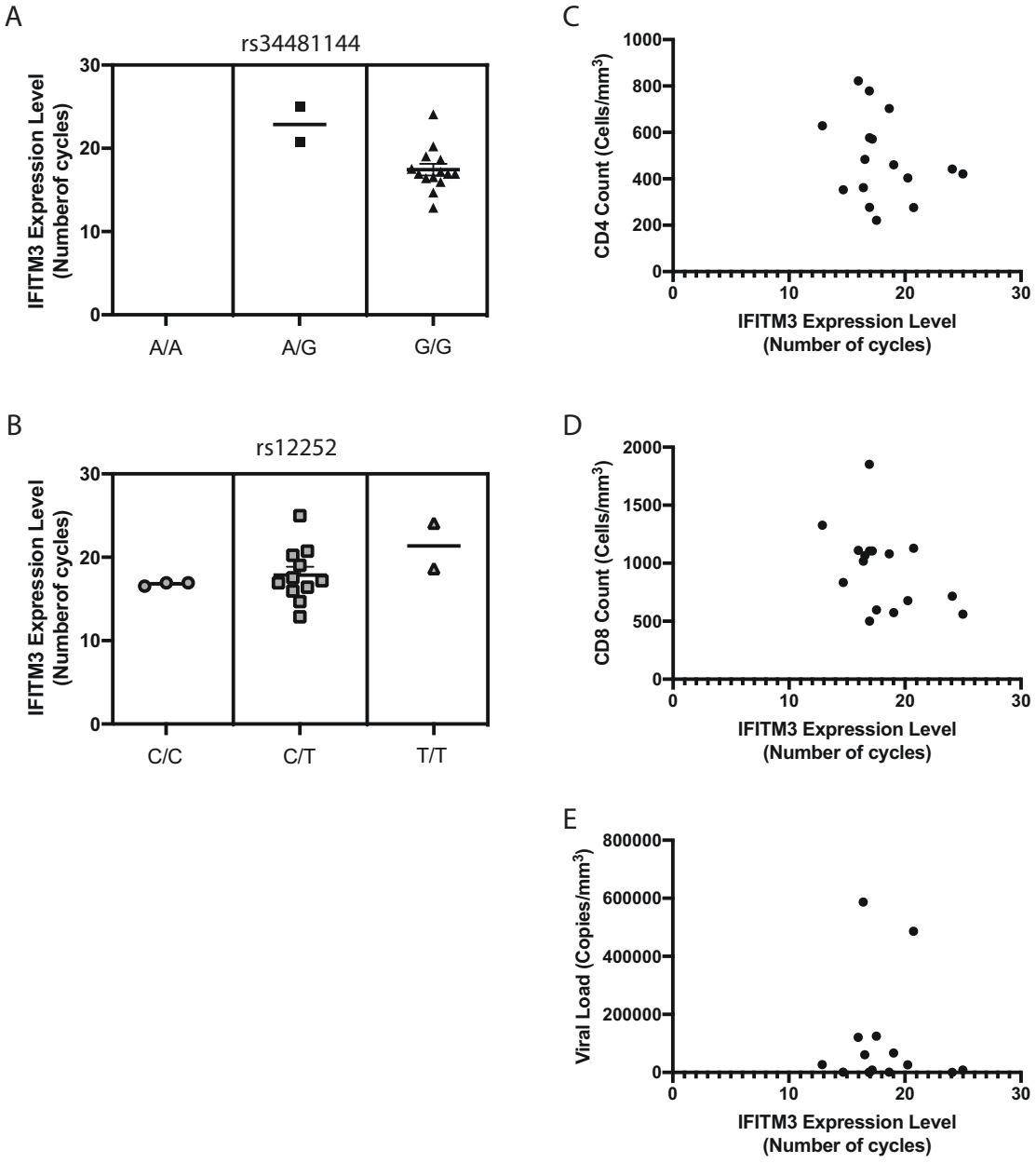

Figure 38: IFITM3 mRNA levels in PBMCs from HIV-1 patients. The frozen PBMCs of the 16 HIV-1 patients from the blood transfusion cohort were cultured five days. The total mRNA was reverse transcribed using poly (T) primer, and the produced cDNA was purified for each sample. The same amount of cDNA was loaded to perform PCR using the primers for GAPDH and IFITM3. The cycle numbers for both genes of the samples were recorded. The cycle numbers of the IFITM3 mRNA were normalized based on the values of the GAPDH cycle

number. (A) The normalized cycle numbers of IFITM3 mRNA were categorized based on the rs34481144 genotypes. There was no A/A homozygote, two A/G heterozygotes, and thirteen G/G homozygotes in the samples. The average level of IFITM3 expression was obtained for both A/G and G/G. The error bars were plotted for G/G samples based on the SEM. (B) The normalized cycle numbers of IFITM3 mRNA were classified based on the rs12252 genotypes. There were three C/C homozygotes, eleven C/T heterozygotes and two T/T homozygotes in the samples. The average level of IFITM3 expression was obtained for all the genotypes. The error bars were plotted for C/C and C/T samples based on their SEM values. (C) (E) The correlation was calculated between the expression levels of IFITM3 and the numbers of CD4+ T cell count, CD8+ T cell count and viral loads. The viral load that was lower than the detectable level was given a value of 0 in the graph.

In Chapter 3.2, I studied the effect of IFITM3 on HIV-1 infection in the human population. The two SNP, rs34481144 and rs12252, shown to modulate IFITM3 expression were investigated. The HIV-1 infected PBMCs showed a wide variation in IFITM3 expression in different individuals. Although some protective effects by rs34481144-G were observed, the outliers significantly mitigated the phenotype. There was no enrichment of the risk allele rs34481144-A in the Han Chinese population. Viral load in the patients without previous treatment was shown to be influenced by the rs34481144 genotype. However, the sample size which was investigated was not large enough to obtain statistically significant conclusions. The implications of these results will be further discussed in Chapter 4.2.2.

3.3 IFITM3 potentiates the anti-HIV-1 activity of CH25H.

As introduced in section 1.5.2, IFN induces the expression of many ISGs with potential anti-HIV-1 activity. Therefore, I proposed to investigate the combined anti-HIV-1 effects of IFITM3 with other ISGs. To gain further insight into the mechanism of the IFITM3 antiviral function, I selected one of the ISGs, cholesterol-25 hydroxylase, as one candidate. Hydroxycholesterols are a group of cholesterol derivatives that have become increasingly recognized for their functions in the immune response. 25-hydroxycholesterol is one of such cholesterol derivatives that are produced by an IFN-inducible enzyme CH25H [407]. 25HC was previously known as a regulator of cholesterol biosynthesis. Recently, two studies reported the antiviral effects of 25HC against Zika virus and HIV-1 [405,406]. The water solubility of 25HC allows it to be secreted extracellularly and act in paracrine to increase CH25H expression. Thereby, 25HC could potentially help the establishment of innate immunity in the uninfected neighbouring cells. Since both 25HC and IFITM3 were shown to inhibit viral entry by modifying cell membrane composition [462,499], I hypothesized that 25HC and IFITM3 might function in an additive or synergistic manner against HIV-1 infection.

3.3.1 25HC exerts different potency in inhibiting HIV-1 in different cell lines.

First, I tried to verify the previous findings that have shown the inhibition of HIV-1 by 25HC. CEM-Rev cells were pre-incubated with different doses of 25HC before the infection by NL4-3. The progeny viruses were harvested and used for infecting TZM-bl cells. The luciferase activity of both CEM-Rev cells and TZM-bl cells were measured. The levels of progeny viruses under different conditions were also determined by measuring the RT activity. The luciferase activity of TZM-bl cells shown in Figure 39 was the result of infections with viruses of the same level of RT activity. The results showed that with 500 nM of 25HC, the infection of CEM-Rev

cells was not affected. However, the level of the progeny viruses was reduced by 4-fold for NL4-3 and 3-fold for AD8-1, respectively. These findings suggest that 25HC suppresses HIV-1 production and reduces virus infectivity.

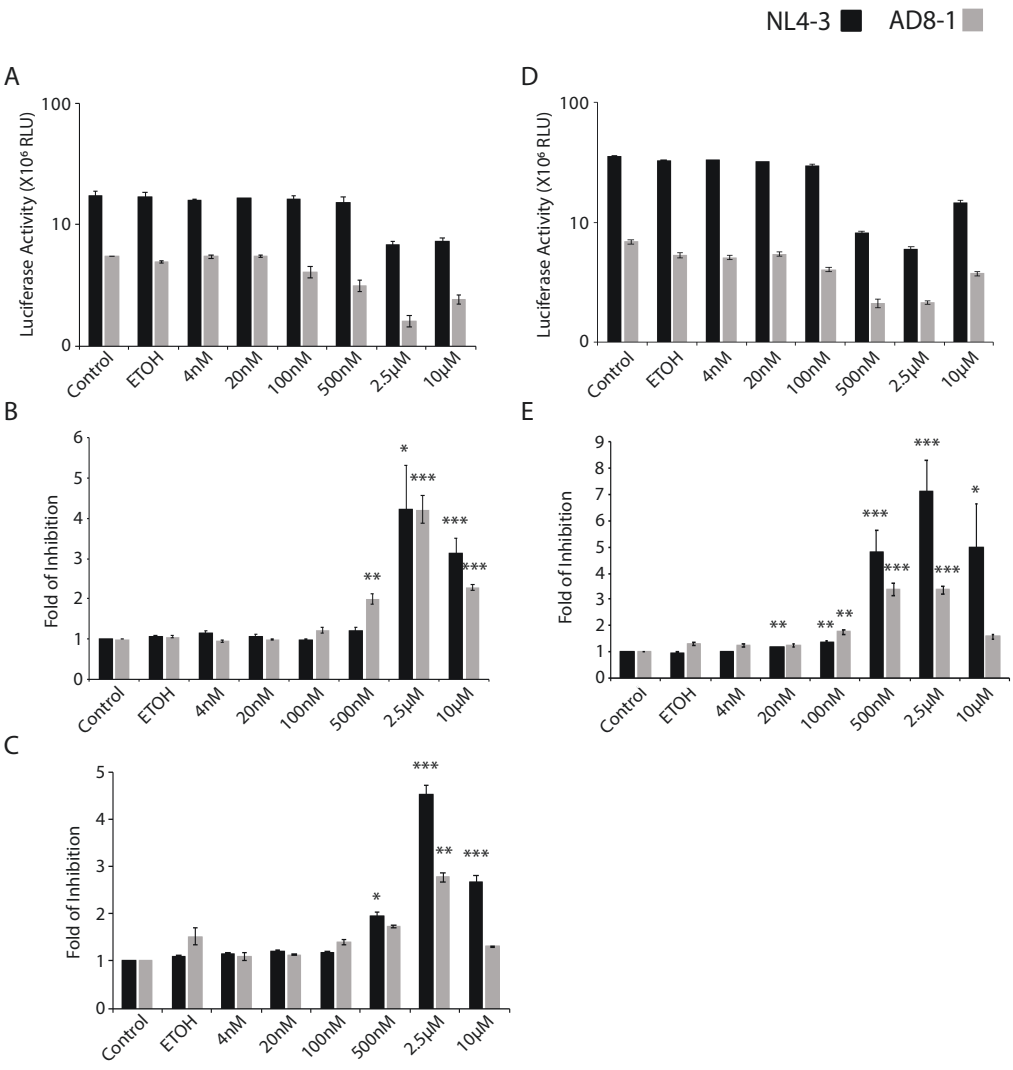

Figure 39: The effect of 25HC on NL4-3 and AD8-1 infection. (A) The representative results of luciferase activity in CEM-Rev cells. The luciferase activity of NL4-3 and AD8-1 infected CEM-Rev cells were quantified. (B) The average of the results from three sets of experiments. The fold inhibition by different doses of 25HC was calculated by comparing the luciferase to the untreated control value. The luciferase activity of the control was arbitrarily set to a value of 1.

(C) Flow cytometry experiment. CEM-Rev cells were analyzed by flow cytometry to measure the number of cells expressing p24. The fold inhibition by 25HC was calculated by comparing the percentage of p24 positive cells under each condition to control treatment. The percentage of p24 positive cells of the control was arbitrarily set a value of 1. (D) The representative result of the luciferase of TZM-bl cells. The progeny viruses produced by CEM-Rev cells were used to infect TZM-bl cells. Luciferase activity of infected TZM-bl cells was shown in the graph. (E) The average results from three sets of TZM-bl cells experiments. The fold inhibition was calculated by comparing the luciferase activity of TZM-bl cells under different treatment to that of the control, which was arbitrarily set to a value of 1. The experiments were repeated three times, with each time done in triplicates. The student t-test was performed to evaluate the statistical significance of the difference between the control and conditioned groups (*, $P < 0.05$; **, $P < 0.01$; ***, $P < 0.001$).

Next, I repeated the same experiments in CBMCs to evaluate the function of 25HC in primary cells. CBMCs were isolated from healthy individuals and were pre-incubated with 25HC before the infection with NL4-3 or AD8-1. The progeny viruses were collected and used for infecting TZM-bl cells. The luciferase activity of TZM-bl cells was measured. The luciferase values produced from the viruses are shown in Figure 40 A. As CBMCs showed higher sensitivity to the toxicity of 25HC, I used a lower amount of 25HC to treat these cells. The results showed that when the concentration of 25HC is below 100 nM, no reduction in HIV-1 infection was observed for NL4-3 and AD8-1. At 500 nM, 25HC treatment reduced the infectivity of the progeny viruses produced from CBMCs at 4.5-fold and 5.3-fold for NL4-3 and AD8-1, respectively. Similar to what has been observed with CEM-rev cells, the efficiency of

the primary infection of CBMCs were analyzed by flow cytometry (Figure 40C). The percentage of Gag positive CBMCs were quantified by detecting the fluorescent signals with anti-p24-FITC antibodies. In accordance with the previous results, NL4-3 was more infectious than AD8-1, which infected 10% of CBMCs. The results showed that the infection of CBMCs with NL4-3 was not significantly affected by 500 nM of 25HC, whereas the infection with AD8-1 was reduced by 3-fold (Figure 40D). Compared to the fold reduction in the infectivity of the progeny viruses (Figure 40B: 4.3-fold for NL4-3 and 5.6-fold for AD8-1), there was less inhibitory effect exhibited by 25HC during the infection of CBMCs. Therefore, these results support my previous findings, in which 25HC also reduces the infectivity of the progeny viruses in addition to inhibiting HIV-1 entry. Together, I showed a novel activity of 25HC in attenuating HIV-1 infection in addition to inhibition of viral entry, as previously reported [406].

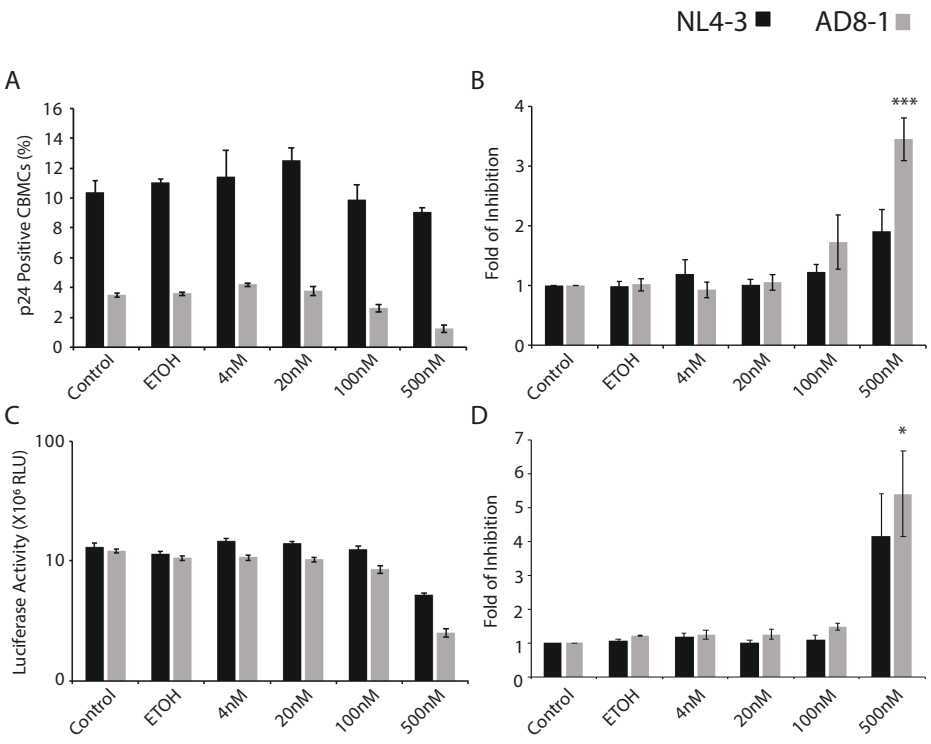

Figure 40: The anti-HIV-1 activity of 25HC in CBMCs. (A) Representative results from HIV-1 infections of CBMCs. The efficiency of infection of CBMCs with NL4-3 and AD8-1 was analyzed by flow cytometry. The percentages of HIV-1 infected CBMCs were measured by immunostaining with Gag/p24 and flow cytometry. The experiments were repeated four times independently. The results of a representative set of data are shown. (B) The average results from four sets of flow cytometry data of CBMCs. The fold inhibition by 25HC was calculated by comparing the percentage of infected CBMCs under each condition to that of the control, which was arbitrarily set to a value of 1. The values of the fold inhibition were obtained for each set of experiments, and the average of the four experiments is presented in the graph. The SEMs were calculated and used to plot the error bars. (C) The representative results from the luciferase experiments of TZM-bl cells. The progeny viruses produced from infected CBMCs were used to infect TZM-bl cells. At 40-hour post-infection, the TZM-bl cells were harvested, and the luciferase activity was measured. The luciferase activity resulting from the infection by the viruses is presented. The experiments were performed in triplicates for four times independently. The results of a representative experiment are shown. The averages and the SEMs were calculated from the data of the triplicates. (D) The average results from four sets of luciferase data of TZM-bl cells. The fold inhibition was calculated by comparing luciferase activity of TZM-bl cells under each condition to that of the control, which was set to a value of 1. The values of the fold inhibition were obtained for each set of experiments, and the average of the four experiments is shown. The SEMs were calculated and used to plot the error bars. The student t-test was performed to evaluate the statistical significance of the difference between the control and conditioned groups (*, $P < 0.05$; **, $P < 0.01$; ***, $P < 0.001$).

3.3.2 25HC inhibits the production of Gag and Env.

Since I observed a reduction in viral production upon 25HC treatment, I next examined HIV-1 protein levels of the infected cells and the progeny virions. First, I harvested NL4-3 infected CEM-rev cells and progeny virions for Western blot analysis (Figure 41). The levels of Env, Gag and IFITM2 and 3 were determined in both cellular and viral lysates. The results showed that when higher than 500 nM 25HC was supplied to the CEM-rev cells, the production of Env, Gag and IFITM proteins were decreased. Similar observations were made for gp120/gp41 Env and Gag in viral lysates. Furthermore, there was a significantly higher reduction of gp120/gp41 at 500 nM 25HC observed in viral than in cell lysate. Similarly, reduced p24 was observed in the viral lysate despite the same level of p55 Gag precursor. This finding suggests that 25HC may interfere with the production of immature gp160, as well as the maturation of Env and Gag.

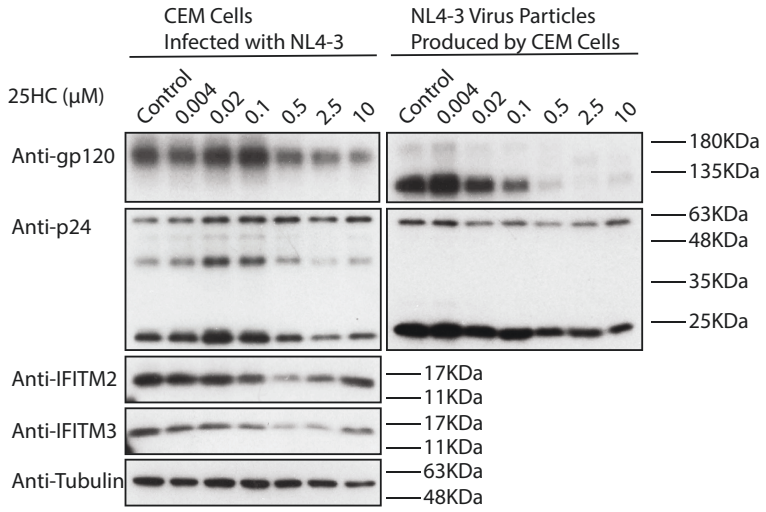

Figure 41: The effect of 25HC on NL4-3 viral expression. The CEM-rev cells were treated with different doses of 25HC for 24 hours prior to infection. The CEM-rev cells were then infected with NL4-3. NL4-3 viruses freshly produced by the infected CEM-rev cells were harvested after 48 hours and concentrated by ultracentrifugation. The CEM-rev cells and the concentrated NL4-3 virions were lysed and examined for viral proteins, IFITM 2 and 3 using antibodies against gp120, p24, IFITM2 and IFITM3. The tubulin expression level was also examined as an internal control.

To further test the implication of 25HC in disrupting Env maturation, I analyzed NL4-3 and AD8-1 infected CEM-rev cells (Figure 42A). At 500 nM 25HC, the reduction of gp120 was shown in the NL4-3 virions produced by CEM-rev cells. With the gp41 level also assessed by WB analysis, this finding confirms my previous observation in Figure 41 that 25HC impairs Env maturation. The levels of gp160 and gp41 at 500 nM 25HC treatment in the cell lysate showed reduction compare to the control, suggesting the Env production in the infected cells was also

interrupted. Similarly, the cell lysate of AD8-1 infected CEM-rev cells demonstrated a significant reduction in gp160 and gp41 (Figure 42).

The cell and viral lysates of CBMCs infected with NL4-3 and AD8-1 were also analyzed (Figure 42B). Interestingly, I observed a more significant decrease in gp120 in the AD8-1 viral lysate than NL4-3. These results are in agreement with the more potent inhibition of AD8-1 infection of CBMCs observed in Figure 40. In the cell lysates, AD8-1 gp160 and gp41 levels were also more potently reduced compared to NL4-3 infected CBMCs. A decrease in gp120 was observed again in the NL4-3 viral lysate. In contrast, the impairment of Env maturation by 25HC was not observed for AD8-1. Therefore, 25HC may affect Env production and maturation by different mechanisms. The activity of each function may also vary for different cell types and different HIV-1 strains. In the case of CEM-rev cell and CBMCs, the impairment of gp160 maturation is more pronounced in NL4-3 infection, whereas the reduction of gp160 production is greater in AD8-1 infection. CBMCs were more sensitive to the interference of 25HC in viral protein production than CEM-rev cells.

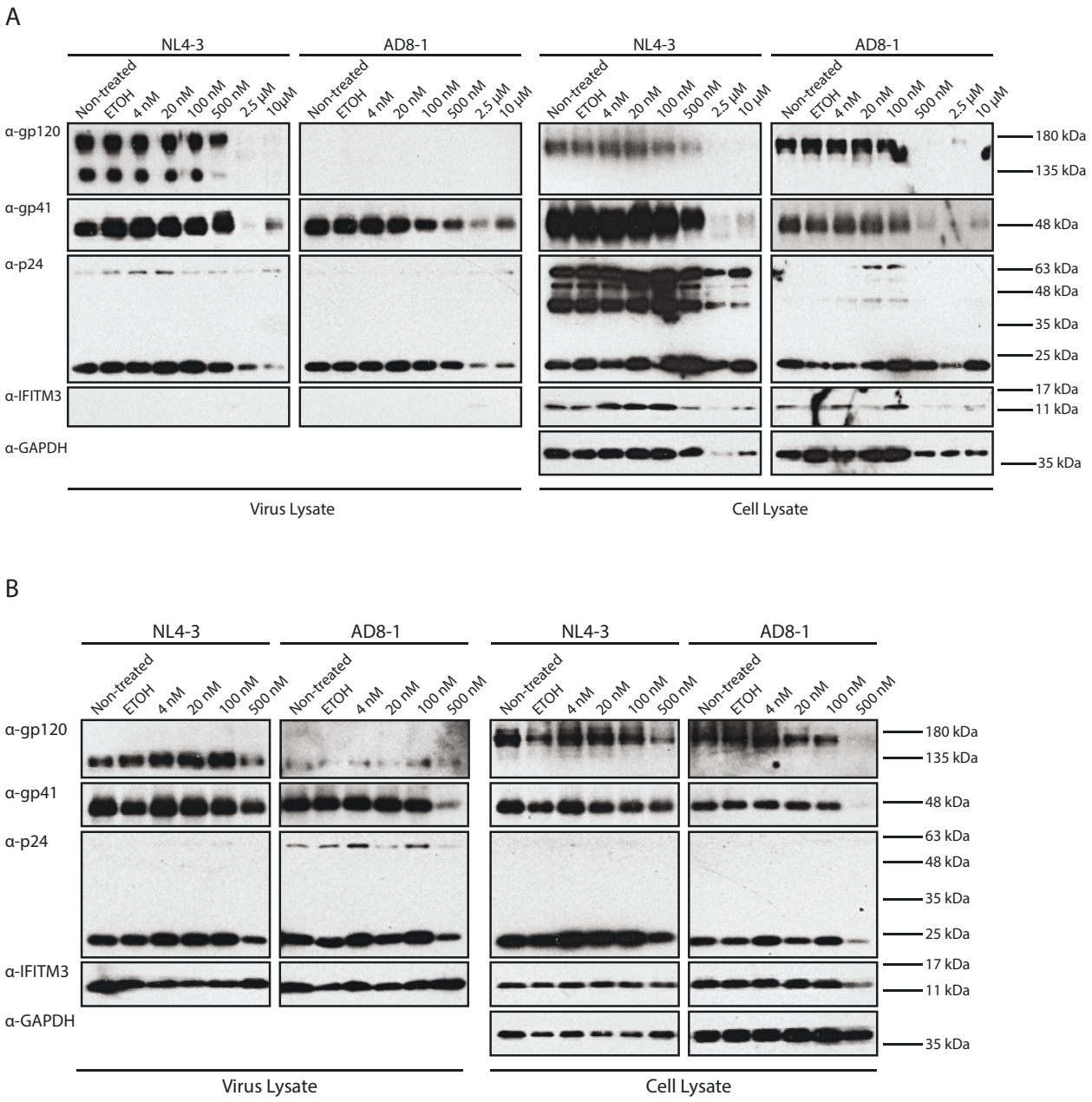

Figure 42: The impact of 25HC on HIV-1 protein levels. (A) The CEM-rev cells were treated with different doses of 25HC for 24 hours prior to infection with NL4-3 and AD8-1. The NL4-3 and AD8-1 virions freshly produced by the infected CEM-rev cells were harvested 48 hours after and concentrated by ultracentrifugation. The infected CEM-rev cells, and the concentrated NL4-3 and AD8-1 virions were lysed and subject to Western blot analysis. Levels of viral proteins and IFITM 3 were determined for the cellular and viral lysates using the antibodies against gp120,

p24, and IFITM3. The level of GAPDH was determined as an internal control. (B) The CBMCs were treated with different doses of 25HC 24 hours prior to infection. NL4-3 and AD8-1 freshly produced by the infected CBMCs were harvested 48 hours later and concentrated via ultracentrifugation. The infected CBMCs, and concentrated NL4-3 and AD8-1 virions were lysed and examined by Western blot for gp120, p24, and IFITM3. GAPDH expression was determined as an internal control.

3.3.3 25HC potentiates the anti-HIV-1 activity of IFITM3.

Since both 25HC and IFITM3 were implicated in modifying the property of cell membranes and inhibiting HIV-1 entry, the combined activity of these two factors was then tested in the MT4-R5 cell line. The control cells, MT4-R5-QCXIN, and the IFITM3-expressing cells, MT4-R5-IFITM3, were used for this experiment. The wild type NL4-3 and AD8-1 were tested in both cell lines. The infected MT4 cells were scored as p24-positive by flow cytometry. The results showed that NL4-3 was more potently inhibited by either 25HC or IFITM3 than AD8-1 (Figure 43A and B). At 250 nM of 25HC, NL4-3 infection was inhibited to 3.2-fold and AD8-1 was barely affected with a 1.6-fold reduction in MT4-R5-QCXIN cells (Figure B). When the cells were not treated with 25HC, IFITM3 alone inhibited NL4-3 infection by 5.9-fold and AD8-1 by 3.8-fold (Figure C). Astonishingly, cells treated with 100 nM of 25HC, which by itself did not inhibit NL4-3, increased the inhibition of NL4-3 by IFITM3 to 14.9-fold (Figure 43C). Therefore, a 2-fold potentiation of anti-HIV-1 activity of IFITM3 was observed. In contrast, the addition of 100 nM 25HC did not increase the potency of IFITM3 against AD8-1, which remained as 3.6-fold (Figure C). This observation implies that 25HC may enhance the anti-HIV-

1 activity of IFITM3 in the infection of some viruses. This implication will be discussed further in Chapter 4.2.3.

Next, I collected NL4-3 and AD8-1 produced by infected MT4-R5 cells. The level of infectivity was measured with TZM-bl cells. When the MT4-R5 cells were not under any treatment, the NL4-3 viruses produced from MT4-R5-IFITM3 cells showed a 10.4-fold decrease in infection when compared to the ones produced from the control cells (Figure 43F). At 100 nM of 25HC, the NL4-3 produced from MT4-R5-IFITM3 demonstrated a 14.9-fold reduction in infection. In the case of AD8-1, no reduction of infection was observed again (Figure 43F). The AD8-1 viruses produced from MT4-R5-IFITM3 cells showed a 1.67- and 1.72-fold reduced infection in untreated and 100 nM 25HC treated conditions, respectively (Figure 43F). The RT activity of the progeny viruses was measured to assess the level of virion production. When incubated with 100 nM of 25HC, MT4-R5-IFITM3 produced 7.44-fold less NL4-3 than the control cells (Figure 43H). When there was no 25HC, a 3.66-fold reduction in NL4-3 production was observed in MT4-R5-IFITM3 cells. The 2-fold decrease in virion production reflects the enhanced IFITM3 entry inhibition by 25HC at 100 nM when MT4-R5 cells were first infected. On the contrary, there was no difference between the AD8-1 production between the untreated and 100 nM 25HC treated conditions. Together, these results suggest that 100 nM of 25HC enhanced the anti-HIV-1 activity of IFITM3 by 2-fold in NL4-3 infection. This enhancement is reflected in the level of progeny viruses produced by the infected cells. In agreement with my previous results, the IFITM3 expressed in MT4-R5 cells reduced the infectivity of NL4-3 but had no effect on AD8-1. Since TZM-bl cells were not treated with 25HC, no further enhancement of entry inhibition was observed.

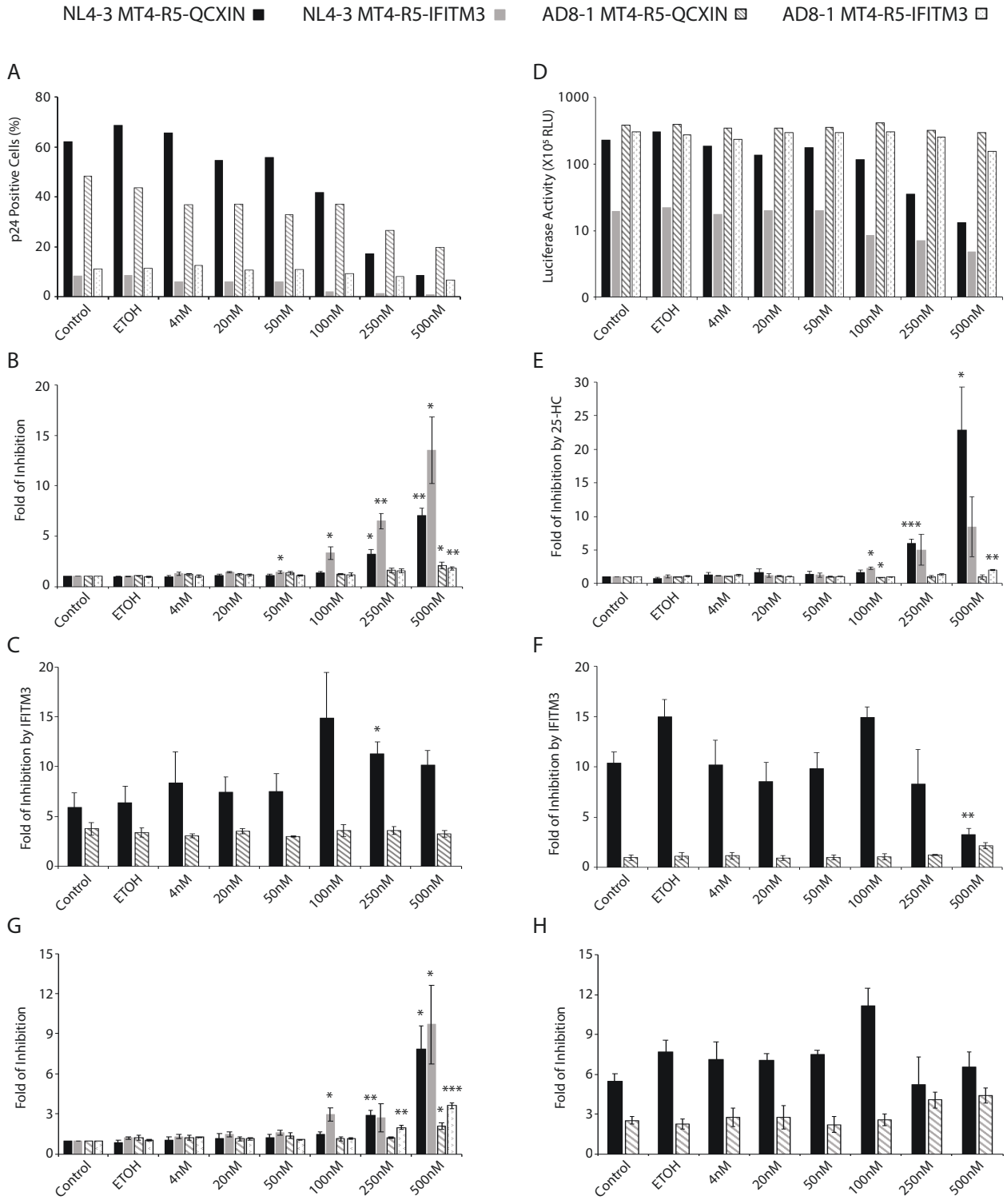
NL4-3 MT4-R5-QCXIN
NL4-3 MT4-R5-IFITM3
AD8-1 MT4-R5-QCXIN
AD8-1 MT4-R5-IFITM3
A
p24 Positive Cells (%)
D
Luciferase Activity (X10⁵ RLU)
B
Fold of Inhibition
E
Fold of Inhibition by 25-HC
C
Fold of Inhibition by IFITM3
F
Fold of Inhibition by IFITM3
G
Fold of Inhibition
H
Fold of Inhibition
Control
ETOH
4nM
20nM
50nM
100nM
250nM
500nM

Figure 43: 25HC increases the anti-HIV-1 activity of IFITM3. (A) The representative results of infection of MT4-R5 cells with HIV-1. The MT4-R5 cells under four different conditions (Control, 25HC only, IFITM3 only and 25HC+IFITM3) were infected with NL4-3 or AD8-1. The MT4-R5 cells were harvested and analyzed by flow cytometry to determine the percentage of cells expressing HIV-1 p24. (B) The averages of data from the two independent MT4-R5 infection experiments with each time done in duplicate. The fold inhibition by 25HC was calculated by comparing the percentage of p24+ MT4-R5 cells of the control condition to the 25HC-treated conditions. (C) The effect of IFITM3 on HIV-1 infection of MT4-R5 cells. The fold inhibition by IFITM3 was calculated by dividing the percentage of p24+ MT4-R5-IFITM3 cells by the percentage of p24+ control MT4-R5 cells under the treatment of various 25HC concentrations. The average of data collected from two independent experiments with each time duplicates was calculated and presented. The SEM of the data is represented by the error bars. (D) Representative results from infection of TZM-bl cells to determine the level of infectious HIV-1. The progeny viruses produced by MT4-R5 cells under each condition were collected and used for infecting TZM-bl cells. At 40 hours post-infection, TZM-bl cells were harvested, and luciferase activity was measured. One representative result is shown. (E) The effect of 25HC treatment on the level of infectious progeny viruses was assessed by calculating the fold inhibition in the same manner as described for (B). The luciferase activity of the control condition for each cell line was arbitrarily set to a value of 1. Luciferase measurements of the TZM-bl cells under other conditions were compared to the control condition from the same cell line. The average values were obtained from the results of two independent experiments with each time duplicates, and the SEM values were presented as the error bars. (F) The effect of IFITM3 on the production of progeny viruses under each concentration of 25HC was assessed by

calculating the fold inhibition by IFITM3. The values were obtained in the same manner as described for (C). The luciferase values of MT4-R5 without IFITM3 expression was arbitrarily set to a value of 1. (G) The amount of virus produced under each condition was determined by measuring viral RT activity. The effect of 25HC on virus production is shown in (G), and the effect of IFITM3 on virus production is shown in (H). The average values were calculated based on the results of two independent experiments with each time duplicates. The error bars are plotted based on the SEM. Different concentrations of 25HC are indicated on the x-axis. The student t-test was performed to evaluate the statistical significance of the difference between the control and conditioned groups (*, $P < 0.05$; **, $P < 0.01$; ***, $P < 0.001$).

Chapter IV: Discussion

4.1 Summary of Results and Contributions to the Field

The role of IFITM3 as an anti-HIV-1 restriction factor was first reported in 2011 by our lab [463]. IFITM3 was the first restriction factor that has been identified to deter HIV-1 entry. Later studies have revealed that inhibition of fusion pore formation serves as the underlying mechanism of IFITM3's entry inhibition [462,480]. While all these previous studies have focused on the function of IFITM3 expressed in the virus-targeting cells, a group from France studied the function of IFITM3 in virus-producing cells [506]. They discovered that expressing IFITM3 on virus-producing cells lead to the incorporation of IFITM3 into the HIV-1 virions, which in result, disrupts the efficiency of HIV-1's cell-to-cell transmission. Therefore, IFITM3 is a unique restriction factor that exhibits anti-HIV-1 in the virions and the virus-targeting cells.

For successfully establishing infection in the target cells, HIV-1 has evolved two mechanisms to antagonize the host restriction factors. First, HIV-1 expresses many accessory viral genes that specifically abrogate the anti-HIV-1 function of some potent restriction factors. For example, Vif targets APOBEC3G and Vpu targets tetherin/BST-2 for proteasomal degradation [521,522]. However, HIV-1 has a small genome that does not accommodate too many accessory proteins. Another way of overcoming the host restriction factors is to mutate the epitopes of the targeted viral proteins. The immune targeting is tolerated by HIV-1 because of its high mutation rate and the tolerance to variations in the viral structural proteins. For example, HIV-1 capsid readily mutates to escape the targeting by TRIM5-alpha and Mx2/MxB [523-525]. Nevertheless, when I started this project, there was no study published showing the viral

countermeasure against IFITM3. Therefore, this study was initiated to identify the viral proteins that ablate the antiviral activity of IFITM3.

The findings of this thesis identified HIV-1 Env as the modulator of the viral sensitivity to IFITM3. In Chapter 3, I first identified HIV-1 strains that are resistant to IFITM3 inhibition. By testing HIV-1 strains for their sensitivity to IFITM3 expressed in the virus-producing cells and the target cells, I found that the IFITM3-resistant phenotype of Env is retained regardless of the location of IFITM3 expression. Further mutagenesis studies mapped the IFITM3-resistant property to the V3-loop region of Env. Next, I looked into the effect of IFITM3 incorporation into the HIV-1 virions. I found that the entry efficiency of the IFITM3 bearing HIV-1 was diminished, and the Env maturation in the virus-producing cells was interrupted. The neutralization assays with sCD4 and neutralization antibodies revealed the correlation between Env conformation and its sensitivity to IFITM3. HIV-1 with IFITM3-sensitive Env are also more susceptible to sCD4 and 17b neutralization. Despite this strong correlation, IFITM3-bearing HIV-1 did not show enhanced inhibition to these blocking agents compared to IFITM3-free HIV-1. Therefore, IFITM3 in the virions does not modulate Env conformation by exposing its epitopes to sCD4 and 17b. A group of JRFL mutants that are differentially sensitive to sCD4 were tested for their sensitivity to IFITM3. The results confirmed that sCD4-sensitive HIV-1 Env is more susceptible to IFITM3 inhibition. As sCD4-sensitive Env is at its higher energy state, "the open conformation", the results of my thesis suggest that Env with an "open" ground state conformation is readily subjected to IFITM3 inhibition.

Next, I looked into the effect of IFITM3 *in vivo*. There is still an ongoing debate on whether SNPs of IFITM3 affect its antiviral activity. Some studies on influenza infection in animal models and the human population have shown that the risk allele of certain SNPs

(rs12252 and rs34481144) appears at a higher frequency in severe illness cases. Only one study has shown that the risk allele at rs12252 correlates with a worse prognosis in HIV-1 infected patients but has no effect on acquiring HIV-1. Therefore, I searched for any correlation between the risk allele at rs34481144 and rs12252 and HIV-1 infection/disease progression. Interestingly, the frequency of risk alleles varies widely among different ethnic groups. Therefore, the data were analyzed for each ethnic group. In my thesis, I found no enrichment of risk allele at rs12252 and rs34481144 in HIV-1 patients regardless of the transmission route. Contrary to Allen et al., I also did not see a correlation between the rs34481144-A homozygotes and reduced IFITM3 expression.

Lastly, I investigated whether HIV-1 uses Env to counteract other entry inhibitors that function similarly to IFITM3. The hydroxylated product of CH25H has been shown to inhibit HIV-1 entry by possibly manipulating the cholesterol homeostasis of the cell membrane. Therefore, I tested how NL4-3 and AD8-1 respond to 25HC during the infection. Unlike our prediction, both strains were inhibited by 25HC to different degrees in two cell types. Therefore, the IFITM3-resistant Env, AD8-1, did not show resistance to 25HC inhibition. Remarkably, I found that at lower than effective dose, 25HC can potentiate the anti-HIV activity of IFITM3. This phenotype was only observed for NL4-3, but not AD8-1. Hence, the augmentation of IFITM3 activity by 25HC only occurs in IFITM3-sensitive HIV-1.

4.2 Outstanding Questions

My thesis revealed the novel function of Env as a viral protein hampering IFITM3 inhibition. However, there are still many unanswered questions that need further investigation. In the following section, I will discuss three outstanding questions from my work and future directions for this research.

4.2.1 How does mutating the V3-loop allow HIV-1 to overcome IFITM3 inhibition?

Consistent with previous reports, I observed the incorporation of IFITM3 in the virus envelope, which was directly proportional to the amount of IFITM3 expressed by the producer cells [506,507]. My results showed that virus infectivity is affected by the level of IFITM3 incorporation in the cell-free system. This observation is also in agreement with what has been observed previously [506]. However, the increase in IFITM3 expression only enhances the entry inhibition of IFITM3 sensitive strains, such as NL4-3, but not IFITM3 resistant strains, such as AD8-1. It is also interesting to note that AD8-1 was shown to downregulate the expression of IFITM3 (Figure 22A and B). However, this observation does not contribute to AD8-1 resistance to IFITM3, as the NL(AD8) and NL(AD8V3) are both IFITM3-resistant without being able to reduce IFITM3 expression (Figure 22A and B). This notion is supported by a recent study on Nef [526], which has shown that this factor downregulates IFITM3 expression. Since all of the V3-loop chimeric viruses have NL4-3 backbone that expresses NL4-3 Nef, these NL4-3 mutants do not downregulate IFITM3 in the viral producer cells. Therefore, changing the V3-loop alone is sufficient to modulate HIV-1 sensitivity to IFITM3.

In Chapter 3.1, I showed that by exchanging the V3-loop of an IFITM3-sensitive strain with the V3-loop of an IFITM3-resistant strain, the mutant HIV-1 becomes resistant to IFITM3 inhibition. The V3-loop in Env is essential for HIV-1 infection as it binds to the coreceptors and mediates viral entry. Together with the V1- and V2-loops, the V3-loop determines the coreceptor tropism of HIV-1. The variability of the V3-loop is high, as HIV-1 needs to mutate this region for overcoming the neutralization by antibodies. In Chapter 3.1.4, V3-loop mutants demonstrated changes in coreceptor tropism from X4 to R5. The study by Foster and colleagues has shown that IFITM3 in the virus-targeting cells preferentially inhibits X4-tropic HIV-1[488]. Therefore, I tested

whether IFITM3 expressed in the virus-producing cells also demonstrates the same characteristic. However, when either of the two coreceptors was disabled by drugs, the degree of IFITM3 inhibition on the duo-tropic 89.6 infections was not affected. Therefore, changing coreceptor tropism is not the underlying reason that explains why the V3-loop mediates IFITM3-resistance. My results agree with another published study showing that IFITM proteins do not differentiate between X4- or R5- tropic viruses when expressed in virus producer cells [527]. Therefore, it is still unclear how the V3-loop confer IFITM3-resistant in HIV-1 infection.

The V3-loop may confer resistance to IFITM3 by changing the conformation of Env. The neutralizing assay in Chapter 3.1.7 indicated a variation in the affinity of the neutralizing antibodies to their epitopes on different Env, suggesting variation in the ligand-free conformation of Env among the V3-loop chimeric viruses. In 2014, Munro and colleagues studied the conformation of Env using the single-molecule fluorescence resonance energy transfer method (FRET) [528]. Their results have shown that Env proteins spontaneously transit between three prefusion conformational states [528]. They proposed a three-state model for ligand-free Env conformation. The low-FRET state, which has the "closed" ground state conformation, where the V1/2 loop is located at the apex of the Env trimer and the V3-loop is buried inside of the trimer; the intermediate-FRET state, which resembles the CD4-bound Env conformation; the high-FRET state, which is required for the Env to transition from the ground state to a CD4-bound state. Munro and colleagues found that despite the fact that all ligand-free Env of NL4-3 and JRFL preferentially occupy a ground state, NL4-3 often spontaneously transitions to a high-FRET state and subsequently the intermediate-FRET CD4-bound state. Intriguingly, they found that sCD4 D1/D2 alone stabilizes the high-FRET state, and the combination of sCD4 D1/D2 and 17b stabilizes the intermediate-FRET state in NL4-3. On the contrary, the high- and

intermediate-FRET states of JRFL were stabilized to the same extent regardless of the presence of 17b. All the evidences suggest that the Env of NL4-3 frequently and spontaneously switches to a CD4-bound conformation, in which the V3-loop becomes more accessible to 17b antibodies.

In Chapter 3.1.7, 17b and sCD4 D1/D4 neutralization experiments revealed a linear correlation between the HIV-1 sensitivity to sCD4 or 17b and the HIV-1 sensitivity to IFITM3. I also tested JRFL for its sensitivity to IFITM3 inhibition, and the results showed resistance. The antibody 17b has been shown to target CD4-binding induced epitopes on Env, which also overlaps with the coreceptor binding sites of Env (the V3-loop) [529]. Therefore, Env with intrinsically more exposed V3-loop at the CD4-bound state is more efficiently targeted by 17b. For the convenience, the Env with an intermediate-FRET state/the CD4-bound state conformation will be referred to as the "open" Env in the subsequent discussion. The Env that intrinsically switches to the "open" state has been shown to facilitate the binding to sCD4, which stabilizes the "open" Env. The pre-mature activation of Env causes gp120 shedding from the HIV-1 virions, resulting in the impaired viral infection [530]. Therefore, this sCD4-induced gp120 shedding is facilitated if the unbound Env protein frequently transits to the "open" state. The linear correlation that I observed between the HIV-1 sensitivity to 17b/sCD4 and IFITM3 provided additional evidence for the correlation between the Env conformation and its resistance to IFITM3 inhibition. Interestingly, our lab's previous findings have revealed that the Env of IFITM1-resistant HIV-1 strain is associated with decreased responsiveness to sCD4 neutralization [483]. Together, these evidences all suggest that the HIV-1 Env that is less frequently switched to the "open" state is more likely to be resistant to IFITM3 inhibition.

Based on the importance of the Env conformation in determining its sensitivity to IFITM3. I then wish to determine whether the Env conformation is the sole factor that predicts

the IFITM3 sensitivity of HIV-1, and tested the JRFL mutants for their sensitivity to IFITM3. The JRFL mutants I used have a single amino acid mutation at their V1/V2 loop, making JRFL Env more frequently in an "open" conformation [517]. The results from section 3.1.8 demonstrated a statistically significant correlation between the "open" Env and the increased IFITM3 susceptibility. However, such a correlation was only significant between cold inactivation sensitivity and the IFITM3-sensitivity of the Env. Surprisingly, IC50 of sCD4 of JRFL mutants did not correlate well with their sensitivity to IFITM3. As the cold inactivation assay directly measures the stability of the Env and can only be indirectly referred to the Env ground state conformation [531], I concluded that the stability of Env is important in determining the viral sensitivity to IFITM3. Since mutations of JRFL Env target the V1/V2 loop, these mutations were able to change how JRFL Env behave at its ground state and the stability of Env spikes. However, these mutations alone were not enough to change the IFITM3-sensitivity of the Env. I suspect that the mutations at the V1/V2 loop are not enough to cause a large window of difference in IFITM3-sensitivity. The observations support the notion that the fold inhibition by IFITM3 among different strains has produced a correlation to 18A with a high statistical significance (data not shown). Therefore, the degree of Env stability is the key determinant of IFITM3-sensitivity. The change in the V3-loop may cause a more drastic difference in Env conformation and stability than a single amino acid in the V1/V2 loop. Hence, mutating the V3-loop modulates the HIV-1 sensitivity to IFITM3, but not the V1/V2 loop.

Section 3.1.5 shows that the V3-loop mutants are more resistant to IFITM3-mediated impediment of gp160 maturation. Yu and the colleagues showed that IFITM3 expression in the virus-producing cells interferes with gp160 processing, and thus reduce the amount of gp120 incorporated into the HIV-1 virions [508]. In my thesis, the defect in Env maturation in the IFITM3

expressing cells was also observed. However, I also observed that the degree of gp120 incorporation into the virus is associated with the ability of the virus to escape IFITM3 inhibition. For example, NL4-3 has the least amount of gp120 incorporation, while it is the most sensitive strain to IFITM3 inhibition, whereas AD8-1 showed almost no defect in gp120 incorporation, and it is completely resistant to IFITM3. The V3-loop chimeric viruses showed that the more IFITM3 resistant strain was able to incorporate more gp120 into their virions. NL(WITOV3) was more resistant to IFITM3 inhibition than NL(YU-2V3), and the former showed more gp120 incorporation to the virions compared to the latter (Figure 22A). Therefore, the V3-loop changes the susceptibility of Env to the IFITM3-mediated impediment of gp160 maturation, although the exact mechanism is not clear.

4.2.2 The impact of IFITM3 inhibition of HIV-1 *in vivo*.

Studying the interaction between Env and IFITM3 at the molecular level in an isolated environment is very important to unveil the effect that IFITM3 has Env mutants. However, to elucidate the macroscopic impact of IFITM3 in the course of HIV-1 infection, it is also critical to study IFITM3 in the context of the human population. The *in vivo* study provides clues to the importance of IFITM3 in disease acquisition and progression. This notion has been highlighted in the study done by Allen and colleagues, which showed a strong correlation between the risk allele A at the rs34481144 SNP position of *ifitm3* and the patients' susceptibility to severe illness caused by influenza [490]. The importance of rs34481144 is based on its location in the core promoter of the *ifitm3* gene. This study has shown that when A is present at rs34481144, the core binding sequence of a chromosome insulator increases its affinity to CTCF compared to the protective genotype G. Consequently, the expression of IFITM3 and other genes in the vicinity are suppressed and provide less protection for the patients upon influenza infection [490]. This

study inspired me to study the effect of SNP of *ifitm3* on IFITM3 expression and the subsequent effect on HIV-1 infection.

In section 3.2, I sequenced PBMCs for their rs34481144 SNP and infected these cells with NL4-3 after IFN treatment. The results did not show a significant difference in the fold inhibition of NL4-3 regardless of the rs34481144SNP because of an outlier. I also tested HIV-1 patient PBMCs and determined the frequency of rs34481144-A in the sample group. However, there was a considerable variation in the frequency of rs34481144-A in the healthy population. I noticed that the population frequency of rs34481144-A in different ethnic groups varied from 1% in Han Chinese to 46% in the British population. By comparing the rs34481144-A frequency that were obtained from the HIV-1 patients to the genome database, a higher rs34481144-A frequency was observed in patients of African ancestry. This finding was very similar to what Allen et al. had published in their study, where a higher enrichment of A allele was present in severe influenza patients of African ancestry. However, the sample size for the patients' group was very small; the statistical power of this finding was minimal. I next genotyped three cohorts of Han Chinese patients that were categorized by transmission routes. The results, however, were not as expected. There was no increase in the rs34481144-A allele observed in any of the three cohorts. One issue with this result is that the population frequency of rs34481144-A in the Han Chinese population is only 1%. If the risk allele frequency is low in a population, a rise in the risk allele in the patient population will be easier to observe only if the sample size is large enough. To achieve statistically significant results, a cohort with at least 1000 patients would have to be tested. With the sample size, I did not find any enrichment of rs34481144-A. However, this result is not conclusive. Therefore, to further this study and obtain a definite

conclusion to the effect of rs34481144-A in HIV-1 infection, a much larger cohort study needs to be done.

Next, I investigated the level of IFITM3 mRNA in the patients' samples. The results showed a huge variation among different individuals in the basal expression of IFITM3 and its inducibility by IFN. The major issue with this set of results is, again, the small sample size. According to the genome database, the frequency of A allele in the Han Chinese population is 1%, which is even smaller than the African population. Among the samples I tested for IFITM3 expression, only two samples carried heterozygous A/G at rs34481144. The variation between these two heterozygous samples was huge, and I could not establish a correlation between rs34481144-A and IFITM3 expression levels. Since the data regarding the CD4+, CD8+ count and viral load of drug-naive patients were only available for the blood transmitted cohort, the IFITM3 RNA level has been measured in PBMCs of blood-transmitted groups. I did not observe any correlation between IFITM3 mRNA level and viral load, CD4+ or CD8+ counts. Again, only two samples were heterozygous A/G, and there were no A/A homozygote. Therefore, the low A allele frequency hampered the statistical significance of this study. Higher number of samples are required for testing before drawing any conclusive statement. In summary, after genotyping and testing for the IFITM3 mRNA level, I could not identify the enrichment of rs34481144-A in the Han Chinese patient population nor a correlation to impaired IFITM3 expression.

Aside from the small sample size, there are other possibilities that could explain why I observed no significant effect of rs34481144-A over susceptibility to HIV-1 infection. First, IFITM3 is primarily localized in the endosomes and only transiently present on the plasma membrane [532]. Therefore, the viruses that enter the cells via endosomes are more potently inhibited by IFITM3 than HIV-1. The change in IFITM3 expression due to the SNP could have a

more profound effect on the influenza virus than HIV-1. It is also possible that IFITM3 reaches its maximum capacity to inhibit HIV-1 at a lower amount than the influenza virus. Although an increase in IFITM3 expression could inhibit the influenza virus, the antiviral effect against HIV-1 might be saturated.

However, a more likely scenario is that TF HIV-1 are resistant to IFITM3, and the infection of TF was not affected by the difference in the level of IFITM3. As shown in Figure 12, the IFITM3-resistant HIV-1 strain is resistant to a high dose of IFITM3 that cannot be achieved in the physiological setting. In section 3.3, I also showed that 25HC only enhances IFITM3-sensitive HIV-1 to IFITM3 inhibition but cannot turn a resistant HIV-1 to become sensitive. Moreover, the TF HIV-1 I tested were mostly resistant to IFITM3, suggesting that IFITM3-resistant property is critical for HIV-1 to successfully establish an infection. As I discussed earlier, Foster and colleagues have already shown that TF HIV-1 are resistant to IFITM3 at the acute stage of infection [488]. However, when these TF viruses replicate for six months after the initial infection, the progeny viruses become sensitive to IFITM3. This study revealed that a robust resistance to IFITM3 is critical for HIV-1 to establish infection; however, after the adaptive immunity is active, the viral resistance to neutralization antibodies takes precedence over the resistance to IFITM3 [488]. Therefore, HIV-1 that can establish infection in the population is resistant to IFITM3. The slight difference in IFITM3 expression caused by rs34481144 SNP was not enough to prevent the IFITM3-resistant HIV-1 from establishing infection. This notion is supported by my results from Figure 34, where NL4-3 infection is more affected by the genotype at rs34481144. Hence, it is possible that rs34481144-A only increases the risk of infection by IFITM3-sensitive viruses.

As the infection of HIV-1 requires its resistance to IFITM3, this restriction factor has a more critical role in serving as the species barrier to SIV infection. Its role as a protective barrier against the initial crossing of species by HIV-1 has been further underlined in a study of the simian-human immunodeficiency virus (SHIV) in macaque [533]. Similar to humans, macaque also has its own set of restriction factors, preventing a persistent HIV-1 infection. Therefore, to study HIV-1 in the macaque model, a chimeric virus SHIV that carries SIV proteins to antagonize macaque restriction factors was generated. However, the replication efficiency is very low for SHIV derived directly from HIV-1 of human origin. After several generations of culturing, the SHIV can finally start to adapt to macaque T-lymphocytes. Previous studies have shown that SHIV Env determines viral replication efficiency and IFN sensitivity [534,535]. Sharma and colleagues attempted to identify the specific macaque restriction factors that affect the transmission efficiency of SHIV. The group specifically focused on ISGs and found that several membrane proteins derived from duplication events of *ifitm3* contribute to the inhibition of SHIV spread in the macaque. They also found that these *ifitm3* duplications do not occur in humans and the unadapted SHIV packages higher level of IFITMs in their virions. The results of this study have unveiled the role of IFITM proteins as the critical species barrier to the adaptation of SHIV [533]. Therefore, when HIV-1 first crossed the species barrier between macaque and human, IFITM proteins could also have a pivotal role in limiting the transmission of unadapted HIV-1. Thus, it is important to study the viral resistance to IFITM proteins to further our understanding of the adaptation of HIV-1 to the human population.

4.2.3 Does Env also contribute to the HIV-1 resistance to other restriction factors?

As previously mentioned, HIV-1 has a very small genome and therefore, effective using of each gene for multiple purposes is critical for virus survival. The same can be observed for

Env. On top of its structural function, I have shown that it is the major modulator of the HIV-1 sensitivity to IFITM3 inhibition. Other studies from our lab have also demonstrated that Env is critical for HIV-1 to escape SERINC5 inhibition [536,537]. As briefly mentioned in Section 1.5.1, SERINC5 is a constitutionally expressed restriction factor against HIV-1 infection that was first identified in 2015 [538,539]. The same studies also identified Nef as the viral inhibiting factor against SERINC5 inhibition, which provided an answer to the mechanism of Nef in increasing the efficiency of HIV-1 infection. Similar to IFITM3, SERINC5 is also a membrane-associated entry inhibitor that prevents HIV-1 entry to the cells. One interesting difference is that SERINC5 is only able to antagonize HIV-1 entry when it is incorporated in the viral particles [536]. When SERINC5 is expressed in the target cells alone, it was not able to reduce HIV-1 infection. To overcome this form of inhibition, HIV-1 uses its Nef protein in the virus-producing cells to downregulate SERINC5 expression. As a membrane-bound protein, Nef associates with SERINC5 and transports SERINC5 from the plasma membrane to the endosomal/lysosomal degradation pathway. However, a recent study raised the possibility that HIV-1 may have other systems to counteract SERINC5 [540]. While studying this possibility, our lab found that HIV-1 Env is the critical protein that determines the viral sensitivity to SERINC5 when Nef is absent [536]. Mutagenesis studies have mapped SERINC5 resistance to the V3-loop of Env. The study also revealed that HIV-1 with the "open" Env are more efficiently inhibited by SERINC5 [536,537]. Despite many similarities shared between IFITM3 and SERINC5, our lab did not see any synergistic effect between IFITM3 and SERINC5.

Nevertheless, in another study that focuses on the role of the T cell Ig and mucin domain (TIM) protein in inhibiting HIV-1 release, SERINC5 has been shown to potentiate the TIM-mediated inhibition of HIV-1 release by increasing TIM-1 expression on the plasma membrane

[541]. This study sheds light on the possible interplay between IFITM3 and other restriction factors. Although our lab has shown that IFITM3 and SERINC5 do not enhance each other's activity, the possibility of interaction between IFITM3 and other restriction factors remains. One such target is CH25H, which shares many similarities with IFITM3. CH25H is an IFN-inducible protein that hydrolyzes cholesterols to 25HC, acting as an effector to impede HIV-1 entry to the cells [406]. Regulation of cholesterol homeostasis by IFITM3 and 25HC has been associated as a part of their function [479,542]. Therefore, I studied the interplay between IFITM3 and 25HC in inhibiting HIV-1 infection. Moreover, I also examined the role of Env in antagonizing 25HC.

Upon stimulation by 25HC, different cell types demonstrated different antiviral potency to either X4- or R5-tropic viruses. AD8-1 was more inhibited in CEM-rev cells compared to NL4-3, whereas NL4-3 was more potently inhibited in MT4-R5 cells than AD8-1. This could be the result of differences in R5 receptor availability in CEM-rev and MT4-R5 cells. Less abundant R5 coreceptor reduces the overall infection efficiency of R5 viruses, and therefore, the difference in infection between 25HC-treated and the control may not be as large as X4-tropic viruses. However, in CBMC infection, AD8-1 demonstrated similar if not more enhanced sensitivity to 25HC compared to NL4-3 (Figure 40B and D). Therefore, unlike IFITM3, 25HC did not inhibit NL4-3 and AD8-1 differentially. Despite many similarities, 25HC is a soluble molecule [406], whereas IFITM3 is a membrane protein, and thus, 25HC inhibits HIV-1 entry through different mechanisms than IFITM3. The Env-dependent mechanism against IFITM3 does not allow HIV-1 to escape 25HC inhibition. Different viral proteins are employed by HIV-1 to attenuate the anti-HIV-1 effect of 25HC, if at all.

A novel phenotype that I observed in my study is the effect of 25HC on viral production (Figure 41). It has been previously shown that 25HC inhibits HIV-1 infection by entry inhibition

[406]. Here, I showed that 25HC might have imposed an additional effect on the progeny HIV-1 particles. At 500 nM of 25HC, treated CEM-rev cells did not show any resistance to NL4-3 infection. However, progeny viruses collected from CEM-rev cells demonstrated a 2.5-fold decrease in infectivity (Figure 39). Together with the RT results and WB data, my results suggest that 25HC affects virion production in addition to entry. The Env production and maturation are hampered when 500 nM of 25HC was used; however, a more precise analysis of gp160 and gp120 is required for a solid conclusion.

Most importantly, 25HC potentiates the anti-HIV-1 effect of IFITM3. When MT4-R5 cells were treated with 100 nM of 25HC, there was no reduction in the NL4-3 and AD8-1 infection (Figure 43). However, when MT4-R5-IFITM3 cells were treated with 100 nM of 25HC, a 12-fold inhibition in NL4-3 infection was observed. Since IFITM3 in MT4-R5 cells alone can achieve a 4-fold inhibition in NL4-3 infection, 25HC was able to sensitize NL4-3 to the anti-HIV-1 activity of IFITM3 by 3-fold. On the contrary, AD8-1 only showed moderate sensitivity to IFITM3 with 3-fold inhibition, and IFITM3 was not able to sensitize AD8-1 to 100 nM of 25HC. These evidences suggest that at a lower than effective dose, 25HC augments the anti-HIV-1 activity of IFITM3 in a strain-dependent manner. The reason that AD8-1 was not subjected to this increased level of inhibition could be due to the difference in coreceptor tropism. It is possible that 25HC preferentially enhances the X4-tropic HIV-1 to IFITM3. However, as I have discussed earlier, coreceptor tropism is less likely differentiated by IFITM3 or 25HC. Another possibility would be that 25HC only enhances the activity of IFITM3 in the infection by IFITM3-sensitive HIV-1. If the HIV-1 is resistant to IFITM3 inhibition, then 25HC cannot make the virus more sensitive to IFITM3. Therefore, 25HC enhances the viral sensitivity to IFITM3 but does not make a resistant HIV-1 sensitive.

The study on the interplay between 25HC and IFITM3 highlighted the complexity in the selection pressure on Env. As discussed in section 4.2.1, Env plays a dominant role in HIV-1 entry by antagonizing host restriction factors. The TF HIV-1 usually is resistant to IFITM3, but the pressure imposed by the humoral response forces the Env to become more sensitive to IFITM3 in the chronic stage. A recent study from our lab has shown that TF HIV-1 Env is also resistant to SERINC5; however, primary isolates do not develop sensitivity to SERINC5 [537]. Although the "open" Env has been shown to be more sensitive to IFITM3 and SERINC5, HIV-1 needs to sacrifice IFITM3 resistance to acquire resistance toward neutralizing antibodies. One explanation is that SERINC5 is constitutively expressed, whereas IFITM3 is IFN-induced. Therefore, HIV-1 cannot afford to eliminate its SERINC5-resistance. Recently, Staropoli and colleagues studied the effects of Nef, CD4 and SERINC5 on the change in the accessibility of Env to neutralization antibodies [543]. In the study, the accessibility of HIV-1 by different neutralization antibodies was called "accessibility profile". Their results showed that SERINC5 and CD4 expressed in the virus-producing cells could shape the accessibility profile of HIV-1. In other words, the change in the conformation of Env is subject to CD4, IFITM3, SERINC5 and neutralization antibodies. Therefore, HIV-1 needs to balance the risks and benefits of modifying its Env to survive through all the complicated evolutionary strains. By understanding the interplay between different pressures and their effects on Env conformation, an optimal vaccine target may finally emerge as a result.

Conclusions

In conclusion, my study first identified the viral protein that modulates the HIV-1 sensitivity to IFITM3 and further mapped the region to the V3-loop of Env. My finding highlights the viral mechanism targeting IFITM3. My study underlined the importance of Env stability in determining the viral sensitivity to IFITM3 inhibition, which has been recently shown to modulate viral response to ADCC[544]. In this study, the more "open" Env expressed on the viral producing cells have demonstrated a higher potency to be targeted by ADCC mediated by HIV+ sera. Since my results also show that unbound Env with more "open" conformation is more susceptible to IFITM3, and that Env with a stable CD4-bound conformation is more susceptible to various host immune pressures. Therefore, by studying IFITM3-Env interaction, small molecules or antibodies could be used to stabilize the Env trimer to the ligand-bound state to sensitize HIV-1 to IFITM3 inhibition at the early stage of infection. Foster and colleagues showed that TF strains develop sensitivity to IFITM3 to withstand the attack from antibodies in chronic infection [488]. Therefore, it is also possible to promote the sensitization of TF Env to IFITM3 using antibodies. A more recent study emphasized the influence of IFITM3 to the adaptive immunity [489]. The *ifitm3* knocked-out mice produced less antibody against CMV infection and resulted in more severe illness. The link between IFITM3 and a proper adaptive immune response provide another insight into the possible use of IFITM3 to enhance HIV-1 vaccine outcome.

References

1 Michael S. Gottlieb, R. S., Howard M. Schanker, Joel D. Weisman, Peng Thim Fan, Robert A. Wolf and Andrew Saxon. Pneumocystis carinii pneumonia and mucosal candidiasis in previously healthy homosexual men: evidence of new acquired cellular immunodeficiency. *The New England Journal of Medicine* **305**, 7 (1981).

2 Prevention, U. S. C. f. D. C. a. Kaposi's sarcoma and Pneumocystic pneumonia among homosexual men--New York City and California. *MMWR Morb Mortal Wkly Rep* **30**, 4 (1981).

3 Prevention, U. S. C. f. D. C. a. Unexplained immunodeficiency and opportunistic infections in infants--New York, New Jersey, California. *MMWR Morb Mortal Wkly Rep* **31**, 3 (1982).

4 Prevention, U. S. C. f. D. C. a. Opportunistic infections and Kaposi's sarcoma among Haitians in the United States. *MMWR Morb Mortal Wkly Rep* **31**, 2, 2 (1982).

5 Prevention, U. S. C. f. D. C. a. Update on Kaposi's sarcoma and opportunistic infections in previously healthy persons--United States. *MMWR Morb Mortal Wkly Rep* **31**, 1, 2 (1982).

6 Barre-Sinoussi, F. *et al.* Isolation of a T-lymphotropic retrovirus from a patient at risk for acquired immune deficiency syndrome (AIDS). *Science* **220**, 868-871 (1983).

7 Gallo, R. C. *et al.* Isolation of human T-cell leukemia virus in acquired immune deficiency syndrome (AIDS). *Science* **220**, 865-867 (1983).

8 P, C. J. H. A. L. J. M. L. O. S. T. N. T. H. T. K. V. H. a. V. Human immunodeficiency viruses [letter]. *Science* **232**, 697 (1986).

9 2015, W. H. O. a. U. AIDS by the numbers 2015. (Geneva, Switzerland, 2015).

10 2015, W. H. O. a. U. Fact Sheet 2015. (Geneva, Switzerland, 2015).

11 Cohen, J. in *Science* (2015).

12 2010, J. U. N. P. i. H. A. Global Report--UNAIDS Report on the Global AIDS Epidemic 2010. (Geneva, Switzerland, 2010).

13 Prevention, U. S. C. f. D. C. a. *HIV Transmission*, <http://www.cdc.gov/hiv/basics/transmission.html> (2015).

14 Shaw, G. M. & Hunter, E. HIV transmission. *Cold Spring Harb Perspect Med* **2**, doi:10.1101/cshperspect.a006965 (2012).

15 Keele, B. F. *et al.* Identification and characterization of transmitted and early founder virus envelopes in primary HIV-1 infection. *Proc Natl Acad Sci U S A* **105**, 7552-7557, doi:10.1073/pnas.0802203105 (2008).

16 Coffin, J. & Swanstrom, R. HIV pathogenesis: dynamics and genetics of viral populations and infected cells. *Cold Spring Harb Perspect Med* **3**, a012526, doi:10.1101/cshperspect.a012526 (2013).

17 Brenchley, J. M. *et al.* CD4+ T cell depletion during all stages of HIV disease occurs predominantly in the gastrointestinal tract. *J Exp Med* **200**, 749-759, doi:10.1084/jem.20040874 (2004).

18 Lackner, A. A., Lederman, M. M. & Rodriguez, B. HIV pathogenesis: the host. *Cold Spring Harb Perspect Med* **2**, a007005, doi:10.1101/cshperspect.a007005 (2012).

19 Schacker, T., Collier, A. C., Hughes, J., Shea, T. & Corey, L. Clinical and epidemiologic features of primary HIV infection. *Ann Intern Med* **125**, 257-264 (1996).

20 Veazey, R. S. *et al.* Gastrointestinal tract as a major site of CD4+ T cell depletion and viral replication in SIV infection. *Science* **280**, 427-431 (1998).

21 Maartens, G., Celum, C. & Lewin, S. R. HIV infection: epidemiology, pathogenesis, treatment, and prevention. *Lancet* **384**, 258-271, doi:10.1016/S0140-6736(14)60164-1 (2014).

22 Chen, P. *et al.* Virological synapses allow HIV-1 uptake and gene expression in renal tubular epithelial cells. *J Am Soc Nephrol* **22**, 496-507, doi:10.1681/ASN.2010040379 (2011).
23 Liu, Y. *et al.* CD4-independent infection of astrocytes by human immunodeficiency virus type 1: requirement for the human mannose receptor. *J Virol* **78**, 4120-4133 (2004).
24 Price, R. W. *et al.* The brain in AIDS: central nervous system HIV-1 infection and AIDS dementia complex. *Science* **239**, 586-592 (1988).
25 Baltimore, D. RNA-dependent DNA polymerase in virions of RNA tumour viruses. *Nature* **226**, 1209-1211 (1970).
26 Temin, H. M. Mechanism of cell transformation by RNA tumor viruses. *Annu Rev Microbiol* **25**, 609-648, doi:10.1146/annurev.mi.25.100171.003141 (1971).
27 Temin, H. M. & Mizutani, S. RNA-dependent DNA polymerase in virions of Rous sarcoma virus. *Nature* **226**, 1211-1213 (1970).
28 Cullen, B. R. Human immunodeficiency virus as a prototypic complex retrovirus. *J Virol* **65**, 1053-1056 (1991).
29 Schneider, J. & Hunsmann, G. Simian lentiviruses--the SIV group. *AIDS* **2**, 1-9 (1988).
30 Clavel, F. *et al.* Isolation of a new human retrovirus from West African patients with AIDS. *Science* **233**, 343-346 (1986).
31 Hemelaar, J. The origin and diversity of the HIV-1 pandemic. *Trends Mol Med* **18**, 182-192, doi:10.1016/j.molmed.2011.12.001 (2012).
32 Keele, B. F. *et al.* Chimpanzee reservoirs of pandemic and nonpandemic HIV-1. *Science* **313**, 523-526, doi:10.1126/science.1126531 (2006).
33 Ho, D. D. a. B., Paul D. HIV-1 at 25. *Cell* **133**, 561-565 (2008).
34 Plantier, J. C. *et al.* A new human immunodeficiency virus derived from gorillas. *Nat Med* **15**, 871-872, doi:10.1038/nm.2016 (2009).
35 Vallari, A. *et al.* Confirmation of putative HIV-1 group P in Cameroon. *J Virol* **85**, 1403-1407, doi:10.1128/JVI.02005-10 (2011).
36 Charneau, P. *et al.* Isolation and envelope sequence of a highly divergent HIV-1 isolate: definition of a new HIV-1 group. *Virology* **205**, 247-253, doi:10.1006/viro.1994.1640 (1994).
37 Gao, F. *et al.* Origin of HIV-1 in the chimpanzee Pan troglodytes troglodytes. *Nature* **397**, 436-441, doi:10.1038/17130 (1999).
38 Roques, P. *et al.* Phylogenetic characteristics of three new HIV-1 N strains and implications for the origin of group N. *AIDS* **18**, 1371-1381 (2004).
39 Simon, F. *et al.* Identification of a new human immunodeficiency virus type 1 distinct from group M and group O. *Nat Med* **4**, 1032-1037, doi:10.1038/2017 (1998).
40 Janssens, W. *et al.* Genetic and phylogenetic analysis of env subtypes G and H in central Africa. *AIDS Res Hum Retroviruses* **10**, 877-879 (1994).
41 Louwagie, J. *et al.* Genetic diversity of the envelope glycoprotein from human immunodeficiency virus type 1 isolates of African origin. *J Virol* **69**, 263-271 (1995).
42 Louwagie, J. *et al.* Phylogenetic analysis of gag genes from 70 international HIV-1 isolates provides evidence for multiple genotypes. *AIDS* **7**, 769-780 (1993).
43 Myers, G., MacInnes, K. & Korber, B. The emergence of simian/human immunodeficiency viruses. *AIDS Res Hum Retroviruses* **8**, 373-386, doi:10.1089/aid.1992.8.373 (1992).
44 Robertson, D. L. *et al.* HIV-1 nomenclature proposal. *Science* **288**, 55-56 (2000).
45 Triques, K. *et al.* Near-full-length genome sequencing of divergent African HIV type 1 subtype F viruses leads to the identification of a new HIV type 1 subtype designated K. *AIDS Res Hum Retroviruses* **16**, 139-151, doi:10.1089/088922200309485 (2000).
46 Vallari, A. *et al.* Four new HIV-1 group N isolates from Cameroon: Prevalence continues to be low. *AIDS Res Hum Retroviruses* **26**, 109-115, doi:10.1089/aid.2009.0178 (2010).

47 Yamaguchi, J. *et al.* Identification of HIV type 1 group N infections in a husband and wife in Cameroon: viral genome sequences provide evidence for horizontal transmission. *AIDS Res Hum Retroviruses* **22**, 83-92, doi:10.1089/aid.2006.22.83 (2006).
48 Ayouba, A. *et al.* HIV-1 group O infection in Cameroon, 1986 to 1998. *Emerg Infect Dis* **7**, 466-467, doi:10.3201/eid0703.010321 (2001).
49 Vessiere, A. *et al.* Diagnosis and monitoring of HIV-1 group O-infected patients in Cameroun. *J Acquir Immune Defic Syndr* **53**, 107-110, doi:10.1097/QAI.0b013e3181b97ec1 (2010).
50 Chen, Z. *et al.* Human immunodeficiency virus type 2 (HIV-2) seroprevalence and characterization of a distinct HIV-2 genetic subtype from the natural range of simian immunodeficiency virus-infected sooty mangabeys. *J Virol* **71**, 3953-3960 (1997).
51 Gao, F. *et al.* Human infection by genetically diverse SIVSM-related HIV-2 in west Africa. *Nature* **358**, 495-499, doi:10.1038/358495a0 (1992).
52 Damond, F. *et al.* Variability of human immunodeficiency virus type 2 (hiv-2) infecting patients living in france. *Virology* **280**, 19-30, doi:10.1006/viro.2000.0685 (2001).
53 Damond, F. *et al.* Identification of a highly divergent HIV type 2 and proposal for a change in HIV type 2 classification. *AIDS Res Hum Retroviruses* **20**, 666-672, doi:10.1089/0889222041217392 (2004).
54 Gao, F. *et al.* Genetic diversity of human immunodeficiency virus type 2: evidence for distinct sequence subtypes with differences in virus biology. *J Virol* **68**, 7433-7447 (1994).
55 Ishikawa, K. *et al.* Genetic analysis of HIV type 2 from Ghana and Guinea-Bissau, West Africa. *AIDS Res Hum Retroviruses* **17**, 1661-1663, doi:10.1089/088922201753342077 (2001).
56 Pieniazek, D. *et al.* Predominance of human immunodeficiency virus type 2 subtype B in Abidjan, Ivory Coast. *AIDS Res Hum Retroviruses* **15**, 603-608, doi:10.1089/088922299311132 (1999).
57 Yamaguchi, J., Devare, S. G. & Brennan, C. A. Identification of a new HIV-2 subtype based on phylogenetic analysis of full-length genomic sequence. *AIDS Res Hum Retroviruses* **16**, 925-930, doi:10.1089/08892220050042864 (2000).
58 Zeh, C. *et al.* Nigerian HIV type 2 subtype A and B from heterotypic HIV type 1 and HIV type 2 or monotypic HIV type 2 infections. *AIDS Res Hum Retroviruses* **21**, 17-27, doi:10.1089/aid.2005.21.17 (2005).
59 De Cock, K. M., Georgette Adjorlolo, Ehounou Ekpini, Toussaint Sibailly, Justin Kouadio, Matthieu Maran, Kari Brattegaard, Kathleen M. Vetter, Ronan Doorly, and Helene D. Gayle. Epidemiology and transmission of HIV-2: why there is no HIV-2 pandemic. *Jama* **270**, 2083-2086 (1993).
60 Kanki, P. J. *et al.* Slower heterosexual spread of HIV-2 than HIV-1. *Lancet* **343**, 943-946 (1994).
61 Matheron, S. *et al.* Vertical transmission of HIV-2. *Lancet* **335**, 1103-1104 (1990).
62 Marx, P. A., Alcabes, P. G. & Drucker, E. Serial human passage of simian immunodeficiency virus by unsterile injections and the emergence of epidemic human immunodeficiency virus in Africa. *Philos Trans R Soc Lond B Biol Sci* **356**, 911-920, doi:10.1098/rstb.2001.0867 (2001).
63 Ancelle, R. *et al.* Long incubation period for HIV-2 infection. *Lancet* **1**, 688-689 (1987).
64 Marlink, R. *et al.* Reduced rate of disease development after HIV-2 infection as compared to HIV-1. *Science* **265**, 1587-1590 (1994).
65 Hemelaar, J. *et al.* Global trends in molecular epidemiology of HIV-1 during 2000-2007. *AIDS* **25**, 679-689, doi:10.1097/QAD.0b013e328342ff93 (2011).
66 Clavel, F. *et al.* Molecular cloning and polymorphism of the human immune deficiency virus type 2. *Nature* **324**, 691-695, doi:10.1038/324691a0 (1986).
67 Frankel, A. D. & Young, J. A. HIV-1: fifteen proteins and an RNA. *Annu Rev Biochem* **67**, 1-25, doi:10.1146/annurev.biochem.67.1.1 (1998).

68 Gallo, R., Wong-Staal, F., Montagnier, L., Haseltine, W. A. & Yoshida, M. HIV/HTLV gene nomenclature. *Nature* **333**, 504, doi:10.1038/333504a0 (1988).
69 Ratner, L. *et al.* Complete nucleotide sequence of the AIDS virus, HTLV-III. *Nature* **313**, 277-284 (1985).
70 Ju, G. & Skalka, A. M. Nucleotide sequence analysis of the long terminal repeat (LTR) of avian retroviruses: structural similarities with transposable elements. *Cell* **22**, 379-386 (1980).
71 Accola, M. A., Hoglund, S. & Gottlinger, H. G. A putative alpha-helical structure which overlaps the capsid-p2 boundary in the human immunodeficiency virus type 1 Gag precursor is crucial for viral particle assembly. *J Virol* **72**, 2072-2078 (1998).
72 de Marco, A. *et al.* Role of the SP2 domain and its proteolytic cleavage in HIV-1 structural maturation and infectivity. *J Virol* **86**, 13708-13716, doi:10.1128/JVI.01704-12 (2012).
73 Krausslich, H. G., Facke, M., Heuser, A. M., Konvalinka, J. & Zentgraf, H. The spacer peptide between human immunodeficiency virus capsid and nucleocapsid proteins is essential for ordered assembly and viral infectivity. *J Virol* **69**, 3407-3419 (1995).
74 Pettit, S. C. *et al.* The p2 domain of human immunodeficiency virus type 1 Gag regulates sequential proteolytic processing and is required to produce fully infectious virions. *J Virol* **68**, 8017-8027 (1994).
75 Gottlinger, H. G., Dorfman, T., Sodroski, J. G. & Haseltine, W. A. Effect of mutations affecting the p6 gag protein on human immunodeficiency virus particle release. *Proc Natl Acad Sci U S A* **88**, 3195-3199 (1991).
76 von Schwedler, U. K. *et al.* The protein network of HIV budding. *Cell* **114**, 701-713 (2003).
77 Cullen, B. R. *et al.* Subcellular localization of the human immunodeficiency virus trans-acting art gene product. *J Virol* **62**, 2498-2501 (1988).
78 Feinberg, M. B., Jarrett, R. F., Aldovini, A., Gallo, R. C. & Wong-Staal, F. HTLV-III expression and production involve complex regulation at the levels of splicing and translation of viral RNA. *Cell* **46**, 807-817 (1986).
79 Muesing, M. A., Smith, D. H. & Capon, D. J. Regulation of mRNA accumulation by a human immunodeficiency virus trans-activator protein. *Cell* **48**, 691-701 (1987).
80 Sodroski, J., Patarca, R., Rosen, C., Wong-Staal, F. & Haseltine, W. Location of the trans-activating region on the genome of human T-cell lymphotropic virus type III. *Science* **229**, 74-77 (1985).
81 Sodroski, J. *et al.* Trans-acting transcriptional regulation of human T-cell leukemia virus type III long terminal repeat. *Science* **227**, 171-173 (1985).
82 Terwilliger, E. *et al.* The art gene product of human immunodeficiency virus is required for replication. *J Virol* **62**, 655-658 (1988).
83 Fisher, A. G. *et al.* The sor gene of HIV-1 is required for efficient virus transmission in vitro. *Science* **237**, 888-893 (1987).
84 Muesing, M. A. *et al.* Nucleic acid structure and expression of the human AIDS/lymphadenopathy retrovirus. *Nature* **313**, 450-458 (1985).
85 Strebel, K., Klimkait, T. & Martin, M. A. A novel gene of HIV-1, vpu, and its 16-kilodalton product. *Science* **241**, 1221-1223 (1988).
86 Wong-Staal, F., Chanda, P. K. & Ghrayeb, J. Human immunodeficiency virus: the eighth gene. *AIDS Res Hum Retroviruses* **3**, 33-39 (1987).
87 Briggs, J. A. & Krausslich, H. G. The molecular architecture of HIV. *J Mol Biol* **410**, 491-500, doi:10.1016/j.jmb.2011.04.021 (2011).
88 Turner, B. G. & Summers, M. F. Structural biology of HIV. *J Mol Biol* **285**, 1-32, doi:10.1006/jmbi.1998.2354 (1999).

89 Ganser, B. K., Li, S., Klishko, V. Y., Finch, J. T. & Sundquist, W. I. Assembly and analysis of conical models for the HIV-1 core. *Science* **283**, 80-83 (1999).
90 Pornillos, O., Ganser-Pornillos, B. K. & Yeager, M. Atomic-level modelling of the HIV capsid. *Nature* **469**, 424-427, doi:10.1038/nature09640 (2011).
91 Nomaguchi, M., Fujita, M. & Adachi, A. Role of HIV-1 Vpu protein for virus spread and pathogenesis. *Microbes Infect* **10**, 960-967, doi:10.1016/j.micinf.2008.07.006 (2008).
92 Wilen, C. B., Tilton, J. C. & Doms, R. W. HIV: cell binding and entry. *Cold Spring Harb Perspect Med* **2**, doi:10.1101/cshperspect.a006866 (2012).
93 Saphire, A. C., Bobardt, M. D., Zhang, Z., David, G. & Gallay, P. A. Syndecans serve as attachment receptors for human immunodeficiency virus type 1 on macrophages. *J Virol* **75**, 9187-9200, doi:10.1128/JVI.75.19.9187-9200.2001 (2001).
94 Arthos, J. *et al.* HIV-1 envelope protein binds to and signals through integrin alpha4beta7, the gut mucosal homing receptor for peripheral T cells. *Nat Immunol* **9**, 301-309, doi:10.1038/ni1566 (2008).
95 Cicala, C. *et al.* The integrin alpha4beta7 forms a complex with cell-surface CD4 and defines a T-cell subset that is highly susceptible to infection by HIV-1. *Proc Natl Acad Sci U S A* **106**, 20877-20882, doi:10.1073/pnas.0911796106 (2009).
96 Geijtenbeek, T. B. *et al.* DC-SIGN, a dendritic cell-specific HIV-1-binding protein that enhances trans-infection of T cells. *Cell* **100**, 587-597 (2000).
97 Orloff, G. M., Orloff, S. L., Kennedy, M. S., Maddon, P. J. & McDougal, J. S. Penetration of CD4 T cells by HIV-1. The CD4 receptor does not internalize with HIV, and CD4-related signal transduction events are not required for entry. *J Immunol* **146**, 2578-2587 (1991).
98 Klatzmann, D. *et al.* Selective tropism of lymphadenopathy associated virus (LAV) for helper-inducer T lymphocytes. *Science* **225**, 59-63 (1984).
99 Maddon, P. J. *et al.* The T4 gene encodes the AIDS virus receptor and is expressed in the immune system and the brain. *Cell* **47**, 333-348 (1986).
100 McDougal, J. S. *et al.* Binding of HTLV-III/LAV to T4+ T cells by a complex of the 110K viral protein and the T4 molecule. *Science* **231**, 382-385 (1986).
101 Klasse, P. J. The molecular basis of HIV entry. *Cellular microbiology* **14**, 1183-1192 (2012).
102 Cordonnier, A., Montagnier, L. & Emerman, M. Single amino-acid changes in HIV envelope affect viral tropism and receptor binding. (1989).
103 Hwang, S. S., Boyle, T. J., Lyerly, H. K. & Cullen, B. R. Identification of the envelope V3 loop as the primary determinant of cell tropism in HIV-1. *Science* **253**, 71-74 (1991).
104 Lasky, L. A. *et al.* Delineation of a region of the human immunodeficiency virus type 1 gp120 glycoprotein critical for interaction with the CD4 receptor. *Cell* **50**, 975-985 (1987).
105 Olshevsky, U. *et al.* Identification of individual human immunodeficiency virus type 1 gp120 amino acids important for CD4 receptor binding. *Journal of virology* **64**, 5701-5707 (1990).
106 Thali, M. *et al.* Characterization of a discontinuous human immunodeficiency virus type 1 gp120 epitope recognized by a broadly reactive neutralizing human monoclonal antibody. *Journal of virology* **65**, 6188-6193 (1991).
107 Kwong, P. D. *et al.* Structure of an HIV gp120 envelope glycoprotein in complex with the CD4 receptor and a neutralizing human antibody. *Nature* **393**, 648-659 (1998).
108 Alkhatib, G. *et al.* CC CKR5: a RANTES, MIP-1alpha, MIP-1beta receptor as a fusion cofactor for macrophage-tropic HIV-1. *Science* **272**, 1955-1958 (1996).
109 Choe, H. *et al.* The beta-chemokine receptors CCR3 and CCR5 facilitate infection by primary HIV-1 isolates. *Cell* **85**, 1135-1148 (1996).
110 Deng, H. *et al.* Identification of a major co-receptor for primary isolates of HIV-1. *Nature* **381**, 661-666, doi:10.1038/381661a0 (1996).

111 Dragic, T. *et al.* HIV-1 entry into CD4+ cells is mediated by the chemokine receptor CC-CKR-5. *Nature* **381**, 667-673, doi:10.1038/381667a0 (1996).
112 Feng, Y., Broder, C. C., Kennedy, P. E. & Berger, E. A. HIV-1 entry cofactor: functional cDNA cloning of a seven-transmembrane, G protein-coupled receptor. *Science* **272**, 872-877 (1996).
113 Berger, E. A. *et al.* A new classification for HIV-1. *Nature* **391**, 240, doi:10.1038/34571 (1998).
114 Lehmann, M. J., Sherer, N. M., Marks, C. B., Pypaert, M. & Mothes, W. Actin- and myosin-driven movement of viruses along filopodia precedes their entry into cells. *J Cell Biol* **170**, 317-325, doi:10.1083/jcb.200503059 (2005).
115 Sherer, N. M., Jin, J. & Mothes, W. Directional spread of surface-associated retroviruses regulated by differential virus-cell interactions. *Journal of virology* **84**, 3248-3258 (2010).
116 Chan, D. C., Fass, D., Berger, J. M. & Kim, P. S. Core structure of gp41 from the HIV envelope glycoprotein. *Cell* **89**, 263-273 (1997).
117 Weissenhorn, W., Dessen, A., Harrison, S. C., Skehel, J. J. & Wiley, D. C. Atomic structure of the ectodomain from HIV-1 gp41. *Nature* **387**, 426-430, doi:10.1038/387426a0 (1997).
118 Melikyan, G. B. Common principles and intermediates of viral protein-mediated fusion: the HIV-1 paradigm. *Retrovirology* **5**, 111 (2008).
119 Stein, B. S. *et al.* pH-independent HIV entry into CD4-positive T cells via virus envelope fusion to the plasma membrane. *Cell* **49**, 659-668 (1987).
120 Miyauchi, K., Kim, Y., Latinovic, O., Morozov, V. & Melikyan, G. B. HIV enters cells via endocytosis and dynamin-dependent fusion with endosomes. *Cell* **137**, 433-444 (2009).
121 Hu, W. S. & Hughes, S. H. HIV-1 reverse transcription. *Cold Spring Harb Perspect Med* **2**, doi:10.1101/cshperspect.a006882 (2012).
122 Baltimore, D. & Smoler, D. F. Association of an endoribonuclease with the avian myeloblastosis virus deoxyribonucleic acid polymerase. *J Biol Chem* **247**, 7282-7287 (1972).
123 Keller, W. & Crouch, R. Degradation of DNA RNA hybrids by ribonuclease H and DNA polymerases of cellular and viral origin. *Proc Natl Acad Sci U S A* **69**, 3360-3364 (1972).
124 Moelling, K., Bolognesi, D. P. & Bauer, H. Polypeptides of avian RNA tumor viruses. 3. Purification and identification of a DNA synthesizing enzyme. *Virology* **45**, 298-302 (1971).
125 Panganiban, A. T. & Fiore, D. Ordered interstrand and intrastrand DNA transfer during reverse transcription. *Science* **241**, 1064-1069 (1988).
126 Schatz, O., Cromme, F. V., Gruninger-Leitch, F. & Le Grice, S. F. Point mutations in conserved amino acid residues within the C-terminal domain of HIV-1 reverse transcriptase specifically repress RNase H function. *FEBS Lett* **257**, 311-314 (1989).
127 Isel, C. *et al.* Specific initiation and switch to elongation of human immunodeficiency virus type 1 reverse transcription require the post-transcriptional modifications of primer tRNA3Lys. *EMBO J* **15**, 917-924 (1996).
128 Lanchy, J. M. *et al.* Contacts between reverse transcriptase and the primer strand govern the transition from initiation to elongation of HIV-1 reverse transcription. *J Biol Chem* **273**, 24425-24432 (1998).
129 Crouch, R. & Dirksen, M. (Cold Spring Harbor Laboratory, Cold Spring Harbor, NY, 1982).
130 Rattray, A. J. & Champoux, J. J. The role of Moloney murine leukemia virus RNase H activity in the formation of plus-strand primers. *J Virol* **61**, 2843-2851 (1987).
131 Hu, W. S. & Temin, H. M. Retroviral recombination and reverse transcription. *Science* **250**, 1227-1233 (1990).
132 Hu, W. S. & Temin, H. M. Genetic consequences of packaging two RNA genomes in one retroviral particle: pseudodiploidy and high rate of genetic recombination. *Proc Natl Acad Sci U S A* **87**, 1556-1560 (1990).

133 van Wamel, J. L. & Berkhout, B. The first strand transfer during HIV-1 reverse transcription can occur either intramolecularly or intermolecularly. *Virology* **244**, 245-251, doi:10.1006/viro.1998.9096 (1998).
134 Yu, H., Jetzt, A. E., Ron, Y., Preston, B. D. & Dougherty, J. P. The nature of human immunodeficiency virus type 1 strand transfers. *J Biol Chem* **273**, 28384-28391 (1998).
135 Charneau, P., Alizon, M. & Clavel, F. A second origin of DNA plus-strand synthesis is required for optimal human immunodeficiency virus replication. *J Virol* **66**, 2814-2820 (1992).
136 Hungnes, O., Tjotta, E. & Grinde, B. Mutations in the central polypurine tract of HIV-1 result in delayed replication. *Virology* **190**, 440-442 (1992).
137 Swanstrom, R., Varmus, H. E. & Bishop, J. M. The terminal redundancy of the retrovirus genome facilitates chain elongation by reverse transcriptase. *J Biol Chem* **256**, 1115-1121 (1981).
138 Pullen, K. A., Ishimoto, L. K. & Champoux, J. J. Incomplete removal of the RNA primer for minus-strand DNA synthesis by human immunodeficiency virus type 1 reverse transcriptase. *J Virol* **66**, 367-373 (1992).
139 Smith, J. S. & Roth, M. J. Specificity of human immunodeficiency virus-1 reverse transcriptase-associated ribonuclease H in removal of the minus-strand primer, tRNA(Lys3). *J Biol Chem* **267**, 15071-15079 (1992).
140 Whitcomb, J. M., Kumar, R. & Hughes, S. H. Sequence of the circle junction of human immunodeficiency virus type 1: implications for reverse transcription and integration. *J Virol* **64**, 4903-4906 (1990).
141 Fassati, A. & Goff, S. P. Characterization of intracellular reverse transcription complexes of human immunodeficiency virus type 1. *J Virol* **75**, 3626-3635, doi:10.1128/JVI.75.8.3626-3635.2001 (2001).
142 Iordanskiy, S., Berro, R., Altieri, M., Kashanchi, F. & Bukrinsky, M. Intracytoplasmic maturation of the human immunodeficiency virus type 1 reverse transcription complexes determines their capacity to integrate into chromatin. *Retrovirology* **3**, 4, doi:10.1186/1742-4690-3-4 (2006).
143 Nermut, M. V. & Fassati, A. Structural analyses of purified human immunodeficiency virus type 1 intracellular reverse transcription complexes. *J Virol* **77**, 8196-8206 (2003).
144 Dismuke, D. J. & Aiken, C. Evidence for a functional link between uncoating of the human immunodeficiency virus type 1 core and nuclear import of the viral preintegration complex. *J Virol* **80**, 3712-3720, doi:10.1128/JVI.80.8.3712-3720.2006 (2006).
145 Forshey, B. M., von Schwedler, U., Sundquist, W. I. & Aiken, C. Formation of a human immunodeficiency virus type 1 core of optimal stability is crucial for viral replication. *J Virol* **76**, 5667-5677 (2002).
146 Arhel, N. J. *et al.* HIV-1 DNA Flap formation promotes uncoating of the pre-integration complex at the nuclear pore. *EMBO J* **26**, 3025-3037, doi:10.1038/sj.emboj.7601740 (2007).
147 Best, S., Le Tissier, P., Towers, G. & Stoye, J. P. Positional cloning of the mouse retrovirus restriction gene Fv1. *Nature* **382**, 826-829, doi:10.1038/382826a0 (1996).
148 Brennan, G., Kozyrev, Y. & Hu, S. L. TRIMCyp expression in Old World primates Macaca nemestrina and Macaca fascicularis. *Proc Natl Acad Sci U S A* **105**, 3569-3574, doi:10.1073/pnas.0709511105 (2008).
149 Frankel, W. N., Stoye, J. P., Taylor, B. A. & Coffin, J. M. Genetic analysis of endogenous xenotropic murine leukemia viruses: association with two common mouse mutations and the viral restriction locus Fv-1. *J Virol* **63**, 1763-1774 (1989).
150 Newman, R. M. *et al.* Evolution of a TRIM5-CypA splice isoform in old world monkeys. *PLoS Pathog* **4**, e1000003, doi:10.1371/journal.ppat.1000003 (2008).

151 Nisole, S., Lynch, C., Stoye, J. P. & Yap, M. W. A Trim5-cyclophilin A fusion protein found in owl monkey kidney cells can restrict HIV-1. *Proc Natl Acad Sci U S A* **101**, 13324-13328, doi:10.1073/pnas.0404640101 (2004).
152 Sayah, D. M., Sokolskaja, E., Berthoux, L. & Luban, J. Cyclophilin A retrotransposition into TRIM5 explains owl monkey resistance to HIV-1. *Nature* **430**, 569-573, doi:10.1038/nature02777 (2004).
153 Stremlau, M. *et al.* The cytoplasmic body component TRIM5alpha restricts HIV-1 infection in Old World monkeys. *Nature* **427**, 848-853, doi:10.1038/nature02343 (2004).
154 Virgen, C. A., Kratovac, Z., Bieniasz, P. D. & Hatziioannou, T. Independent genesis of chimeric TRIM5-cyclophilin proteins in two primate species. *Proc Natl Acad Sci U S A* **105**, 3563-3568, doi:10.1073/pnas.0709258105 (2008).
155 Wilson, S. J. *et al.* Independent evolution of an antiviral TRIMCyp in rhesus macaques. *Proc Natl Acad Sci U S A* **105**, 3557-3562, doi:10.1073/pnas.0709003105 (2008).
156 Wu, X., Anderson, J. L., Campbell, E. M., Joseph, A. M. & Hope, T. J. Proteasome inhibitors uncouple rhesus TRIM5alpha restriction of HIV-1 reverse transcription and infection. *Proc Natl Acad Sci U S A* **103**, 7465-7470, doi:10.1073/pnas.0510483103 (2006).
157 Bowerman, B., Brown, P. O., Bishop, J. M. & Varmus, H. E. A nucleoprotein complex mediates the integration of retroviral DNA. *Genes Dev* **3**, 469-478 (1989).
158 Suzuki, Y. & Craigie, R. The road to chromatin—nuclear entry of retroviruses. *Nature Reviews Microbiology* **5**, 187-196 (2007).
159 Craigie, R. & Bushman, F. D. HIV DNA integration. *Cold Spring Harb Perspect Med* **2**, a006890, doi:10.1101/cshperspect.a006890 (2012).
160 Coffin, J. M., Hughes, S. H. & Varmus, H. E. in *Retroviruses* (eds J. M. Coffin, S. H. Hughes, & H. E. Varmus) (1997).
161 Weiss, R., Teich, N., Varmus, H. & Coffin, J. RNA tumor viruses. (1985).
162 Pruss, D., Bushman, F. D. & Wolffe, A. P. Human immunodeficiency virus integrase directs integration to sites of severe DNA distortion within the nucleosome core. *Proc Natl Acad Sci U S A* **91**, 5913-5917 (1994).
163 Pryciak, P. M., Sil, A. & Varmus, H. E. Retroviral integration into minichromosomes in vitro. *EMBO J* **11**, 291-303 (1992).
164 Pryciak, P. M. & Varmus, H. E. Nucleosomes, DNA-binding proteins, and DNA sequence modulate retroviral integration target site selection. *Cell* **69**, 769-780 (1992).
165 Wang, G. P., Ciuffi, A., Leipzig, J., Berry, C. C. & Bushman, F. D. HIV integration site selection: analysis by massively parallel pyrosequencing reveals association with epigenetic modifications. *Genome Res* **17**, 1186-1194, doi:10.1101/gr.6286907 (2007).
166 Bor, Y. C., Bushman, F. D. & Orgel, L. E. In vitro integration of human immunodeficiency virus type 1 cDNA into targets containing protein-induced bends. *Proc Natl Acad Sci U S A* **92**, 10334-10338 (1995).
167 Bushman, F. D. & Craigie, R. Integration of human immunodeficiency virus DNA: adduct interference analysis of required DNA sites. *Proc Natl Acad Sci U S A* **89**, 3458-3462 (1992).
168 Katz, R. A., Gravuer, K. & Skalka, A. M. A preferred target DNA structure for retroviral integrase in vitro. *J Biol Chem* **273**, 24190-24195 (1998).
169 Barr, S. D. *et al.* HIV integration site selection: targeting in macrophages and the effects of different routes of viral entry. *Mol Ther* **14**, 218-225, doi:10.1016/j.ymthe.2006.03.012 (2006).
170 Berry, C., Hannenhalli, S., Leipzig, J. & Bushman, F. D. Selection of target sites for mobile DNA integration in the human genome. *PLoS Comput Biol* **2**, e157, doi:10.1371/journal.pcbi.0020157 (2006).

171 Brady, T. *et al.* HIV integration site distributions in resting and activated CD4+ T cells infected in culture. *AIDS* **23**, 1461-1471, doi:10.1097/QAD.0b013e32832caf28 (2009).
172 Ciuffi, A. & Bushman, F. D. Retroviral DNA integration: HIV and the role of LEDGF/p75. *Trends Genet* **22**, 388-395, doi:10.1016/j.tig.2006.05.006 (2006).
173 Mitchell, R. S. *et al.* Retroviral DNA integration: ASLV, HIV, and MLV show distinct target site preferences. *PLoS Biol* **2**, E234, doi:10.1371/journal.pbio.0020234 (2004).
174 Schroder, A. R. *et al.* HIV-1 integration in the human genome favors active genes and local hotspots. *Cell* **110**, 521-529 (2002).
175 Lewinski, M. K. *et al.* Retroviral DNA integration: viral and cellular determinants of target-site selection. *PLoS Pathog* **2**, e60, doi:10.1371/journal.ppat.0020060 (2006).
176 Ciuffi, A. *et al.* A role for LEDGF/p75 in targeting HIV DNA integration. *Nat Med* **11**, 1287-1289, doi:10.1038/nm1329 (2005).
177 Llano, M. *et al.* Identification and characterization of the chromatin-binding domains of the HIV-1 integrase interactor LEDGF/p75. *J Mol Biol* **360**, 760-773, doi:10.1016/j.jmb.2006.04.073 (2006).
178 Marshall, H. M. *et al.* Role of PSIP1/LEDGF/p75 in lentiviral infectivity and integration targeting. *PLoS One* **2**, e1340, doi:10.1371/journal.pone.0001340 (2007).
179 Shun, M. C. *et al.* LEDGF/p75 functions downstream from preintegration complex formation to effect gene-specific HIV-1 integration. *Genes Dev* **21**, 1767-1778, doi:10.1101/gad.1565107 (2007).
180 Cherepanov, P. *et al.* HIV-1 integrase forms stable tetramers and associates with LEDGF/p75 protein in human cells. *J Biol Chem* **278**, 372-381, doi:10.1074/jbc.M209278200 (2003).
181 De Rijck, J., Bartholomeeusen, K., Ceulemans, H., Debyser, Z. & Gijsbers, R. High-resolution profiling of the LEDGF/p75 chromatin interaction in the ENCODE region. *Nucleic Acids Res* **38**, 6135-6147, doi:10.1093/nar/gkq410 (2010).
182 Emiliani, S. *et al.* Integrase mutants defective for interaction with LEDGF/p75 are impaired in chromosome tethering and HIV-1 replication. *J Biol Chem* **280**, 25517-25523, doi:10.1074/jbc.M501378200 (2005).
183 Maertens, G. *et al.* LEDGF/p75 is essential for nuclear and chromosomal targeting of HIV-1 integrase in human cells. *J Biol Chem* **278**, 33528-33539, doi:10.1074/jbc.M303594200 (2003).
184 Turlure, F., Devroe, E., Silver, P. A. & Engelman, A. Human cell proteins and human immunodeficiency virus DNA integration. *Front Biosci* **9**, 3187-3208 (2004).
185 Llano, M. *et al.* An essential role for LEDGF/p75 in HIV integration. *Science* **314**, 461-464, doi:10.1126/science.1132319 (2006).
186 Marini, B. *et al.* Nuclear architecture dictates HIV-1 integration site selection. *Nature* **521**, 227-231, doi:10.1038/nature14226 (2015).
187 Karn, J. & Stoltzfus, C. M. Transcriptional and posttranscriptional regulation of HIV-1 gene expression. *Cold Spring Harb Perspect Med* **2**, a006916, doi:10.1101/cshperspect.a006916 (2012).
188 Garcia, J. A. *et al.* Human immunodeficiency virus type 1 LTR TATA and TAR region sequences required for transcriptional regulation. *EMBO J* **8**, 765-778 (1989).
189 Jones, K. A., Kadonaga, J. T., Luciw, P. A. & Tjian, R. Activation of the AIDS retrovirus promoter by the cellular transcription factor, Sp1. *Science* **232**, 755-759 (1986).
190 Rittner, K., Churcher, M. J., Gait, M. J. & Karn, J. The human immunodeficiency virus long terminal repeat includes a specialised initiator element which is required for Tat-responsive transcription. *J Mol Biol* **248**, 562-580, doi:10.1006/jmbi.1995.0243 (1995).

191 Zenzie-Gregory, B., Sheridan, P., Jones, K. A. & Smale, S. T. HIV-1 core promoter lacks a simple initiator element but contains a bipartite activator at the transcription start site. *J Biol Chem* **268**, 15823-15832 (1993).
192 Kim, S. Y., Byrn, R., Groopman, J. & Baltimore, D. Temporal aspects of DNA and RNA synthesis during human immunodeficiency virus infection: evidence for differential gene expression. *J Virol* **63**, 3708-3713 (1989).
193 Pomerantz, R. J., Trono, D., Feinberg, M. B. & Baltimore, D. Cells nonproductively infected with HIV-1 exhibit an aberrant pattern of viral RNA expression: a molecular model for latency. *Cell* **61**, 1271-1276 (1990).
194 Narita, T. *et al.* Human transcription elongation factor NELF: identification of novel subunits and reconstitution of the functionally active complex. *Mol Cell Biol* **23**, 1863-1873 (2003).
195 Yamaguchi, Y. *et al.* NELF, a multisubunit complex containing RD, cooperates with DSIF to repress RNA polymerase II elongation. *Cell* **97**, 41-51 (1999).
196 Zhang, Z., Klatt, A., Gilmour, D. S. & Henderson, A. J. Negative elongation factor NELF represses human immunodeficiency virus transcription by pausing the RNA polymerase II complex. *J Biol Chem* **282**, 16981-16988, doi:10.1074/jbc.M610688200 (2007).
197 Churcher, M. J. *et al.* High affinity binding of TAR RNA by the human immunodeficiency virus type-1 tat protein requires base-pairs in the RNA stem and amino acid residues flanking the basic region. *J Mol Biol* **230**, 90-110 (1993).
198 Karn, J. The molecular biology of HIV latency: breaking and restoring the Tat-dependent transcriptional circuit. *Curr Opin HIV AIDS* **6**, 4-11, doi:10.1097/COH.0b013e328340ffbb (2011).
199 Siliciano, R. F. & Greene, W. C. HIV latency. *Cold Spring Harb Perspect Med* **1**, a007096, doi:10.1101/cshperspect.a007096 (2011).
200 Kao, S. Y., Calman, A. F., Luciw, P. A. & Peterlin, B. M. Anti-termination of transcription within the long terminal repeat of HIV-1 by tat gene product. *Nature* **330**, 489-493, doi:10.1038/330489a0 (1987).
201 Berkhout, B., Silverman, R. H. & Jeang, K. T. Tat trans-activates the human immunodeficiency virus through a nascent RNA target. *Cell* **59**, 273-282 (1989).
202 Selby, M. J., Bain, E. S., Luciw, P. A. & Peterlin, B. M. Structure, sequence, and position of the stem-loop in tar determine transcriptional elongation by tat through the HIV-1 long terminal repeat. *Genes Dev* **3**, 547-558 (1989).
203 Dingwall, C. *et al.* HIV-1 tat protein stimulates transcription by binding to a U-rich bulge in the stem of the TAR RNA structure. *EMBO J* **9**, 4145-4153 (1990).
204 Dingwall, C. *et al.* Human immunodeficiency virus 1 tat protein binds trans-activation-responsive region (TAR) RNA in vitro. *Proc Natl Acad Sci U S A* **86**, 6925-6929 (1989).
205 Herrmann, C. H., Gold, M. O. & Rice, A. P. Viral transactivators specifically target distinct cellular protein kinases that phosphorylate the RNA polymerase II C-terminal domain. *Nucleic Acids Res* **24**, 501-508 (1996).
206 Herrmann, C. H. & Rice, A. P. Lentivirus Tat proteins specifically associate with a cellular protein kinase, TAK, that hyperphosphorylates the carboxyl-terminal domain of the large subunit of RNA polymerase II: candidate for a Tat cofactor. *J Virol* **69**, 1612-1620 (1995).
207 Marshall, N. F., Peng, J., Xie, Z. & Price, D. H. Control of RNA polymerase II elongation potential by a novel carboxyl-terminal domain kinase. *J Biol Chem* **271**, 27176-27183 (1996).
208 Marshall, N. F. & Price, D. H. Purification of P-TEFb, a transcription factor required for the transition into productive elongation. *J Biol Chem* **270**, 12335-12338 (1995).
209 Wei, P., Garber, M. E., Fang, S. M., Fischer, W. H. & Jones, K. A. A novel CDK9-associated C-type cyclin interacts directly with HIV-1 Tat and mediates its high-affinity, loop-specific binding to TAR RNA. *Cell* **92**, 451-462 (1998).

210 Zhu, Y. *et al.* Transcription elongation factor P-TEFb is required for HIV-1 tat transactivation in vitro. *Genes Dev* **11**, 2622-2632 (1997).
211 Isel, C. & Karn, J. Direct evidence that HIV-1 Tat stimulates RNA polymerase II carboxyl-terminal domain hyperphosphorylation during transcriptional elongation. *J Mol Biol* **290**, 929-941, doi:10.1006/jmbi.1999.2933 (1999).
212 Tahirov, T. H. *et al.* Crystal structure of HIV-1 Tat complexed with human P-TEFb. *Nature* **465**, 747-751, doi:10.1038/nature09131 (2010).
213 Fujinaga, K. *et al.* Dynamics of human immunodeficiency virus transcription: P-TEFb phosphorylates RD and dissociates negative effectors from the transactivation response element. *Mol Cell Biol* **24**, 787-795 (2004).
214 Bourgeois, C. F., Kim, Y. K., Churcher, M. J., West, M. J. & Karn, J. Spt5 cooperates with human immunodeficiency virus type 1 Tat by preventing premature RNA release at terminator sequences. *Mol Cell Biol* **22**, 1079-1093 (2002).
215 Ivanov, D., Kwak, Y. T., Guo, J. & Gaynor, R. B. Domains in the SPT5 protein that modulate its transcriptional regulatory properties. *Mol Cell Biol* **20**, 2970-2983 (2000).
216 Yamada, T. *et al.* P-TEFb-mediated phosphorylation of hSpt5 C-terminal repeats is critical for processive transcription elongation. *Mol Cell* **21**, 227-237, doi:10.1016/j.molcel.2005.11.024 (2006).
217 Yamaguchi, Y., Inukai, N., Narita, T., Wada, T. & Handa, H. Evidence that negative elongation factor represses transcription elongation through binding to a DRB sensitivity-inducing factor/RNA polymerase II complex and RNA. *Mol Cell Biol* **22**, 2918-2927 (2002).
218 Kim, Y. K., Bourgeois, C. F., Isel, C., Churcher, M. J. & Karn, J. Phosphorylation of the RNA polymerase II carboxyl-terminal domain by CDK9 is directly responsible for human immunodeficiency virus type 1 Tat-activated transcriptional elongation. *Mol Cell Biol* **22**, 4622-4637 (2002).
219 Rausch, J. W. & Le Grice, S. F. HIV Rev Assembly on the Rev Response Element (RRE): A Structural Perspective. *Viruses* **7**, 3053-3075, doi:10.3390/v7062760 (2015).
220 Malim, M. H., Hauber, J., Le, S. Y., Maizel, J. V. & Cullen, B. R. The HIV-1 rev trans-activator acts through a structured target sequence to activate nuclear export of unspliced viral mRNA. *Nature* **338**, 254-257, doi:10.1038/338254a0 (1989).
221 Mann, D. A. *et al.* A molecular rheostat. Co-operative rev binding to stem I of the rev-response element modulates human immunodeficiency virus type-1 late gene expression. *J Mol Biol* **241**, 193-207 (1994).
222 Sodroski, J. *et al.* A second post-transcriptional trans-activator gene required for HTLV-III replication. *Nature* **321**, 412-417, doi:10.1038/321412a0 (1986).
223 Watts, J. M. *et al.* Architecture and secondary structure of an entire HIV-1 RNA genome. *Nature* **460**, 711-716, doi:10.1038/nature08237 (2009).
224 Daly, T. J., Cook, K. S., Gray, G. S., Maione, T. E. & Rusche, J. R. Specific binding of HIV-1 recombinant Rev protein to the Rev-responsive element in vitro. *Nature* **342**, 816-819, doi:10.1038/342816a0 (1989).
225 Heaphy, S. *et al.* HIV-1 regulator of virion expression (Rev) protein binds to an RNA stem-loop structure located within the Rev response element region. *Cell* **60**, 685-693 (1990).
226 Malim, M. H. & Cullen, B. R. HIV-1 structural gene expression requires the binding of multiple Rev monomers to the viral RRE: implications for HIV-1 latency. *Cell* **65**, 241-248 (1991).
227 Zapp, M. L., Hope, T. J., Parslow, T. G. & Green, M. R. Oligomerization and RNA binding domains of the type 1 human immunodeficiency virus Rev protein: a dual function for an arginine-rich binding motif. *Proc Natl Acad Sci U S A* **88**, 7734-7738 (1991).

228 Fischer, U., Huber, J., Boelens, W. C., Mattaj, I. W. & Luhrmann, R. The HIV-1 Rev activation domain is a nuclear export signal that accesses an export pathway used by specific cellular RNAs. *Cell* **82**, 475-483 (1995).
229 Henderson, B. R. & Percipalle, P. Interactions between HIV Rev and nuclear import and export factors: the Rev nuclear localisation signal mediates specific binding to human importin-beta. *J Mol Biol* **274**, 693-707, doi:10.1006/jmbi.1997.1420 (1997).
230 Bolinger, C. & Boris-Lawrie, K. Mechanisms employed by retroviruses to exploit host factors for translational control of a complicated proteome. *Retrovirology* **6**, 8, doi:10.1186/1742-4690-6-8 (2009).
231 Brierley, I. & Dos Ramos, F. J. Programmed ribosomal frameshifting in HIV-1 and the SARS-CoV. *Virus Res* **119**, 29-42, doi:10.1016/j.virusres.2005.10.008 (2006).
232 Chamorro, M., Parkin, N. & Varmus, H. E. An RNA pseudoknot and an optimal heptameric shift site are required for highly efficient ribosomal frameshifting on a retroviral messenger RNA. *Proc Natl Acad Sci U S A* **89**, 713-717 (1992).
233 Jacks, T. *et al.* Characterization of ribosomal frameshifting in HIV-1 gag-pol expression. *Nature* **331**, 280-283, doi:10.1038/331280a0 (1988).
234 Brakch, N., Dettin, M., Scarinci, C., Seidah, N. G. & Di Bello, C. Structural investigation and kinetic characterization of potential cleavage sites of HIV GP160 by human furin and PC1. *Biochem Biophys Res Commun* **213**, 356-361 (1995).
235 Hallenberger, S. *et al.* Inhibition of furin-mediated cleavage activation of HIV-1 glycoprotein gp160. *Nature* **360**, 358-361, doi:10.1038/360358a0 (1992).
236 Vollenweider, F. *et al.* Comparative cellular processing of the human immunodeficiency virus (HIV-1) envelope glycoprotein gp160 by the mammalian subtilisin/kexin-like convertases. *Biochem J* **314 (Pt 2)**, 521-532 (1996).
237 Freed, E. O. HIV-1 assembly, release and maturation. *Nat Rev Microbiol* **13**, 484-496, doi:10.1038/nrmicro3490 (2015).
238 Sundquist, W. I. & Krausslich, H. G. HIV-1 assembly, budding, and maturation. *Cold Spring Harb Perspect Med* **2**, a006924, doi:10.1101/cshperspect.a006924 (2012).
239 Massiah, M. A. *et al.* Three-dimensional structure of the human immunodeficiency virus type 1 matrix protein. *J Mol Biol* **244**, 198-223, doi:10.1006/jmbi.1994.1719 (1994).
240 Ono, A., Ablan, S. D., Lockett, S. J., Nagashima, K. & Freed, E. O. Phosphatidylinositol (4,5) bisphosphate regulates HIV-1 Gag targeting to the plasma membrane. *Proc Natl Acad Sci U S A* **101**, 14889-14894, doi:10.1073/pnas.0405596101 (2004).
241 Saad, J. S. *et al.* Structural basis for targeting HIV-1 Gag proteins to the plasma membrane for virus assembly. *Proc Natl Acad Sci U S A* **103**, 11364-11369, doi:10.1073/pnas.0602818103 (2006).
242 Shkriabai, N. *et al.* Interactions of HIV-1 Gag with assembly cofactors. *Biochemistry* **45**, 4077-4083, doi:10.1021/bi052308e (2006).
243 Hogue, I. B., Grover, J. R., Soheilian, F., Nagashima, K. & Ono, A. Gag induces the coalescence of clustered lipid rafts and tetraspanin-enriched microdomains at HIV-1 assembly sites on the plasma membrane. *J Virol* **85**, 9749-9766, doi:10.1128/JVI.00743-11 (2011).
244 Nikolaitchik, O. A. *et al.* Dimeric RNA recognition regulates HIV-1 genome packaging. *PLoS Pathog* **9**, e1003249, doi:10.1371/journal.ppat.1003249 (2013).
245 Summers, M. F. *et al.* Nucleocapsid zinc fingers detected in retroviruses: EXAFS studies of intact viruses and the solution-state structure of the nucleocapsid protein from HIV-1. *Protein Sci* **1**, 563-574, doi:10.1002/pro.5560010502 (1992).

246 Chen, J. *et al.* Cytoplasmic HIV-1 RNA is mainly transported by diffusion in the presence or absence of Gag protein. *Proc Natl Acad Sci U S A* **111**, E5205-5213, doi:10.1073/pnas.1413169111 (2014).
247 Jouvenet, N., Simon, S. M. & Bieniasz, P. D. Imaging the interaction of HIV-1 genomes and Gag during assembly of individual viral particles. *Proc Natl Acad Sci U S A* **106**, 19114-19119, doi:10.1073/pnas.0907364106 (2009).
248 Kutluay, S. B. & Bieniasz, P. D. Analysis of the initiating events in HIV-1 particle assembly and genome packaging. *PLoS Pathog* **6**, e1001200, doi:10.1371/journal.ppat.1001200 (2010).
249 Briggs, J. A. *et al.* Structure and assembly of immature HIV. *Proc Natl Acad Sci U S A* **106**, 11090-11095, doi:10.1073/pnas.0903535106 (2009).
250 Fuller, S. D., Wilk, T., Gowen, B. E., Krausslich, H. G. & Vogt, V. M. Cryo-electron microscopy reveals ordered domains in the immature HIV-1 particle. *Curr Biol* **7**, 729-738 (1997).
251 Kutluay, S. B. *et al.* Global changes in the RNA binding specificity of HIV-1 gag regulate virion genesis. *Cell* **159**, 1096-1109, doi:10.1016/j.cell.2014.09.057 (2014).
252 Wright, E. R. *et al.* Electron cryotomography of immature HIV-1 virions reveals the structure of the CA and SP1 Gag shells. *EMBO J* **26**, 2218-2226, doi:10.1038/sj.emboj.7601664 (2007).
253 Gitti, R. K. *et al.* Structure of the amino-terminal core domain of the HIV-1 capsid protein. *Science* **273**, 231-235 (1996).
254 Tang, C., Ndassa, Y. & Summers, M. F. Structure of the N-terminal 283-residue fragment of the immature HIV-1 Gag polyprotein. *Nat Struct Biol* **9**, 537-543, doi:10.1038/nsb806 (2002).
255 Gamble, T. R. *et al.* Crystal structure of human cyclophilin A bound to the amino-terminal domain of HIV-1 capsid. *Cell* **87**, 1285-1294 (1996).
256 Checkley, M. A., Luttge, B. G. & Freed, E. O. HIV-1 envelope glycoprotein biosynthesis, trafficking, and incorporation. *J Mol Biol* **410**, 582-608, doi:10.1016/j.jmb.2011.04.042 (2011).
257 Murakami, T. & Freed, E. O. The long cytoplasmic tail of gp41 is required in a cell type-dependent manner for HIV-1 envelope glycoprotein incorporation into virions. *Proc Natl Acad Sci U S A* **97**, 343-348 (2000).
258 Tedbury, P. R., Ablan, S. D. & Freed, E. O. Global rescue of defects in HIV-1 envelope glycoprotein incorporation: implications for matrix structure. *PLoS Pathog* **9**, e1003739, doi:10.1371/journal.ppat.1003739 (2013).
259 Carlton, J. G. & Martin-Serrano, J. Parallels between cytokinesis and retroviral budding: a role for the ESCRT machinery. *Science* **316**, 1908-1912, doi:10.1126/science.1143422 (2007).
260 Fossen, T. *et al.* Solution structure of the human immunodeficiency virus type 1 p6 protein. *J Biol Chem* **280**, 42515-42527, doi:10.1074/jbc.M507375200 (2005).
261 Fujii, K. *et al.* Functional role of Alix in HIV-1 replication. *Virology* **391**, 284-292, doi:10.1016/j.virol.2009.06.016 (2009).
262 Strack, B., Calistri, A., Craig, S., Popova, E. & Göttlinger, H. G. AIP1/ALIX is a binding partner for HIV-1 p6 and EIAV p9 functioning in virus budding. *Cell* **114**, 689-699 (2003).
263 Demirov, D. G., Ono, A., Orenstein, J. M. & Freed, E. O. Overexpression of the N-terminal domain of TSG101 inhibits HIV-1 budding by blocking late domain function. *Proc Natl Acad Sci U S A* **99**, 955-960, doi:10.1073/pnas.032511899 (2002).
264 Garrus, J. E. *et al.* Tsg101 and the vacuolar protein sorting pathway are essential for HIV-1 budding. *Cell* **107**, 55-65 (2001).
265 Martin-Serrano, J., Zang, T. & Bieniasz, P. D. HIV-1 and Ebola virus encode small peptide motifs that recruit Tsg101 to sites of particle assembly to facilitate egress. *Nat Med* **7**, 1313-1319, doi:10.1038/nm1201-1313 (2001).

266 VerPlank, L. *et al.* Tsg101, a homologue of ubiquitin-conjugating (E2) enzymes, binds the L domain in HIV type 1 Pr55(Gag). *Proc Natl Acad Sci U S A* **98**, 7724-7729, doi:10.1073/pnas.131059198 (2001).
267 Hanson, P. I., Roth, R., Lin, Y. & Heuser, J. E. Plasma membrane deformation by circular arrays of ESCRT-III protein filaments. *J Cell Biol* **180**, 389-402, doi:10.1083/jcb.200707031 (2008).
268 Shen, Q. T. *et al.* Structural analysis and modeling reveals new mechanisms governing ESCRT-III spiral filament assembly. *J Cell Biol* **206**, 763-777, doi:10.1083/jcb.201403108 (2014).
269 Wollert, T., Wunder, C., Lippincott-Schwartz, J. & Hurley, J. H. Membrane scission by the ESCRT-III complex. *Nature* **458**, 172-177, doi:10.1038/nature07836 (2009).
270 Wlodawer, A. & Erickson, J. W. Structure-based inhibitors of HIV-1 protease. *Annu Rev Biochem* **62**, 543-585, doi:10.1146/annurev.bi.62.070193.002551 (1993).
271 Alfadhli, A., Barklis, R. L. & Barklis, E. HIV-1 matrix organizes as a hexamer of trimers on membranes containing phosphatidylinositol-(4,5)-bisphosphate. *Virology* **387**, 466-472, doi:10.1016/j.virol.2009.02.048 (2009).
272 Frank, G. A. *et al.* Maturation of the HIV-1 core by a non-diffusional phase transition. *Nat Commun* **6**, 5854, doi:10.1038/ncomms6854 (2015).
273 Hill, M., Tachedjian, G. & Mak, J. The packaging and maturation of the HIV-1 Pol proteins. *Curr HIV Res* **3**, 73-85 (2005).
274 Keller, H., Krausslich, H. G. & Schwille, P. Multimerizable HIV Gag derivative binds to the liquid-disordered phase in model membranes. *Cell Microbiol* **15**, 237-247, doi:10.1111/cmi.12064 (2013).
275 Rustagi, A. & Gale, M., Jr. Innate antiviral immune signaling, viral evasion and modulation by HIV-1. *J Mol Biol* **426**, 1161-1177, doi:10.1016/j.jmb.2013.12.003 (2014).
276 Loo, Y. M. & Gale, M., Jr. Viral regulation and evasion of the host response. *Curr Top Microbiol Immunol* **316**, 295-313 (2007).
277 Schoggins, J. W. & Rice, C. M. Interferon-stimulated genes and their antiviral effector functions. *Curr Opin Virol* **1**, 519-525, doi:10.1016/j.coviro.2011.10.008 (2011).
278 Stetson, D. B. & Medzhitov, R. Antiviral defense: interferons and beyond. *J Exp Med* **203**, 1837-1841, doi:10.1084/jem.20061377 (2006).
279 Doehle, B. P. *et al.* Vpu mediates depletion of interferon regulatory factor 3 during HIV infection by a lysosome-dependent mechanism. *Journal of virology* **86**, 8367-8374 (2012).
280 Okumura, A. *et al.* HIV-1 accessory proteins VPR and Vif modulate antiviral response by targeting IRF-3 for degradation. *Virology* **373**, 85-97 (2008).
281 Park, S. Y., Waheed, A. A., Zhang, Z.-R., Freed, E. O. & Bonifacino, J. S. HIV-1 Vpu accessory protein induces caspase-mediated cleavage of IRF3 transcription factor. *Journal of Biological Chemistry* **289**, 35102-35110 (2014).
282 Laguette, N. *et al.* Premature activation of the SLX4 complex by Vpr promotes G2/M arrest and escape from innate immune sensing. *Cell* **156**, 134-145 (2014).
283 Goujon, C. *et al.* Human MX2 is an interferon-induced post-entry inhibitor of HIV-1 infection. *Nature* **502**, 559-562 (2013).
284 Kane, M. *et al.* MX2 is an interferon-induced inhibitor of HIV-1 infection. *Nature* **502**, 563-566 (2013).
285 Liu, Z. *et al.* The interferon-inducible MxB protein inhibits HIV-1 infection. *Cell host & microbe* **14**, 398-410 (2013).
286 Gao, D. *et al.* Cyclic GMP-AMP synthase is an innate immune sensor of HIV and other retroviruses. *Science* **341**, 903-906, doi:10.1126/science.1240933 (2013).
287 Jakobsen, M. R. *et al.* IFI16 senses DNA forms of the lentiviral replication cycle and controls HIV-1 replication. *Proc Natl Acad Sci U S A* **110**, E4571-4580, doi:10.1073/pnas.1311669110 (2013).

288 Li, X. D. *et al.* Pivotal roles of cGAS-cGAMP signaling in antiviral defense and immune adjuvant effects. *Science* **341**, 1390-1394, doi:10.1126/science.1244040 (2013).
289 Sun, L., Wu, J., Du, F., Chen, X. & Chen, Z. J. Cyclic GMP-AMP synthase is a cytosolic DNA sensor that activates the type I interferon pathway. *Science* **339**, 786-791, doi:10.1126/science.1232458 (2013).
290 Thompson, M. R. *et al.* Interferon gamma-inducible protein (IFI) 16 transcriptionally regulates type i interferons and other interferon-stimulated genes and controls the interferon response to both DNA and RNA viruses. *J Biol Chem* **289**, 23568-23581, doi:10.1074/jbc.M114.554147 (2014).
291 Lee, M. N. *et al.* Identification of regulators of the innate immune response to cytosolic DNA and retroviral infection by an integrative approach. *Nat Immunol* **14**, 179-185, doi:10.1038/ni.2509 (2013).
292 Wu, J. *et al.* Cyclic GMP-AMP is an endogenous second messenger in innate immune signaling by cytosolic DNA. *Science* **339**, 826-830, doi:10.1126/science.1229963 (2013).
293 Zhang, X. *et al.* Cyclic GMP-AMP containing mixed phosphodiester linkages is an endogenous high-affinity ligand for STING. *Mol Cell* **51**, 226-235, doi:10.1016/j.molcel.2013.05.022 (2013).
294 Ablasser, A. *et al.* Cell intrinsic immunity spreads to bystander cells via the intercellular transfer of cGAMP. *Nature* **503**, 530-534, doi:10.1038/nature12640 (2013).
295 Price, A. J. *et al.* Active site remodeling switches HIV specificity of antiretroviral TRIMCyp. *Nat Struct Mol Biol* **16**, 1036-1042, doi:10.1038/nsmb.1667 (2009).
296 Lahaye, X. *et al.* The capsids of HIV-1 and HIV-2 determine immune detection of the viral cDNA by the innate sensor cGAS in dendritic cells. *Immunity* **39**, 1132-1142, doi:10.1016/j.immuni.2013.11.002 (2013).
297 Manel, N. *et al.* A cryptic sensor for HIV-1 activates antiviral innate immunity in dendritic cells. *Nature* **467**, 214-217, doi:10.1038/nature09337 (2010).
298 Altfeld, M. & Gale, M., Jr. Innate immunity against HIV-1 infection. *Nat Immunol* **16**, 554-562, doi:10.1038/ni.3157 (2015).
299 Lester, S. N. & Li, K. Toll-like receptors in antiviral innate immunity. *J Mol Biol* **426**, 1246-1264, doi:10.1016/j.jmb.2013.11.024 (2014).
300 Kawai, T. & Akira, S. The role of pattern-recognition receptors in innate immunity: update on Toll-like receptors. *Nature immunology* **11**, 373-384 (2010).
301 Nazli, A. *et al.* HIV-1 gp120 induces TLR2- and TLR4-mediated innate immune activation in human female genital epithelium. *J Immunol* **191**, 4246-4258, doi:10.4049/jimmunol.1301482 (2013).
302 Schlaepfer, E., Audige, A., Joller, H. & Speck, R. F. TLR7/8 triggering exerts opposing effects in acute versus latent HIV infection. *J Immunol* **176**, 2888-2895 (2006).
303 Akira, S., Uematsu, S. & Takeuchi, O. Pathogen recognition and innate immunity. *Cell* **124**, 783-801 (2006).
304 Kawai, T. & Akira, S. TLR signaling. *Cell Death & Differentiation* **13**, 816-825 (2006).
305 Beignon, A.-S. *et al.* Endocytosis of HIV-1 activates plasmacytoid dendritic cells via Toll-like receptor–viral RNA interactions. *The Journal of clinical investigation* **115**, 3265-3275 (2005).
306 Lepelley, A. *et al.* Innate sensing of HIV-infected cells. *PLoS Pathog* **7**, e1001284 (2011).
307 Botos, I., Segal, D. M. & Davies, D. R. The structural biology of Toll-like receptors. *Structure* **19**, 447-459 (2011).
308 Berg, R. K. *et al.* Genomic HIV RNA induces innate immune responses through RIG-I-dependent sensing of secondary-structured RNA. *PLoS One* **7**, e29291, doi:10.1371/journal.pone.0029291 (2012).

309 Liu, H. M. *et al.* The mitochondrial targeting chaperone 14-3-3ε regulates a RIG-I translocon that mediates membrane association and innate antiviral immunity. *Cell host & microbe* **11**, 528-537 (2012).
310 Loo, Y. M. & Gale, M., Jr. Immune signaling by RIG-I-like receptors. *Immunity* **34**, 680-692, doi:10.1016/j.immuni.2011.05.003 (2011).
311 Wang, Y., Wang, X., Li, J., Zhou, Y. & Ho, W. RIG-I activation inhibits HIV replication in macrophages. *J Leukoc Biol* **94**, 337-341, doi:10.1189/jlb.0313158 (2013).
312 Loo, Y.-M. *et al.* Distinct RIG-I and MDA5 signaling by RNA viruses in innate immunity. *Journal of virology* **82**, 335-345 (2008).
313 Paz, S. *et al.* Induction of IRF-3 and IRF-7 phosphorylation following activation of the RIG-I pathway. *Cellular and molecular biology (Noisy-le-Grand, France)* **52**, 17-28 (2005).
314 Neil, S. J., Zang, T. & Bieniasz, P. D. Tetherin inhibits retrovirus release and is antagonized by HIV-1 Vpu. *Nature* **451**, 425-430, doi:10.1038/nature06553 (2008).
315 Perez-Caballero, D. *et al.* Tetherin inhibits HIV-1 release by directly tethering virions to cells. *Cell* **139**, 499-511, doi:10.1016/j.cell.2009.08.039 (2009).
316 Tokarev, A., Skasko, M., Fitzpatrick, K. & Guatelli, J. Antiviral activity of the interferon-induced cellular protein BST-2/tetherin. *AIDS Res Hum Retroviruses* **25**, 1197-1210, doi:10.1089/aid.2009.0253

10.1089/aid.2009.9991 (2009).
317 Galão, R. P., Le Tortorec, A., Pickering, S., Kueck, T. & Neil, S. J. Innate sensing of HIV-1 assembly by Tetherin induces NFκB-dependent proinflammatory responses. *Cell host & microbe* **12**, 633-644 (2012).
318 Matsuda, A. *et al.* Large-scale identification and characterization of human genes that activate NF-κB and MAPK signaling pathways. *Oncogene* **22**, 3307-3318 (2003).
319 Tokarev, A. *et al.* Stimulation of NF-κB activity by the HIV restriction factor BST2. *Journal of virology* **87**, 2046-2057 (2013).
320 Rustagi, A. & Gale, M. Innate antiviral immune signaling, viral evasion and modulation by HIV-1. *Journal of molecular biology* **426**, 1161-1177 (2014).
321 Chen, W. & Royer, W. E. Structural insights into interferon regulatory factor activation. *Cellular signalling* **22**, 883-887 (2010).
322 Anders, H. J., Lichtnekert, J. & Allam, R. Interferon-alpha and -beta in kidney inflammation. *Kidney Int* **77**, 848-854, doi:10.1038/ki.2010.71 (2010).
323 Chevaliez, S. & Pawlotsky, J.-M. in *Antiviral Strategies* 203-241 (Springer, 2009).
324 Harris, R. S., Petersen-Mahrt, S. K. & Neuberger, M. S. RNA editing enzyme APOBEC1 and some of its homologs can act as DNA mutators. *Molecular cell* **10**, 1247-1253 (2002).
325 Mariani, R. *et al.* Species-specific exclusion of APOBEC3G from HIV-1 virions by Vif. *Cell* **114**, 21-31 (2003).
326 Refsland, E. W. *et al.* Quantitative profiling of the full APOBEC3 mRNA repertoire in lymphocytes and tissues: implications for HIV-1 restriction. *Nucleic acids research* **38**, 4274-4284 (2010).
327 Sheehy, A. M., Gaddis, N. C., Choi, J. D. & Malim, M. H. Isolation of a human gene that inhibits HIV-1 infection and is suppressed by the viral Vif protein. *Nature* **418**, 646-650 (2002).
328 Mangeat, B. *et al.* Broad antiretroviral defence by human APOBEC3G through lethal editing of nascent reverse transcripts. *Nature* **424**, 99-103 (2003).
329 Apolonia, L. *et al.* Promiscuous RNA binding ensures effective encapsidation of APOBEC3 proteins by HIV-1. *PLoS Pathog* **11**, e1004609, doi:10.1371/journal.ppat.1004609 (2015).

330 Zennou, V., Perez-Caballero, D., Gottlinger, H. & Bieniasz, P. D. APOBEC3G incorporation into human immunodeficiency virus type 1 particles. *J Virol* **78**, 12058-12061, doi:10.1128/JVI.78.21.12058-12061.2004 (2004).
331 Bishop, K. N. *et al.* Cytidine deamination of retroviral DNA by diverse APOBEC proteins. *Curr Biol* **14**, 1392-1396, doi:10.1016/j.cub.2004.06.057 (2004).
332 Suspene, R., Rusniok, C., Vartanian, J. P. & Wain-Hobson, S. Twin gradients in APOBEC3 edited HIV-1 DNA reflect the dynamics of lentiviral replication. *Nucleic Acids Res* **34**, 4677-4684, doi:10.1093/nar/gkl555 (2006).
333 Desimmie, B. A. *et al.* Multiple APOBEC3 restriction factors for HIV-1 and one Vif to rule them all. *J Mol Biol* **426**, 1220-1245, doi:10.1016/j.jmb.2013.10.033 (2014).
334 Refsland, E. W. & Harris, R. S. in *Intrinsic Immunity* 1-27 (Springer, 2013).
335 Bishop, K. N., Verma, M., Kim, E. Y., Wolinsky, S. M. & Malim, M. H. APOBEC3G inhibits elongation of HIV-1 reverse transcripts. *PLoS Pathog* **4**, e1000231, doi:10.1371/journal.ppat.1000231 (2008).
336 Conticello, S. G., Harris, R. S. & Neuberger, M. S. The Vif protein of HIV triggers degradation of the human antiretroviral DNA deaminase APOBEC3G. *Current Biology* **13**, 2009-2013 (2003).
337 Yu, X. *et al.* Induction of APOBEC3G ubiquitination and degradation by an HIV-1 Vif-Cul5-SCF complex. *Science* **302**, 1056-1060 (2003).
338 Guo, Y. *et al.* Structural basis for hijacking CBF-[bgr] and CUL5 E3 ligase complex by HIV-1 Vif. *Nature* **505**, 229-233 (2014).
339 Bergeron, J. R. *et al.* The SOCS-box of HIV-1 Vif interacts with ElonginBC by induced-folding to recruit its Cul5-containing ubiquitin ligase complex. *PLoS Pathog* **6**, e1000925 (2010).
340 Jäger, S. *et al.* Vif hijacks CBF-[bgr] to degrade APOBEC3G and promote HIV-1 infection. *Nature* **481**, 371-375 (2012).
341 Ooms, M. *et al.* HIV-1 Vif adaptation to human APOBEC3H haplotypes. *Cell host & microbe* **14**, 411-421 (2013).
342 Russell, R. A. & Pathak, V. K. Identification of two distinct human immunodeficiency virus type 1 Vif determinants critical for interactions with human APOBEC3G and APOBEC3F. *Journal of virology* **81**, 8201-8210 (2007).
343 Kim, E.-Y. *et al.* Human APOBEC3 induced mutation of human immunodeficiency virus type-1 contributes to adaptation and evolution in natural infection. *PLoS Pathog* **10**, e1004281 (2014).
344 Kim, E.-Y. *et al.* Human APOBEC3G-mediated editing can promote HIV-1 sequence diversification and accelerate adaptation to selective pressure. *Journal of virology* **84**, 10402-10405 (2010).
345 Fourati, S. *et al.* Partially active HIV-1 Vif alleles facilitate viral escape from specific antiretrovirals. *Aids* **24**, 2313-2321 (2010).
346 Nisole, S., Stoye, J. P. & Saib, A. TRIM family proteins: retroviral restriction and antiviral defence. *Nat Rev Microbiol* **3**, 799-808, doi:10.1038/nrmicro1248 (2005).
347 Johnson, W. E. & Sawyer, S. L. Molecular evolution of the antiretroviral TRIM5 gene. *Immunogenetics* **61**, 163-176 (2009).
348 Sawyer, S. L., Wu, L. I., Emerman, M. & Malik, H. S. Positive selection of primate TRIM5α identifies a critical species-specific retroviral restriction domain. *Proceedings of the National Academy of Sciences of the United States of America* **102**, 2832-2837 (2005).
349 Song, B. *et al.* The B30. 2 (SPRY) domain of the retroviral restriction factor TRIM5α exhibits lineage-specific length and sequence variation in primates. *Journal of virology* **79**, 6111-6121 (2005).
350 Perez-Caballero, D., Hatziioannou, T., Yang, A., Cowan, S. & Bieniasz, P. D. Human tripartite motif 5α domains responsible for retrovirus restriction activity and specificity. *Journal of virology* **79**, 8969-8978 (2005).

351 Stremlau, M., Perron, M., Welikala, S. & Sodroski, J. Species-specific variation in the B30. 2 (SPRY) domain of TRIM5α determines the potency of human immunodeficiency virus restriction. *Journal of virology* **79**, 3139-3145 (2005).
352 Yap, M. W., Nisole, S. & Stoye, J. P. A single amino acid change in the SPRY domain of human Trim5α leads to HIV-1 restriction. *Current Biology* **15**, 73-78 (2005).
353 Stremlau, M. *et al.* Specific recognition and accelerated uncoating of retroviral capsids by the TRIM5α restriction factor. *Proceedings of the National Academy of Sciences* **103**, 5514-5519 (2006).
354 Li, X. & Sodroski, J. The TRIM5α B-box 2 domain promotes cooperative binding to the retroviral capsid by mediating higher-order self-association. *Journal of virology* **82**, 11495-11502 (2008).
355 Diaz-Griffero, F. *et al.* A B-box 2 surface patch important for TRIM5α self-association, capsid binding avidity, and retrovirus restriction. *Journal of virology* **83**, 10737-10751 (2009).
356 Ganser-Pornillos, B. K. *et al.* Hexagonal assembly of a restricting TRIM5α protein. *Proceedings of the National Academy of Sciences* **108**, 534-539 (2011).
357 Diaz-Griffero, F. *et al.* Modulation of retroviral restriction and proteasome inhibitor-resistant turnover by changes in the TRIM5α B-box 2 domain. *Journal of virology* **81**, 10362-10378 (2007).
358 Malim, M. H. & Bieniasz, P. D. HIV restriction factors and mechanisms of evasion. *Cold Spring Harbor perspectives in medicine* **2**, a006940 (2012).
359 Neil, S. J., Sandrin, V., Sundquist, W. I. & Bieniasz, P. D. An interferon-α-induced tethering mechanism inhibits HIV-1 and Ebola virus particle release but is counteracted by the HIV-1 Vpu protein. *Cell host & microbe* **2**, 193-203 (2007).
360 Hinz, A. *et al.* Structural basis of HIV-1 tethering to membranes by the BST-2/tetherin ectodomain. *Cell host & microbe* **7**, 314-323 (2010).
361 Venkatesh, S. & Bieniasz, P. D. Mechanism of HIV-1 virion entrapment by tetherin. *PLoS Pathog* **9**, e1003483 (2013).
362 Van Damme, N. *et al.* The interferon-induced protein BST-2 restricts HIV-1 release and is downregulated from the cell surface by the viral Vpu protein. *Cell host & microbe* **3**, 245-252 (2008).
363 Douglas, J. L. *et al.* Vpu directs the degradation of the human immunodeficiency virus restriction factor BST-2/Tetherin via a βTrCP-dependent mechanism. *Journal of virology* **83**, 7931-7947 (2009).
364 Mitchell, R. S. *et al.* Vpu antagonizes BST-2–mediated restriction of HIV-1 release via β-TrCP and endo-lysosomal trafficking. *PLoS Pathog* **5**, e1000450 (2009).
365 Sauter, D. *et al.* Differential regulation of NF-κB-mediated proviral and antiviral host gene expression by primate lentiviral Nef and Vpu proteins. *Cell reports* **10**, 586-599 (2015).
366 Willey, R., Maldarelli, F., Martin, M. & Strebel, K. Human immunodeficiency virus type 1 Vpu protein induces rapid degradation of CD4. *Journal of virology* **66**, 7193-7200 (1992).
367 Schubert, U. *et al.* CD4 glycoprotein degradation induced by human immunodeficiency virus type 1 Vpu protein requires the function of proteasomes and the ubiquitin-conjugating pathway. *Journal of virology* **72**, 2280-2288 (1998).
368 Bour, S. & Strebel, K. The human immunodeficiency virus (HIV) type 2 envelope protein is a functional complement to HIV type 1 Vpu that enhances particle release of heterologous retroviruses. *Journal of virology* **70**, 8285-8300 (1996).
369 Jia, B. *et al.* Species-specific activity of SIV Nef and HIV-1 Vpu in overcoming restriction by tetherin/BST2. *PLoS Pathog* **5**, e1000429 (2009).
370 Zhang, F. *et al.* Nef proteins from simian immunodeficiency viruses are tetherin antagonists. *Cell host & microbe* **6**, 54-67 (2009).

371 Goldstone, D. C. *et al.* HIV-1 restriction factor SAMHD1 is a deoxynucleoside triphosphate triphosphohydrolase. *Nature* **480**, 379-382 (2011).
372 Hrecka, K. *et al.* Vpx relieves inhibition of HIV-1 infection of macrophages mediated by the SAMHD1 protein. *Nature* **474**, 658-661 (2011).
373 Laguette, N. *et al.* SAMHD1 is the dendritic-and myeloid-cell-specific HIV-1 restriction factor counteracted by Vpx. *Nature* **474**, 654-657 (2011).
374 Brandariz-Nuñez, A. *et al.* Role of SAMHD1 nuclear localization in restriction of HIV-1 and SIVmac. *Retrovirology* **9**, 4690-4699 (2012).
375 Hofmann, H. *et al.* The Vpx lentiviral accessory protein targets SAMHD1 for degradation in the nucleus. *Journal of virology* **86**, 12552-12560 (2012).
376 Lahouassa, H. *et al.* SAMHD1 restricts the replication of human immunodeficiency virus type 1 by depleting the intracellular pool of deoxynucleoside triphosphates. *Nature immunology* **13**, 223-228 (2012).
377 Powell, R. D., Holland, P. J., Hollis, T. & Perrino, F. W. Aicardi-Goutieres syndrome gene and HIV-1 restriction factor SAMHD1 is a dGTP-regulated deoxynucleotide triphosphohydrolase. *Journal of Biological Chemistry* **286**, 43596-43600 (2011).
378 Gramberg, T. *et al.* Restriction of diverse retroviruses by SAMHD1. *Retrovirology* **10**, 1-1 (2013).
379 Cribier, A., Descours, B., Valadão, A. L. C., Laguette, N. & Benkirane, M. Phosphorylation of SAMHD1 by cyclin A2/CDK1 regulates its restriction activity toward HIV-1. *Cell reports* **3**, 1036-1043 (2013).
380 Gelais, C. S. *et al.* Identification of cellular proteins interacting with the retroviral restriction factor SAMHD1. *Journal of virology* **88**, 5834-5844 (2014).
381 Pauls, E. *et al.* Cell cycle control and HIV-1 susceptibility are linked by CDK6-dependent CDK2 phosphorylation of SAMHD1 in myeloid and lymphoid cells. *The Journal of Immunology* **193**, 1988-1997 (2014).
382 White, T. E. *et al.* The retroviral restriction ability of SAMHD1, but not its deoxynucleotide triphosphohydrolase activity, is regulated by phosphorylation. *Cell host & microbe* **13**, 441-451 (2013).
383 Beloglazova, N. *et al.* Nuclease activity of the human SAMHD1 protein implicated in the Aicardi-Goutieres syndrome and HIV-1 restriction. *Journal of Biological Chemistry* **288**, 8101-8110 (2013).
384 Ryoo, J. *et al.* The ribonuclease activity of SAMHD1 is required for HIV-1 restriction. *Nature medicine* **20**, 936-941 (2014).
385 Hofmann, H. *et al.* Inhibition of CUL4A neddylation causes a reversible block to SAMHD1-mediated restriction of HIV-1. *Journal of virology* **87**, 11741-11750 (2013).
386 Tristem, M., Marshall, C., Karpas, A. & Hill, F. Evolution of the primate lentiviruses: evidence from vpx and vpr. *The EMBO journal* **11**, 3405 (1992).
387 Guyader, M., Emerman, M., Montagnier, L. & Peden, K. VPX mutants of HIV-2 are infectious in established cell lines but display a severe defect in peripheral blood lymphocytes. *The EMBO journal* **8**, 1169 (1989).
388 Baldauf, H.-M. *et al.* SAMHD1 restricts HIV-1 infection in resting CD4+ T cells. *Nature medicine* **18**, 1682-1689 (2012).
389 Srivastava, S. *et al.* Lentiviral Vpx accessory factor targets VprBP/DCAF1 substrate adaptor for cullin 4 E3 ubiquitin ligase to enable macrophage infection. *PLoS Pathog* **4**, e1000059 (2008).
390 Jáuregui, P., Logue, E. C., Schultz, M. L., Fung, S. & Landau, N. R. Degradation of SAMHD1 by Vpx is Independent of Uncoating. *Journal of virology* **89**, 5701-5713 (2015).

391 Kim, B., Nguyen, L. A., Daddacha, W. & Hollenbaugh, J. A. Tight interplay among SAMHD1 protein level, cellular dNTP levels, and HIV-1 proviral DNA synthesis kinetics in human primary monocyte-derived macrophages. *Journal of Biological Chemistry* **287**, 21570-21574 (2012).
392 Li, M. *et al.* Codon-usage-based inhibition of HIV protein synthesis by human schlafen 11. *Nature* **491**, 125-128 (2012).
393 Abdel-Mohsen, M. *et al.* Expression profile of host restriction factors in HIV-1 elite controllers. *Retrovirology* **10**, 106 (2013).
394 Fribourgh, J. L. *et al.* Structural insight into HIV-1 restriction by MxB. *Cell host & microbe* **16**, 627-638 (2014).
395 Miles, R. J. *et al.* MxB sensitivity of HIV-1 is determined by a highly variable and dynamic capsid surface. *Elife* **9**, doi:10.7554/eLife.56910 (2020).
396 Yi, D. R. *et al.* Human MxB Inhibits the Replication of Hepatitis C Virus. *J Virol* **93**, doi:10.1128/JVI.01285-18 (2019).
397 Crameri, M. *et al.* MxB is an interferon-induced restriction factor of human herpesviruses. *Nat Commun* **9**, 1980, doi:10.1038/s41467-018-04379-2 (2018).
398 Schilling, M. *et al.* Human MxB Protein Is a Pan-herpesvirus Restriction Factor. *J Virol* **92**, doi:10.1128/JVI.01056-18 (2018).
399 Staeheli, P. & Haller, O. Human MX2/MxB: a Potent Interferon-Induced Postentry Inhibitor of Herpesviruses and HIV-1. *J Virol* **92**, doi:10.1128/JVI.00709-18 (2018).
400 Goto, E. *et al.* c-MIR, a human E3 ubiquitin ligase, is a functional homolog of herpesvirus proteins MIR1 and MIR2 and has similar activity. *Journal of Biological Chemistry* **278**, 14657-14668 (2003).
401 Bartee, E., Mansouri, M., Nerenberg, B. T. H., Gouveia, K. & Früh, K. Downregulation of major histocompatibility complex class I by human ubiquitin ligases related to viral immune evasion proteins. *Journal of virology* **78**, 1109-1120 (2004).
402 Tada, T. *et al.* MARCH8 inhibits HIV-1 infection by reducing virion incorporation of envelope glycoproteins. *Nature medicine* **21**, 1502-1507 (2015).
403 Kim, B.-H., Shenoy, A. R., Kumar, P., Bradfield, C. J. & MacMicking, J. D. IFN-inducible GTPases in host cell defense. *Cell host & microbe* **12**, 432-444 (2012).
404 Krapp, C. *et al.* Guanylate Binding Protein (GBP) 5 Is an Interferon-Inducible Inhibitor of HIV-1 Infectivity. *Cell Host Microbe* **19**, 504-514, doi:10.1016/j.chom.2016.02.019 (2016).
405 Li, C. *et al.* 25-Hydroxycholesterol Protects Host against Zika Virus Infection and Its Associated Microcephaly in a Mouse Model. *Immunity* **46**, 446-456, doi:10.1016/j.immuni.2017.02.012 (2017).
406 Liu, S. Y. *et al.* Interferon-inducible cholesterol-25-hydroxylase broadly inhibits viral entry by production of 25-hydroxycholesterol. *Immunity* **38**, 92-105, doi:10.1016/j.immuni.2012.11.005 (2013).
407 Holmes, R. S., Vandeberg, J. L. & Cox, L. A. Genomics and proteomics of vertebrate cholesterol ester lipase (LIPA) and cholesterol 25-hydroxylase (CH25H). *3 Biotech* **1**, 99-109, doi:10.1007/s13205-011-0013-9 (2011).
408 Kandutsch, A. A. & Chen, H. W. Inhibition of sterol synthesis in cultured mouse cells by cholesterol derivatives oxygenated in the side chain. *J Biol Chem* **249**, 6057-6061 (1974).
409 Goldstein, J. L., Dana, S. E., Faust, J. R., Beaudet, A. L. & Brown, M. S. Role of lysosomal acid lipase in the metabolism of plasma low density lipoprotein. Observations in cultured fibroblasts from a patient with cholesteryl ester storage disease. *J Biol Chem* **250**, 8487-8495 (1975).
410 McDonald, J. G. & Russell, D. W. Editorial: 25-Hydroxycholesterol: a new life in immunology. *J Leukoc Biol* **88**, 1071-1072, doi:10.1189/jlb.0710418 (2010).

411 Schule, R. *et al.* Marked accumulation of 27-hydroxycholesterol in SPG5 patients with hereditary spastic paresis. *J Lipid Res* **51**, 819-823, doi:10.1194/jlr.M002543 (2010).
412 Park, K. & Scott, A. L. Cholesterol 25-hydroxylase production by dendritic cells and macrophages is regulated by type I interferons. *J Leukoc Biol* **88**, 1081-1087, doi:10.1189/jlb.0610318 (2010).
413 Diczfalusy, U. *et al.* Marked upregulation of cholesterol 25-hydroxylase expression by lipopolysaccharide. *J Lipid Res* **50**, 2258-2264, doi:10.1194/jlr.M900107-JLR200 (2009).
414 Bauman, D. R. *et al.* 25-Hydroxycholesterol secreted by macrophages in response to Toll-like receptor activation suppresses immunoglobulin A production. *Proc Natl Acad Sci U S A* **106**, 16764-16769, doi:10.1073/pnas.0909142106 (2009).
415 Gomes, B., Goncalves, S., Disalvo, A., Hollmann, A. & Santos, N. C. Effect of 25-hydroxycholesterol in viral membrane fusion: Insights on HIV inhibition. *Biochim Biophys Acta Biomembr* **1860**, 1171-1178, doi:10.1016/j.bbamem.2018.02.001 (2018).
416 Shrivastava-Ranjan, P. *et al.* 25-Hydroxycholesterol Inhibition of Lassa Virus Infection through Aberrant GP1 Glycosylation. *mBio* **7**, doi:10.1128/mBio.01808-16 (2016).
417 Doms, A., Sanabria, T., Hansen, J. N., Altan-Bonnet, N. & Holm, G. H. 25-Hydroxycholesterol Production by the Cholesterol-25-Hydroxylase Interferon-Stimulated Gene Restricts Mammalian Reovirus Infection. *J Virol* **92**, doi:10.1128/JVI.01047-18 (2018).
418 Civra, A. *et al.* Inhibition of pathogenic non-enveloped viruses by 25-hydroxycholesterol and 27-hydroxycholesterol. *Sci Rep* **4**, 7487, doi:10.1038/srep07487 (2014).
419 Chen, Y. *et al.* Interferon-inducible cholesterol-25-hydroxylase inhibits hepatitis C virus replication via distinct mechanisms. *Sci Rep* **4**, 7242, doi:10.1038/srep07242 (2014).
420 Ke, W. *et al.* Cholesterol 25-Hydroxylase Inhibits Porcine Reproductive and Respiratory Syndrome Virus Replication through Enzyme Activity-Dependent and -Independent Mechanisms. *J Virol* **91**, doi:10.1128/JVI.00827-17 (2017).
421 Friedman, R. L., Manly, S. P., McMahon, M., Kerr, I. M. & Stark, G. R. Transcriptional and posttranscriptional regulation of interferon-induced gene expression in human cells. *Cell* **38**, 745-755 (1984).
422 LEWIN, A. R., REID, L. E., McMAHON, M., STARK, G. R. & KERR, I. M. Molecular analysis of a human interferon-inducible gene family. *European Journal of Biochemistry* **199**, 417-423 (1991).
423 Siegrist, F., Ebeling, M. & Certa, U. The small interferon-induced transmembrane genes and proteins. *J Interferon Cytokine Res* **31**, 183-197, doi:10.1089/jir.2010.0112 (2011).
424 Moffatt, P. *et al.* Bril: a novel bone-specific modulator of mineralization. *Journal of Bone and Mineral Research* **23**, 1497-1508 (2008).
425 Lazarus, S. *et al.* The IFITM5 mutation c.-14C> T results in an elongated transcript expressed in human bone; and causes varying phenotypic severity of osteogenesis imperfecta type V. *BMC musculoskeletal disorders* **15**, 1 (2014).
426 Oren, R., Takahashi, S., Doss, C., Levy, R. & Levy, S. TAPA-1, the target of an antiproliferative antibody, defines a new family of transmembrane proteins. *Molecular and Cellular Biology* **10**, 4007-4015 (1990).
427 Behr, S. & Schriever, F. Engaging CD19 or target of an antiproliferative antibody 1 on human B lymphocytes induces binding of B cells to the interfollicular stroma of human tonsils via integrin alpha 4/beta 1 and fibronectin. *The Journal of experimental medicine* **182**, 1191-1199 (1995).
428 Smith, R., Young, J., Weis, J. & Weis, J. Expression of the mouse fragilis gene products in immune cells and association with receptor signaling complexes. *Genes and immunity* **7**, 113-121 (2006).
429 Saitou, M., Barton, S. C. & Surani, M. A. A molecular programme for the specification of germ cell fate in mice. *Nature* **418**, 293-300 (2002).

430 Zucchi, I., Montagna, C., Susani, L., Vezzoni, P. & Dulbecco, R. The rat gene homologous to the human gene 9–27 is involved in the development of the mammary gland. *Proceedings of the National Academy of Sciences* **95**, 1079-1084 (1998).
431 El-Tanani, M., Jin, D., Campbell, F. & Johnston, P. Interferon-induced transmembrane 3 binds osteopontin in vitro: expressed in vivo IFITM3 reduced OPN expression. *Oncogene* **29**, 752-762 (2010).
432 Zucchi, I. *et al.* Association of rat8 with Fyn protein kinase via lipid rafts is required for rat mammary cell differentiation in vitro. *Proceedings of the National Academy of Sciences of the United States of America* **101**, 1880-1885 (2004).
433 Tanaka, S. S. & Matsui, Y. Developmentally regulated expression of mil-1 and mil-2, mouse interferon-induced transmembrane protein like genes, during formation and differentiation of primordial germ cells. *Mechanisms of development* **119**, S261-S267 (2002).
434 Tanaka, S. S., Yamaguchi, Y. L., Tsoi, B., Lickert, H. & Tam, P. P. IFITM/Mil/fragilis family proteins IFITM1 and IFITM3 play distinct roles in mouse primordial germ cell homing and repulsion. *Developmental cell* **9**, 745-756 (2005).
435 Lange, U. C. *et al.* Normal germ line establishment in mice carrying a deletion of the Ifitm/Fragilis gene family cluster. *Molecular and cellular biology* **28**, 4688-4696 (2008).
436 Gutterman, J. U. Cytokine therapeutics: lessons from interferon alpha. *Proceedings of the National Academy of Sciences* **91**, 1198-1205 (1994).
437 Yang, G., Xu, Y., Chen, X. & Hu, G. IFITM1 plays an essential role in the antiproliferative action of interferon-γ. *Oncogene* **26**, 594-603 (2007).
438 Xu, Y., Yang, G. & Hu, G. Binding of IFITM1 enhances the inhibiting effect of caveolin-1 on ERK activation. *Acta biochimica et biophysica Sinica* **41**, 488-494 (2009).
439 Daniel-Carmi, V. *et al.* The human 1-8D gene (IFITM2) is a novel p53 independent pro-apoptotic gene. *International Journal of Cancer* **125**, 2810-2819 (2009).
440 Brem, R., Oraszlan-Szovik, K., Foser, S., Bohrmann, B. & Certa, U. Inhibition of proliferation by 1-8U in interferon-α-responsive and non-responsive cell lines. *Cellular and Molecular Life Sciences CMLS* **60**, 1235-1248 (2003).
441 Huang, H. *et al.* Gene expression profiling of low-grade diffuse astrocytomas by cDNA arrays. *Cancer research* **60**, 6868-6874 (2000).
442 Brem, R., Certa, U., Neeb, M., Nair, A. P. & Moroni, C. Global analysis of differential gene expression after transformation with the vH-ras oncogene in a murine tumor model. *Oncogene* **20** (2001).
443 Abba, M. C. *et al.* Transcriptomic changes in human breast cancer progression as determined by serial analysis of gene expression. *Breast Cancer Res* **6**, R499-513 (2004).
444 Andreu, P. *et al.* Identification of the IFITM family as a new molecular marker in human colorectal tumors. *Cancer research* **66**, 1949-1955 (2006).
445 Pellagatti, A. *et al.* Gene expression profiles of CD34+ cells in myelodysplastic syndromes: involvement of interferon-stimulated genes and correlation to FAB subtype and karyotype. *Blood* **108**, 337-345 (2006).
446 Yang, Y. *et al.* The interferon-inducible 9-27 gene modulates the susceptibility to natural killer cells and the invasiveness of gastric cancer cells. *Cancer letters* **221**, 191-200 (2005).
447 Hatano, H. *et al.* IFN-induced transmembrane protein 1 promotes invasion at early stage of head and neck cancer progression. *Clinical Cancer Research* **14**, 6097-6105 (2008).
448 Akyerli, C. B. *et al.* Expression of IFITM1 in chronic myeloid leukemia patients. *Leukemia research* **29**, 283-286 (2005).

449 Hisamatsu, T. *et al.* Interferon-inducible gene family 1-8U expression in colitis-associated colon cancer and severely inflamed mucosa in ulcerative colitis. *Cancer Research* **59**, 5927-5931 (1999).
450 Wu, F. *et al.* Genome-wide gene expression differences in Crohn's disease and ulcerative colitis from endoscopic pinch biopsies: insights into distinctive pathogenesis. *Inflammatory bowel diseases* **13**, 807-821 (2007).
451 Younossi, Z. M. *et al.* Gene expression profile associated with superimposed non-alcoholic fatty liver disease and hepatic fibrosis in patients with chronic hepatitis C. *Liver International* **29**, 1403-1412 (2009).
452 Bailey, C. C., Kondur, H. R., Huang, I. C. & Farzan, M. Interferon-induced transmembrane protein 3 is a type II transmembrane protein. *J Biol Chem* **288**, 32184-32193, doi:10.1074/jbc.M113.514356 (2013).
453 Ling, S. *et al.* Combined approaches of EPR and NMR illustrate only one transmembrane helix in the human IFITM3. *Scientific reports* **6** (2016).
454 Jia, R. *et al.* The N-terminal region of IFITM3 modulates its antiviral activity by regulating IFITM3 cellular localization. *Journal of virology* **86**, 13697-13707 (2012).
455 Jia, R. *et al.* Identification of an endocytic signal essential for the antiviral action of IFITM3. *Cellular microbiology* **16**, 1080-1093 (2014).
456 Zhu, X. *et al.* IFITM3-containing exosome as a novel mediator for anti-viral response in dengue virus infection. *Cellular microbiology* **17**, 105-118 (2015).
457 ALBER, D. & STAEHELI, P. Partial inhibition of vesicular stomatitis virus by the interferon-induced human 9-27 protein. *Journal of interferon & cytokine research* **16**, 375-380 (1996).
458 Brass, A. L. *et al.* The IFITM proteins mediate cellular resistance to influenza A H1N1 virus, West Nile virus, and dengue virus. *Cell* **139**, 1243-1254, doi:10.1016/j.cell.2009.12.017 (2009).
459 Everitt, A. R. *et al.* IFITM3 restricts the morbidity and mortality associated with influenza. *Nature* **484**, 519-523, doi:10.1038/nature10921 (2012).
460 Huang, I. C. *et al.* Distinct patterns of IFITM-mediated restriction of filoviruses, SARS coronavirus, and influenza A virus. *PLoS Pathog* **7**, e1001258, doi:10.1371/journal.ppat.1001258 (2011).
461 Jiang, D. *et al.* Identification of five interferon-induced cellular proteins that inhibit west nile virus and dengue virus infections. *Journal of virology* **84**, 8332-8341 (2010).
462 Li, K. *et al.* IFITM proteins restrict viral membrane hemifusion. *PLoS Pathog* **9**, e1003124, doi:10.1371/journal.ppat.1003124 (2013).
463 Lu, J. *et al.* The IFITM proteins inhibit HIV-1 infection. *J Virol* **85**, 2126-2137, doi:10.1128/JVI.01531-10 (2011).
464 Mudhasani, R. *et al.* IFITM-2 and IFITM-3 but not IFITM-1 restrict Rift Valley fever virus. *Journal of virology* **87**, 8451-8464 (2013).
465 Smith, S. E. *et al.* Chicken interferon-inducible transmembrane protein 3 restricts influenza viruses and lyssaviruses in vitro. *J Virol* **87**, 12957-12966, doi:10.1128/JVI.01443-13 (2013).
466 Weidner, J. M. *et al.* Interferon-induced cell membrane proteins, IFITM3 and tetherin, inhibit vesicular stomatitis virus infection via distinct mechanisms. *J Virol* **84**, 12646-12657, doi:10.1128/JVI.01328-10 (2010).
467 Wilkins, C. *et al.* IFITM1 is a tight junction protein that inhibits hepatitis C virus entry. *Hepatology* **57**, 461-469 (2013).
468 Wrensch, F. *et al.* Interferon-Induced Transmembrane Protein-Mediated Inhibition of Host Cell Entry of Ebolaviruses. *J Infect Dis* **212 Suppl 2**, S210-218, doi:10.1093/infdis/jiv255 (2015).

469 Zhang, Z., Liu, J., Li, M., Yang, H. & Zhang, C. Evolutionary dynamics of the interferon-induced transmembrane gene family in vertebrates. *PLoS One* **7**, e49265, doi:10.1371/journal.pone.0049265 (2012).
470 Anafu, A. A., Bowen, C. H., Chin, C. R., Brass, A. L. & Holm, G. H. Interferon-inducible transmembrane protein 3 (IFITM3) restricts reovirus cell entry. *J Biol Chem* **288**, 17261-17271, doi:10.1074/jbc.M112.438515 (2013).
471 Warren, C. J. *et al.* The antiviral restriction factors IFITM1, 2 and 3 do not inhibit infection of human papillomavirus, cytomegalovirus and adenovirus. *PloS one* **9**, e96579 (2014).
472 Zhao, X. *et al.* Interferon induction of IFITM proteins promotes infection by human coronavirus OC43. *Proceedings of the National Academy of Sciences* **111**, 6756-6761 (2014).
473 Ranjbar, S., Haridas, V., Jasenosky, L. D., Falvo, J. V. & Goldfeld, A. E. A Role for IFITM Proteins in Restriction of Mycobacterium tuberculosis Infection. *Cell reports* **13**, 874-883 (2015).
474 Yount, J. S. *et al.* Palmitoylome profiling reveals S-palmitoylation–dependent antiviral activity of IFITM3. *Nature chemical biology* **6**, 610-614 (2010).
475 Yount, J. S., Karssemeijer, R. A. & Hang, H. C. S-palmitoylation and ubiquitination differentially regulate interferon-induced transmembrane protein 3 (IFITM3)-mediated resistance to influenza virus. *Journal of Biological Chemistry* **287**, 19631-19641 (2012).
476 Shiratori, T. *et al.* Tyrosine phosphorylation controls internalization of CTLA-4 by regulating its interaction with clathrin-associated adaptor complex AP-2. *Immunity* **6**, 583-589 (1997).
477 John, S. P. *et al.* The CD225 domain of IFITM3 is required for both IFITM protein association and inhibition of influenza A virus and dengue virus replication. *Journal of virology* **87**, 7837-7852 (2013).
478 Smith, S., Weston, S., Kellam, P. & Marsh, M. IFITM proteins—cellular inhibitors of viral entry. *Current opinion in virology* **4**, 71-77 (2014).
479 Amini-Bavil-Olyaee, S. *et al.* The antiviral effector IFITM3 disrupts intracellular cholesterol homeostasis to block viral entry. *Cell Host Microbe* **13**, 452-464, doi:10.1016/j.chom.2013.03.006 (2013).
480 Desai, T. M. *et al.* IFITM3 restricts influenza A virus entry by blocking the formation of fusion pores following virus-endosome hemifusion. *PLoS Pathog* **10**, e1004048, doi:10.1371/journal.ppat.1004048 (2014).
481 Perreira, J. M., Chin, C. R., Feeley, E. M. & Brass, A. L. IFITMs restrict the replication of multiple pathogenic viruses. *Journal of molecular biology* **425**, 4937-4955 (2013).
482 Bailey, C. C., Zhong, G., Huang, I. C. & Farzan, M. IFITM-Family Proteins: The Cell's First Line of Antiviral Defense. *Annu Rev Virol* **1**, 261-283, doi:10.1146/annurev-virology-031413-085537 (2014).
483 Ding, S., Pan, Q., Liu, S. L. & Liang, C. HIV-1 mutates to evade IFITM1 restriction. *Virology* **454-455**, 11-24, doi:10.1016/j.virol.2014.01.020 (2014).
484 Chutiwitoonchai, N. *et al.* Characteristics of IFITM, the newly identified IFN-inducible anti-HIV-1 family proteins. *Microbes and Infection* **15**, 280-290 (2013).
485 Compton, A. A. *et al.* IFITM proteins incorporated into HIV-1 virions impair viral fusion and spread. *Cell host & microbe* **16**, 736-747 (2014).
486 Tartour, K. *et al.* IFITM proteins are incorporated onto HIV-1 virion particles and negatively imprint their infectivity. *Retrovirology* **11**, doi:10.1186/s12977-014-0103-y (2014).
487 Yu, J. *et al.* IFITM Proteins Restrict HIV-1 Infection by Antagonizing the Envelope Glycoprotein. *Cell Rep* **13**, 145-156, doi:10.1016/j.celrep.2015.08.055 (2015).
488 Foster, T. L. *et al.* Resistance of Transmitted Founder HIV-1 to IFITM-Mediated Restriction. *Cell Host Microbe* **20**, 429-442, doi:10.1016/j.chom.2016.08.006 (2016).

489 Stacey, M. A. *et al.* The antiviral restriction factor IFN-induced transmembrane protein 3 prevents cytokine-driven CMV pathogenesis. *J Clin Invest* **127**, 1463-1474, doi:10.1172/JCI84889 (2017).
490 Allen, E. K. *et al.* SNP-mediated disruption of CTCF binding at the IFITM3 promoter is associated with risk of severe influenza in humans. *Nat Med* **23**, 975-983, doi:10.1038/nm.4370 (2017).
491 Qian, J. *et al.* Primate lentiviruses are differentially inhibited by interferon-induced transmembrane proteins. *Virology* **474**, 10-18, doi:10.1016/j.virol.2014.10.015 (2015).
492 Jia, R. *et al.* The C-terminal sequence of IFITM1 regulates its anti-HIV-1 activity. *PLoS One* **10**, e0118794, doi:10.1371/journal.pone.0118794 (2015).
493 Bailey, C. C., Huang, I.-C., Kam, C. & Farzan, M. Ifitm3 limits the severity of acute influenza in mice. *PLoS Pathog* **8**, e1002909 (2012).
494 Xuan, Y. *et al.* IFITM3 rs12252 T> C polymorphism is associated with the risk of severe influenza: a meta-analysis. *Epidemiology and infection* **143**, 2975-2984 (2015).
495 Zhang, Y.-H. *et al.* Interferon-induced transmembrane protein-3 genetic variant rs12252-C is associated with severe influenza in Chinese individuals. *Nature communications* **4**, 1418 (2013).
496 Zhang, Y. *et al.* Interferon-induced transmembrane protein-3 rs12252-C is associated with rapid progression of acute HIV-1 infection in Chinese MSM cohort. *AIDS (London, England)* **29**, 889 (2015).
497 Compton, A. A. *et al.* Natural mutations in IFITM3 modulate post-translational regulation and toggle antiviral specificity. *EMBO Rep* **17**, 1657-1671, doi:10.15252/embr.201642771 (2016).
498 Shen, C. *et al.* A functional promoter polymorphism of IFITM3 is associated with susceptibility to pediatric tuberculosis in Han Chinese population. *PloS one* **8**, e67816 (2013).
499 Olsen, B. N., Schlesinger, P. H., Ory, D. S. & Baker, N. A. 25-Hydroxycholesterol increases the availability of cholesterol in phospholipid membranes. *Biophys J* **100**, 948-956, doi:10.1016/j.bpj.2010.12.3728 (2011).
500 Freed, E. O., Englund, G. & Martin, M. A. Role of the basic domain of human immunodeficiency virus type 1 matrix in macrophage infection. *J Virol* **69**, 3949-3954 (1995).
501 Cavrois, M., De Noronha, C. & Greene, W. C. A sensitive and specific enzyme-based assay detecting HIV-1 virion fusion in primary T lymphocytes. *Nat Biotechnol* **20**, 1151-1154, doi:10.1038/nbt745 (2002).
502 Cavrois, M., Neidleman, J., Bigos, M. & Greene, W. C. Fluorescence resonance energy transfer-based HIV-1 virion fusion assay. *Methods Mol Biol* **263**, 333-344, doi:10.1385/1-59259-773-4:333 (2004).
503 Ding, S. *et al.* Lineage-Specific Differences between the gp120 Inner Domain Layer 3 of Human Immunodeficiency Virus and That of Simian Immunodeficiency Virus. *J Virol* **90**, 10065-10073, doi:10.1128/JVI.01215-16 (2016).
504 Desormeaux, A. *et al.* The highly conserved layer-3 component of the HIV-1 gp120 inner domain is critical for CD4-required conformational transitions. *J Virol* **87**, 2549-2562, doi:10.1128/JVI.03104-12 (2013).
505 Finzi, A. *et al.* Topological layers in the HIV-1 gp120 inner domain regulate gp41 interaction and CD4-triggered conformational transitions. *Mol Cell* **37**, 656-667, doi:10.1016/j.molcel.2010.02.012 (2010).
506 Compton, A. A. *et al.* IFITM proteins incorporated into HIV-1 virions impair viral fusion and spread. *Cell Host Microbe* **16**, 736-747, doi:10.1016/j.chom.2014.11.001 (2014).
507 Tartour, K. *et al.* IFITM proteins are incorporated onto HIV-1 virion particles and negatively imprint their infectivity. *Retrovirology* **11**, 103, doi:10.1186/s12977-014-0103-y (2014).
508 Yu, J. *et al.* IFITM Proteins Restrict HIV-1 Infection by Antagonizing the Envelope Glycoprotein. *Cell Rep* **13**, 145-156, doi:10.1016/j.celrep.2015.08.055 (2015).

509 Cordonnier, A., Montagnier, L. & Emerman, M. Single amino-acid changes in HIV envelope affect viral tropism and receptor binding. *Nature* **340**, 571-574, doi:10.1038/340571a0 (1989).
510 Hwang, S. S., Boyle, T. J., Lyerly, H. K. & Cullen, B. R. Identification of the envelope V3 loop as the primary determinant of cell tropism in HIV-1. *Science* **253**, 71-74, doi:10.1126/science.1905842 (1991).
511 Hamoudi, M., Simon-Loriere, E., Gasser, R. & Negroni, M. Genetic diversity of the highly variable V1 region interferes with Human Immunodeficiency Virus type 1 envelope functionality. *Retrovirology* **10**, 114, doi:10.1186/1742-4690-10-114 (2013).
512 Hendrix, C. W. *et al.* Pharmacokinetics and safety of AMD-3100, a novel antagonist of the CXCR-4 chemokine receptor, in human volunteers. *Antimicrob Agents Chemother* **44**, 1667-1673, doi:10.1128/aac.44.6.1667-1673.2000 (2000).
513 Fatkenheuer, G. *et al.* Efficacy of short-term monotherapy with maraviroc, a new CCR5 antagonist, in patients infected with HIV-1. *Nat Med* **11**, 1170-1172, doi:10.1038/nm1319 (2005).
514 Dimitrov, D. S., Hillman, K., Manischewitz, J., Blumenthal, R. & Golding, H. Kinetics of soluble CD4 binding to cells expressing human immunodeficiency virus type 1 envelope glycoprotein. *J Virol* **66**, 132-138 (1992).
515 Hart, T. K. *et al.* Binding of soluble CD4 proteins to human immunodeficiency virus type 1 and infected cells induces release of envelope glycoprotein gp120. *Proc Natl Acad Sci U S A* **88**, 2189-2193, doi:10.1073/pnas.88.6.2189 (1991).
516 Moore, J. P., McKeating, J. A., Weiss, R. A. & Sattentau, Q. J. Dissociation of gp120 from HIV-1 virions induced by soluble CD4. *Science* **250**, 1139-1142, doi:10.1126/science.2251501 (1990).
517 Herschhorn, A. *et al.* A broad HIV-1 inhibitor blocks envelope glycoprotein transitions critical for entry. *Nat Chem Biol* **10**, 845-852, doi:10.1038/nchembio.1623 (2014).
518 Herschhorn, A. *et al.* Release of gp120 Restraints Leads to an Entry-Competent Intermediate State of the HIV-1 Envelope Glycoproteins. *mBio* **7**, doi:10.1128/mBio.01598-16 (2016).
519 Moore, J. P. *et al.* A human monoclonal antibody to a complex epitope in the V3 region of gp120 of human immunodeficiency virus type 1 has broad reactivity within and outside clade B. *J Virol* **69**, 122-130 (1995).
520 Zhang, Y. *et al.* Interferon-induced transmembrane protein-3 rs12252-C is associated with rapid progression of acute HIV-1 infection in Chinese MSM cohort. *AIDS* **29**, 889-894, doi:10.1097/QAD.0000000000000632 (2015).
521 Conticello, S. G., Harris, R. S. & Neuberger, M. S. The Vif protein of HIV triggers degradation of the human antiretroviral DNA deaminase APOBEC3G. *Curr Biol* **13**, 2009-2013, doi:10.1016/j.cub.2003.10.034 (2003).
522 Douglas, J. L. *et al.* Vpu directs the degradation of the human immunodeficiency virus restriction factor BST-2/Tetherin via a {beta}TrCP-dependent mechanism. *J Virol* **83**, 7931-7947, doi:10.1128/JVI.00242-09 (2009).
523 Goujon, C. *et al.* Human MX2 is an interferon-induced post-entry inhibitor of HIV-1 infection. *Nature* **502**, 559-562, doi:10.1038/nature12542 (2013).
524 Kane, M. *et al.* MX2 is an interferon-induced inhibitor of HIV-1 infection. *Nature* **502**, 563-566, doi:10.1038/nature12653 (2013).
525 Liu, Z. *et al.* The interferon-inducible MxB protein inhibits HIV-1 infection. *Cell Host Microbe* **14**, 398-410, doi:10.1016/j.chom.2013.08.015 (2013).
526 Lee, W. J., Fu, R. M., Liang, C. & Sloan, R. D. IFITM proteins inhibit HIV-1 protein synthesis. *Sci Rep* **8**, 14551, doi:10.1038/s41598-018-32785-5 (2018).
527 Yu, J. & Liu, S. L. The Inhibition of HIV-1 Entry Imposed by Interferon Inducible Transmembrane Proteins Is Independent of Co-Receptor Usage. *Viruses* **10**, doi:10.3390/v10080413 (2018).

528 Munro, J. B. *et al.* Conformational dynamics of single HIV-1 envelope trimers on the surface of native virions. *Science* **346**, 759-763, doi:10.1126/science.1254426 (2014).
529 Hoffman, T. L. *et al.* Stable exposure of the coreceptor-binding site in a CD4-independent HIV-1 envelope protein. *Proc Natl Acad Sci U S A* **96**, 6359-6364, doi:10.1073/pnas.96.11.6359 (1999).
530 Zhuang, K. *et al.* Adoption of an "open" envelope conformation facilitating CD4 binding and structural remodeling precedes coreceptor switch in R5 SHIV-infected macaques. *PLoS One* **6**, e21350, doi:10.1371/journal.pone.0021350 (2011).
531 Medjahed, H., Pacheco, B., Desormeaux, A., Sodroski, J. & Finzi, A. The HIV-1 gp120 major variable regions modulate cold inactivation. *J Virol* **87**, 4103-4111, doi:10.1128/JVI.03124-12 (2013).
532 Jia, R. *et al.* The N-terminal region of IFITM3 modulates its antiviral activity by regulating IFITM3 cellular localization. *J Virol* **86**, 13697-13707, doi:10.1128/JVI.01828-12 (2012).
533 Sharma, A. *et al.* Macaque interferon-induced transmembrane proteins limit replication of SHIV strains in an Envelope-dependent manner. *PLoS Pathog* **15**, e1007925, doi:10.1371/journal.ppat.1007925 (2019).
534 Chen, Z. *et al.* Enhanced infectivity of an R5-tropic simian/human immunodeficiency virus carrying human immunodeficiency virus type 1 subtype C envelope after serial passages in pig-tailed macaques (Macaca nemestrina). *J Virol* **74**, 6501-6510, doi:10.1128/jvi.74.14.6501-6510.2000 (2000).
535 Siddappa, N. B. *et al.* Neutralization-sensitive R5-tropic simian-human immunodeficiency virus SHIV-2873Nip, which carries env isolated from an infant with a recent HIV clade C infection. *J Virol* **83**, 1422-1432, doi:10.1128/JVI.02066-08 (2009).
536 Beitari, S., Ding, S., Pan, Q., Finzi, A. & Liang, C. Effect of HIV-1 Env on SERINC5 Antagonism. *J Virol* **91**, doi:10.1128/JVI.02214-16 (2017).
537 Beitari, S., Pan, Q., Finzi, A. & Liang, C. Differential Pressures of SERINC5 and IFITM3 on HIV-1 Envelope Glycoprotein over the Course of HIV-1 Infection. *J Virol* **94**, doi:10.1128/JVI.00514-20 (2020).
538 Rosa, A. *et al.* HIV-1 Nef promotes infection by excluding SERINC5 from virion incorporation. *Nature* **526**, 212-217, doi:10.1038/nature15399 (2015).
539 Usami, Y., Wu, Y. & Gottlinger, H. G. SERINC3 and SERINC5 restrict HIV-1 infectivity and are counteracted by Nef. *Nature* **526**, 218-223, doi:10.1038/nature15400 (2015).
540 Passos, V. *et al.* Characterization of Endogenous SERINC5 Protein as Anti-HIV-1 Factor. *J Virol* **93**, doi:10.1128/JVI.01221-19 (2019).
541 Li, M. *et al.* TIM-mediated inhibition of HIV-1 release is antagonized by Nef but potentiated by SERINC proteins. *Proc Natl Acad Sci U S A* **116**, 5705-5714, doi:10.1073/pnas.1819475116 (2019).
542 Waltl, S. *et al.* 25-Hydroxycholesterol regulates cholesterol homeostasis in the murine CATH.a neuronal cell line. *Neurosci Lett* **539**, 16-21, doi:10.1016/j.neulet.2013.01.014 (2013).
543 Staropoli, I. *et al.* Flow Cytometry Analysis of HIV-1 Env Conformations at the Surface of Infected Cells and Virions: Role of Nef, CD4, and SERINC5. *J Virol* **94**, doi:10.1128/JVI.01783-19 (2020).
544 Richard, J., Prevost, J., Alsahafi, N., Ding, S. & Finzi, A. Impact of HIV-1 Envelope Conformation on ADCC Responses. *Trends Microbiol* **26**, 253-265, doi:10.1016/j.tim.2017.10.007 (2018).